DEVELOPMENT OF LINEAR REGRESSION MODEL FOR PREDICTING WATER QUALITY PARAMETERS FROM ANAEROBIC TREATMENT OF VINASSE

by

SHAMMI RAHMAN

Presented to the Faculty of the Graduate School of

The University of Texas at Arlington in Partial Fulfillment

of the Requirements

for the Degree of

DOCTOR OF PHILOSOPHY

THE UNIVERSITY OF TEXAS AT ARLINGTON

December 2014

Acknowledgements

All praise is due to God alone, the sustainer of all the worlds.

Additionally, my heartiest gratitude to Dr. Melanie Sattler for her unconditional support, guidance, and encouragement throughout the four years of graduate school. Her valuable suggestions towards my research have given me enthusiasm to successfully accomplish my work. Words cannot express my gratitude towards Dr. Hossain for his advice and ideas towards my research. I would like to thank Dr. Chen for her technical support and suggestions towards the research from experimental design to model building. Dr. Grover has been an invaluable asset for this research team. His prompt ideas towards the research have benefitted my work tremendously. I am grateful to my other committee member, Dr. Choi, for his time and interest towards the research.

Special thanks to Dr. Arpita Bhatt, Dr. Luciana Marcia, and Gautam, for mentoring me on my research work. I would like to thank my research colleague, Dr. Madhu Sabnis for her support on the research. My friends – Hesam, Zak, Wasiu, and Anna played a great role in this wonderful journey of grad school.

And at the end, I would like to take this moment to appreciate the contributions of my family members – my true strength. I am thankful to my kids, Umair and Mariyam, for being patient with busy mom. And I want to thank my husband for his patience, love and support, without which the Ph.D. would have been an unfulfilled dream.

November 14, 2014

Abstract

DEVELOPMENT OF LINEAR REGRESSION MODELS FOR PREDICTING WATER QUALITY PARAMETERS FROM ANAEROBIC TREATMENT OF VINASSE

Shammi Rahman, Ph.D.

The University of Texas at Arlington, 2014

Supervising Professor: Melanie Sattler

One of the most prominent biofuels today is ethanol. The production of ethanol from biomass, whether from sugar crops, starch crops, dairy products, or cellulosic materials, results in the production of a high-strength liquid waste called vinasse. Approximately 12 liters of vinasse are produced for every 1 liter of ethanol. Vinasse is high in solids and organic content, with biochemical oxygen demand (BOD) ranging from 30 to 40 g/L, and a low pH, typically from 3-5. Traditionally, in countries such as India, Brazil, and other Latin American countries, vinasse has been disposed of by applying it as a fertilizer on agricultural land. This can produce short-term benefits, because the vinasse contains nutrients like potassium, magnesium, and calcium which are needed for crops like sugarcane. However, over the long term, such disposal can cause severe deterioration of soil, surface water and ground water.

The research described here increases our knowledge of anaerobic biological treatment of vinasse. Such treatment reduces the vinasse waste strength and produces stabilized residuals that can be used as fertilizer without creating water pollution problems. Anaerobic biological treatment of vinasse also produces methane, which can be used as a renewable energy resource.

This research explored the behavior of the different compositions of vinasse in an anaerobic environment at three different temperatures (30, 35, and 40^0C). The primary goals of this research were 1) to develop laboratory scale anaerobic treatments to study the effect of temperature and vinasse composition on waste composition over time, and 2) to develop regression models for predicting water quality parameters as functions of temperature, time, and vinasse composition. Water quality parameters measured included biochemical oxygen demand (BOD), chemical oxygen demand (COD), ammonia-nitrogen, phosphorus, potassium, sulfate, pH, conductivity, total dissolved solids (TDS), total suspended solids (TSS), and volatile suspended solid (VSS)

6-L glass lab-scale reactors were filled with vinasse of 6 different compositions and operated at 3 different mesophilic temperatures (30, 35, 40°C). In the experimental design, the primary constituents of environmental interest - chemical oxygen demand (COD), nitrogen (N), phosphorus (P), potassium (K) and sulfur (S) - were varied over the ranges observed in vinasse, as described in the literature Synthetic vinasse was made from glucose, ammonia, phosphoric acid, potassium hydroxide, and calcium sulfate, in various amounts. For our experiments, we also obtained real vinasse from White Energy, Texas and MGP Ingredient, KS.

Percent of methane gas and water quality parameters were monitored as functions of time. Chemical oxygen demand was substantially reduced. Little reduction in BOD was observed. No significant changes in ammonia, potassium, or sulfate were observed. COD and BOD followed first-order decay. Statistical Analysis Software (SAS) was used to conduct Multiple Linear Regressions (MLR) on these water quality parameters (COD and BOD). The other water quality parameters did not decrease substantially with time; thus, no regression was performed.

Table of Contents

List of Illustrations

List of Tables

Chapter 1

Introduction

1.1 Biofuel

Throughout most of the Earth's history, especially before the existence of humans, natural forces were the primary cause of climate change. The scenario started to change with human emergence and accelerated with the start of the Industrial Revolution, reaching its peak today. Increasing human activities in industry, agriculture, transportation and modernization has made us enormously dependent on energy, mostly oil. Worldwide consumption of energy is 370 exajoules of energy per year, which is like 170 million barrels of oil per day and 11.73 terrawatts (TW) per hour (Somerville, 2007). The majority (more than 90 percent) is from fossil fuels.

There has been increasing interest in biofuels to combat the growing demand of energy with a cleaner and environment friendly alternative. Biofuels are defined as any gas, liquid or solid predominantly extracted from biomass; they include bioethanol, biomethanol, vegetable oils, biodiesel, biogas, bio-synthetic gas (bio-syngas), bio-oil, bio-char, Fischer-Tropsch liquids, and bio hydrogen (Demirbas, 2008).

Two of the most widely used biofuels are bioethanol and biodiesel. Bioethanol is almost entirely obtained from food crops. Biodiesel is primarily extracted from oil seeds like sunflower, mustard, and canola and has gained much attention recently due to its environmental benefits. Another category of biofuels is bio-crude or bio –synthetic oils. This is essentially a mixture of biofuel and traditional fossil fuels. The different categories of biofuels are depicted in the flow chart in Figure 1-1.

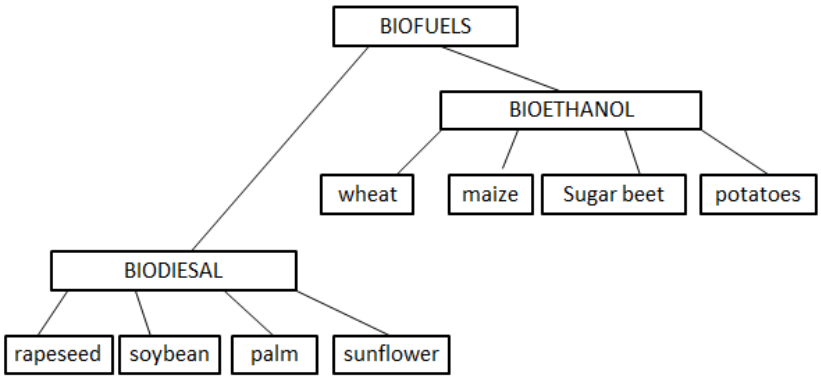

Fig. 1.1 - Sources of Bioethanol and Biodiesel (Demirbas, 2008)

According to the Worldwatch Institute's Climate and Energy Program, worldwide biofuel production reached an all-time high in 2010 of 105 billion liters (28 billion gallons US), a rise of 17% from 2009. The institute considers high oil prices, a global economic rebound, and new laws and mandates in Argentina, Brazil, Canada, China, and the United States, among other countries, to be the main reasons behind the accelerated production. The US and Brazil together top in ethanol production, generating 90 percent of total world production. The largest producer of biodiesel is the European Union, which generated 53 percent of all biodiesels in 2010.

As mentioned earlier, United States and Brazil remain the two largest producers of ethanol. In 2010, the United States generated 49 billion liters, or 57 percent of global output, and Brazil produced 28 billion liters, or 33 percent of the total. Corn is the primary feedstock for U.S. ethanol, and sugarcane is the dominant source of ethanol in Brazil. Globally Brazil tops in sugar cane production with 5 million hectares of land allocated for this purpose (Bassanta et al., 2003). In 2011/2012 crop, Brazil processed 492.70 million of tons of sugarcane to produce 12.71 billion of liters of hydrated ethanol (CANAOESTE, 2012). India, China, Pakistan, Thailand, and Mexico follow Brazil in the sugarcane

industry. Worldwide sugarcane production shown below in Figure 1-2 confirms Indian Subcontinent produces the largest amount of sugarcane.

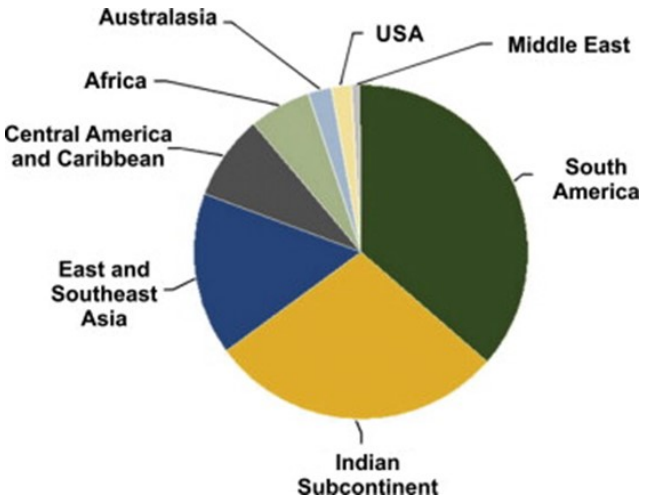

Fig. 1.2 - Sugarcane worldwide distribution. Source: Food and Agriculture Organization of United Nations (FAO), 2007 and FAO, 2013

Biofuels generate certain benefits over traditional gasoline, including the following:

- Renewable supply/sustainable.
- Perhaps lower emissions of greenhouse gases, depending on the feedstock and production process.
- Low sulfur and aromatic content, reducing emissions of these traditional pollutants (Conserve Energy Future, 2014).

Biodegradable (mainly biodiesel): the organics in biofuels are much simpler thus easily broken down

- Easily obtained since food crops can be grown potentially everywhere.

- Helps in social, regional and agricultural development.

However, there are some significant drawbacks associated with biofuels, mainly because the production is not completely fossil fuel free. Some of the noted disadvantages are mentioned below:

- Uses tractors and refinery machineries in agricultural fields that use fossil fuels.
- Uses trucks to transport biofuels.
- Increased pressure on food crops.
- Fertilizers and pesticides used increase soil and water pollution.
- Depending on the source, biofuel price can vary.
- High-strength liquid wastes like vinasse.

1.2 Vinasse

The production of ethanol from biomass, whether from sugar crops, starch crops, dairy products, or cellulosic materials, results in the production of a high-strength liquid waste called vinasse. Approximately 12 liters of vinasse are produced for every 1 liter of ethanol. Vinasse is high in solids and organic content (biochemical oxygen demand, or BOD, ranging from 30 to 40 g/L, Polack *et al.*, 1981), with a low pH, typically from 3-5 (Wilkie *et al.*, 2000).

The thick residual liquid from ethanol industry is given many names like stillage, mosto, dunder or distillery pot ale (Camargo et al., 2009, Gianchini and Ferraz, 2009 and Wilkie et al., 2000). Vinasse is produced all over the world and as the feedstocks can be chosen from a wide variety of crops, properties of the by-product also differ widely. Common crops used for the production of ethanol are as follows: sugarcane in South America (Haanon and Trenkle, 1990), beet, wine, and fruits in Europe, and corn and tequila in North America (Gianchini and Ferraz,2009 and España-Gamboa et al., 2011).

According to Almeida (1952), vinasse is an organic liquid residue primarily comprised of about water (93%), organic matter (5% mainly unfermented sugars and other carbohydrates) and inorganic dissolved solids (2%). Robertiello (1982) suggested that the molasses mosto has higher concentrations of organic matter, potassium, calcium, and magnesium. Sugarcane mosto has considerably lower concentrations of these elements – produced mainly in autonomous distilleries

Traditionally, in countries such as India, Brazil, and other Latin American countries, vinasse has been disposed of by applying it as a fertilizer or disposed as irrigation water on agricultural land (Korndorfer and Anderson, 1997). This can produce short-term benefits, because the vinasse contains nutrients like potassium, magnesium, and calcium, which are needed for crops like sugarcane (Glória, 1975). However, over the long term, such disposal can cause severe deterioration of soil, surface water and ground water. If released untreated to the environment, depending on the mixture composition, possess the potential of serious damage to the environment. The difficulty in disposal is due to the high temperature (65º to 105° C), persistent brown color, a smell that goes from astringent to nauseating, a solid content from 20,000 to 40,000 mg/l when obtained from straight sugarcane juice(can be high as 50,000 to 100,000mg/L if obtained from sugarcane molasses) (Octavio, 2012 and Smith 2006). Furthermore, vinasse is highly acidic (pH between 4 and 5) and high chemical oxygen demand (COD) content. The threat due to inappropriate disposal of vinasse has concerned many researchers. The high organic load is the primary problem. In addition, the hydrogen sulfide, amines and other offensive-smelling chemicals that are generated by decomposition of the organic matter make vinasse a difficult byproduct. In USA, Australia, Europe and in other places, vinasse must be treated before disposal.

1.3 Research Objectives

Anaerobic digestion is a comparatively cheap and easy procedure that significantly decreases the waste strength and at the same time generates methane gas, which can be used as an energy resource.

The primary objectives of this research were:

1. To develop and operate laboratory scale anaerobic reactors to study the effect of temperature and vinasse composition on waste composition over time.
2. To develop regression models for predicting water quality parameters as functions of temperature, time, and vinasse composition.

1.4 Dissertation Organization

Chapter 2 provides a detailed literature review of vinasse composition, sources, applications, and different treatments of vinasse. Further, it has extensive detail on anaerobic treatment in general – the pros and cons related to the method and a section on the previous studies conducted on anaerobic treatment of vinasse. Biogas was discussed in this section, too, since an integral part of anaerobic treatment is biogas formation.

Chapter 3 describes the methods and procedures used to conduct the experiments. The experimental design is discussed, and analytical procedures for the liquid parameters are summarized. Also included is a section on how data was collected, stored, reported and analyzed.

Chapter 4 elaborately discusses the results, primarily the methane generation and the water quality analysis. COD and BOD and its relationship with the methane generation, batch time and species richness have also been discussed.

Chapter 5 concentrates on the statistical analysis for the model development of COD and BOD. The final models have been chosen after many steps. All the steps are discussed.

Chapter 6 summarizes the conclusions and future recommendations for the research.

Chapter 2

Literature review

2.1 Background

Vinasse is classified as a class II residue, which means vinasse is not inert and not dangerous. It is a dark brown liquid and rich in nutrients, though the composition varies primarily depending on the kind of feedstock. Irrespective of the source, whether produced from corn, beets, or sugarcane, vinasse composition is dominated by organic matter in the form of organic acids and cations such as K, Ca and Mg (Gianchini and Ferraz, 2009; Laime et al., 2011). The presence of ions in vinasse, mainly potassium, phosphorus (phosphate) and nitrogen compounds (nitrite and nitrate) could cause groundwater salinization.

Vinasse, a waste product from ethanol distillery is characterized by low pH (3 – 4.5), distinguished odor, brown color and high inorganic and organic content (Octavio, 2012). Such unique properties make it difficult to dispose of. Several methods have been proposed but two processes remain the most common. One is the direct disposal to land (Conde et al., 2009) and the other is the anaerobic treatment to generate methane (Espinoza-Escalante et al., 2009). The former is a common practice in India, Brazil and many Latin American countries where untreated vinasse is applied to land to be used as fertilizers. This is primarily because of high nutrient content, particularly calcium, potassium, and organic materials, and the vast quantity of vinasse generated during ethanol production (España-Gamboa, 2011). Vinasse is not applied in a concentrated form. Rather it is applied to crops after diluting it with water, and subsequently crops are sprayed with the aqueous solutions. Depending on soil and plant nutrient requirements, vinasse may be applied as a 1–2% diluted solution to land (80–160 liters per acre) through irrigation or foliar spray for direct absorption by the plant. Though it has some

short-term benefits of land application of vinasse, there have been numerous reports of severe contamination of land and ground water.

Anaerobic treatment produces methane, a greenhouse gas but if trapped efficiently can be a renewable source of energy and an excellent example of converting waste to energy. The major drawbacks to this process are the long time required to generate methane and the limitations in treatment. Industries are often challenged with the high cost involved in the proper disposal and treatment of waste. A relatively cheap and simple method like anaerobic digestion can help to lower costs of waste disposal; if methane is trapped efficiently, companies may generate profit from the process, too.

2.2 Sources of vinasse

Vinasse, a highly colored residue represents a mixture of water, organic and inorganic compounds (Cortez and Brossard Pérez, 1997). The composition is solely dependent on the raw material used in the fermentation process. In general it is obtained through distillation of fermented cane and beet molasses, and molasses are a residue of cane and beet juice processing for the production of pure or refined sugar. In summary, vinasse is produced with the harvesting of sugar cane and sugar beets. Separating cellulosic components from the cane or beet juice produces sugarcane or sugar beet. Vinasse has a dark brown persistent color. To get rid of it, sulfur dioxide is sometimes added during the beet juice processing prior to crystallization. Multiple crystallization procedures are conducted on the syrup made from the juice after clarification to produce sugar crystals; the crystals are separated from the molasses by centrifugation and then harvested. The residue formed is then mixed with yeast or other microorganisms and fermented. The ethanol production from sugarcane is depicted in the flow chart shown in Figure 2 - 1.

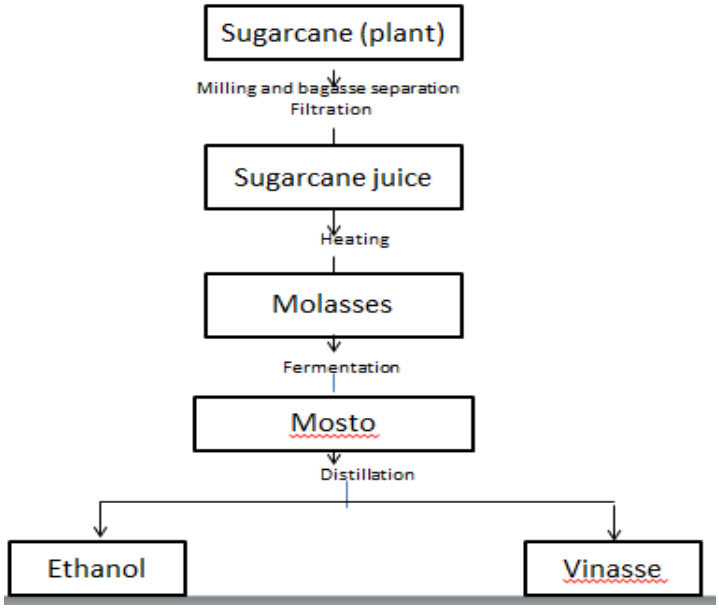

Fig. 2.1 - Flowchart of ethanol production process and co-production of sugar cane vinasse

The kind of yeast or microorganism used determines the conversion of carbohydrates (i.e., sugars) by fermentation within the molasses to ethyl alcohol, organic acids, and or other desired organic compounds. While producing ethanol, small amounts of sulfuric acid added prior to fermentation help to decrease the populations and activity of undesired bacterial species by adjusting the pH to between 4 and 5. Finally, distillation of the resulting fermentation broth separates ethanol from the mother liquor. Vinasse is the final byproduct of the distillation procedure, with 9-20 liters of vinasse generated per liter of ethanol (Parnaudeau, 2008; España-Gamboa, 2011), depending on the feedstock.

Along with vinasse, bagasse (the fibrous matter that remains following sugarcane processing), molasses, and filtercake are examples of bi products formed during the production of ethanol. The production of ethanol from sugarcane is accomplished in several steps:

Cane juice production

Vinasse production from sugarcane begins with the production of sugarcane and subsequent extraction of cane juice at a sugarcane factory. The crushed cane fibers exiting the mill are referred to as bagasse. The cane juice is filtered to remove large particles and clarified to get rid of turbid and suspended particles using heat and lime. The large insoluble particles are separated from lime juice by gravity and are mostly discarded or sometimes recycled back into the juice to maximize sugar yields (U.S. EPA, 1997).

Sucrose crystallization and processing

This step involves concentration of cane juice into cane syrup through heating in various steps. The final syrup is generally 65% solids and 35% water. Sucrose crystallization occurs in vacuum pans, where the syrup is heated until it reaches a supersaturated stage. At the supersaturated stage, if “seeding” or “shocking” is initiated, crystallization will take place that would separate sugar crystals from the mother liquor (i.e., molasses). The crystals are washed with water and the washed water centrifuged from the crystals (U.S. EPA, 1997).

Molasses and wash water from the first crystallization are recycled to the vacuum pan, reheated to form a second massecuite, which in turn produces a second batch of sucrose crystals. The third repetition would produce very low grade sugar. The final batch of molasses, which is a thick, viscous liquid, is used for the production of ethanol, yeast, and organic acids, leaving vinasse as the byproduct.

Molasses Fermentation

Ethanol production requires the fermentation of musts made of raw materials (i.e., cane juice, molasses) diluted with water followed by distillation of the fermented media. *Saccharomyces*, *Schizosaccharomyces*, *Pichia*, 359 *Hansenula*, *Candida*, and

Toulopsis are the yeast strains are traditionally used to perform the alcoholic fermentation of diluted molasses (Fahrasmane, 1998). Fermentation procedures using molasses also helps in the synthesis of amino acids, organic acids, and flavoring agents. Lactic acid can also be produced through the bacterial or fungal fermentation of molasses.

Distillation

Distillation is a common procedure to separate ethanol and lactic acid from other components of the fermentation mixture. To obtain thick ethanol, batch distillation is conducted; thin ethanol requires continuous distillation. Distillation is a process of separating component substances from liquid mixtures through vaporization and condensation, based on different volatility (vaporization point) of components in the mixture. From the first distillation, the residue (i.e., vinasse or stillage) is removed from the pot and the distillate is returned from the storage tank to the pot to be redistilled. The term “vinasse” or “stillage” refers to the collection of all residues obtained during the distillation process (Martagh, 1999).

Vinasse Processing

Vinasse can be obtained in a diluted or concentrated form, based on the application. It can be processed for various agricultural needs as well (Parnaudeau, 2008). The formation of diluted and concentrated vinasse is shown below in Figure 2-2.

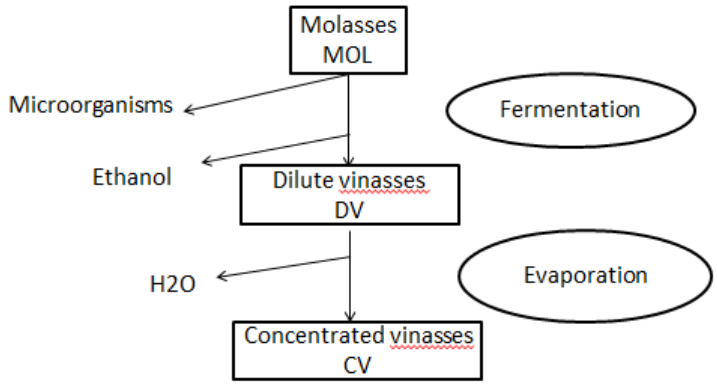

Fig. 2.2 - Industrial fermentation process leading to vinasse generation (Parnaudeau, 2008)

Moreover, processing of vinasse to separate the organic and inorganic fractions has been described by Paananen (2000). This is achieved by adding sulfuric acid to the vinasse, which in turn liberates the potassium from vinasse to form salt (like potassium sulfate). The procedure generates two fractions - one organic, used as an animal feeding additive, and the other inorganic, mostly used as fertilizer.

2.3 Applications of Vinasse

Historically in several tropical countries and Europe, vinasse has been applied as an additive for feed supplement for the feeding of ruminant and non-ruminant animals. Its use as fertilizer became prominent at the onset of 20th century. Vinasse has also been used as a compost ingredient. According to *Pesticide Research Institute for the USDA National Organic Program,* when vinasse is applied in appropriate ways, it is expected to:

- Improve the quality of soils with macro-nutrients (e.g., nitrogen, phosphorus, sulfur).
- Improve the quality of soils with micro-nutrients (e.g., vitamins and trace minerals).

- Maintain soil organic carbon levels.
- Increase micro flora and fauna development within soils.
- Improve the nutritional profile of crops for human and animal consumption.
- Increase the growth potential of crops.

ProLico®, a vinasse-containing product manufactured in Belgium and used in Europe, published a product information sheet stating that vinasse can be applied in soils or substrates for horticulture, tree nurseries, amenity planting, and landscaping. Cortez and Pere´ z, (1997) and Rodrı´guez (2000) reported that disposal of vinasse from sugarcane on land improves the quality of the land and has the potential to replace traditional inorganic fertilizers. This procedure requires proximity of disposal site and production site. Invitti (2012) described a method of decontamination and drying of vinasse using a micrionizing procedure and transformation of the residue into an organic mineral fertilizer.

Hidalgo (2011) suggested that the cost of animal feed is substantially decreased and the efficiency of outcome increases when vinasse is used as a feed supplement for conventional ruminant and non-ruminant livestock. There is a direct relationship between the consumption of vinasse and animal behavior, probably due to the presence of high content of organic acids and B complex vitamins contained within vinasse. Hidalgo further emphasized that the addition of vinasse to chicken feed with the goal for meat production enhanced live weight conversions and increased weights for carcass and edible parts.

Wilkie (2000) reported that calcium magnesium acetate, an organic acid salt produced during fermentation of carbohydrates in vinasse, can be used as an alternative di-icing agent for roadways. Earlier vinasse was concentrated, neutralized with an alkali

and incorporated into road building material (Wilkie, 2000). Recently, production methods for enzyme synthesis have utilized the necessary nutrient components of vinasse. For example, the combination of vinasse and bagasse is a useful substrate for the microbiological production of cellulolytic and lignolytic enzymes (Aguiar, 2010). Vinasse has also been incinerated and the ash used as fertilizer (Cortez, 1997; Willington, 1982).

Methane generation is possible with the anaerobic treatment of vinasse. Aerobic treatment of vinasse with fungi of the genus *Penicillium* and *Aspergillus* caused significant decolorization of the wastewater and also decreased the COD (Jiménez, 2003). After the treatment, the organic loading of vinasse is sufficiently decreased so that it can be used as a fertilizer without any threat of soil, ground or water pollution.

2.4 Vinasse Composition

Vinasse is a dark brown color liquid and weakly caramel, non-pungent odor (Tate & Lyle, 2005; DCM, 2010). It has a low viscosity at 25^0C is also slightly acidic which varies considerably based on the natural source and/or production method employed. It contains both organic (e.g., carbohydrates, proteins, and vitamins) and inorganic (e.g., nitrogen, sulfur, and minerals) compounds. Vinasse is dense at room temperature (vinasse density = 1.25–1.33 g/mL) and also infinitely soluble in water (Tate & Lyle, 2005; DCM, 2010). Although there is no vapor pressure reported for vinasse, components such as lactic acid and acetic acid in vinasse will volatize from soils. Table 2-1 shows the inorganic composition of vinasse obtained from cane and beet molasses.

Table 2.1 - Composition and yield of vinasse from cane and beet molasses (España-Gamboa, 2011)

	Vinasse from Cane Molasses	Vinasse from Beet Molasses
BOD (g/L)	39.5	27.5–44.9
COD (g/L)	84.9–95	55.5–91.1
Nitrogen total	153–1230	1800–4750
Phosphorus	1–190	160–163
Potassium	4893–11000	10000–10030
Sulfate total	1500–3480	3500–3720
pH	4.46–4.80	4.30–5.35
Copper	0.27–1.71 mg/L	2.1–5.0 mg/kg
Cadmium	0.04–1.36 mg/L	<1 mg/kg
Lead	0.02–0.48 mg/L	<5 mg/kg
Iron	12.8–157.5 mg/L	203–226 mg/kg
Phenols	34 mg/L	450 mg/kg
Vinasse Yield	12–20	9–15

Based on the data available from the literature and chemical analysis conducted by specialized laboratories, Table 2-2 presents the main elements found in the different types of vinasse.

Table 2.2 - Composition of vinasse from different kinds of feedstock

Parameters	Vinasse			
	Sugarcane	Grape (wine)	Beet	Sweet Sorghum
pH	3.9	2.9	5.1	4.5
BOD	5046	18900	78300	46
DQO	13380	na	na	na
Potassium	2056	118–800	10.000–10.030	na
Socium	50.2	na	3.79	na
Sulfate	710	120	0.62	na
Calcium	719	na	0.71	na
Magnesium	237	na	1.23	na
Total Phosphorus	190	83	91	1990
Hardness	2493	na	na	na
As	na	na	na	na
Ba	0.41	na	na	na
Cd	na	0.05–0.08	<1∗	na
Cr	0.04	na	na	na
Cu	0.35	0.2–3.26	2.1–5∗	37
Hg	0.0019	na	na	na
Mo	0.008	na	na	na
Ni	0.03	na	na	na
Pb	na	0.55–1.34	<5∗	na
Se	na	na	na	na
Zn	1.66	na	na	na

All values, except pH are expressed in mg L^{-1}.

Source: adapted from Robertiello (1982) and España-Gamboa et al. (2012).

∗ Unit is mg kg^{-1}; na: data not available

As mentioned before vinasse composition is highly dependent on the feed stock and location of production. Table 2-3 below describes the different parameters of vinasse obtained from sugar cane in different countries.

Table 2.3 - Comparative composition of vinasse derived from sugar cane

	Brazil(1)	Brazil(2)	Australia(1)	Australia(2)	India	USA(LA)
Component	Juice	Molasses	Molasses	Molasses	Molasses	Molasses
K, mg/L	1733	4893	8767	10704	4078	9073
P, mg/L	71	102	20	12	5097	1
N, mg/L	102	408	3160	1835	1019	153
Ca, mg/L	408	714	1121	2039	n.a	143
Mg, mg/L	102	204	1529	1325	n.a	61
Ash, mg/L	15292	19879	32622	n.a	n.a	50972
Organic solids, mg/L	52399	47200	n.a	n.a	n.a	n.a
Total solids, mg/L	68201	n.a	n.a	91750	69322	n.a
pH	4.6	4.8	n.a	n.a	4.3	4.5

Source: Cortez, L.A.B., and L.E. Brossard Perez. Experiences on vinasse disposal. Part III: Combustion of vinasse-#6 fuel oil emulsions, Brazilian Journal of Chemical Engineering, Vol. 14, No.1, 1997, São Paulo, Brazil.

Note: Data converted to mg/l from original % composition; n.a. means not available

The physio-chemical characteristics of concentrated vinasse are shown in the following table 2-4. The mineral composition is shown in Table 2-5. The concentrated vinasse was obtained from Havana Club rum factory of the Mixed Enterprise Havana Club, located in San José de las Lajas municipality, Mayabeque province. The samples were obtained from five production lots stored in tanks placed in Swine Unit (sample 1) and in “Atrevido” Unit (sample 2) of the Institute of Animal Science.

Table 2.4 - Physical-chemical characterization of concentrated vinasse (Scull, 2012)

Indicators	Sample 1 (n = 5)	Statistics		Sample 2 (n = 5)	Statistics	
		SD	VC (%)		SD	VC (%)
pH	4.08	0.07	1.92	3.92	0.008	0.21
Specific wt(%)	1.12	0.004	0.37	1.085	0.008	0.07
Dry Matter (%)	29.31	0.02	0.07	21.33	0.20	0.94
OM (%)	77.01	2.71	1.21	76.37	0.19	0.26
Ash (%)	25.00	0.04	0.18	23.63	0.20	0.83
CP (%)	12.39	0.63	5.13	13.26	0.40	3.05
TP (%)	8.89	0.10	1.18	9.29	0.79	8.46
Reducing sugars (%)	4.43	0.9	1.02	4.01	1.10	0.96

SD = Standard Deviation

VC = Variation coefficient.

Table 2.5 - Mineral composition of vinasse (Scull, 2012).

	Statistics			Statistics		
Mineral	Sample1	SD (%)	VC (%)	Sample2	SD (%)	VC (%)
Ca (%)	4.06	0.14	5.32	3.02	0.16	3.57
Mg	1.14	0.04	3.12	1.27	0.03	3.57
P (%)	0.24	0.01	1.03	0.28	0.04	0.98
K (%)	6.36	0.06	3.83	7.2	0.28	1.08
Na (%)	1.58	0.14	3.01	1.84	0.05	8.72
Fe (%)	0.07	0.003	1.37	0.08	0.001	4.56
Zn (%)	0.04	0.004	32.5	0.08	0.002	11.32
Cu (ppm)	6.6	0.004	1.93	5	0.0009	5.39
Pb (ppm)	12.9	0.69	11.18	19.34	2.16	5.34
Co (ppm)	6.49	0.46	1.77	8.67	0.15	7.04

The content and composition of amino acids mainly determine the protein quality in protein nutrition. But other structural characteristics and solubility may also affect the digestibility and nutritional value of vinasse (Millward, 2004).Table 2-6 shows the amino acidic profile of vinasse.

Table 2.6 - Amino acid composition of vinasse (Scull, 2012)

Amino acids	g/100 g Sample 1	g/100 g Sample 2	g/100 g FAO pattern
Aspartic acid	7.69	8.85	-
Threonine	5.66	7.31	2.9
Serine	4.64	4.81	-
Glutamic acid	12.11	13.23	-
Prolina	4.98	6.02	-
Glycine	4.08	3.61	-
Alanine	3.74	2.5	-
Cysteine	1.81	1.81	2
Valine	5.66	7.13	1.3
Methionine	4.53	nd	2.3
Isoleucine	6.79	5.76	4.3
Leucine	4.53	3.1	4.9
Tyrosine	6.23	4.99	2.9
Phenylalanine	5.09	4.73	2.9
Histidine	5.09	4.72	-
Lysine	9.96	9.28	4.9
Arginine	7.47	10.57	-

Table 2.7- Results of the microbiological analysis of vinasse (Scull, 2012)

Indicators	Sample 1	Sample 2
Counting of microorganisms mL	$< 1x10^4$	$< 1x10^4$
Counting of total coliforms mL	$< 1x10^2$	$< 1x10^2$
Counting of molds and yeasts mL	$< 5.7 x10^4$	$< 5.7 x10^4$
Determination of salmonella 25 ml	Ausente	Ausente

The original raw material of the organic fraction is mainly dependent on the plant-derived material. The characteristics of the plant material differ on the basis of the nature, soil, fertilizers, weather and many other factors. The procedures followed in the processing of the plant material also influence the composition of the final product. The composition of the organic fraction therefore varies considerably.

In Table 2.8, the percentage of the organic fraction from sugar beet is chosen. The concentrations are shown as percentages based on the dry solid matter.

Table 2.8 – Composition of the organic fraction from sugar beet (Parnaudeau, 2008).

Organic Component	**Percentage (%)**
Monosaccharide	0.2
Disaccharides	1.2
Other carbohydrates	8
Total nitrogen	6.5
Betaine	2.4
Amino acids	7
Organic acids	36
Potassium	4
Ash	15

Organic acid comprises 18 to 45%, typically 30 to 45% based on the dry solid matter % of the organic fraction. Almost 10 – 20 % of the organic acid is comprised of lactic acid and pyrrolidone carboxylic acid (PCA) (Parnaudeau, 2008).

Table 2.9 - Biochemical C and N components of the molasses and vinasses tested (Parnaudeau, 2008).

	MOL0	**MOL 30**	**MOL 100**	**DV0**	**DV30**	**DV 100**	**CV0**	**CV 30**	**CV 100**
Carbonaceous compounds (% organic C)									
Lactate	1.3	1	0.3	4	3.5	1	5.8	2.9	0.4
Acetate	1.3	0.8	0.3	3.7	2.8	2.6	3.4	2.6	8.4
Propionate	0	0	0	0.1	0.3	0.8	0	0	3.3
Formate	0.2	0.2	0.1	0.7	0.1	0.3	0.8	0.3	0.5
Butyrate	0.1	0	0	0.4	0.1	0.1	0	0.1	0.9
Pyruvate	0	0	0	2.3	0.3	0.8	0.5	0.1	0
Valerate	0	0	0	0	0	0	0	0	0.9
Malate	0.3	0.3	0.3	2.9	1	1.2	2.1	1.4	0.2
Tartrate	0	0	0.1	0.3	0.2	0.2	0	0.1	0

Table 2.9 continued

Oxalate	0.3	0.4	1.3	7.2	7.9	4	1.6	1.8	5.5
Citrate	0	0	0.1	0.3	0.1	0.1	0.1	0.1	0
Iso-citrate	0	0	0.1	0.1	0.4	0.1	0.1	0	0.2
cis-Aconitate	0.2	0.3	0.3	1.1	0.1	1.4	1	0.9	0.2
trans-Aconitate	0	0	0.1	0	0.8	0.5	0	0.4	6.7
Ethanol	8.8	0	0	0	1.2	0	0	6.9	0
Inositol	0.2	0.2	0.3	0.2	0.1	0.2	2.9	0.2	0.2
Glycerol	0.1	0.2	0.1	3.6	0	0	8	0.3	0.2
Arabitol	0	0	0	0.1	0.1	0.3	0.9	0.1	0.1
Sorbitol	0.1	0	0	0	0.1	0.1	0	0.1	0
Mannitol	0.1	0.2	0.3	0.3	0	0.2	1.5	1.9	0.1
Trehalose	0	0	0.1	1.6	0	0.1	2.4	0	0.2
Arabinose	0	0	0	0	0	0	0	0	0
Galactose	0	0	0	0	0	0.1	0.9	0	0
Mannose	0	0.3	0.4	0	0	0	1.1	0	0
Lactose	0	0	0	0	0	0	0	0	0
Ribose	0.2	0	0	0	0.1	0	0.1	0.1	0.1
Fructose	0	5.8	9.4	3.4	0	0.1	1.9	0.7	0
Glucose	0	4.2	4.9	0.3	0.1	0.4	0.7	0.8	0
Saccharose	64.4	69	57.5	0.1	0.1	0.3	2.8	0.5	1.3
Organic acids	3.7	3.1	3	23.1	17.7	13	15.5	10.7	27.3
Alcohols and polyols	9.2	0.7	0.7	4.3	1.5	0.7	13.3	9.3	0.6
Carbohydrates	64.6	79.4	72.3	5.6	0.4	1	9.8	1.9	1.5
Total	77.5	83.2	75.9	33	19.6	14.7	38.6	21.9	29.4
Nitrogenous compounds (% organic N)									
Betain	46.1	34.9	0	45.1	45	0	39.3	37.3	0

MOl 0 – Molasses from sugar beet only

DV0 and CV0 – Dilute vinasse and concentrated vinasse produced from a factory using molasses from sugar beet only.

DV30 and CV 30 – Dilute vinasse and concentrated vinasse produced in a factory based on molasses from a 30% sugar cane + 70% sugar beet mixture (MOL30)

DV100 and CV100 = Dilute vinasse and Concentrated vinasse came from a factory that only used sugar cane molasses (MOL100)

Table 2.10 - Characterization of the phenolic compounds in the molasses and vinasses tested (Parnaudeau, 2008).

	MOL0	**MOL 30**	**MOL 100**	**DV 0**	**DV 30**	**DV 100**	**CV 0**	**CV 30**	**CV 100**
λmax	263	267	271	261	271	271	261	271	271
Phenolic compounds absorbance	0.498	1.074	1.575	1.055	2.549	3.702	2.089	2.949	5.5

2.5 Vinasse Treatment

Recently (after 1970), the practice of land disposal of vinasse has been frowned on. There have been many concerns about the odor and volume of waste to deal. Joshi (1999) warned about the serious after-effects of such disposal. Deep well disposal is an option but is limited by underground storage availability and specific geological location. Other procedures like evaporation and combustion of the waste on site are alternatives (Sheehan and Greenfield, 1980; Wilkie et al., 2000). Some of the waste disposal or treatment methods have been compiled by Satyawali and Wilkie (2000) and are described below:

2.5.1 Biological Treatment

2.5.1.1 Anaerobic treatment

Anaerobic treatment of vinasse is a relatively easy and economical procedure because it generates biogas that could contribute to the plant's vast energy need. Furthermore, it has about 10% of the sludge yield and lower nutrient requirements compared to aerobic treatment (Wilkie et al., 2000).The major drawback of anaerobic treatment is the long time required for the process completion. In addition, not all compounds are biodegradable. Aerobic treatment is fast and the success of COD

removal is also high. However, the disadvantage compared to anaerobic treatment is that the cost of energy to maintain the aerated aerobic environment and no potential for methane gas production. Moreover, after aerobic treatment, almost 50% of the COD is converted to sludge (Sennitt, 2005), which requires further treatment and disposal, whereas anaerobic treatment converts over half of the effluent COD into biogas (Wilkie et al., 2000).

Anaerobic lagoons are considered the most natural method to conduct anaerobic treatment (Rao, 1972). Two lagoons in series have the potential to significantly degrade BOD. Due to the odor, however, large area requirement and potential leaching, lagoons have limited its use.

Suspended Bed Reactor

Upflow anaerobic sludge blanket (UASB) reactors are used in various types of industrial settings (Akunna and Clark, 2000; Syutsubo et al., 1997). 75% of COD removal is possible while treating sugarcane molasses (Goodwin and Stuart, 1994; Sanchez Riera et al., 1985). Mesophilic conditions are provided in most practical UASB systems, although thermophilic operation results in higher methanogenic activity.

Vlyssides (2010) introduced an alternative method to conventional anaerobic treatment. He tried a lab-scale UASB reactor of 20 L volume at 45^0 C with a retention time of 24 hours. There were three systems - conventional UASB reactor (system 1), UASB reactor with iron (system 2) and System 3 consisted of the UASB reactor supplemented with an iron performing Anammox process. All had high COD removal (almost 75%). Systems 2 and 3 were efficient in removing sulfur. Past studies have determined that ferrous iron enhances biological activity of the sludge and promotes COD removal (Vlyssides et al., 2007). Ferrous iron encourages good settling characteristics (Vlyssides et al, 2008, 2009). It promotes the removal of sulfide ions by forming

precipitate of ferrous sulfide and thus prevents hydrogen sulfide formation in the biogas. System 3 converts the nitrogen in the waste because the biogas bags were high in nitrogen.

UASB has been used for a long time to treat industrial wastewater, including vinasse, due to a high removal rate of organic load. It produces less sludge, produces biogas and requires less energy compared to other treatments. A table 2-11 comparing the performance of UASB for different types of vinasse is shown below:

Table 2.11 - Comparison of performance parameters of UASB by different types of vinasse (Espana, 2012)

Vinasse	**OLR kg COD/m^3-day**	**HRT days**	**COD removed%**	**CH_4%**	**M.Y. m^3CH_4/kg COD_{added}**	**Ref.**
Vinasse from hydrous alcohol distillery plant, using UASB (laboratory scale)	24	4	75	58	0.217	Sanchez, 1985
Cane molasses vinasse from hydrous alcohol distillery plant diluted ten-fold, using UASB (pilot scale)	19	0.5	40	na	0.21	Harada,1996
Cane molasses hydrous alcohol stillage, using UASB (laboratory scale)	14.49	9	65	na	0.055	Yeoh, 1997
Diluted brewery wastewater, using UASB (laboratory scale)	1.53	0.75	91	67	0.209	Cronin, 1998
Winery effluent treatment in an anaerobic hybrid USBF (pilot scale)	12	7	96	74	0.33	Molina, 2007

Table 2.11 continued

Wheat straw vinasse, using a UASB (laboratory scale)	17.1	2	76	64	0.155	Kaparaju, 2010
Vinasse from hydrous ethanol distillation, using a modified UASB reactor (laboratory scale)	17.05	7.5	69	84	0.263	España, 2012

na: data not available.

Fixed Bed Reactor

A fixed bed reactor restrains the movement of microorganisms on an inert support to encourage the biological activity per unit of reactor volume and thus decrease the loss of biomass. It is more suited for toxic materials with high COD removal and short hydraulic retention time (HRT). Packing materials like polyurethane, clay brick, granular activated carbon (GAC), and polyvinyl chloride (PVC) media have been applied, resulting in 67–98% reduction in COD (Bories et al., 1988; Seth et al., 1995; Goyal et al., 1996; Vijayaraghavan and Ramanujam, 2000). GAC has the best removal efficiency because of its adsorption capacity but it is quite expensive.

Fluidized Bed reactor

A fluidized bed reactor has an appropriate media like sand, gravel or plastics that attracts bacterial attachments and growth. Both up flow or down flow modes are in use. Fluidization is normally achieved by effluent recycling. Garcıa-Bernet et al. (1998) found in their experiments that downflow fluidized bed system using ground perlite (an expanded volcanic rock) can accomplish 75–95% reduction in carbon content.

Two Stage Process and Hybrid Reactor

Akunna and Clark (2000) worked with granular-bed anaerobic baffled reactor (GRABBR). It has ten equal compartments, each of which is further divided into two with baffles. 32 – 90 % COD removal is possible with HRT of 4 days. Vlissidis and Zoubolis

(1993) investigated the treatment of beet molasses in two stages: anaerobic digestion in an upflow sludge bed reactor (HRT of 11 days), followed by coagulation–flocculation with lime (2.5 hrs). 86% BOD and 71% COD removal was possible with 76% methane content in biogas.

2.5.1.2 Aerobic treatment

Aerobic digestion of high strength vinasse has been conducted satisfactorily in many places.

Luty (2008) studied the aerobic treatment of vinasse by a mixed culture of thermo- and mesophilic bacteria of the genus Bacillus after optimizing the pH, temperature and oxygenation state. The experiments were conducted in two stages. Initially a series of experiments from temperature 30 to 65^0C and from pH 5.4 to 9.5 were conducted to obtain the optimum condition. The optimum condition was 58^0C and the pH was 8.35 where COD removal was 60.88%. Then batch biodegradation processes were conducted with the optimum conditions in a Single Tank Reactor (STR) with aeration at 1.0 vvm and two stirrer speeds, 550 rpm and 900 rpm. The maximum COD removal (83.57%) was obtained with pH of 8.35, a temperature of 58°C and a stirrer speed of 900 rpm.

Aerobic treatment is often conducted after the anaerobic digestion because the post anaerobic treatment effluent still has relatively high organic loading and brown color. Solar drying is a natural method to get rid of this problem but it requires large space and rain or lack of sunshine will diminish its use. The other treatments applied to biomethanated distillery effluent are as follows:

Aquaculture – In Channai, India a pissiculture utilized the effluent, first spreading it over a 6 hectare bioconversion pond. The BOD decreased to zero and the residue,

which is high in nutrients, was used for fish food (Vorion Chemicals & Distilleries Ltd., 1999).

Constructed wetlands (CWs) - Trivedy and Nakate (2000), studied a lab scale CW using T.latipholia to treat diluted distillery effluent. An area of around 1.5m× 0.3 m× 0.3m was filled with sand and gravels (75%) and soil (25%). The diluted effluent was added after 4 weeks of plantation. In 10 days, 78% COD and 47% BOD removal is possible.

Biocomposting – This method is a common practice in Indian distilleries. Effluents from distilleries are thrown in sugarcane pressmud (filter cake obtained from juice clarification while producing sugar). It results in a formation of rich humus that can be applied as fertilizers.

The most common practice of post anaerobic treatment of vinasse is the activated sludge method.

Fungal treatment

To improve the efficiency of aerobic systems, some studies have focused on treatment by pure cultures. White rot fungus secreting ligninolytic enzymes has the potential to break xenobiotics and organopollutants. Kumar et al. (1998) and Dahiya et al. (2001a) *used P. chrysosporium* JAG 40 and resulted in 80% decolorization of diluted synthetic melanoidin, and 6.25% digested spentwash. *Coriolus hirsutus* resulted in 71 – 75% reduction in color and 90% reduction in COD (Kumar et al., 1998).

Apart from white rod fungi and filamentous fungi, yeast grows quickly, is less susceptible to contamination by other microorganisms, and can greatly degrade vinasse. The removal efficiencies for diluted waste (absorbance unit of 3.5 at 475nm) were 75% for color intensity and 76% for BOD (Sirianuntapiboon et al., 2004a).

Bacterial treatment

Ghosh et al. (2002) performed treatment of distillery wastewater with *Pseudomonas putida* followed *by Aeromonas sp*. in a two-stage bioreactor. P. putida is good in color removal because it secretes hydrogen peroxide, a strong decolorizing agent*. Aeromonas sp* utilizes carbon as its food and removes COD level up to 66% in 24 hours. Sirianuntapiboon et al. (2004) first observed the decolorization power of acetogenic bacteria. Arora et al. (1992) stated that significant removal of chloride and toxic content is possible with the nitrifying bacteria *Nitrosococcus oceanus.*

Algal treatment

This is the most reliable source of nitrogen and phosphorus removal from vinasse. It is conducted naturally by growing algae which feeds on the pollutant. Valderrama et al. (2002) treated 10% distillery effluent using the algae *Chlorella vulgaris* followed by *Lemna minuscula*. They observed 52% color removal. Kalavathi et al. (2001) conducted work on the effluent by marine cyanobacterium *Oscillatoria boryana* BDU 92181. It resulted in 5% melanoidin destruction.

2.5.2 Physio chemical Treatment

Molasses, after being treated anaerobically and aerobically, will still have significant organic load color and odor (Mall and Kumar, 1997). Melanoidins, the color causing pigment in vinasse, is not affected by the conventional biological treatment (Migo et al., 1993). Pena et al. (2003) suggested that multistage biological treatment decreases the organic load but has the disadvantage of repolymerization of the colored compounds.

Adsorption

Activated carbon (AC) is the most common adsorber in wastewater treatment to remove organic load. However, use of AC can be expensive in an industrial setting. Bernardo et al. (1997) compared the breakdown of synthetic melanoidins by

commercially used AC and synthetic AC made from bagasse. AC made from 2-diethylaminoethyl chloride hydrochloride and 3-chloro-2-hydroxypropyl trimethylammonium chloride has the potential of decolorizing diluted vinasse (Mane et al., 2006).

Coagulation and flocculation

In wastewater treatment, flocculation is a common practice. Numerous flocculants are in use like aluminum sulfate, poly-aluminum chloride (PAC) and synthetic polymers such as polyacrylamide (PAM). However aluminum has been linked to Alzheimer's disease (Campbell et al., 2000) and the polyacrylamide monomer poses concern as a strong neurotoxin (Takahashia et al., 2005). Octavio (2012) worked with harmless biological flocculants which will not have the above mentioned problems and are biodegradable. He found that poly-γ-glutamic acid (PGA), a polyamide flocculant, is the most desirable option because of its high yield, high flocculating activity and ability to flocculate a wide range of organic and inorganic compounds (Shih and Van, 2001). He used raw and treated vinasse from a tequila storage company treated with PGA by a by a flocculation–coagulation process. The results were impressive. PGA (250–300 ppm) combined with sodium hypochlorite and sand filtration managed removed about 70% of the turbidity and reduced chemical oxygen demand (COD) by 79.5%; in addition, there was substantial color removal. Table 2-12 shows removal of different parameters after a combined (coagulation/flocculation)/sand filtration/NaClO/sand filtration treatment using different PGA concentrations.

Table 2.12 - Summary of COD, pH, turbidity and sedimentable solids parameters obtained after a combined (coagulation/flocculation)/sand filtration/NaClO/sand filtration treatment using different PGA concentration for the coagulation/flocculation step (Octavio, 2012)

PGα21Ca (mg/L)	COD (mg/L)[a]	Removal (%)[a]	Turbidity (NTU)[a]	Removal (%)[a]	Sedimentable solids (mL)	pH
0	40,000 ± 3850		440 ± 40		420	3.5
100	27,250 ± 2580	31.9 ± 6.45	342 ± 18	22 ± 4.1	310	5.6
200	12,700 ± 1790	68.3 ± 6.6	253 ± 23	43 ± 5.2	250	5.6
300	8200 ± 920	79.5 ± 11.2	134 ± 33			

PGA by itself cannot remove the color. Sodium hypochlorite, an oxidant used with PGA, is successful in removing the melanoidin group (that causes the color) formed during the processing of raw materials or during broth sterilization for the fermentation process (Iñiguez-Cobarrubias and Peraza-Luna, 2007). This is a simple and cheap method, more suitable for industrial settings where time and money to deal with wastes are scarce.

Oxidation

Ozone is a common practice in treating waste with concern for color, phenolics, pesticides, etc. (Pena et al., 2003). Treating the distillery resulted in 15 to 25% COD removal and 80% decolorization, and it improved the biodegradability of the effluent significantly. Alfafara et al. (2000) mentioned on the inability of ozone to destroy the dark colored polymeric compounds. Chlorine destroys color more than 97% but the color

comes back after some time (Mandal et al., 2003). Combinations of oxidation methods were tried. Ozone with UV had significant success but ozone with hydrogen peroxide made few changes.

Sangave and Pandit (2004) worked with sonication for 2 hours as a pretreatment procedure of vinasse wastewater, resulting in 44% removal of COD. Aerobic digestion alone removed 24% COD. Gaikwad and Naik (2000) conducted research on a combination of wet air oxidation and adsorption. 57% COD, 72% BOD, 83% TOC and 94% sulfates were successfully removed.

The treatment of distillery from grain, potato, beet and some other plant materials were conducted with the combination of electron beam and coagulation by Pikaev et al. (2001). Optical absorption in the UV region decreased 65 – 70%.

Membrane treatment

Chang et al. (1994) reported removal of half of organic load when pretreatment with ceramic membranes were conducted before anaerobic digestion. Furthermore, the treatment improved anaerobic digestion by removing inhibiting substances. Vlyssides et al. (1997) worked with the electrodialysis of beet molasses using a stainless steel cathode, titanium alloy anode and NaCl as electrolytic agent. COD removal as high as 88% was achieved.

Evaporation / Combustion

The diluted waste from a distillery can be evaporated with thermal vapor recompression (Bhandari et al., 2004; Gulati, 2004). The concentrated liquor can be dried using hot air to form dry powder. The dry powder after mixing with agricultural waste is burned in a boiler. Cortez and Pere´z (1997) emphasized that vinasse can be combusted onsite to produce potassium rich ash that can be applied on land as fertilizers.

2.6 Anaerobic Digestion

Anaerobic digestion is a series of biological processes by which microorganisms break down organic materials in the absence of oxygen. The process produces methane, carbon dioxide and traces of other gases. Methane is a greenhouse gas but if trapped can be an excellent source of renewable energy. The biogas can be used to facilitate industry's need of energy, in combined heat and power gas engines or upgraded to natural gas-quality bio methane. The digestate, the final solid or liquid product from the digestion, is rich in nutrients and can be applied to land as fertilizers.

Klein et al. (1972) explained the different steps of anaerobic breakdown of organic matter with the following equations:

Carbon, C $\longrightarrow$ organic acids ($R\cdot COOH$) $CH_4 + CO_2 \longrightarrow$

Nitrogen, N $\longrightarrow$ amino acids [$R\cdot(NH_2)\cdot COOH$] $\longrightarrow$ NH_3 + amines

Sulfur, S $\longrightarrow$ H_2S + organic S compounds

Phosphorus P $\longrightarrow$ PH_3 + organic P compounds

The breakdown of organic matter in an anaerobic treatment is accomplished in four recognized steps:

Hydrolysis – The first step of the anaerobic treatment is conversion of organic matter into liquefied monomers and polymers, i.e. proteins, carbohydrates and fats are transformed to amino acids, monosaccharides and fatty acids, respectively. Ostrem (2004) described the breakdown of glucose through hydrolysis:

$$C_6H_{10}O_4 + 2H_2O \rightarrow C_6H_{12}O_6 + 2H_2$$

Acidogenesis – In this step the products from the first step are further degraded into short chains of volatile acids, ketones, alcohols, hydrogen and carbon dioxide by acidogenic bacteria. The common products are propionic acid (CH_3CH_2COOH), butyric acid ($CH_3CH_2CH_2COOH$), acetic acid (CH_3COOH), formic acid ($HCOOH$), lactic acid

($C_3H_6O_3$), ethanol (C_2H_5OH) and methanol (CH_3OH). Ostrem (20040 and Bilitewski et al. (1997) described the acidogenesis steps through the following equations:

$$C_6H_{12}O_6 \leftrightarrow 2CH_3CH_2OH + 2CO_2$$

$$C_6H_{12}O_6 + 2H_2 \leftrightarrow 2CH_3CH_2COOH + 2H_2O$$

$$C_6H_{12}O_6 \rightarrow 3CH_3COOH$$

The degradation steps of anaerobic treatment are shown in Figure 2-3.

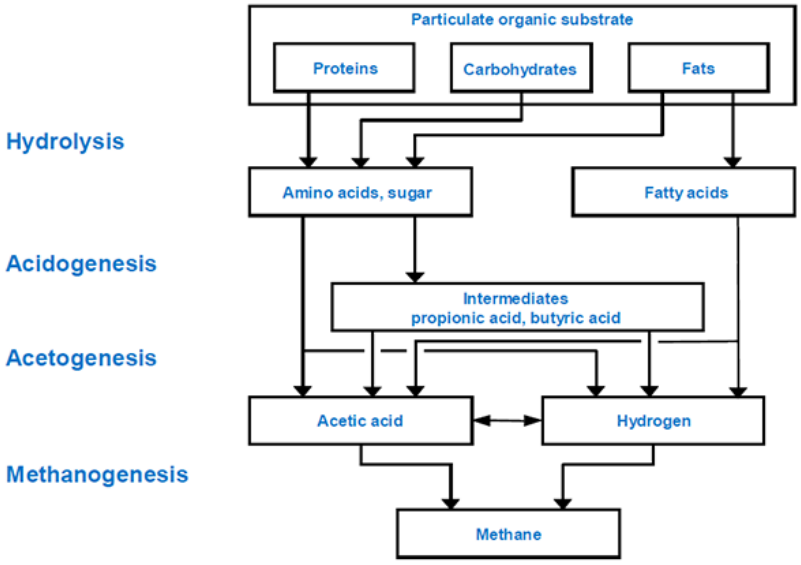

Fig. 2.3 - Degradation steps of anaerobic digestion process (Waste to Energy Research and Technology council, 2014)

Acetogenesis – This step primarily breaks down the products from the former step into hydrogen, carbon dioxide and acetic acid. These conversions are possible only if the partial pressure of hydrogen is low enough to thermodynamically allow the conversion of all the acids. Ostrem (2004) described the acetogenesis stage through the following equations:

$$CH_3CH_2COO^- + 3H_2O \leftrightarrow CH_3COO^- + H^+ + HCO_3^- + 3H_2$$

$$C_6H_{12}O_6 + 2H_2O \leftrightarrow 2CH_3COOH + 2CO_2 + 4H_2$$

$CH_3CH_2OH + 2H_2O \leftrightarrow CH_3COO^- + 2H_2 + H^+$

Methanogenesis – The final waste stabilization stage is the methanogenesis stage. The bacteria responsible for converting the hydrogen and acetic acid (formed in the prior stage) into methane and carbon dioxide are called methanogens. These microbes are anaerobes and very sensitive. A little oxygen at this stage might kill the microbes and methane will not form. Verma (2002) described this final stage with the following equations:

$CO_2 + 4H_2 \rightarrow CH_4 + 2H_2O$

$2C_2H_5OH + CO_2 \rightarrow CH_4 + 2CH_3COOH$

$CH_3COOH \rightarrow CH_4 + CO_2$

Since methane generation from anaerobic digestion decreases pressure on fossil fuels, it also decreases production of another greenhouse gas, CO_2, which results from fossil fuels combustion. Furthermore, the anaerobic digestion also decreases the organic load of the polluted waste stream. Due to its multipurpose benefits, anaerobic digestion has become a common treatment procedure.

Environmental benefits of anaerobic digestion (Zafar, 2008) include:

1. Elimination of odorous compounds.
2. Destruction of pathogens.
3. Deactivation of weed seeds.
4. Production of sanitized compost.
5. Reduction in GHG emissions.
6. Decreased dependence on inorganic fertilizers by capture and reuse of nutrients.
7. Promotion of carbon sequestration
8. Beneficial reuse of recycled water

9. Protection of groundwater and surface water resources.

10. Improved social acceptance

Anaerobic digestion is advantageous in terms of energy in the following ways:

1. Anaerobic digestion is a net energy-producing process.

2. A biogas facility generates high-quality renewable fuel.

3. Surplus energy as electricity and heat is produced during anaerobic digestion of biomass.

4. Anaerobic digestion reduces reliance on energy imports.

5. Such a facility contributes to decentralized, distributed power systems.

6. Biogas is a rich source of electricity, heat, and transportation fuel.

Economic benefits associated with a biomass-to-biogas facility include:

1. Anaerobic digestion transforms waste liabilities into new profit centers.

2. The time devoted to moving, handling and processing manure is minimized.

3. Anaerobic digestion adds value to negative value feedstock.

4. Income can be obtained from the processing of waste (tipping fees), sale of organic fertilizer, carbon credits and sale of power.

5. Power tax credits may be obtained from each kWh of power produced.

6. A biomass-to-biogas facility reduces water consumption.

7. It reduces dependence on energy imports.

8. Anaerobic digestion plants increases self-sufficiency.

Although there are many advantages of anaerobic digestion, the method also poses challenges. A list of disadvantages adopted from Stuart (2013) is mentioned below:

- Environmental Sensitivities

Anaerobic processes are much slower and sensitive to environmental conditions. Successful anaerobic treatment relies on:

pH – A pH close to neutral is favourable for the anaerobic microbes.

*Temperatur*e – Mesophilic and thermophilic temperature must be maintained to promote the growth of microbes.

Salts – Bacteria requires some nutrients for their growth. An excess of nutrient accumulation is detrimental for the microbes. Thus a balance of nutrients is must.

Alkalinity – The acids produced during the digestion process can be toxic to the microbes. Thus enough alkalinity must be present to avoid such situation.

Other materials like heavy metals, ammonia, and sulfate in high amounts can be inhibitory for the anaerobic digestion. Also oxygen after the methanogens are in action can disrupt biogas production.

- Fluctuating Loads

Since the methane production is performed by a series of bacteria, each having their different set of optimum level of parameters, it becomes very difficult for the microbes to perform their work in a fast-changing digester environment. Figure 2-4 shows the different bacteria in an anaerobic environment.

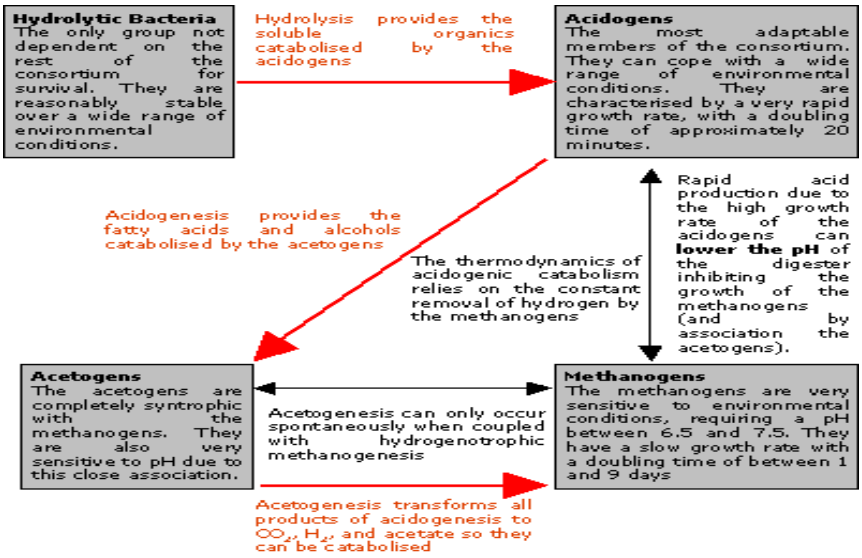

Fig. 2.4 - Interdependence of anaerobes (Stuart, 2014)

- Economic Viability

In some situations, anaerobic treatment fails to be economically feasible. Different processes like stabilization, optimum inorganic nutrient recycle savings on synthetic fertilizers, sale of liquid fertilizer and compost need to be accomplished to make the anaerobic digestion a successful venture for renewable energy.

- Comparatively Low COD Removal

Although anaerobic digestion can reduce the organic load quite efficiently (85 – 90%), it may not enough to be discharged directly to rivers. A secondary method like aerobic treatment or chemical oxidation is often required.

- Required Expertise

Such sensitive treatment requires continuous monitoring. In a developed country, the skill required for such a system often discourages the industrialists.

- Hydrogen Sulfide Production

If sulfur is present in the waste, it will be converted to hydrogen sulfide. Though small in quantity, hydrogen sulfide is extremely corrosive and needs to be stripped out from methane. Moreover, sturdy collection bags are required to combat the corrosive nature.

- Persistence of Heavy Metals

The heavy metals and persistent organic pollutants present in the feedstock cannot be digested by the anaerobes thus more intensive treatments are required after the digestion.

2.7 Biogas

Biogas is defined as the gas produced from the degradation of organic matter by anaerobes in absence of oxygen. The primary composition of biogas is methane and carbon dioxide and trace of other gases like hydrogen sulfide. Biogas has gained a lot of attention in recent years because of its potential to reduce pressure on fossil fuels and combat global warming. The gas can be converted into energy and utilized in gas engines. Biogas is compressible thus can be made useful to power motor vehicles; it can be also upgraded to biomethane for introduction into the local natural gas grid. The composition of biogas is very much dependent on the kind of organic matter used to produce it. Composition of biogas can vary. A typical composition of biogas is shown in Table 2-13.

Table 2.13 – Typical composition of biogas (The Biogas, 2014)

Components	Household waste	Wastewater treatment sludge	Agricultural waste	Waste of Agrifood Industry
CH4 % vol	50 - 60	60 - 75	60 - 75	68
CO2 % vol	38 - 34	33 - 19	33 - 19	26
N2 % vol	5 - 0	1 - 0	1 - 0	-
O2 % vol	1 - 0	< 0.5	< 0.5	-
H2O % vol	6 (at 40 C)	6 (at 40 C)	6 (at 40 C)	6 (at 40C)
Total % vol	100	100	100	100
H2S mg/m3	100 - 900	1000 - 4000	3000 -10000	400
NH3 mg/m3	-	-	50 - 100	-
Aromatic mg/m3	0 - 200	-	-	-
Organochlorinated or organofluorated mg/m3	100 - 800	-	-	-

Biogas Utilization

For better usage of biogas, one needs to desulfurize and dry it. The H_2S proportion can be from 100 to 3000 ppm, depending on the feedstock and the procedures used. H_2S above 250 ppm is never desired to avoid deterioration from corrosive H_2S. Schneider et al. (2002) advocated biological desulfurization. Air containing Sulfobacter oxydans bacteria is injected into raw gas, which oxidizes H_2S. Another procedure of desulfurization is to add ferrous solution in the digester. It binds the sulfur in the waste

into insoluble compounds in the liquid phase, thus combating the production of H_2S in biogas.

It is necessary have about 95% of methane in the biogas for use as pipeline-quality natural gas. CO_2 is present in the biogas and requires removal. Water scrubbing or scrubbing with organic solvents like polyethylene glycol are common methods applied to remove CO_2 (Kapdi et al., 2005). Schulte-Schulze Berndt (2005) encouraged the use of pressure swing adsorption using activated carbon or molecular sieves. Some other less popular methods are chemical washing by alkanol amines like mono ethanolamine or dimethyl ethanolamine (Wünsche, 2008), membrane technologies (Miltner et al, 2009) and cryogenic separation at low temperature (Peterson, 2008). There is often a risk of methane escape while removing CO_2. To enhance efficiency and to decrease global warming, the escaping must be kept at a minimum level.

Moisture is removed from the biogas through coalescing filters and refrigeration dryers. High-efficiency particulate air (HEPA) filters are used to get rid of bacteria and other microorganisms that might threaten human health and equipment (Dumont, 2008). Biogas is preserved at a pressure of 200 to 250 bars in gas bottles to improve the utilization of biogas.

2.8 Anaerobic Digestion of Vinasse

Since the research is on the anaerobic treatment of vinasse, it is worth writing in detail on the similar work performed. Anaerobic treatment is typically defined as a process in which microbes breakdown organic matter into biogas in the absence of oxygen. Anaerobic treatment is an energy-efficient process primarily utilized to treat high-strength industrial wastewaters containing high concentrations of biodegradable organic matter (measured as BOD, COD and/or TSS). Carmen (2006) studied the anaerobic treatment of vinasse from a sugar cane distillery to assess the production of methane and

to determine the technical feasibility of the process. The study was conducted for 10 days at 40^0 C (thermophilic) in a complete mix reactor. A Mathematical Anaerobic Digestion model (MADM) was built and the model implied that a 90 percent removal of BOD is possible producing 1,500,000 cu ft per year of ethanol (38,000,000L per year).

Espana (2012) conducted a study on vinasse produced during the production of hydrous ethanol from sugar cane molasses using a lab scale upflow anaerobic sludge blanket (UASB) reactor. The goal of this study was to figure out the optimum organic loading rate (OLR) for operating a modified upflow anaerobic sludge blanket (UASB) reactor to treat vinasse from sugar cane molasses. The reactor was operated at 30 ± 5^0C (mesophilic) at pH 7 with 2.5L of granulated sludge. 69% of COD was removed at an optimum organic loading rate (OLR) of 17.05 kg COD/m^3-day. The methane content reached 84%, achieving a methane yield of 0.263 m^3/kg COD added. The study also found that the methanogens, namely Methanobacteriales and Methanosarcinales, detected by PCR favored methane production. The chemical analysis performed were COD, total nitrogen (N_T), ammonia nitrogen ($N\text{-}NH_3$), phosphate (PO_4^{3-}), sulfate (SO_4^{2-}), sulfide (S^{2-}) content, potassium content (K^+) and VFA. This experiment confirmed that anaerobic digestion does not remove K^+, which is considered good since the final goal of the study was to produce a product that can be used as a fertilizer. K^+ is nutrient and when applied to land can improve the soil fertility, with the exception of alkaline effluents, which can dissolve soil organic carbon.

Budiyono (2013) worked with batch mode anaerobic digestion of vinasse from the ethanol industry located in Solo, Central Java, Indonesia. The goal of the research was to investigate the kinetics of biogas production. The vinasse was diluted in the ratio of 1:3 (vinasse: water). The author used the Gompertz equation to model biogas production kinetics. He worked with a 5 L batch reactor for the anaerobic treatment and

used 1 L rumen fluid as the source of methanogenic bacteria. Urea was added to the vinasse at different proportions to make four sets of COD/N ratios -400/7, 500/7, 600/7, 700/7. Furthermore, a control of 1436/7 was also used. Biogas was collected by water displacement method. The result was the reactor with COD/N of 600/7 had the best biogas production potential, equal to 109,368 mL/kg COD; maximum biogas production rate was equal to 23,466 mL/kg COD day and λ (minimum time to produce biogas) was 0.803 day. In terms of biodegradability, the COD/N ratio of 600/7 broke down most easily, with the maximum negative k (biodegradability rate constant) value of 0.2876 /day.

Belhadj (2013) worked with vinasse from the production of ethyl alcohol in Kenitra, Morocco with the aim to produce the potential of biogas from anaerobic digestion. He conducted the study in a 0.5 L batch reactor at mesophilic temperature (30 $\pm 2^0$ C) for 16 days with 70% of inoculum obtained from a wastewater treatment plant (source of microbes) and a daily charge of 0.25g SV vinasse; the load increased to 0.50 g SV vinasse when the production of the biogas stopped. In this particular study, the organic load (TS, MS and VS) increased rather than decreased. The author believes it is due to the accumulation of non- biodegradable substrate. However, the study was successful in terms of biogas production. Almost 300 mL of accumulated biogas was extracted from 0.25 g VS and 370 mL of biogas were obtained from 0.5 g VS. Thus, increasing the load increases the biogas potential, mainly due to the breakdown of extra organic matter added. The author suggested chemical pretreatment like ozonation can be performed to increase the efficiency of organic load removal.

Anaerobic digestion, though simple and energy efficient, does not degrade all compounds. Heinze et al. (1995) suggested an idea of combining biological and chemical treatment of vinasse to increase removal efficiency of complex compounds. Chemical treatments like ozonation, sonication and UV can degrade complexes effectively, but

these processes usually increase the cost of operation. Limited chemical treatment followed by biological treatment can effectively remove pollutants at a reduced cost. Keeping this strategy in mind, Siles (2011) worked extensively on a combination treatment of ozonation and anaerobic treatment on vinasse from sugar cane distillery from SOTRAMEG Company in Kenitra, Morocco. In 1 L Pyrex flask, vinasse was treated with oxygen 4 g O_3/m^3 (0ºC and 1atm) for 15 minutes through a porous plate diffuser. The second step was batch mode lab-scale anaerobic digestion via 2 1 L CSTRs maintained at 35^0 C (mesophilic). The innoculum with a concentration of 10g VSS/L was used in the experiment. At the beginning only glucose, lactic acid and sodium acetate was used. Later the pretreated vinasse was added slowly until a concentration of 3g COD/L was reached. The ozonation substantially decreased the phenolic compounds; the relationship between ozone treatment and phenol degradation was direct: the longer the ozonation time, the more breakdown. Ozonation did not play any role in TOC or COD breakdown but it improved the biodegradability of the vinasse. Furthermore, the methane generation potential increased with the pretreatment.

Martin (2002) executed a comprehensive study on different kinds of pretreatment of vinasse followed by anaerobic digestion. The waste was obtained from vinasse produced from ethyl alcohol. Four types of vinasse were treated at 35^0 C – un-pretreated vinasse, vinasse pretreated with ozone, vinasse pretreated with ozone and UV and finally vinasse pretreated with ozone, UV and titanium oxide. The goal was to develop a kinetic model to observe the effects of the mentioned pretreatments on vinasse methane production and biodegradability. In terms of biodegradability, the vinasse pretreated with ozone and UV in presence of titanium oxide had the best result. Furthermore, it had a positive effect on the rate of methane production. The other pretreatments had almost no effect on the biodegradability.

Wilkson (2011) conducted a study as part of his master's thesis on anaerobic treatment of thin stillage at a variety of organic concentrations and food-to-microorganisms ratios by Down-flow Fixed Film Reactor. 85% of COD removal was achieved in 5 days with an organic loading rate of 7.4 g TCOD/L/d.

Previous studies were mainly focused on methane generation and building the model for methane. Only one vinasse was studied in each work. To my knowledge, there was no research that worked with six different types of vinasses. Also, modelling the liquid parameters in terms of temperature and compositions were also not seen in any of the literatures that I have reviewed. My research emphasizes on the development of regression models for predicting COD or BOD on anaerobic treatment of vinasse. Six different kinds of vinasses (three synthetic and three real) were operated on mesophilic temperatures (30 ^{0}C, 35 ^{0}C and 40 ^{0}C) and a list of water quality parameters were measured using the Standard procedures over the entire batch time.

Chapter 3

Material and Methods

3.1 Introduction

This chapter discusses the experimental design, reactor building and setup procedure, reactor monitoring, and procedures to measure methane percentage and water quality parameters: pH, biochemical oxygen demand (BOD), chemical oxygen demand (COD), pH, conductivity, total dissolved solids (TDS), total suspended solids (TSS), volatile suspended solid (VSS), ammonia-nitrogen (NH3-N), Phosphorus (P) , Potassium (K), and Sulfur (S) from 18 stimulated lab scale anaerobic reactors at three different temperatures.

3.2 Design of Experiment

The first step of conducting a research is to design the experiment. An effective experimental design has the ability to predict future responses. Initially the scope of the project was to conduct research on a wide range of combinations of vinasse so that vinasse from every feedstock was covered. Wilkie (2000) compiled composition data from a wide range of vinasse from different sources and countries. Based on Wilkie's work, 18 combinations at 3 different temperatures were picked. The goal was to cover the entire range of vinasse composition and its potential to produce methane. Unfortunately, few of the combinations worked. One particular reason was that certain elements at an excessive level can be toxic to the methanogens. Furthermore, the importance of pH adjustment was not understood at the initial stage of the research. The temperatures that were picked were 50, 55 and 60 ^{0}C. Methane generation is maximum at thermophilic temperature. In our case, the high temperature was not the optimum situation for the methanogens. Thus the initial design was not followed. Six compositions of vinasse that generated methane were run at three mesophilic temperatures (30, 35, and 40^{0} C).

3.2.1 Vinasse Composition

Variations in methane generation and water quality parameters with time are very much dependent on the constituents of vinasse. Depending on the feedstock, that is whether the waste is produced from wheat, barley, milo, sugarcane or any other food crops, the vinasse composition will vary. The composition of this by-product also varies according to the conditions of the fermentation and distillation process and the raw materials used.

The primary vinasse constituents of environmental interest are Chemical Oxygen Demand, nitrogen, phosphorous, potassium, and sulfur. The parameters were chosen based on the capability of conducting the research and influence on the environment. Depending on the ethanol feedstock (sugar crops, starch crops, and cellulose-based ethanol), the composition of vinasse varies. Therefore, in the experimental design, the primary constituents of environmental interest - chemical oxygen demand (COD), nitrogen (N), phosphorus (P), potassium (K) and sulfur (S) - were varied over the ranges observed in vinasse, as described in the literature (Wilkie *et al.*, 2000). Synthetic vinasse was made from glucose, ammonia, phosphoric acid, potassium hydroxide, and calcium sulfate, in the amounts shown in Table 3-1. For our experiments, we also obtained real vinasse from White Energy, Texas and MGP Ingredient, KS.

Table 3.1- Different Amount of Components added in the six vinasse compositions.

Comp.	Low or high COD	Real or synthetic	Synthetic Vinasse Composition (g of constituents per 6.8L of vinasse)					Real Vinasse Comp.
			COD	N	P	K	S	
			$C_6H_{12}O_6$ (g)	NH_3 (g)	H_3PO_4 (g)	KOH (g)	H_2SO_4 (g)	
1	Low	Synthetic	14.625	0.44	0.156	0.336	0.289	0
2	Medium		62.78	0.44	0.02	0	0	0
3	High		204	12.67	6.49	0	0	0
4	Low	Real	30	0	0	0	0	300
5	High		0	0	0	0	0	3.5L
6	Medium		0	0	0	0	0	4.0L

The different water quality parameters of the vinasse before adding the sludge and after adding the sludge were measured. For our experimental design, we considered the initial values after adding the sludge. Sludge adds a lot of COD, N, P, K, and S to the composition. The composition of sludge is not constant. Depending on the time and kind of waste received in the treatment plant, the composition of sludge will vary. The following table depicts the measured values of the different parameters after adding the sludge. In Table 3-2 only the compositions at 30°C has been shown. The initial values of the parameters were pretty consistent at the different temperatures with very little deviation.

Table 3.2 – Values for different water quality parameters for the 6 vinasse compositions at 30°C.

Composition	Real or synthetic	Strength of COD	COD (g/L)	N(g/L)	P(g/L)	K(g/L)	S(g/L)
1	synthetic	low	2.53	0.19	0.16	0.07	0.08
2		medium	9.84	0.22	0.13	0.02	0.12
3		high	30.49	19.06	1.17	0.01	0.15
4	real	low	23.95	40.10	0.67	0.08	0.44
5		high	32.17	28.64	1.39	0.17	0.62
6		medium	27.11	23.69	1.14	0.15	0.62

The other constituents were measured and added to the reactor. In addition, 1L of trace mineral solution (TMS) was added for the synthetic combinations to provide nutrients to the microbes. Real vinasse has substantial nutrients thus additional TMS solution was not required. The composition of TMS solution was adopted from Revised Anaerobic Mineral Medium (RAMM) (Shelton and Tiedje, 1984). A modification was made based on the availability of the components and nature of vinasse: the article had sodium and potassium as nutrients. Sodium in excess amount can be toxic and potassium is already added in the synthetic vinasse. Thus, these two nutrients were eliminated in our experimental design. Table 3-3 lists the chemicals and amounts used in TMS preparation.

Table 3.3 - Composition of TMS solution used in the synthetic vinasse

Salt	**Concentration, mg/L**
Calcium Chloride ($CaCl_2.2H_2O$)	75
Magnesium Chloride ($MgCl_2.6H_2O$)	100
Ferrous Chloride ($FeCl_2.4H_2O$)	20
Trace Metals	
Manganese (ii) Chloride ($MnCl_2.4H_2O$)	0.5
Boric Acid (H_3BO_3)	0.05
Zinc Chloride ($ZnCl_2$)	0.05
Cupper Chloride ($CuCl_2$)	0.03
Cobalt Chloride ($CoCl_2$. 6 H_2O)	0.5
Nickel Chloride ($NiCl_2$. 6 H_2O)	0.05

5 g of sodium carbonate (buffer) was added to the synthetic compositions to buffer the pH around 7 to 8.5, which is good for the microbial community. The pH was adjusted by adding HCl or NaOH. The desired pH ranges from 7 to 8.5. Anaerobic digester sludge obtained from the Fort Worth Village Creek Wastewater Treatment Plant was used to seed to each reactor (10 – 12% by volume).

Some combinations of vinasse required alkali treatment, which is raising the pH of the vinasse composition to pH 12 for 24 hours using sodium hydroxide prior to anaerobic treatment, then decreasing the pH around 7 to 8 using hydrochloric acid after 24 hours of raised pH. Alkali treatment was conducted on the vinasses obtained from White Energy. Alkali treatment tends to increase the activity of microbes on real vinasse combinations. The pre-treatment provides a contact surface and a rupture in the structure of the lignin and cellulose fibers, thus facilitating the hydrolysis to simple sugars (Kuhad

et al., 1990; Kuwahara *et al,.* 1984; Bon et al., 2008). The other real vinasse composition was hybrid, meaning it had some glucose in it. Since alkali treatment was not performed on synthetic compositions, it was not performed on the hybrid one either.

After the sludge was added, each reactor was filled to 6.8L with deionized water and for the last time pH was measured. If required, we adjusted the pH again to the desired range.

3.2.2.Temperature

Temperature plays an important role in the generation of methane gas and degradation of the waste. It is expected that higher the temperature, the sooner we obtain the peak concentration of methane for a combination. Six combinations of vinasse at 30, 35 and 40^0 C were run to predict the methane generation and water quality parameters over time.

3.3 Reactor Experimental Set-Up

3.3.1 Vinasse Collection

There were essentially two types of vinasse used in the experiment - real and Synthetic. Real vinasse was collected from three facilities: White Energy, Plainview, TX; White Energy, Hereford, TX; and MGP Ingredients, KS. White Energy in both the plants produced ethanol from corn and milo. Composition nos.5 and 6 were made from White Energy vinasse. Only different amounts were used: 4 L in Composition 5 and 3.5 L in Composition 6. These went through alkali treatment to increase the microbial activity on the organic composition of vinasse. No TMS solution was required because real vinasse is high in nutrients. No buffer was used for these compositions either. There were no effects of buffer on these compositions. Extra sodium can be toxic to the microbes. Thus, buffer was eliminated in these compositions.

Another source of real vinasse was MGP Ingredients. Their vinasse was not like the thin stillage in White Energy: it was more concentrated. Probably the thin stillage went through evaporation. It is common practices in many industries to air dry their waste to make it easier to handle. This particular vinasse was used to make Composition 4, in which some glucose was added (30 g of real vinasse from MGP and 30 g of glucose). This particular Composition (Comp no. 4) is often termed as hybrid because of its unique component (both glucose and real vinasse were added). Moreover 25 – 30 g of sodium bicarbonate was used to buffer the solution. It helped to stabilize the composition, which was essential for an effective run. Though sodium bicarbonate was added, regular dosages of sodium hydroxide and sometimes hydrochloric acid had to be added to adjust the pH. No alkali treatment was conducted for the hybrid because the microbes would not have trouble in degrading the glucose. TMS solution was not added to it because the composition had the real concentrated vinasse, which was high in nutrients.

The synthetic compositions had glucose to provide COD, ammonia to provide N, potassium hydroxide to provide K, phosphoric acid to provide P, and sulfuric acid to provide S at various amounts. Compositions 1, 2 and 3 were synthetic. TMS solution was added to these compositions to provide extra food for the microbes, as the synthetic is not rich in other nutrients. 25 g of sodium bicarbonate was added as buffer. No alkali treatment was required for the synthetic compositions, as glucose is simple to degrade.

Then in each reactors, both real and synthetic, 900 mL of sludge from Village Creek was added and then DI water was added to make it 6.8 L of liquid.

3.3.2 Reactors

12-L borosilicate glass lab-scale reactors (VWR part#22877-082, shown in Figure 3-1) were filled with vinasse of different compositions and operated at 3 different mesophilic temperatures (30, 35, 40°C), via placement in constant-temperature rooms.

The reactors, though 12 L in size, had the capacity to mix 6 to 7 L of liquid. Magnetic stirrers were used to provide continuous mixing. The reactors were designed to optimize maximum cell growth and prevent and cell damage from crushing. Silicon sealant was used to ensure that the reactors were air-tight.

Fig. 3.1- ProCulture® Glass Spinner Reactor with Angled Side Arms

There were three openings on each reactor. One of the side arm openings was connected to the gas bag to collect and measure the percentage and volume of the generated gas. Gas and media handling fittings, shown in Figure 3.2 below, with 3.2 mm (1/8'') and 6.4 mm (1/4'') inlets with two long tubes from VWR International were used to connect with gas bags.

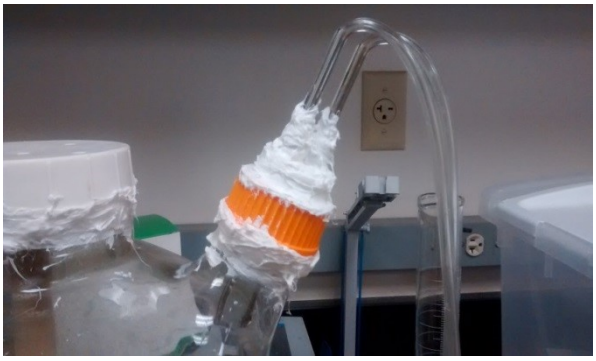

Fig. 3.2 - Gas fittings

The cap of the other arm was replaced with septa. The septa was used to draw vinasse for water quality monitoring and also to adjust pH by injecting HCl or NaOH. The septa, shown in Fig. 3.3, was butyl rubber (thickness 0.125 inch) purchased in sheet locally from a website (http://www.rubbersheetroll.com/butyl-rubber.htm). It was cut from UTA workshop to the shape that fits the cap. The septa was used because it has long durability and flexibility and there is no possible damage from gas and puncturing through syringes.

Fig. 3.3 - Septa

The large opening in the center of the reactor was used to insert the magnetic stirrer. It is very important to have a homogenous mixture for the vinasse analysis. Thus a stirrer capable to handle 6.8 L of vinasse was adjusted from 2 – 2.5 rpms range.

An essential task of the experiment was to provide a gas-tight environment. It was accomplished through sealing the openings with Teflon tape and silicon sealants. The reactors were then left alone for a couple of hours to be dried. Different tests were conducted on the reactors to locate any leakage. The reactors were inserted in a large bucket of soap water. If there is a leakage, chain of bubbles will rise from that location. After the leak test, the reactors were put through pressure tests. The reactors were connected to an U-tube manometer for 1 or 2 days. A head difference of 0.3 – 3 inches

was desired. If the pressure difference was above the range, additional sealing was conducted.

One opening of the reactor was connected to an air-tight gas-collecting bag (22-L Cali-5-Bond™ Bag, Calibrated Instruments, Inc.), as shown in Figure 3-4. The goal was to monitor the composition and volume of the gas.

Fig. 3.4 - Reactors connected to the gas bags.

The various fittings used in the reactor build up are shown in Figs. 3-5 – 3-8.

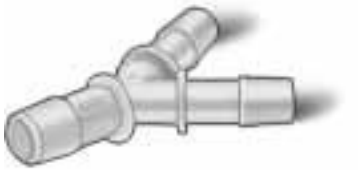

Fig. 3.5 - Single-barb 'Y' for joining the 2 flexible tubes (McMaster part # 5117K61)

Fig. 3.6 - Expansion joint, from 1/8 to ¼" (McMaster part # 5117K61

Fig. 3.7 - 2-Way Valve, OD = ¼" (US Plastic part # 17220)

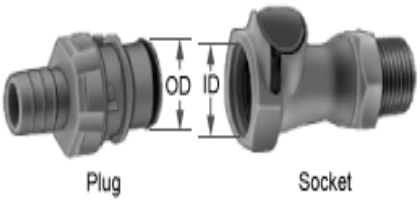

Fig. 3.8 - Quick-Disconnect Tube Couplings (McMaster part # 5012K58)

3.4 Reactor Monitoring

In order to maintain an anaerobic sludge with a high metabolic activity, it was necessary to maintain favorable environmental conditions. Among these factors, the most important ones were temperature, pH, the absence of toxic materials and the availability of nutrients. The methanogens are very sensitive to adverse environmental conditions and for this reason it was always attempted to maintain optimal conditions for these bacteria. The desirable pH range for the reactors was from 6 – 9. It was not possible to install a pH adjuster to our set up. Thus it was done manually. During the initial stages known as the hydrolysis and acidogenesis phase of microbes, the gas production was high and there was a drastic drop in pH. The pH needed to be adjusted every 3 hours. If the pH dropped below 5 for any reason, the process of anaerobic digestion as a whole may fail due to "souring" of the reactor contents. pH adjustment was crucial in the preliminary phase. Later, the pH is pretty stable and monitoring it once a day is enough. During the initial stage, gas bags were changed frequently too (sometimes 3 bags per

day). The reactors were observed for leakage. If necessary, caps were recoated with DAP silicon sealant. Reactors were operated until methane generation ceased.

3.4.1 Sample Extraction

Samples were extracted using syringe, as shown in Fig. 3-9. The 30 mL luer-Lok PK56 Syringe (Product Number BD3028321) and needles (Product Number 305129) were ordered from BD Medic. Based on the water quality parameters that needed to be measured, almost 20 to 25 mL of samples were withdrawn from the reactors every day. Another research student analyzed the microbes in the vinasse.

(a) (b)

Fig. 3.9 – a.) Sample Collection (b) Syringe

3.4.2 Sample Storage

Samples were stored in high performance 15 mL centrifugal tubes with plug caps made of polypropylene, shown in Fig. 3-10. The tubes were purchased from VWR International ((VWR Catalog Number 89039-668). Most of the time, samples were analyzed the same day they were collected. However, sometimes they needed to be refrigerated (at 4^0 C) to be used later. The tubes which are sterile can be easily refrigerated.

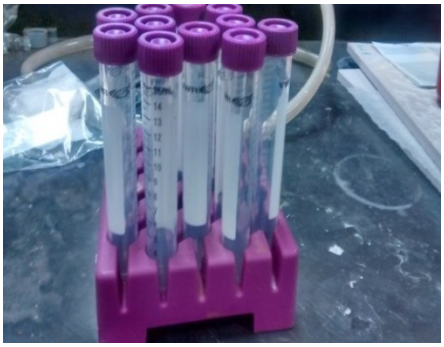

Fig. 3.10 - Empty tubes in the stand

3.5 Analytical Methods for Biogas Measurements

Biogas was collected in air-tight bags and the composition was measured with the help of LANDTECGEM 2000 PLUS with infrared gas analyzer (±3% accuracy). The main components of the gas that were measured are % Methane (CH_4), % Carbon Dioxide (CO_2), and %Oxygen (O_2). Trace gases like Hydrogen Sulfide (H_2S), Carbon monoxide (CO) and Hydrogen (H_2) were also recorded. Gas volume was measured by pumping gas out of the collection bag through a standard SKC grab air sampler (SKC Aircheck sampler model 224-44XR) at 1.0 L/min connected to a calibrator (Bios Defender 510M). This provided a minute by minute gas pumping rate. The gas bags were measured based on the production. At the beginning of the treatment, gas production is high and for certain combinations sometimes 3 to 4 bags needed to be changed in a single day. This was more seen in 40^0 C reactors. Then after couple of days of gas production, the reactors come to a lag period when the gas bags remain empty for many days. At 30^0C, the lag period could reach 25 to 30 days. The gas produced after this stagnant period is smaller in quantity but high in methane percent. It is during this time the peak methane percent is achieved.

3.6 Analytical Methods for Water Quality Parameters

The vinasse parameters were chosen keeping in mind the goal of model development. It was not an easy task to choose the vinasse parameters from dozens of parameters. Furthermore, there was a challenge of choosing the methods for monitoring the parameters. Since the experiment was a batch reactor and no additional vinasse was added during the treatment time, vinasse samples had to be extracted wisely, using minimal volumes. The time required to accomplish the experiment was also an important consideration in determining sampling frequency. The ability of the civil engineering department and the cost to execute the experiments were other criteria.

Vinasse was extracted almost daily in the preliminary stage to conduct tests. It was observed that the water quality parameters were also dependent on biogas formation. There are substantial changes in the water quality parameters for the first couple of days; however, the parameters are almost constant during the lag period. Changes became dramatic after the stagnant period was over. Some parameters were tested at least 5 times a week (like COD, BOD) and the rest of the parameters that did not make significant changes thus were not tested as frequently.

Water quality parameters, including biochemical oxygen demand (BOD5), chemical oxygen demand (COD), pH, total dissolved solids, conductivity, ammonia-nitrogen, phosphorus, potassium and sulfate - sulfur, Total Suspended Solids, Volatile Suspended Solids, were measured using Standard Methods for the Examination of Water and Wastewater, probes and spectrophotometer, as appropriate. Table 3.4 shows the methods used to measure each parameter. Liquid samples of volume 20-25 ml were also collected via syringe every alternate day and refrigerated for DNA extraction for microbe identification.

Table 3.4 - Measurement Methods for Leachate Parameters.

Leachate Parameters	**Methods**
Biochemical Oxygen Demand-5 (BOD_5)	Standard Method 5210 B
Chemical Oxygen Demand (COD)	Standard Method 5220 C
Total Suspended Solids (TSS)	Standard Method 2540 D
Volatile Suspended Solids (VSS)	Standard Method 2540 E
pH, Conductivity and Total Dissolved Solids (TDS)	IntelliCAL probes from Hach
Ammonia-Nitrogen (NH_3-N)	10205 HR TNTplus from Hach
Reactive Phosphorus	10209 Spectrophotometer HR, TNTplus 844 from Hach
Potassium	8049 Spectrophotometer Powder Pillows from Hach
Sulfate	10227 Spectrophotometer HR TNTplus 865

3.6.1 pH

In chemistry, pH is defined as a measure of the amount of free hydrogen ions in water. Specifically, pH is the negative logarithm of the molar concentration of hydrogen ions.

$$pH = -\log[H+]$$

Since pH is measured on a logarithmic scale, an increase of one unit indicates an increase of ten times the amount of hydrogen ions. For this study, the pH of the vinasse samples was immediately measured using a pH probe (IntelliCAL, Hach) on a daily basis. In an anaerobic study, pH is a good indicator of the stage of degradation. The

concern in the anaerobic digestion process is that equilibrium has to be maintained between acid- and methanogenic fermentation. Otherwise methanogens will not form and methane generation will be hampered. The intermediates formed during the conversion of organic matter are mostly acid. Thus during the acetogenesis stage the pH tends to drop. If equilibrium is maintained, the conversion of hydrolyzed products to the final products is substantially complete. In the methanogenesis stage, the acid is consumed and pH will increase. At the final stage, the pH becomes stabilized indicating that the reaction is essentially complete.

Fig. 3.11- pH meter probe

3.6.2 Biochemical Oxygen Demand

Biochemical oxygen demand (BOD) is defined as the amount of dissolved oxygen required by aerobic organisms in a body of water to break down organic material present in a given water sample at certain temperature over a specific time period (in our case 5 days). This is not a precise quantitative test, although it is widely accepted as an indication of the organic quality of water. The BOD_5 value is most commonly expressed in milligrams of oxygen consumed per liter of sample during 5 days of incubation at 20 °C and is often used as an indicator of the degree of organic pollution of water. The BOD was determined by following instructions from Standard Methods 5210 B. Because most

samples of wastewater will have a BOD higher that the amount of oxygen available in the BOD bottle during the incubation period, the samples must be diluted. The first step was to prepare the required amount of dilution water (1 ml of each of phosphate buffer, $MgSO_4$, $CaCl_2$, and $FeCl_3$ and finally added deionized water to mark 1 L). The dilution water was aerated for 2 hours. The source of microorganisms was polyseed (InterLab Supply). The seed control bottles with different dilutions of 15, 20, 25, and 30 mg/l were prepared along with glucose-glutamic acid standard check on a regular basis for quality control. A blank with only dilution water was run to compare the strength of microbes (if any) in the water. 4 – 10 mL (depending on the kind and the stage of vinasse) of sample were added to the 300mL flask, 4 mLof seed water and then filled to neck with dilution water so that insertion of the stopper would displace all air, leaving no bubbles. The initial and final (after 5 days) DO was determined using the IntelliCAL probe (Hach). The DO meter and the bottles are shown n Figure 3-5. The BOD calculations for each bottle meeting the 2 mg/l minimum DO depletion and the 1 mg/l residual DO were as follows:

BOD, mg/L = $\frac{(D1-D2)-(B1-B2)f}{P}$

Where,

f = (volume of seed in diluted sample)/(volume of seed in seed control)

D1 = initial DO of diluted sample immediately after preparation, mg/l

D2 = final DO of diluted sample after incubation at 20 °C, mg/l

P = decimal volumetric fraction of sample used

B1 = DO of seed control before incubation, mg/l

B2 = DO of seed control after incubation, mg/L

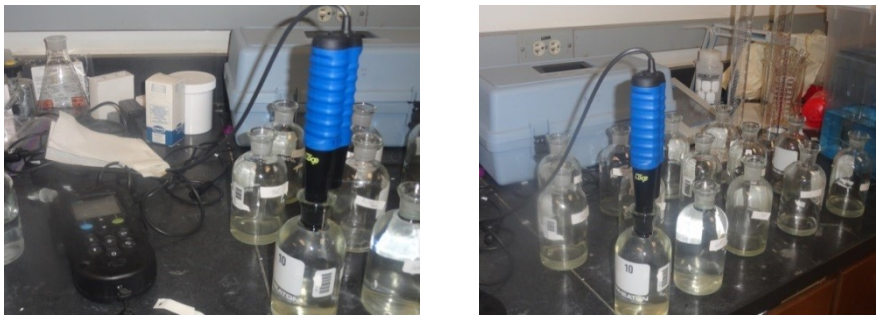

Fig. 3.12 – Dissolved oxygen probe and meter

If vinasse with high BOD levels is discharged into a stream or river, it will enhance bacterial growth in the river. This in turn will replenish oxygen levels in the river. The oxygen may diminish to levels that are detrimental for most fish and many aquatic insects.

3.6.3 Chemical Oxygen Demand

Chemical Oxygen Demand (COD) is the standard method for the indirect measurement of the amount of pollution (that cannot be oxidized biologically) in a sample of water. The COD test procedure is based on the chemical decomposition of organic and inorganic contaminants, dissolved or suspended in water. The result of a chemical oxygen demand test indicates the amount of water-dissolved oxygen (expressed as parts per million or milligrams per liter of water) consumed by the contaminants, during two hours of digestion from a solution of boiling potassium dichromate. The higher the chemical oxygen demand, the higher the amount of pollution in the test sample.

COD does not differentiate between biologically available and inert organic matter: it is a measure of the total quantity of oxygen required to oxidize all organic material into carbon dioxide and water. COD values are always greater than BOD values since COD includes both biological and chemical constituents, but COD measurements can be made in a few hours while BOD measurements take five days. The ratio of

BOD/COD is very important. It helps to determine a stage when anaerobic digestion is no more capable of degrading the complex organic content of vinasse.

Standard Method 5220 C was followed while testing for COD. 2 mL of samples after appropriate dilutions were added to vials containing premixed digestion solution. The mixture was capped and inverted to mix the contents. Finally the vials were placed into a preheated digester for 2 hours at 150 °C, as shown in Figure. After two hours the vials were allowed to cool in a room temperature for about 30 minutes and then absorption of each sample at 620 nm was measured using a Spectronic-D spectrophotometer, as displayed in Figure 3-6. A calibration curve was prepared at the very beginning incorporating all the ranges of the COD used in the experiment using 6 standards from potassium hydrogen phthalate solution. COD was determined using the best fit line from the calibration curve.

(a) (b)

Fig. 3.13 – a) Spectrophotometer b) Digester

3.6.4 Total Suspended Solids (TSS) and Volatile Suspended Solids (VSS)

An increase of TSS causes a water body to lose its ability to support a diversity of aquatic life. Suspended solids absorb heat from sunlight, which increases water temperature and subsequently decreases levels of dissolved oxygen (warmer water holds less oxygen than cooler water). Trout and stoneflies, which are cold water species,

are especially sensitive to changes in dissolved oxygen. Photosynthesis also disrupted, since less light penetrates the water. Plants and algae produce less oxygen thus there is a further drop in dissolved oxygen levels.

To measure the TSS, burned filters were used to increase the porosity of the filters. They were prepared by placing the filters using forceps into filtration apparatus and then applying vacuum. The filter was washed with approximately 20 ml of distilled water for 3 times. The washed filter was removed and placed in an aluminum pan and for an hour dried in an oven at 103 to 105 °C. Finally the filters were ignited in a muffle furnace at 550 °C and placed in a desiccator until ready to use.

Standard Method 2540 D and Standard Method 2540 D were applied to test for TSS and VSS. The filter with aluminum pan before analysis was weighed and then the filter paper was placed in a set up as shown in Figure. A little water was added to open the pores of the filter. Then a measured volume of the diluted sample was added to the filter. The filter paper was then taken out and placed in the pan using the forceps and dried in an oven at 103 to 105 °C for one hour. The weight of the filter and the pan was taken again. Then the filter paper was ignited in a muffle furnace at 550 °C for 15 – 20 minutes. The filter paper and pan were measured again. The following equations were used to calculate TSS and VSS.

Total Suspended Solids, mg/L = (A-B) x 1,000/C

Where:

A = weight of filter and dish + residue in mg

B = weight of filter and dish in mg

C = volume of sample filtered in mL

Volatile Suspended Solids, mg/L = (A-B) x 1,000/C

Where:

A = weight of residue + filter and crucible in mg from Total Suspended Solids test

B = weight of residue + filter and crucible in mg after ignition

C = volume of sample filtered in mL

3.6.5 Conductivity and Total Dissolved Solids (TDS)

Conductivity is a measure of the ability of water to pass an electrical current. Conductivity in water is affected by the presence of inorganic dissolved solids such as chloride, nitrate, sulfate, and phosphate anions (ions that carry a negative charge) or sodium, magnesium, calcium, iron, and aluminum cations (ions that carry a positive charge). Organic compounds like oil, phenol, alcohol, and sugar do not conduct electrical current very well and therefore have a low conductivity when in water. Significant changes in conductivity could then be an indicator that a discharge or some other source of pollution has entered a stream.

Total dissolved solids (TDS) are a measure of the combined content of all inorganic and organic substances contained in a liquid in molecular, ionized or micro-granular (colloidal sol) suspended form. Generally the operational definition is that the solids must be small enough to survive filtration through a filter with two-micrometer (nominal size, or smaller) pores. This parameter is more significant in freshwater.

Conductivity has a direct relationship with total dissolved solids (TDS). Total dissolved solids (in mg/l) in a sample can be estimated by multiplying conductivity (micromhos per centimeter) by an empirical factor, which ranges from 0.55 to 0.9, depending on the soluble components of the water and on the temperature of measurements (Standard Methods). For this study, the conductivity and TDS measurements were obtained using single probe (IntelliCAL probe, Hach) as shown in Figure 3.7. The meter provided the readings for conductivity (µs/cm) and TDS (mg/l) simultaneously.

Fig. 3.14 – Probe to measure TDS and Conductivity

3.6.6 Ammonia Nitrogen (NH_3 – N)

Nutrients such as phosphorous and nitrogen are essential for the growth of algae and other plants. Aquatic life is dependent upon these nutrients, which usually occur in low levels in surface water. Excessive concentrations of nutrients, however, can accelerate aquatic plant and algae growth. Bacterial respiration and organic decomposition can use up available dissolved oxygen, depriving fish and invertebrates of available oxygen in the water (eutrophication).

Ammonia nitrogen was measured in accordance with10205 HR TNT plus from Hach. This is a Salicylate method in which after appropriate dilutions, 0.2 mL of sample is added to the vial. The vial cap is flipped to the other side to face the reagent side to the vial. The vials are shaken couple of time to encourage thorough mixing. After 15 minutes absorption is measured in a spectrophotometer (DR 2800) with 690 nm wavelength. Figure 3-8 shows the spectrophotometer and the test cells used in the experiment.

The mechanism applied in this test is that ammonium ions react at pH 12.6 with hypochlorite ions and salicylate ions in the presence of sodium nitroprusside as a catalyst to form indophenol. The amount of color formed is directly proportional to the ammonia nitrogen present in the sample (HACH manual).

(a) (b)

Fig. 3.15 - a.) Spectrophotometer b.) Ammonia and Phosphate vials

3.6.7 Reactive Phosphorus (PO4–P)

Phosphorus is an essential element for plant life, but when there is too much of it in water, it can speed up eutrophication (a reduction in dissolved oxygen in water bodies caused by an increase of mineral and organic nutrients) of rivers and lakes. Soil erosion is a major contributor of phosphorus to streams. Bank erosion occurring during floods can transport a lot of phosphorous from the river banks and adjacent land into a stream.

Reactive phosphorus or Orthophosphate was measured in this experiment and the method 10209 Spectrophotometer HR, TNT plus 844 from Hach was applied. From a diluted sample, 0.5 mL is pipetted out and added to the vial. 0.2 mL of Reagent B is added to the vial and then capped with Dosi C. Finally the vials are thoroughly mixed and the absorbance is measured after 10 minutes of reaction time.

The reactive or orthophosphate ions react with molybdate and antimony ions in an acidic solution to form an antimonyl phosphomolybdate complex, which is reduced by ascorbic acid to phosphomolybdenum blue. Test results are measured at 890 nm (HACH manual).

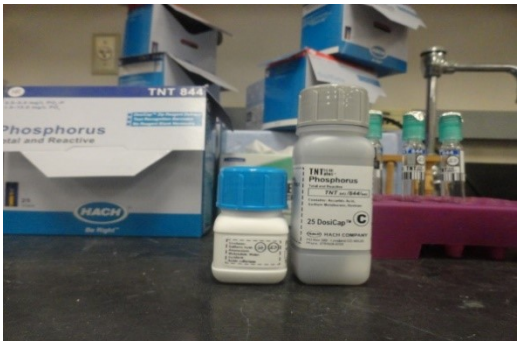

Fig. 3.16 – Reagents used to measure Orthphosphate.

3.6.8 Sulfate - S

Recent studies have shown that excessive sulfate in drinking water might cause diarrhea. It is an important constituent of vinasse thus has been regularly measured following 10227 Spectrophotometer HR TNTplus 865.

2 mL of diluted samples were pipetted into the vial and quickly one spoonful of reagent A was added. The mixture was shaken for 1 minute and then after 30 seconds the vial was inserted into the spectrophotometer (DR 2800).This is known as turbidimetric method where sulfate ions in the sample react with barium chloride in aqueous solution and form a precipitate of barium sulfate. The resulting turbidity was measured photometrically at 880 nm (HACH manual).

Fig. 3.17– Reagents used to measure Sulfate - S

3.6.9 Potassium (K)

Potassium is a dietary requirement for nearly any organism. Potassium salts may kill plant cells because of high osmotic activity. Potassium is weakly hazardous in water, but it does spread pretty rapidly, because of its relatively high mobility and low transformation potential. Potassium toxicity is usually caused by other components in a compound, for example cyanide in potassium cyanide.

Potassium was tested in accordance of 8049 Spectrophotometer Powder Pillows Method. 25 mL of diluted sample was added to a cylinder. Then Potassium 1 and Potassium 2 reagents were added subsequently to the cylinder. Then the cylinder was stoppered and inverted a couple of times to encourage mixing. The contents of one Potassium 3 Reagent Pillow were added after the solution cleared. Again the cylinder was stoppered and mixed for 30 seconds. A white turbidity would form if potassium was present. A blank was prepared with only the sample and none of the reagents were added. After 3 minutes 10 mL of the solution was poured into a sample cell and inserted into the spectrophotometer.

This method is also known as the Tetraphenylborate method for powder pillows. Potassium in the sample reacts with sodium tetraphenylborate to form potassium tetraphenylborate, an insoluble white solid. The amount of turbidity produced is proportional to the potassium concentration. Test results are measured at 650 (HACH manual). The powder pillows and the sample cell used are shown below in Figure 3-18.

Fig. 3.18 – Reagents to measure potassium

3.7 Multiple Linear Regression Modeling

Statistical Analysis Software (SAS) was used to conduct Multiple Linear Regression (MLR) on each response variable (water quality parameters), using an equation of a form similar to that shown in Eq. 1 below.

$$Y = \beta_0 + \beta_1 COD + \beta_2 N + \beta_3 P + \beta_4 K + \beta_5 S + \beta_6 T + \beta_7 t + \varepsilon \quad \text{(Eq. 1)}$$

where

Y = Water Quality Parameters (pH, BOD, COD, and NH_3-N, P, K, S)

βs = Parameters to be determined using SUR

COD = initial COD concentration of vinasse

N = initial nitrogen concentration of vinasse

P = initial phosphorous concentration of vinasse

K = initial potassium concentration of vinasse

S = initial sulfur concentration of vinasse

T = Temperature, °F

t = Time

ε = Model error term

Furthermore, the volume and percentage of methane are measured over time at different temperatures. The cumulative methane gas is calculated by the following equation:

$$V = L_o(1-e^{-kt}) \qquad \text{(Eq. 2)}$$

Or can be re-written as,

$$\ln(1-V/L_o) = -kt \qquad \text{(Eq.3)}$$

where,

V= Cumulative volume of methane per liter of vinasse (mL/L),

L_o = Ultimate methane potential (mL/L),

k = first-order methane generation rate constant (day-1),

t = time (days).

K and L_o were computed from Eq. using Simple Linear Regression (SLR) analysis using SAS software.

Chapter 4

Results and Discussion

The chapter discusses the results of methane generation and water quality analyses for three different temperatures. Later the chapter elaborates on the development of two models using multiple linear regression. The goal of the models is to predict K_{COD} and K_{CH4} at three different temperatures and six different compositions.

4.1 Methane Results.

The methane and oxygen data (in percentage) for the six compositions at three different temperatures are depicted in graphs (Figure 4.1 to Fig 4.19) along with the pH. For some reactors it took almost 50 days before the highest methane concentration was obtained. The reason was that the microbes known as Methanogens, responsible for the generation of methane gas, become active in the final stage after hydrolysis, acidogenesis and acetogenesis. At the methanogenesis stage, microorganisms convert the hydrogen and acetic acid formed by the acid formers to methane gas and carbon dioxide (Verma, 2002). Another reason is that the experiments were conducted in batch reactors where vinasse was added once at the beginning of operation. Thus the acclimation of the digester sludge to the vinasse took a long lag time. In future work, continuous flow reactors can be tested instead of batch reactors which would eliminate the lag time, except for the very beginning of operation, and would be a more representative of a real-world scenario. Depending on the temperature and waste composition, methane generation can reach as high as 87%.

Table 4.1 - Maximum Methane Concentration of 6 Compositions at Different Temperatures

Composition			Maximum Methane Concentration (%) (time to reach peak percent)		
Number	Real or synthetic	COD	30°C	35°C	40°C
1	Synthetic	low	37.4 (32 days)	19.9 (18 days)	38.6 (15 days)
2		medium	74.1 (48 days)	81.5 (40 days)	81.1 (26 days)
3		high	87.9 (70 days)	87.7 (64 days)	44.6 (11 days)
4	Real	low	31.8 (36 days)	78.2 (22 days)	29.6 (14 days)
5		high	24 (37 days)	48.3 (23 days)	34.5 (12 days)
6		medium	2.3 (35 days)	41.1 (24 days)	25.2 (17 days)

Table 4.1 above illustrates the maximum methane percent generated by the vinasse combinations. As expected, the higher the temperature, the sooner we obtain the maximum concentration. However not all combinations had the same peak methane percent at the three temperatures, especially in the real vinasse scenario. The first three combinations are synthetic and they had pretty similar peak methane vinasse concentrations (except Comp 1 at 35°C and Comp 3 at 40°C). For the real vinasses, 35°C seems to be a better temperature to generate higher methane gas percentages.. Combination 4 was a hybrid with both glucose and real vinasse. Moreover, the 35°C was conducted in a 1 L reactor. The 30 ^{0}C and 40 ^{0} C were performed in regular 6.8 L reactors. Since the headspace was small for 35 ^{0}C, it generated higher methane gas concentration than other reactors at different temperatures. Only Composition 4 at 35 ^{0}C was conducted in a 1L reactor. No other compositions were tried on the 1 L reactor because of the need of larger volume of samples. Composition 5 and Composition 6 have no consistent trend in methane concentration vs. temperature. We cannot say higher the temperature, the more is the methane percent. They both had the maximum

concentration at 35 ^{0}C. Composition 4 also had the highest concentration at 35^0 C, although 35 ^{0}C was different in terms of reactors size. Thus 35 ^{0}C can be considered the optimum temperature for the real vinasse. It is important to see if high COD incorporates higher methane percent. For this comparison the highest methane concentration reached among the three temperatures was considered. For synthetic vinasse, the highest methane concentration was obtained for high COD. But the difference in methane concentration between the medium and high COD is not much. It is almost same. From this limited study we can say that high COD increases the COD for a certain extent. Like the increase in peak methane concentration from low (14.625 g glucose) to medium (62.78 g glucose) COD was substantial (a rise form 38.6% to 81.5%). Likewise the increase in methane concentration from medium (62.78 g glucose) to high (204 g glucose) COD was not much (a rise from 81.5% to 87.9 %). More studies are recommended between the medium and high COD and higher to come to any conclusion. It might be interesting to see whether there is any threshold level, meaning whether there is existence of any level beyond which increase in COD has no impact on peak methane concentration.

For real vinasse, all the peak methane concentration and COD were around the same interval. Composition 4 at 35^0 C, will not be considered in this comparison because it was conducted in 1 L reactor. All the others were operated in 6.8 L reactor. The real vinasse followed a trend. The lower is the COD, the lower is the peak methane concentration. Real and low vinasse (23.95g COD) had 31.8% highest peak methane concentration. Real and medium vinasse (27.12g COD) had 41.1% and Real and high vinasse (32.17 g COD) had 48.3%.

If comparison is made between the synthetic and real vinasse compositions, it is evident that the synthetic combinations will generate more methane gas in terms of

percentage and volume compared to real vinasse. The reason is simple: glucose has been used in synthetic combinations, which is easily degraded by the microbes, whereas real vinasse is a complex combination of various organic and inorganic matter, different amino acids group, phenolic compounds and others. The high concentration of real vinasse can be a tough challenge for the microbes. It is difficult for the microbes to disintegrate real vinasse compounds. Thus methane concentration in most of the real vinasse was around 20 to 40% , where as high as 88 % methane composition was achieved for some synthetic vinasses. Moreover, since all the reactors were not run at the same time, real vinasse was stored in the refrigerator. Though stored in frozen condition, slow degradation might have taken place and changed the consistency of the vinasse composition. It might disrupt the concept of same composition but different temperature.

4.1.1 Gas Components for the 6 Combinations of Vinasse.

The methane and oxygen data, along with the pH data, are depicted in graphs (Fig. 4.1 – Fig. 4.3) and presented below. Figures below show the methane and oxygen data for Comp. 1 at 30 ^{0}C, 35 ^{0}C and 40 ^{0}C.

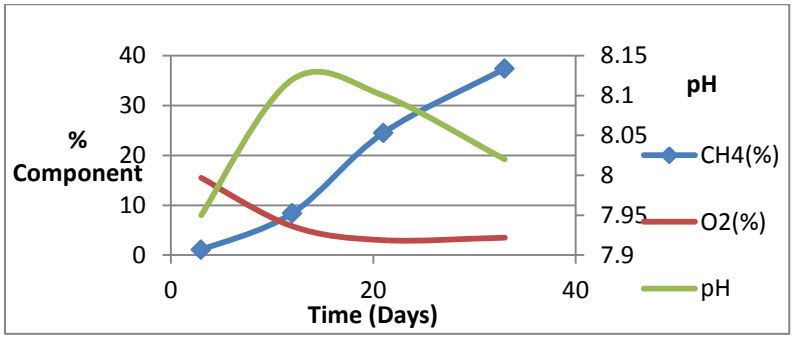

Fig. 4.1 - Gas Components of Composition 1 (synthetic and low COD) at 30 ^{0}C

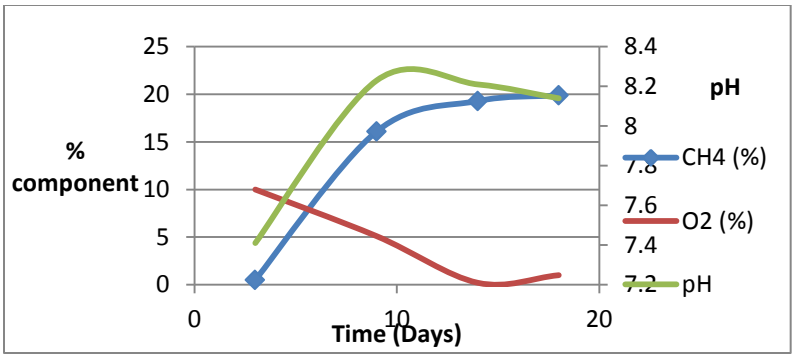

Fig.4.2 - Gas Components of Composition 1 (synthetic and low COD) at 35 ^{0}C

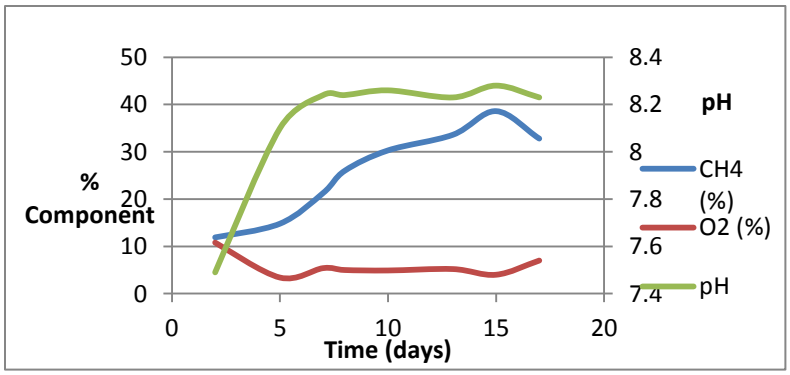

Fig. 4.3 - Gas Components of Composition 1 (synthetic and low COD) at 40^0 C

Temperature definitely played a role in the rate of reaction to reach the methanogens stage. The higher the temperature, the higher is the rate of reaction and thus lower is the number of days required to reach the maximum concentration. The lag time or the time when there is no gas generation and no drastic pH fluctuation was longer for 30 ^{0}C than for 35 ^{0}C and 40 ^{0}C. Also for the total length of operating period, at 30 ^{0}C, the reactors were kept for 35 days and for 35 and 40 ^{0}C we kept the reactors for 19 and 13 days, respectively. However, regarding the value of the peak methane concentration there was no such trend for this particular composition. Oxygen concentration decreases with increasing methane concentration in all three reactors.

Figs. 4.4, 4.5 and 4.6 show the gas components for Composition 2 at 30, 35 and 40 ^{0}C.

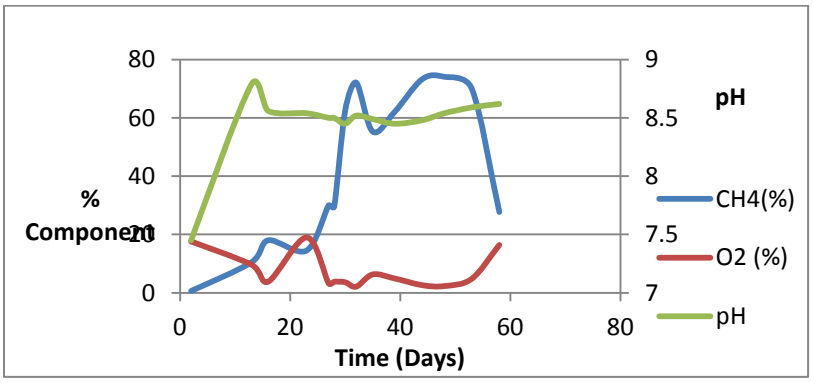

Fig. 4.4 - Gas components of Composition 2 (synthetic and medium COD) at 30 ^{0}C

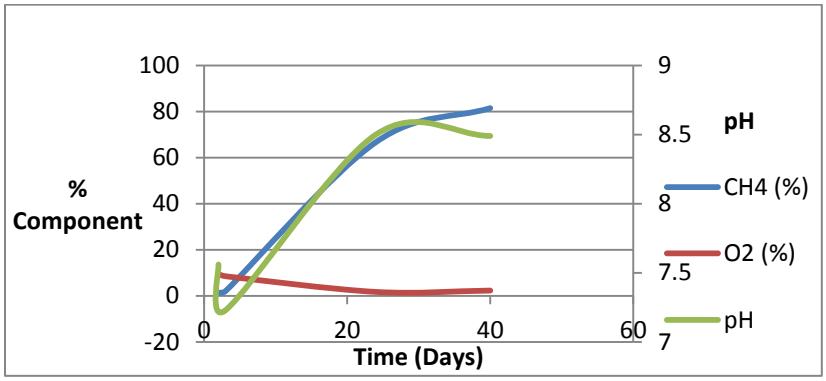

Fig. 4.5 - Gas components of Composition 2 (synthetic and medium COD) at 35 ^{0}C

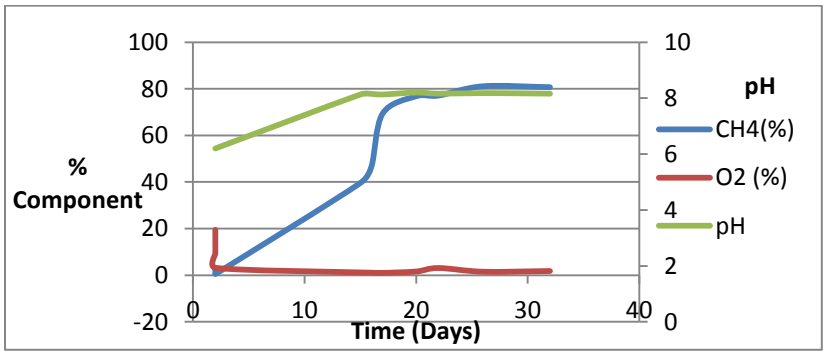

Fig. 4.6 - Gas components of Composition 2 (synthetic and medium COD) at 40 ^{0}C

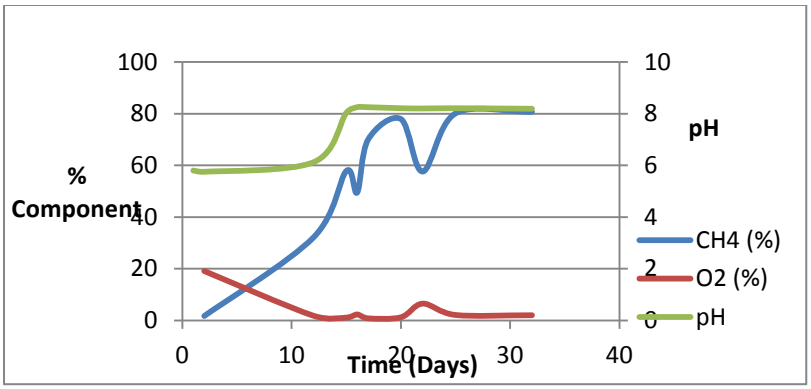

Fig. 4.7 - Gas components of Composition 2 (Duplicate of synthetic and medium COD) at 40 ^{0}C

For combination no. 2 the peak methane concentration was almost the same at all three temperatures. Looking at this particular combination, it seems that temperature plays no significant role in peak methane concentration. The operating period and also the lag phase as expected are longest for 30 ^{0}C and shortest for 40 ^{0}C. A duplicate was run at 40 ^{0}C and it was observed that the methane peak, the time to reach the peak methane concentration and the total operating period were very similar.

Figures 4.8, 4,9, 4,10 show the gas components of Composition 3 at 30, 35 and 40 ^{0}C.

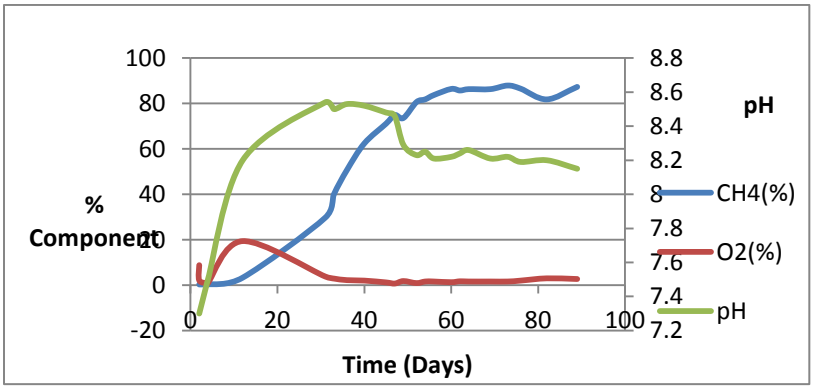

Fig. 4.8 – Gas components of Composition 3 (synthetic and high COD) at 30 ^{0}C

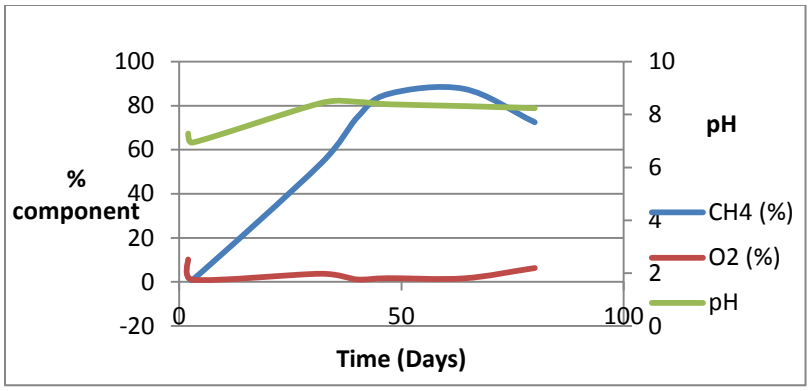

Fig. 4.9 – Gas components of Composition 3 (synthetic and high COD) at 35 ^{0}C

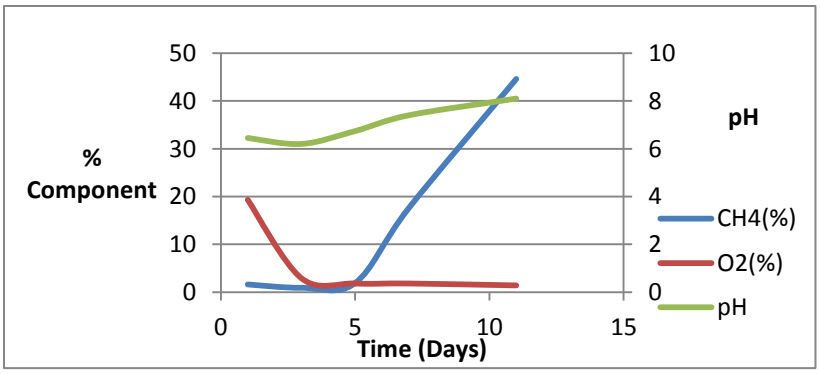

Fig. 4.10 – Gas components of Composition 3 (synthetic and high COD) at 35 ^{0}C

Composition no. 3 was unique for 40 ^{0}C in some ways. The residence time of the reactor at 30 ^{0}C was 87 days and at 35 ^{0}C was 89 days. The reactor at 40 ^{0}C stopped generating gas after 12 days. No specific reason can be provided for such unusual behavior at 40 ^{0}C, except that there was accumulation of toxics or oxygen in the anaerobic reactor at 40 ^{0}C.

The three figures below show the gas components of Composition 4 at 30, 35 and 40 ^{0}C.

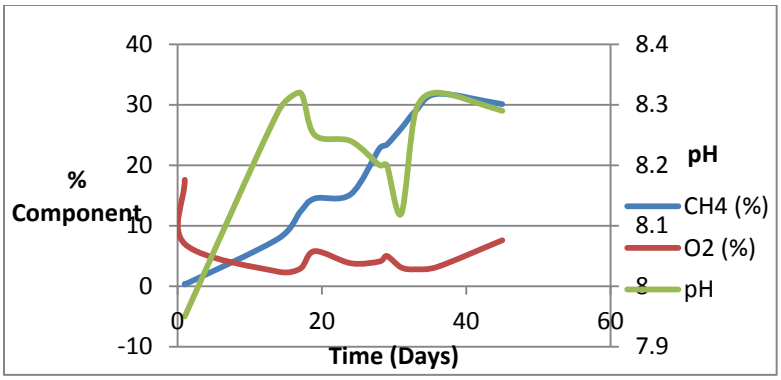

Fig. 4.11 – Gas components of Composition 4 (real and low COD) at 30 ^{0}C

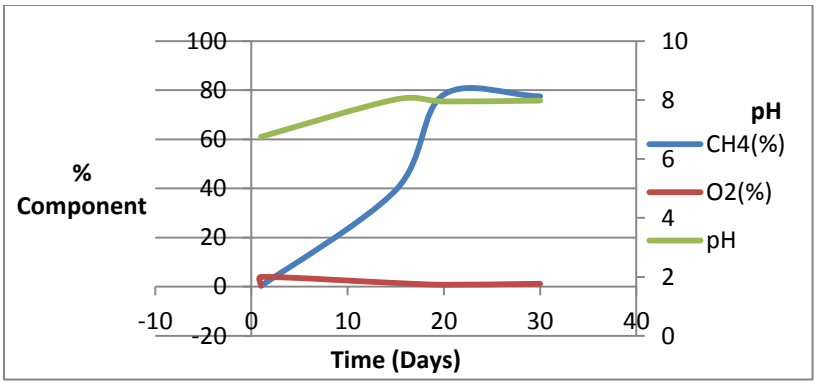

Fig. 4.12 – Gas components of Composition 4 (real and low COD) at 35 ^{0}C

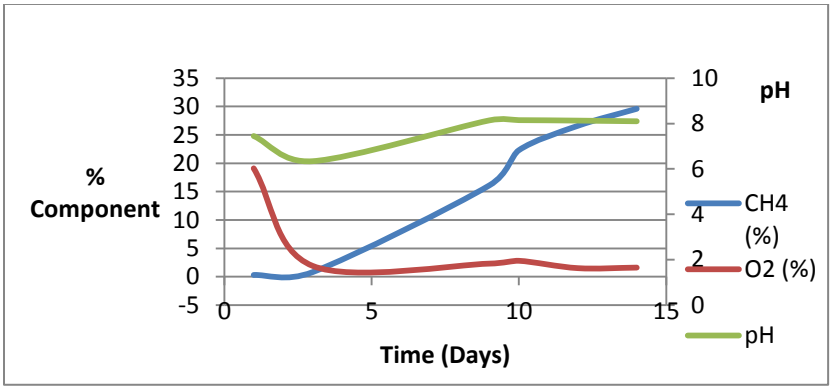

Fig. 4.13 – Gas components of Composition 4 (real and low COD) at 40 ^{0}C

Composition 4 was a mixture of glucose and real vinasse. At 30 ^{0}C and 40 ^{0}C, the highest methane concentration achieved was around 30 %. However, at 35 ^{0}C, 78.2

% was achieved. For this temperature we used a 1 liter anaerobic vessel rather than the 6.8 L vessels. This can be the reason for such high methane concentration. Since the one liter vessel had much lesser headspace, it meant the microbes can work more efficiently in oxygen conversion compared to the six liter vessel.

The 30 ^{0}C reactor in Figure 4.11 seems to have multiple peaks. It suggests different organic compounds being broken down at different times broken down at different times. Why these peaks were not seen in the other reactors is not clear.

Below are the graphs (Fig. 4.14 – Fig. 4.17) are the gas components for Composition 5 at different temperatures.

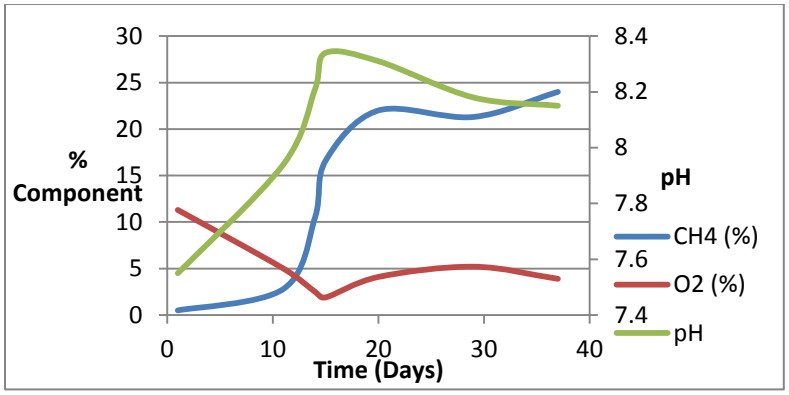

Fig. 4.14– Gas components of Composition 5 (real and high COD) at 30 ^{0}C

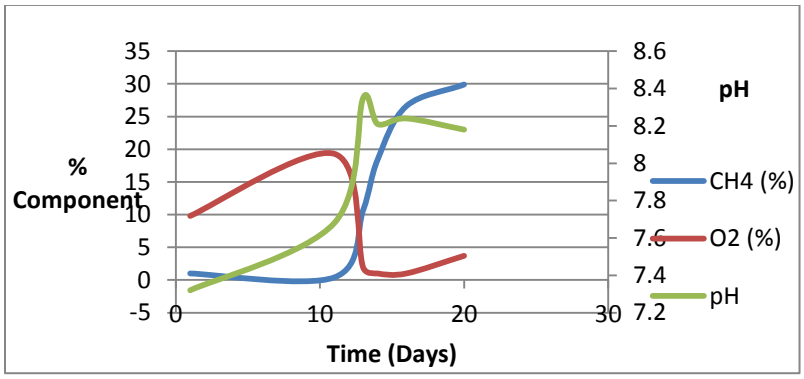

Fig. 4.15 – Gas components of Composition 5 (real and high COD) at 30 ^{0}C

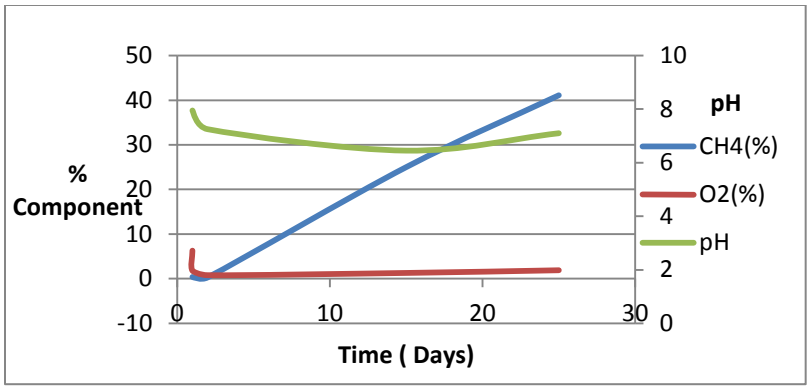

Fig. 4.16 – Gas components of Composition 5 (real and high COD) at 35 ^{0}C

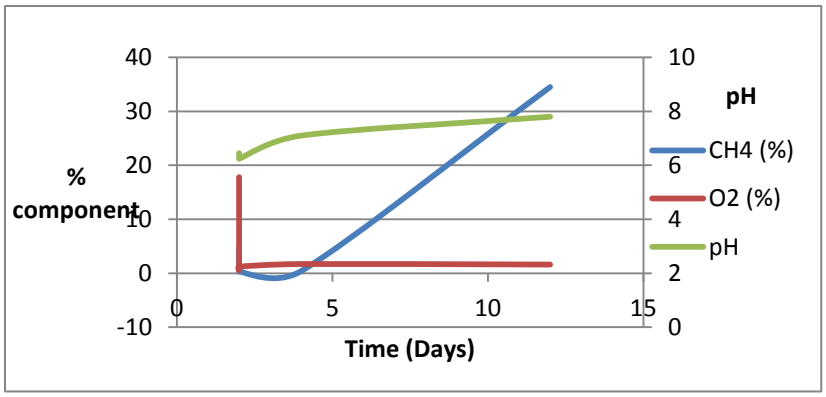

Fig. 4.17 – Gas components of Composition 5 (real and high COD) at 40 ^{0}C

In this case for composition 5, the highest concentration (48.3%) was obtained for 35 ^{0}C over a batch time of 24 days. The methane concentration was high compared to the reactors operated at the other two temperatures. As methane concentration increases, concentration of oxygen decreases. A duplicate was run at 30 ^{0}C. The peak methane percent was similar but the duplicate did not have a descending trend of methane after reaching the peak as was observed with the other one.

Below are the graphs (Fig. 4.18 – Fig. 4.20) for gas components for composition 6 at 30 ^{0}C, 35 ^{0}C and 40 ^{0}C.

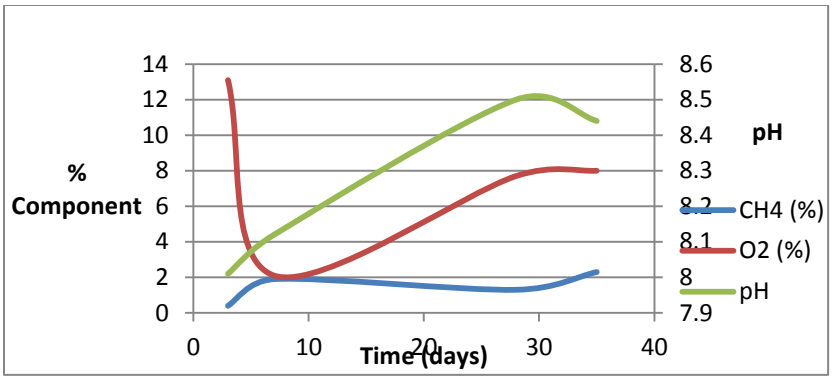

Fig. 4.18 – Gas components of Composition 6 (real and medium COD) at 30 ^{0}C

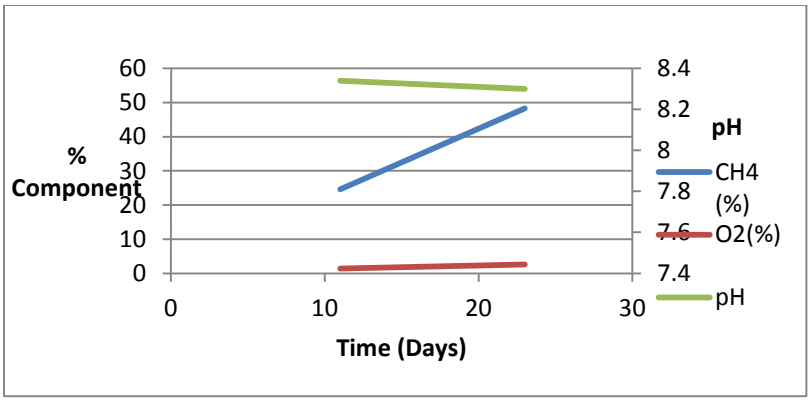

Fig. 4.19 – Gas components of Composition 6 (real and medium COD) at 35 ^{0}C

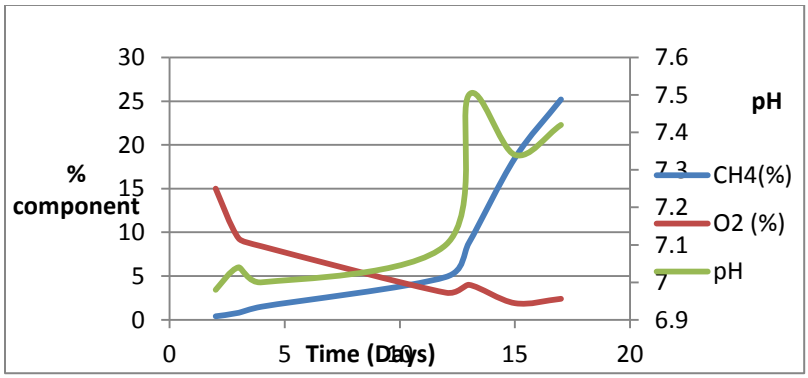

Fig. 4.20 – Gas components of Composition 6 (real and medium COD) at 40 ^{0}C

Composition 6 at 30 ^{0}C did not work as expected. It reached a maximum methane concentration of 2.1% in 35th day. When Composition 6 at 30 ^{0}C was

conducted, Village Creek (our source of sludge) was going through some maintenance issues. The sludge was very thin. Since it was real vinasse, it was not possible to repeat the experiment because the company was reluctant to supply additional vinasse. The peak methane concentration was subsequently 48.3 and 25.2 % for 35 and 40 ^{0}C.

Based on the above results it seems 35 ^{0}C is the most desirable temperature, especially for the real vinasses, because most of the combinations had peak methane concentration at this temperature. More combinations need to be tried to conclude whether 35 ^{0}C is the optimum temperature for anaerobic treatment of vinasse.

4.1.2 Comparison of Methane Generation Rates and Cumulative Methane Generation

The cumulative methane generation rate is computed by adding the daily methane generation rate and is expressed in terms of mL of methane at STP / L of vinasse. Methane generation rate is also compared with the cumulative methane generation. The methane generation rate is expressed in terms of mL of methane at STP per L of vinasse per day. We expect to see similar cumulative methane generation for a particular combination at different temperatures, because theoretically they have the same COD content and should thus generate a similar amount of methane. For rate of methane generation, the higher the temperature, the higher is the microbial activity and thus the lesser the time to reach the peak methane generation.

The following Figures 21 and 22 show the methane generation and cumulative methane generation (mL per liter) of Composition 1 at 30 ^{0}C and 35 ^{0}C, which is the synthetic vinasse with the least glucose. The volume for 40 ^{0}C was not measured because the machine was sent for calibration.

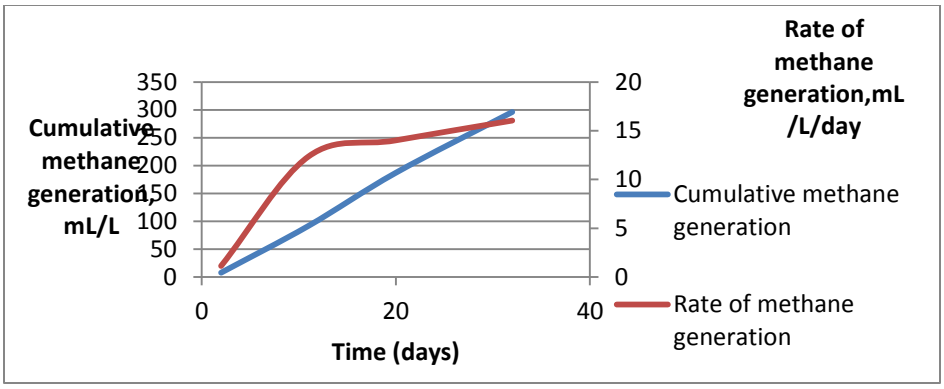

Fig. 4.21– Cumulative methane generation (mL per liter) and rate of methane generation (ml per Liter per day) for Composition 1 (synthetic and low COD) at 30 ^{0}C.

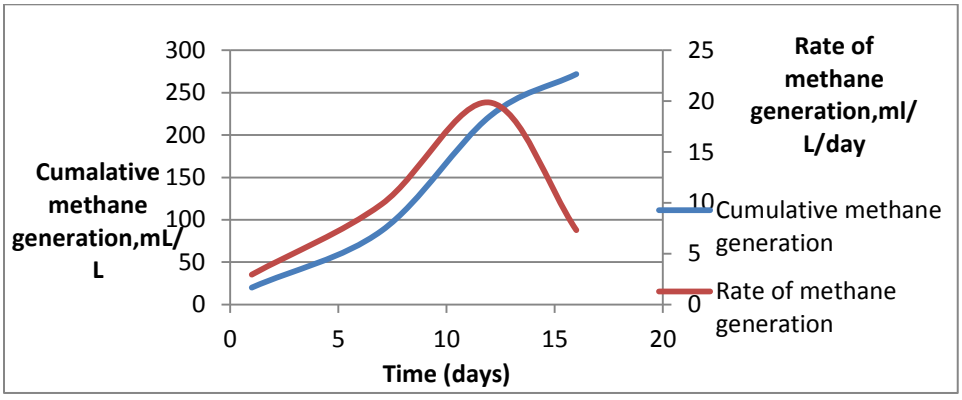

Fig. 4.22– Cumulative methane generation (mL per liter) and rate of methane generation (ml per liter per day) for Composition 1 (synthetic and low COD) at 35 ^{0}C.

Almost 300mL/L of methane was obtained from this reactor at 30 ^{0}C over a period of 32 days. The reactor at 35 ^{0}C produced 271 mL/L of methane gas over a period of 16 days. Thus the volume of methane produced is almost same for these two reactors. Temperature did not play a role in the cumulative methane generation. This is exactly what we expect since they had the similar initial COD. As expected, 35 ^{0}C reactor was active for a much shorter time.

For rate of methane generation, there were some obvious differences in the pattern of the graphs. For 30 ^{0}C, the rate of methane generation (mL/L/day) kept increasing, peaking at 16 mL/L/day on day 32. However, at 35 ^{0}C, the rate topped in 12 days with 20 mL/L/day and then decreased to 7.3 mL/L/day. Thus as expected, the higher the temperature, the greater is the methane generation rate at a particular time.

The four figures (Fig. 23 – Fig. 26) below depict the cumulative methane generation and rate of methane generation of Composition 2 at 30 C and 35 ^{0}C, 40 ^{0}C and 40 ^{0}C duplicate. Composition 2 was synthetic with medium COD.

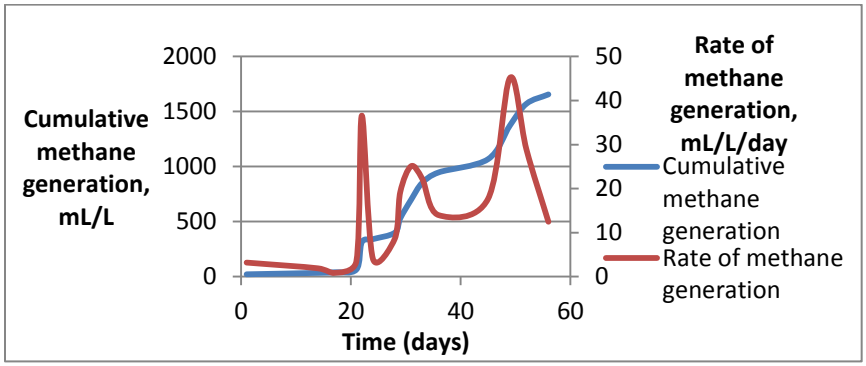

Fig. 4.23 – Cumulative methane generation (mL per liter) and rate of methane generation (ml per liter per day) for Composition 2 (synthetic and low COD) at 30 ^{0}C.

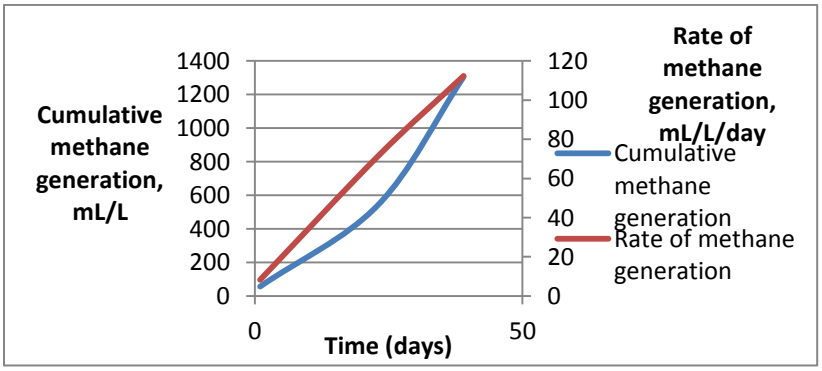

Fig. 4.24 – Cumulative methane generation (mL per liter) and rate of methane generation (ml per liter per day) for Composition 2 (synthetic and medium COD) at 35 ^{0}C.

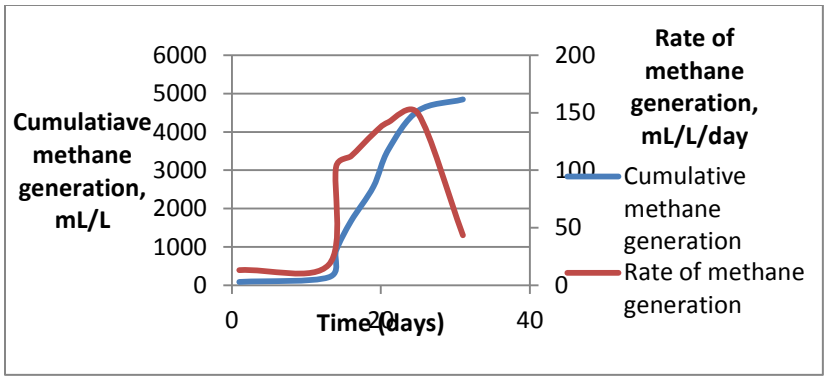

Fig. 4.25 – Cumulative methane generation (mL per liter) and rate of methane generation (ml per liter per day) for Composition 2 (synthetic and medium COD) at 40 ^{0}C.

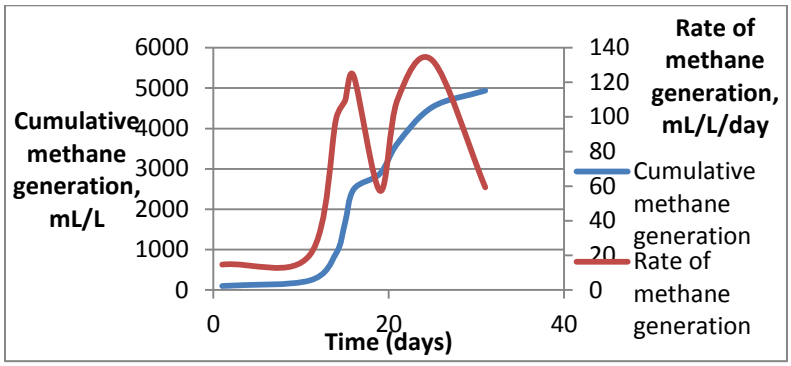

Fig. 4.26 – Cumulative methane generation (mL per liter) and rate of methane generation (ml per liter per day) for Composition 2 (duplicate of synthetic and medium COD) at 40 ^{0}C.

Composition 2 is a synthetic vinasse. At 30 ^{0}C the cumulative methane generation was 1655 mL/L over a period of 56 days, at 35 ^{0}C it was 1305 mL/L over 39 days and at 40 ^{0}C the methane generation was 4846 mL/L over a period of 31 days. The higher the temperature, the shorter the reactor run time, as expected. By far 40 ^{0}C was the most successful reactor in this combination. It produced more than three times of methane (mL/L) than the ones at 30 ^{0}C and 35 ^{0}C. The reason can be some unwanted toxics or oxygen in the 30 and 35 ^{0}C reactors. Sometimes the sealants got loose and air

entered the system. In an anaerobic treatment, a little addition of oxygen might result in the microbe killing. Alternatively, higher temperature might have increased the activity of the microbes, especially the methanogens that led to such high methane generation.

The rate of methane generation at 30 ^{0}C is very undulating with multiple peaks and drops. The peaks were 36.6 mL/L/day at 22 days, then 25.1mL/L/days at 31 days and 45.1mL/L/day at 49 days. At 35 ^{0}C, the rate graph was straight peaking and stopping at 112.36 mL/L/day at 39 days. The pattern at 40 ^{0}C is a kind of asymmetrical bell shape. The graph peaks at 149.1mL/L/days at 25 days and then drops down. The higher the temperature, the greater is the microbial activity, thus the greater the methane generation at a specific time.

A duplicate at 40 ^{0}C was run in this composition. Both the original reactor and the duplicate had similar cumulative methane generation (4846.7 and 4937.7 mL/L) and the batch time was similar, too (both 31 days). Thus this composition was consistent with the duplicate result. The methane generation rate at 40 ^{0}C and the duplicate had similar values over the operation time.

Below are the graphs (Fig. 27 – Fig. 29) for the cumulative methane generation and rate of methane generation at three different temperatures for Composition 3. Composition 3 is synthetic with the highest COD.

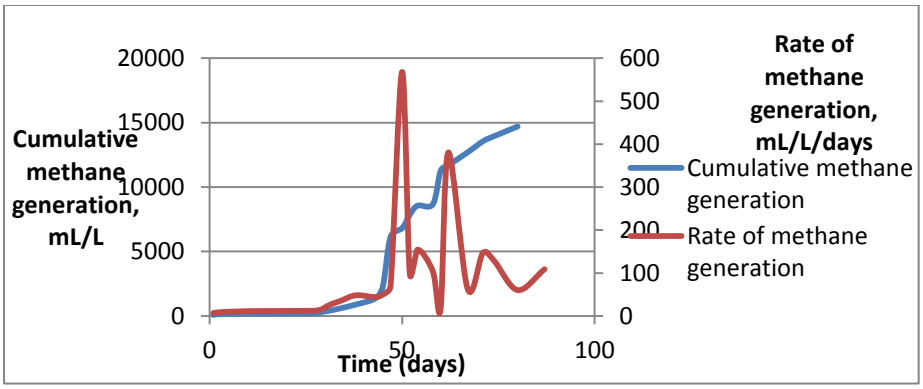

Fig. 4.27– Cumulative methane generation (mL per liter) and rate of methane generation (ml per liter per day) for Composition 3 (synthetic and high COD) at 30 ^{0}C.

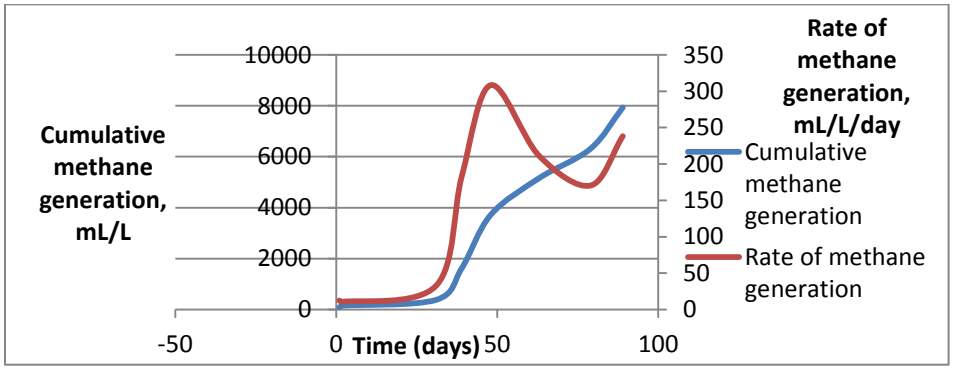

Fig. 4.28 – Cumulative methane generation (mL per liter) and rate of methane generation (ml per liter per day) for Composition 3 (synthetic and high COD) at 35 ^{0}C.

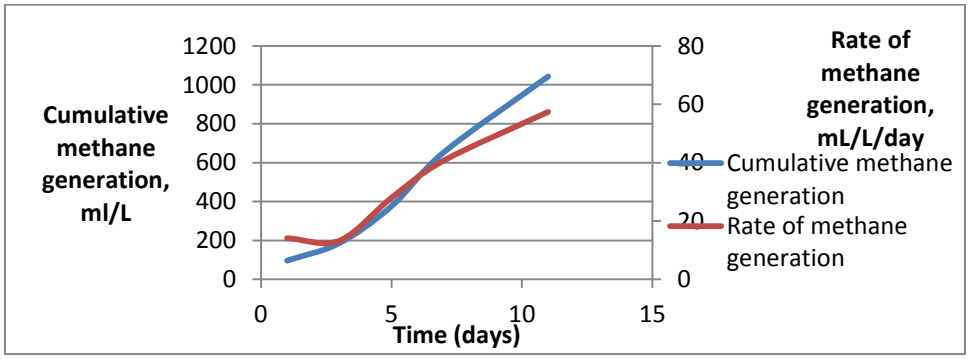

Fig. 4.29 – Cumulative methane generation (mL per liter) and rate of methane generation (ml per liter per day) for Composition 3 (synthetic and high COD) at 40 ^{0}C.

Composition 3 was unique in many ways. At 30 ^{0}C, the cumulative methane generation was 14,706 mL/L in 87 days. At 35 ^{0}C, the methane generation was 7935 mL/L in 89 days. However, at 40 ^{0}C the cumulative methane generation reached only 1043 mL/L in 11 days. There likely was some accumulation of oxygen and toxics at 40 ^{0}C and some at 35 ^{0}C, since their cumulative methane generation was so much lower than for that at 30 ^{0}C. Alternatively, for this synthetic composition, the microbes most adept at methane generation may have flourished at 30 ^{0}C.

The rate of methane generation for 30 ^{0}C reached a at 568.1 ml/L/day in 50 days, then dropped for a while and rose to 380.7 mL/L/day in 62 days and 147 ml/L/day in 80 days. At 35^0 C, the rate reached a peak of 308 m/L/day in 48 days and 238 mL/L in 89 days. At 40 ^{0}C, the rate was 57.3 in 11 days. The 40 ^{0}C reactors did not follow the same pattern.

The two figures below are the cumulative methane generation and rate of methane generation for Composition 4 at 30 ^{0}C and 40 ^{0}C. The 35 ^{0}C was not measured because the machine was sent for calibration.

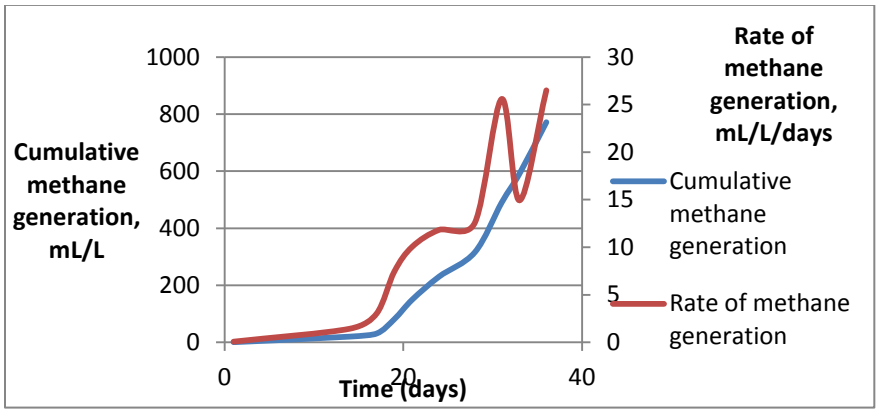

Fig. 4.30 – Cumulative methane generation (mL per liter) and rate of methane generation (ml per liter per day) for Composition 4 (hybrid and low COD) at 30 ^{0}C.

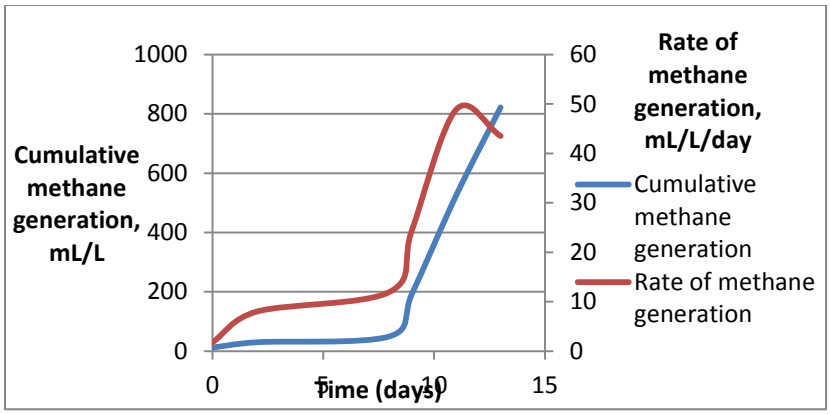

Fig. 4.31– Cumulative methane generation (mL per liter) and rate of methane generation (ml per liter per day) for Composition 4 (hybrid and low COD) at 40 ^{0}C.

Composition 4 is a combination of real vinasse and glucose. The volume data at 35 ^{0}C is not available but the concentration of methane was very high ; however, the reactor at this temperature was 1 L rather than 6.8 L. Cumulative methane generation at 30 ^{0}C reached 771 mL/L in 36 days and at 40 ^{0} C , it reached 821 mL/L in 13 days. The cumulative methane generation was similar for the two reactors and at 40 ^{0}C, the batch time was less, as expected.

The rate of methane generation at 30 ^{0}C was 25 mL/L/day at 31 days, whereas at 40 ^{0}C it was 43.5 mL/L/day at 13 days. The higher the temperature, the greater the microbial activity and less time it should take to reach the maximum rate of methane generation.

Below are the graphs (Figure 4.32 – Figure 4.35) for Composition 5 at 30 ^{0}C, 30 ^{0}C duplicate and 40 ^{0}C. Composition 5 is a real vinasse from White Energy with the highest COD among the real vinasses tested.

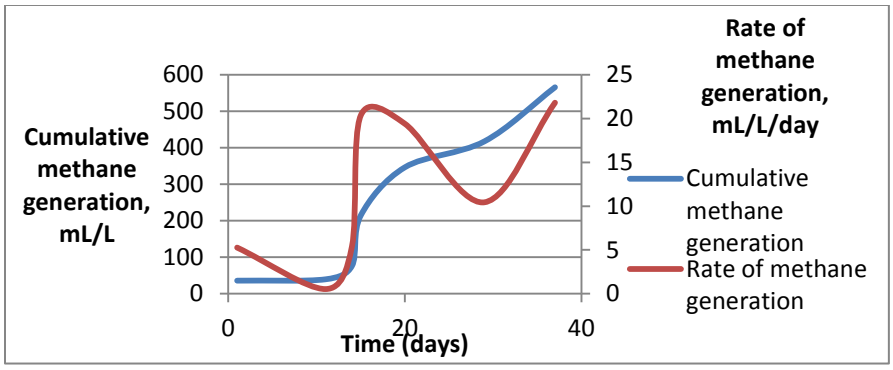

Fig. 4.32 – Cumulative methane generation (mL per liter) and rate of methane generation (ml per Liter per day) for Composition 5 (real and high COD) at 30 ^{0}C.

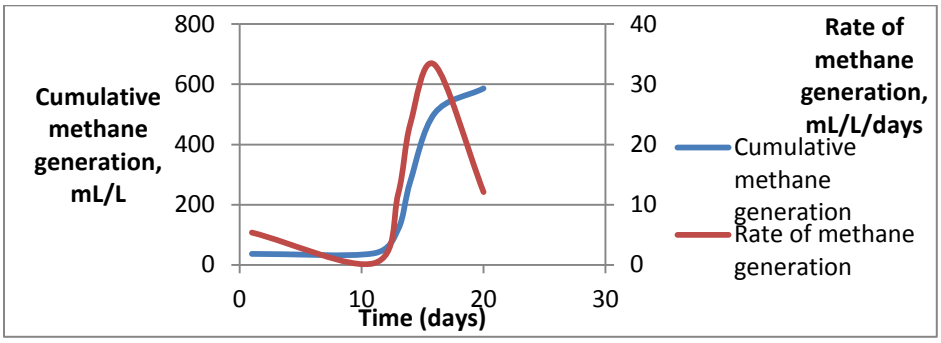

Fig. 4.33 – Cumulative methane generation (mL per liter) and rate of methane generation (ml per liter per day) for Composition 5 (duplicate of real and high COD) at 30 ^{0}C.

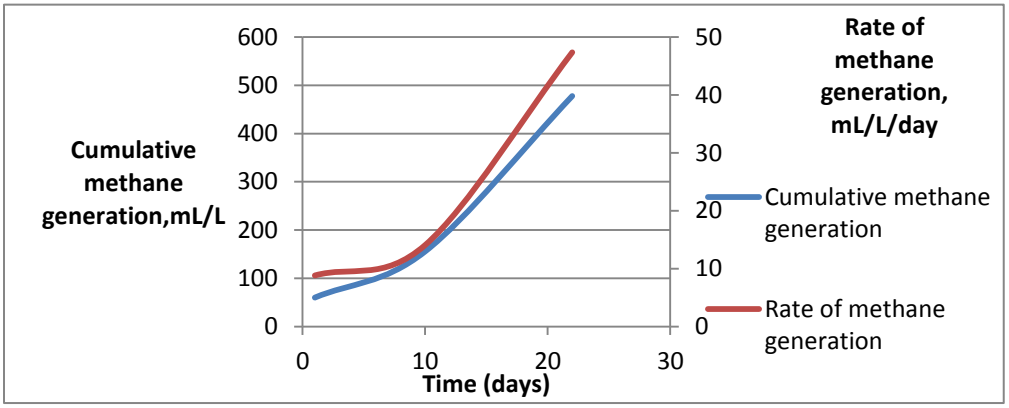

Fig. 4.34 – Cumulative methane generation (mL per liter) and rate of methane generation (ml per liter per day) for Composition 5 (real and high COD) at 35 ^{0}C.

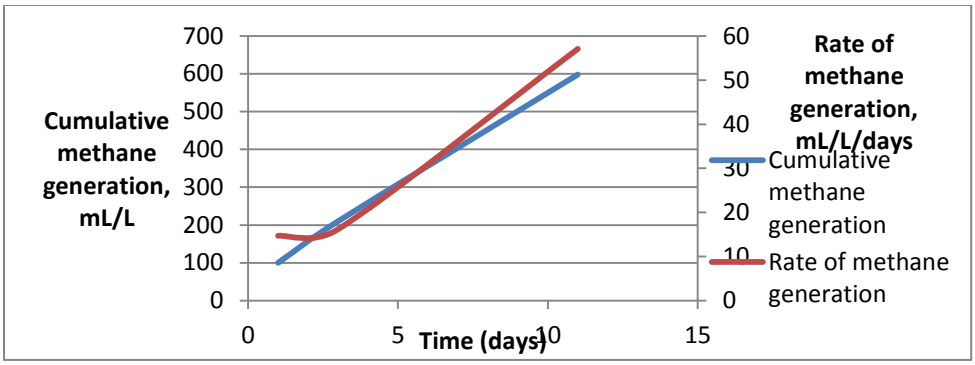

Fig. 4.35 – Cumulative methane generation (mL per liter) and rate of methane generation (ml per liter per day) for Composition 5 (real and high COD) at 40 ^{0}C.

Cumulative methane generation at 30 ^{0}C reached 565 mL/L in 37 days, at 35 ^{0}C it reached 477 mL/L in 22 days and at 40 ^{0}C it reached 598 in 11 days. The methane generation was quite similar, especially for 30 ^{0}C and 40 ^{0}C. The batch time was greater for the 30 ^{0}C reactor and least for the 40 ^{0}C reactor, as expected.

The rate of methane generation for 30 ^{0}C peaked at 20.3 ml/L/day in 15 days, then dropped and again rise to 21.8 ml/L/day in 37 days. At 35 ^{0}C it reached 47 mL/L/day at 22 days and at 40 ^{0}C within 11 days it reached 57 mL/L/day. The rate also followed the expected trend. The higher the temperature, the greater is the methane generation at a specific time.

A duplicate at 30 ^{0}C was run for the real vinasse. The cumulative methane generation was almost the same (565.9 and 586.2 mL/L) over a residence time of 37 and 20 days. The batch time showed some discrepancy. The methane generate rate was also different. At 30 ^{0}C, the rate of methane generation had some undulating features, rising and dropping. The duplicate had more like a bell shape.

Below are the graphs (Figure 4.36 and Figure 4.37) for Composition 6 at 30 and 40 ^{0} C.

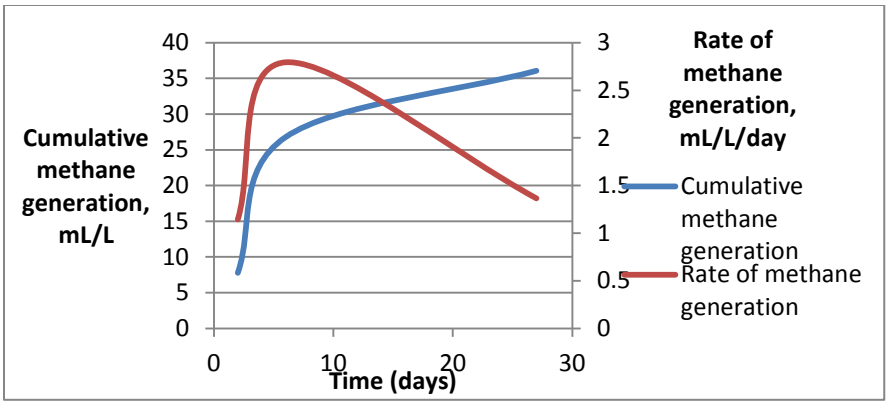

Fig. 4.36 – Cumulative methane generation (mL per liter) and rate of methane generation (ml per liter per day) for Composition 6 (real and medium COD) at 30 ^{0}C.

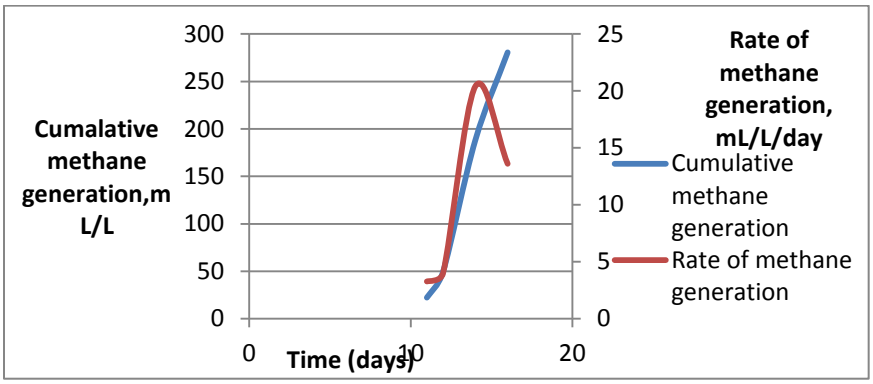

Fig. 4.37– Cumulative methane generation (mL per liter) and rate of methane generation (ml per liter per day) for Composition 6 (real and medium COD) at 40 ^{0}C.

Composition 6 had 3.5 L of vinasse. The volume data was not available for the reactor at 35 ^{0}C due to maintenance issue of the calibrator. Cumulative methane generation at 30 ^{0}C was reached 36.1 mL/L within 27 days and at 40 ^{0}C the cumulative methane generation reached 280 ml/L. There is clearly a difference between the two reactors. The volume data at 40 ^{0}C was measured at 10th day because of the lack of availability of the machine. There were some problems in the reactor at 30 ^{0}C. The

sludge was very thin and the experiment could not be repeated because of reluctance of the companies to supply any more.

The real vinasse did not behave accordingly like most synthetics did. The reason can be a leak in the reactor or the fact that the vinasse might become toxic (even though refrigerated at 4 ^{0}C). At the end of the experiments, the vinasse turned greenish and lost its original color. This is because though sludge was added to increase the microbial activity, the vinasse itself has microbes inside. Although slowly (since refrigerated), the vinasse lost its original form with time.

For the rate of methane generation, at 30 ^{0}C, the reactor topped 2.8 mL/L/day in 6 days and at 40 ^{0}C, the rate was maximum within 14 days with 20.4 mL/L/day. There is no point in comparing this since the volume data till 10th days for 40 ^{0}C was not measured.

Table 4.3 summarizes the cumulative methane generation and the batch time for all the different compositions of vinasse. It is interesting to compare the trend of cumulative methane generation in synthetics and real vinasse. For synthetics, higher the initial COD, higher the methane generation. It is expected because the more carbon in the vinasse, the greater is the conversion to methane. For real vinasse, such a trend was not seen. The methane generation varied very little on the basis of composition. Also the methane output was very little. Again the complex composition of real vinasse may be the reason for this low methane generation.

Table 4.2 – Cumulative methane generation and batch time for all the reactors

	Temperature (^{0}C)	Cumulative methane generation (mL/L)	Batch Time (days)
Comp1 (low and synthetic)			
	30	296.1	32
	35	271.9	16
	40		18
Comp2 (medium and synthetic)			
	30	1655.6	56
	35	1305.2	39
	40	4846.7	31
	40 duplicate	4937	32
Comp3 (high and synthetic)			
	30	14706.9	87
	35	7935.9	89
	40	1042.9	11
Comp4 (low and real)			
	30	771.5	36
	35		32
	40	821.8	13
Comp5 (high and real)			
	30	565.9	37
	30 duplicate	586	21
	35	477.6	22
	40	598.1	11
Comp6 (medium and real)			
	30	36.1	27
	35		23
	40	280.1	16

4.2 Water Quality Analysis

4.2.1 COD Analysis

4.2.1.1 By Temperature

COD analysis was conducted almost 5 days in a week. The reason is the drastic changes in the COD especially at 40 ^{0}C and to obtain as many as data to form the model. The initial COD for the six combinations ranges from 2630 to 32,231 mg/L. It is necessary to mention that we used the COD after addition of the sludge as our initial COD. The COD of all the combinations increased after introducing the sludge. The initial COD for each combination at three different temperatures was measured separately (both before adding and after adding sludge). For all the combinations, the initial COD before adding the sludge was almost the same for all three temperatures. Table 4.3 shows the COD values before and after adding the sludge at 30 ^{0}C. However, after adding the sludge, there were some significant changes in the combinations. The reason is that the sludge was taken at different times from Village Creek; thus, the sludge concentration was not always uniform.

Table 4.3 - COD values measured before and after adding sludge for all the Compositions at 30 ^{0}C

Composition			COD	
Number	Strength	Type	Before adding sludge	After adding sludge
1	low	synthetic	2127	2537
2	medium		8843	9837
3	high		29661	30,493
4	low	real	23083	23,950
5	high		31676	32,172
6	medium		26140	26,528

Figure 4.38 depicts the COD degradation of Composition 1 at the three different temperatures.

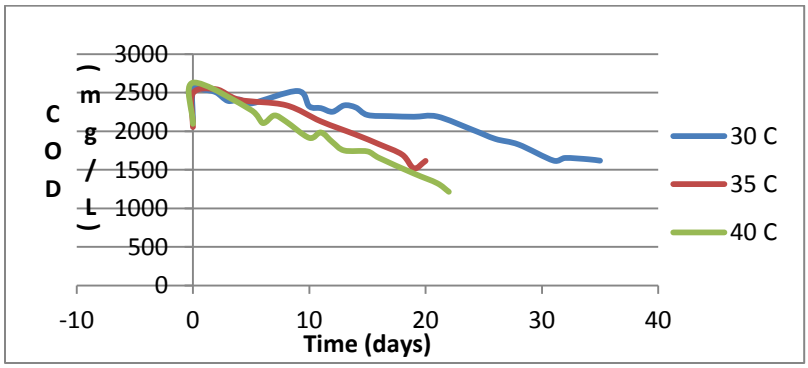

Fig. 4.38 - COD vs Time for Composition 1(synthetic and low COD) at different temperatures

As expected, the decrease in COD took place over a longer period at 30 ^{0}C. As temperature increases, stability is reached earlier. At 30 ^{0}C, almost 36.2% removal of COD was observed over a period of 35 days. At 35 ^{0}C, we had 36.5 % and at 40 ^{0}C, 52.3% removal.

Figure 4.39 describes the COD removal with time for Composition 2 at 30 ^{0}C, 35 ^{0}C, 40 ^{0}C and the duplicate at 40 ^{0}C.

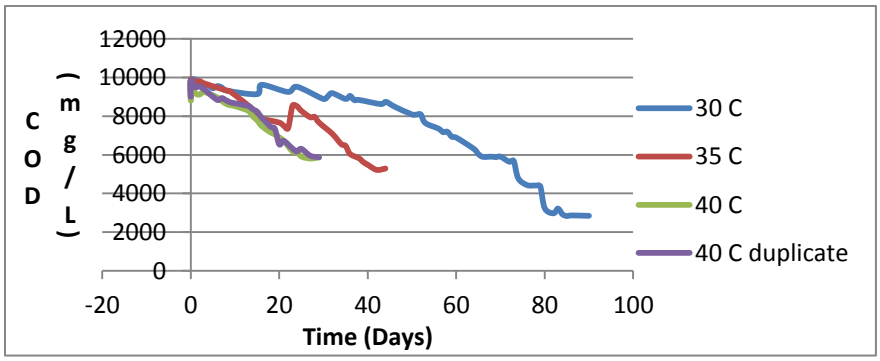

Fig. 4.39 - COD vs Time for Composition 2 (synthetic and medium COD) at different temperatures.

At this combination, 71% removal of COD occurred at 30 ^{0}C over a period of 90 days. It can be observed that this did not follow a first-order reaction. The graph shape is concave. Composition 2 at 35 ^{0}C removed 46 % of COD for a period of 44 days and at 40 ^{0}C it removed 40 % COD within 29 days. A duplicate was run at 40 ^{0}C too and the removal observed was almost 40 %, too. One reason for such high removal at 30 ^{0} C may be the long residence time (90 days). Thus it had more time to react and degrade and produce more methane.

Figure 4.40 below depicts COD vs. Time at 30 ^{0}C, 35 ^{0}C and 40 ^{0}C.

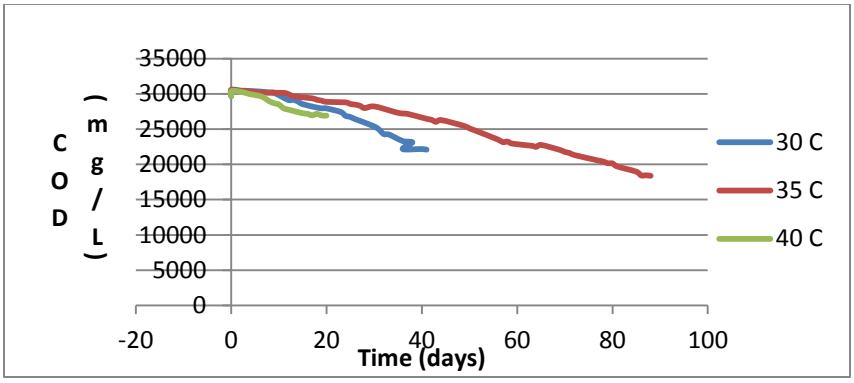

Fig. 4.40 - COD vs Time for Composition 3 (synthetic and high COD) at different temperatures

The results of Combination 3 are a little unusual. At 30 ^{0}C COD removal was 27.6 % over a period of 41 days. At 35 ^{0}C, 40 % removal was achieved over a period of 88 days. At 40 ^{0}C, only 13.3 % removal was achieved within 20 days. At 35 ^{0}C combination 3 had the maximum COD removal. 30 ^{0}C went for almost 89 days, but the water analysis has conducted for 41 days. It was unknown to the researcher about the generation of gas in later days thus water parameters were measured only for 42 days. However it seems that Composition 3 at 30 ^{0}C, would have a much higher COD removal

than the other two reactors because of the long residence time. At 40 ^{0} C, the reactor was operated only for 20 days. It will not be unusual to believe that some toxicity must have caused the early death of the reactor.

Fig. 4.41 below is the COD vs. time at the three different temperatures for Composition 4.

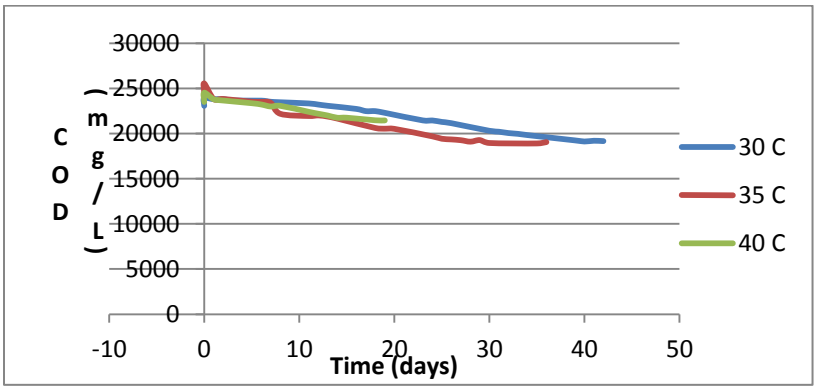

Fig. 4.41- COD vs Time for Composition 4 (low and real COD) at different compositions

Combination 4 was a mixture of glucose and real vinasse. At 30 ^{0}C the anaerobic treatment reduced COD by 30% in 42 days. At 35 ^{0}C, 20 % removal was achieved in 40 days. At 40 ^{0}C, COD was reduced by 10 % in 20 days. The 35 ^{0}C reactor was not the usual 6.8 L vessel used for the experiment: it was the 1 L reactor. Thus it had little head space and comparatively better results. The removal percentage and rate are very similar to that of 30 ^{0}C.

Figure 4.42 below are the figures for COD vs. Time at 30 ^{0}C, 30 ^{0}C duplicate, 35 ^{0}C and 40 ^{0}C for Composition 5.

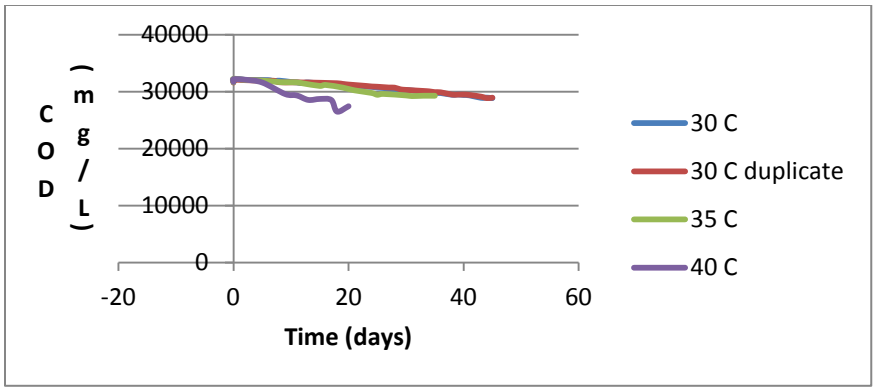

Fig. 4.42- COD vs Time for Composition 5 (real and high COD) at different temperatures

Combination 5 had 4 L of vinasse from Hereford Company, with 10.3 % removed COD over 45 days at 30 ^{0}C. A duplicate run at this temperature had a similar removal efficiency (10%). At 35 ^{0}C, 9.1 % COD was removed and at 40 ^{0}C 14.8 % COD was removed in 20 days.

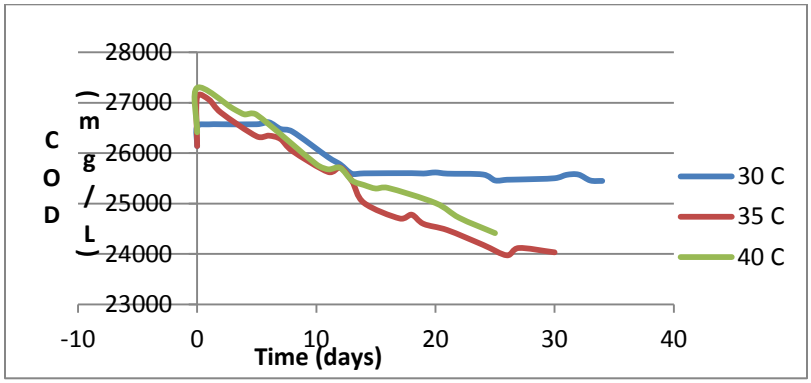

Fig. 4.43 - COD vs Time for Composition 6 (real and medium COD) at different temperatures

Composition 6 had 3.5 L of real vinasse. At 30 ^{0}C, the composition did not work like the other reactors at different temperatures. This was due to thin sludge from Village Creek. The removal was 4.1%. At 35 ^{0}C, a removal of 11.4 % was accomplished within 30 days. At 40 ^{0}C, 10 % removal was possible. Table 4.4 summarizes COD removal for different compositions at three temperatures.

Table 4.4 – Comparison of COD removal (%) and batch time with different compositions at three temperatures.

	Temperature (C)	Batch Time (days)	COD removal (%)
Comp1 (synthetic and low COD)			
	30	32	36.2
	35	16	36.5
	40	18	52.3
Comp2 (synthetic and medium COD)			
	30	56	71
	35	39	46
	40	31	40
	40 duplicate	32	40
Comp3 (synthetic and high COD)			
	30	87	27.6
	35	89	40
	40	11	13.3
Comp4 (real and low COD)			
	30	36	20
	35	32	20
	40	13	10
Comp5 (real and high COD)			
	30	37	10.3
	30 duplicate	21	9.6
	35	22	10
	40	11	9.1
Comp6 (real and medium COD)			
	30	27	4.1
	35	23	11.4
	40	16	10

As expected, the synthetic compositions have higher COD removal percentages than the real vinasses. The highest removal was observed in Composition 2 at 30 ^{0}C (71%). Real vinasse had the highest removal for Composition 4 at 30 and 35 ^{0} C (only 20%). This proves again the complexity involved, dealing with real vinasse.

4.2.1.2 By Composition

As expected, the synthetic compositions (first 3 compositions) had better performance in removal of COD than the real compositions (Composition no. 4, 5 and 6). Fig. 4.44 – Fig. 4.46 below show the COD vs. time at different temperatures for all the compositions used.

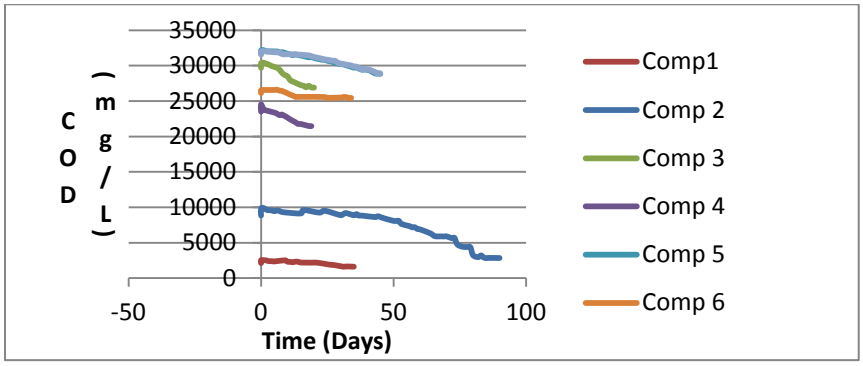

Fig. 4.44 – COD of real and synthetic vinasse at 30 ^{0}C

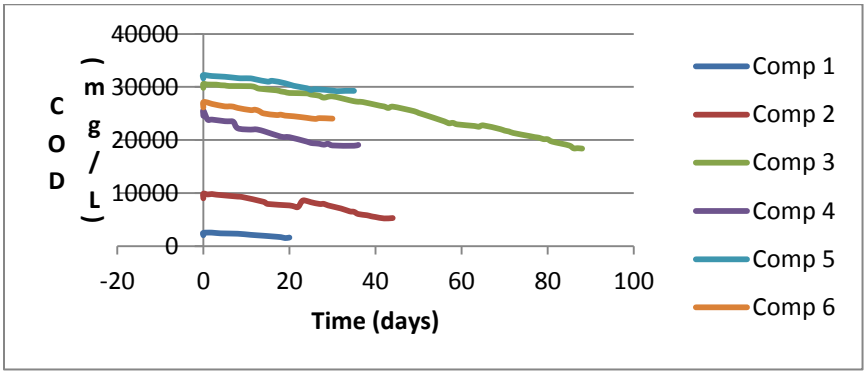

Fig. 4.45 – COD of real and synthetic vinasse at 35 ^{0}C

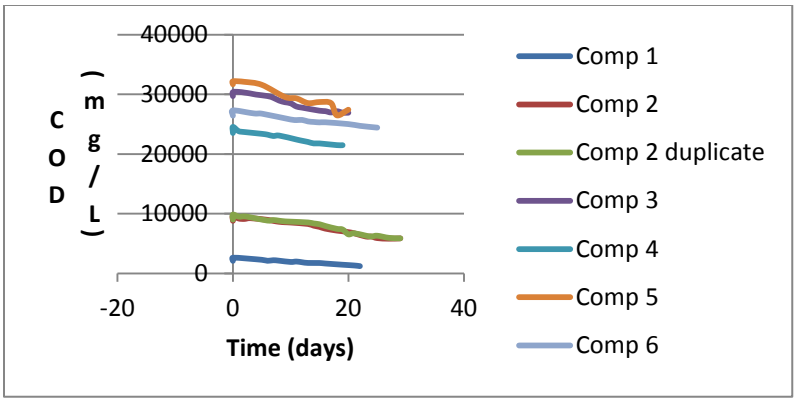

Fig. 4.46 – COD of real and synthetic vinasse at 40 ^{0}C

Composition 1 and 2 had lower initial COD. It was seen that at all temperatures, the reactor operating time was substantially longer for these two combinations. At 30 ^{0}C and 35 ^{0}C, Composition 3 also had a longer batch time. The longer the residence time, the longer is the microbial activity that contributes to the degradation of vinasse, resulting in better removal of COD. Due to certain misunderstandings (the researcher was unaware of the generation of gas), the researcher can only calculate the COD at 30 ^{0}C only for 35 days. It was not measured for 87 days.

By composition, we can observe that the synthetic compositions had better removal efficiency than the real vinasse, which was expected. The synthetic compositions are composed of simple glucose, whereas vinasse is a complex combination of organic and inorganic matter, amino acids, phenolic compounds and many more. Thus certain synthetic combinations had as high as 70 % COD removal efficiency. The real vinasse had an average 10 % removal efficiency. Such low removal efficiency is not enough for vinasse treatment. It must be accompanied by other treatments like advanced oxidation methods. Ozonation, UV and sonication are often used as a pre or post anaerobic treatment. The primarily goal of the research was not to optimize the removal efficiency; thus such secondary treatments were not tried. The low

removal efficiency is quite consistent with other studies. Belhadj (2013) worked with vinasse from the production of ethyl alcohol in Kenitra, Morocco. The aim was to produce the potential of biogas from anaerobic digestion. In this particular study, the organic load (TS, MS and VS) increased but the extraction of biogas was successful.The author believes it was due to the accumulation of non- biodegradable substrate.

4.2.1.3 Relation of initial COD with cumulative methane generation, COD removal, and batch time.

Fig.4.47 (a) and (b) shows the COD vs. cumulative methane generation (ml/L) at the three different temperatures for synthetic and real vinasses. The initial COD used in the graph has been taken from the 30 0C after adding the sludge. Since there was little difference between the initial value of COD at different temperatures, only 30 0C has been used.

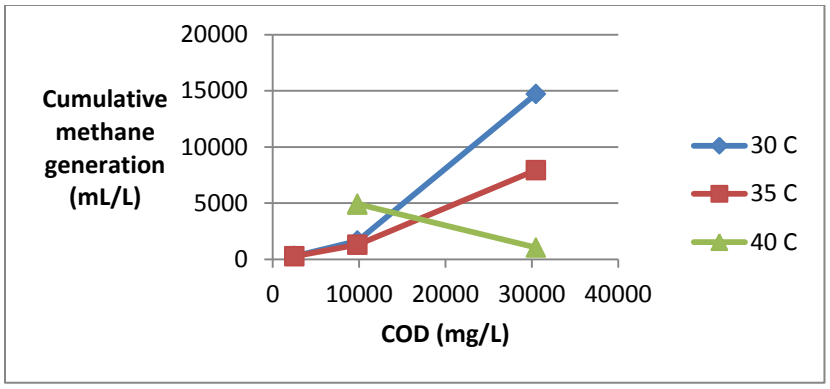

(a)

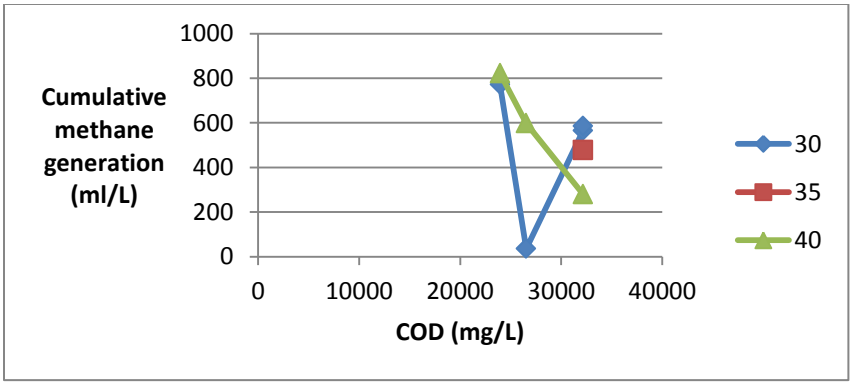

(b)

Fig. 4.47 - COD (mg/L) vs. cumulative methane generation (ml/L) at different temperatures for (a) synthetic vinasses (b) real vinasses.

Composition 3 (synthetic and high) has the highest methane generation (mL/L) for 30 ^{0}C and 35 ^{0}C. At these temperature, the higher the initial COD, the greater is the cumulative methane generation. It is an expected trend. The more Carbon in vinasse, the greater would be the expected conversion to methane. At 40 ^{0}C, the methane generation for Composition 3 was not maximum. Leakage or unexpected toxicity are the possible reasons for such unusual behavior. Real vinasse had no trend for any of the temperatures. Again, the complexities involved in dealing with real vinasses is a possible explanation for such trends.

Fig. 4.48 depicts the COD vs. COD removal at different temperatures.

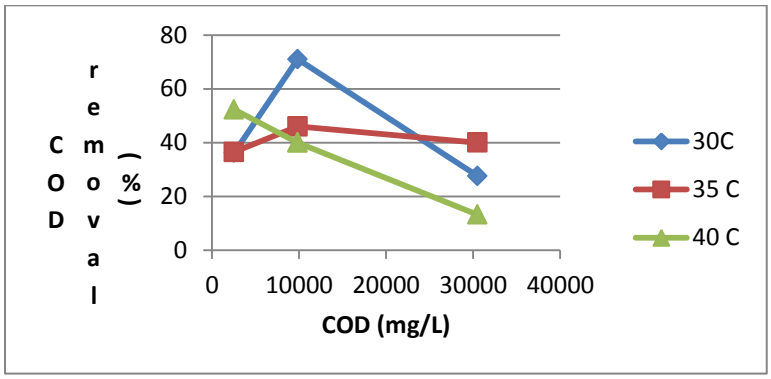

(a)

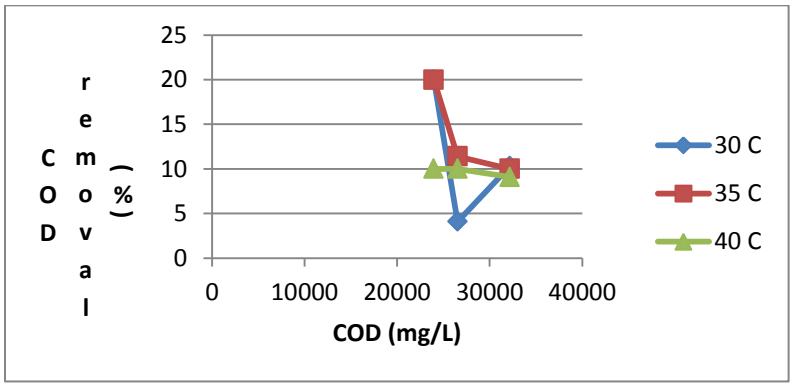

(b)

Fig. 4.48 - COD (mg/L) vs. COD removal (%) at different temperatures for (a) synthetic vinasses and (b) real vinasses.

30 ^{0}C and 35 ^{0}C behave in a similar fashion for synthetic vinasses. The highest COD removal occurs for Composition 2 (synthetic and medium COD). For real vinasses, Composition 4 (low and real), had the highest removal percent. This composition had also glucose, so that can be a possible reason for such removal efficiency in all three temperatures. There are no specific trends for both synthetic and real vinasses. It can be concluded that there is no relationship between COD removal and initial COD.

Figure 4.49 describes the COD vs. batch time. Batch time is the operated time for the reactors. It was seen for synthetic vinasse that the higher the COD, the longer the batch time, since the microbes required more time to degrade the organic matter.

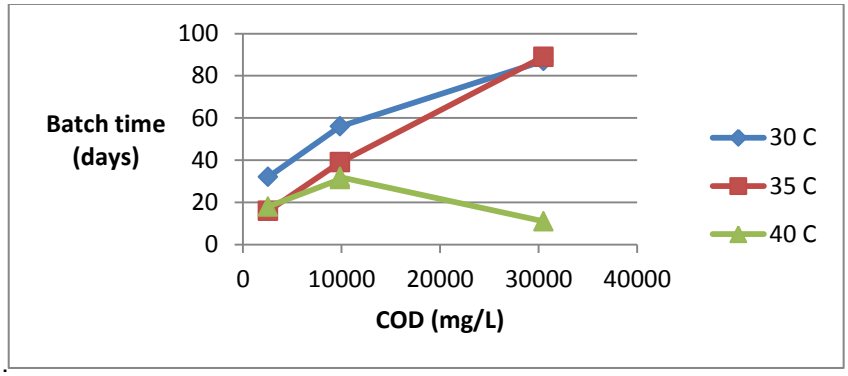

(a)

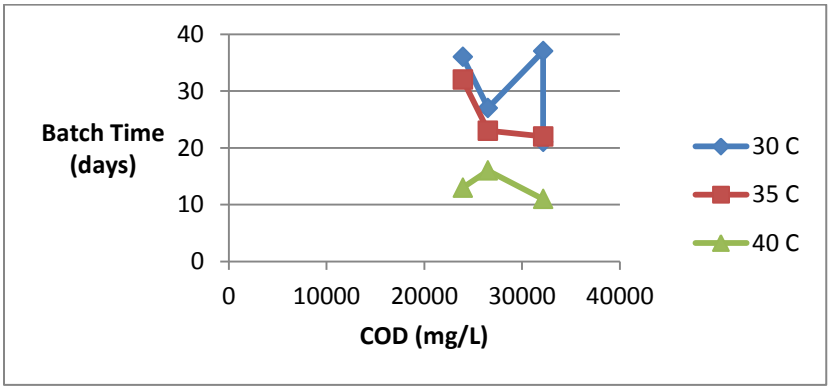

(b)

Fig. 4.49 – COD (mg/L) vs. Batch time at different temperatures for (a) synthetic vinasses and (b) real vinasses.

For synthetics, Composition 3 (synthetic and high) had the highest batch time for 30 ^{0}C and 35 ^{0}C. At 40 ^{0}C, some toxicity must have caused the early death of the reactor. There is an increase in batch time with increasing COD at all temperatures (except for Composition 3 at 40 ^{0} C). In real vinasse there are no trends between the COD and batch time. Synthetic vinasse is easy to break, and thus can be operated for a long time.

Real vinasse is a challenge for the microbes and possibility of toxicity can be there; thus batch times are comparatively shorter.

4.2.2 BOD analysis

4.2.2.1 By Temperature

According to US Clean Water Act, BOD is considered as a conventional pollutant. BOD and COD are similar in function, as both measure the organic matter in water. However, COD is more general, measuring all the matters that are chemically oxidized. BOD specifically targets biodegradable compounds. BOD of vinasse is normally very high, ranging between 17,000 to 50,000 mg/l (Carmen, 2006). The untreated vinasse, if disposed of in water or soil, as is practiced in many parts of the world, will cause severe water and soil pollution.

The removal percent of BOD was calculated by subtracting the final BOD (measured at the last day of the resident time) from the initial BOD (BOD measured at the beginning of the run , after adding sludge), then dividing by the initial BOD and multiplying it by 100. Table 4.4 depicts the BOD removal for different compositions. As expected, the synthetics had higher BOD removal than the real vinasses.

Table 4.5 - Comparison between BOD removals (%) in different compositions.

	Temperature (°C)	BOD removal (%)
Comp1 (low and synthetic)	30	28.7
	35	46.5
	40	39.9
Comp2 (medium and synthetic)	30	75.1
	35	47
	40	33.7
	40 duplicate	27.6

Table 4.5 continued

Comp3 (high and synthetic)	30	25.9
	35	17.7
	40	10.2
Comp4 (low and real)	30	8
	35	12
	40	7.5
Comp5 (high and real)	30	9.5
	30 duplicate	4.9
	35	4.8
	40	3.4
Comp6 (medium and real)	30	2.4
	35	8.1
	40	9.5

This particular section discusses the BOD trends of the 6 different types of vinasse at 3 different temperatures. Below is the figure of BOD vs. time at the three different temperatures for Composition 1.

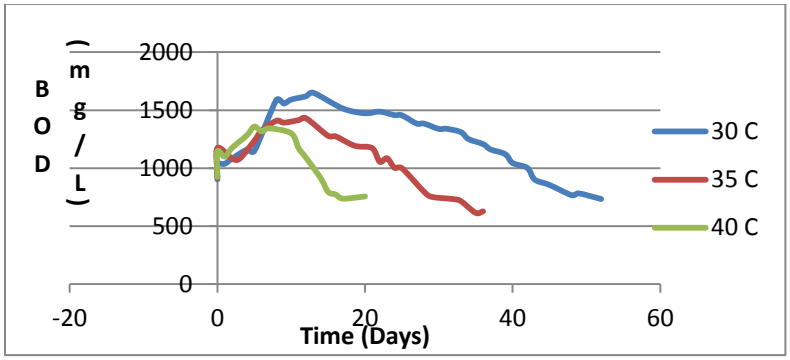

Fig. 4.50 – BOD vs. Time for Composition 1 (low and synthetic COD) at three different temperatures.

The BOD removal at 30 ^{0}C was 28.7%. At 35 ^{0}C, the percent removal was 46.5% and at 40 ^{0}C the removal was 39.9%. So for this particular synthetic composition, the removal percent increased with the temperature.

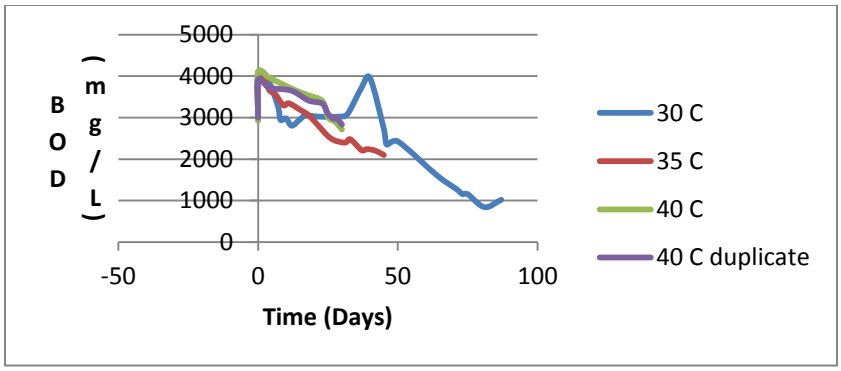

Fig. 4.51– BOD vs. Time for Composition 2 (synthetic and medium COD) at three different temperatures

Composition 2 is also synthetic. At 30 ^{0}C the BOD removal percent was 75.1%, at 35 ^{0}C the removal percent was 47% and at 40 ^{0}C the BOD removal is 33.7%. For this particular combination, the BOD removal decreases with increasing temperature. This makes sense since the operation time was greater at 30 ^{0}C: vinasse had more time to be degraded, though at a slower pace. A duplicate was run at 40 ^{0}C which exhibited a similar pattern of BOD removal.

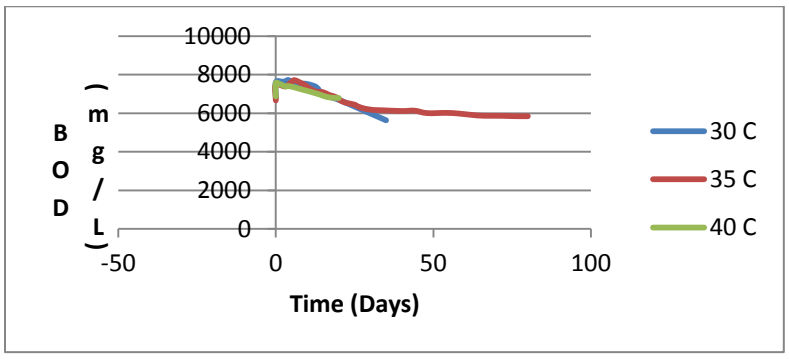

Fig. 4.52– BOD vs. Time for Composition 3 (synthetic and high COD) at three different temperatures

Composition 3 is synthetic, too. The BOD removal at 30 ^{0}C was 25.9%. At 35 ^{0}C, the BOD removal was 17.7% and 40 ^{0}C the removal was 10.2%. There is a lower in

efficiency in terms of BOD removal with increasing temperature. Again, the more is the resident time, the more is the removal percent of BOD. Figure 4.49 depicts the BOD vs. Time for Composition 3.

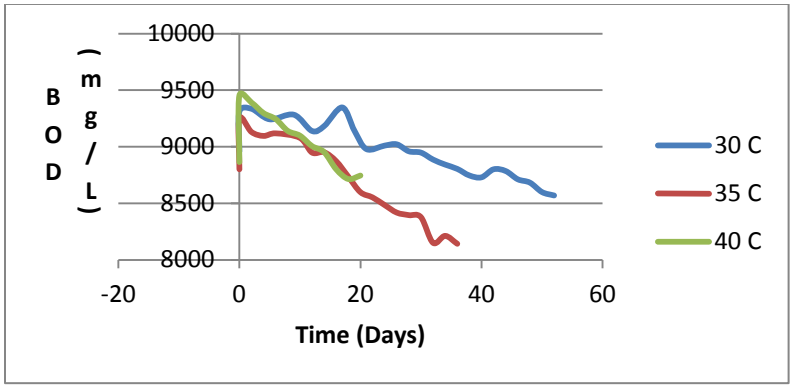

Fig. 4.53 – BOD vs. Time for Composition 4 (real and low COD) at three different temperatures

Composition 4 was the concentrated vinasse from Hereford and a little glucose was added to it. The BOD removal at 30 ^{0}C was around 8%. At 35^{0} C the anaerobic treatment was able to remove 12% and at 40 ^{0}C the removal was 7.5%. The efficiency was considerably lower compared to previous compositions. This particular composition had real vinasse and as expected, the constituents were much harder to degrade, resulting in lower BOD removal. Figure 4.50 depicts the BOD vs. Time for Composition 4.

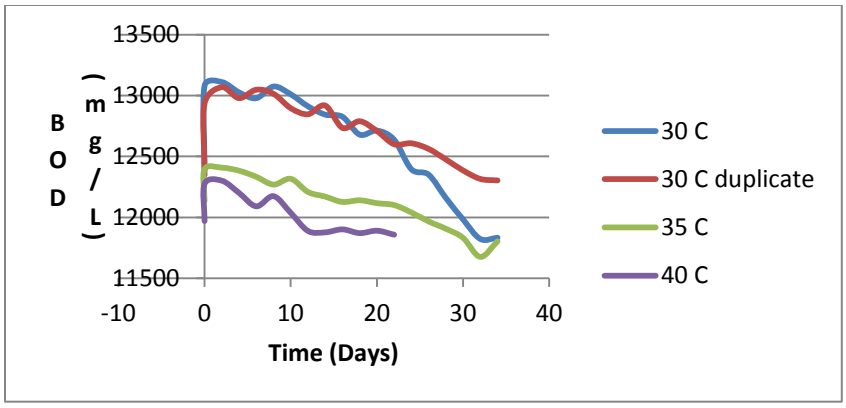

Fig. 4.54 – BOD vs. Time for Composition 5 (real and high COD) at three different temperatures

Composition 5 had 4 L of liquid real vinasse from White Energy. Figure 4.51 depicts the BOD vs. Time for Composition 5. At 30 ^{0}C the removal was 9.5%. At 35 ^{0}C, the removal was 4.8% and at 40 ^{0}C it was 3.4%. There was a duplicate at 30 ^{0}C, which had a removal rate of around 4.9%. The removal percent was very low. Many researches have obtained higher removal efficiencies with real vinasse. Carmen (2006) stated that a 90% BOD removal is possible in an anaerobic digestion method. Our lower rate may be due to the kind of vinasse we used. Each plant has its own unique composition. Another reason can be the kind of microbes used to seed the reactors. Microbes play the key roles in this treatment. It is an absolute necessity to provide the right kind and the optimum environment for the microbes.

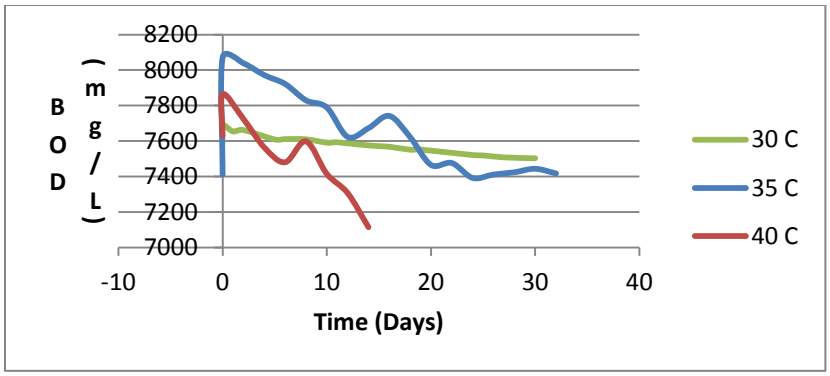

Fig. 4.55 – BOD vs. Time for Composition 6 (real and medium COD) at three different temperatures

Composition 6 had 3.5 L of liquid vinasse. Figure 4.52 depicts the BOD vs. Time for Composition 6. The reactor at 30 ^{0}C did not work as expected. Only 2.4% removal of BOD was observed. At 35 ^{0}C, the BOD removal was 8.1% and at 40 ^{0}C the removal rate was 9.5%. This too had low efficiency.

4.2.2.2 By Composition

It is interesting to see how compositions impacts BOD removal, provided temperature and other parameters remain constant. Below are the figures (Fig. 4.53 – Fig. 4.55) of the BOD removal of real and synthetic vinasses at 30, 35 and 40 ^{0} C.

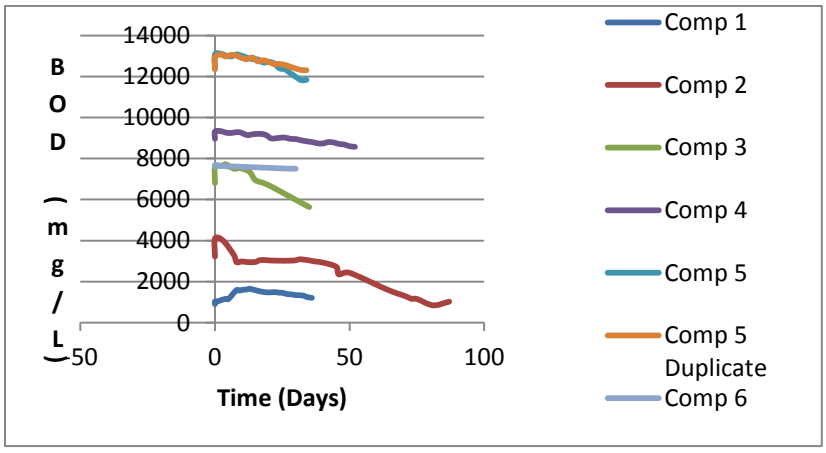

Fig. 4.56 – BOD of synthetic and real vinasse at 30 ^{0}C

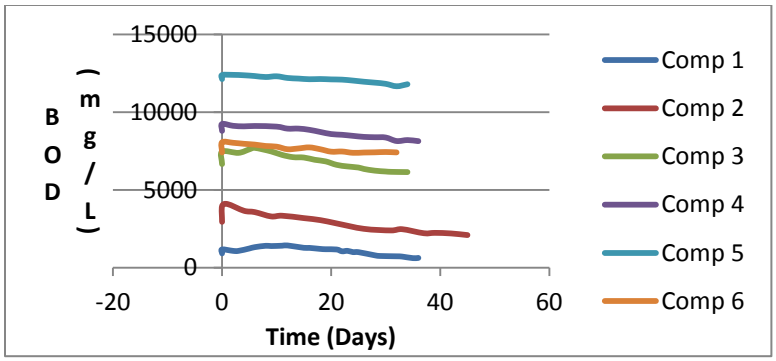

Fig 4.57– BOD of synthetic and real vinasse at 35 ^{0}C

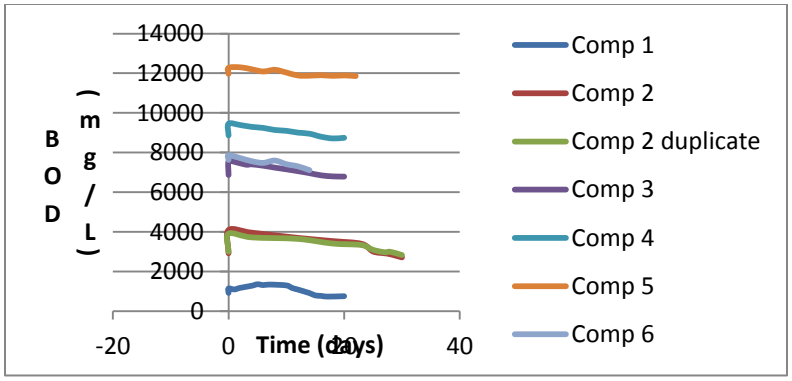

Fig. 4.58 – BOD of synthetic and real vinasse at 40 ^{0}C

Like all the other parameters, synthetics performed substantially better in terms of removal of BOD than the real vinasse. The reason is the simple composition (like glucose) of synthetic vinasses, whereas real vinasse is comprised of much complex materials.

4.2.3. Relationship between methane generation and COD and BOD removal

It is expected that the greater the methane generation, the greater would be the removal of COD and BOD. Below is the table for the cumulative methane generation and COD and BOD removal.

Table 4.6 - Cumulative methane generation and COD and BOD removal.

	Temp. (C)	Peak methane Conc. (%)	Cumulative methane generation (mL/L)	Batch Time (days)	COD removal (%)	BOD removal (%)
Comp1 (low and synthetic)	30	37.4	296.1	32	36.2	28.7
	35	19.9	271.9	16	36.5	46.5
	40	38.6		18	52.3	39.9
Comp2 (medium and synthetic)	30	74.1	1655.6	56	71	75.1
	35	81.5	1305.2	39	46	47
	40	81.1	4846.7	31	40	33.7
	40 dup.	80.7	4937	32	40	27.6
Comp3 (high and synthetic)	30	87.9	14706.9	87	27.6	25.9
	35	87.7	7935.9	89	40	17.7
	40	44.6	1042.9	11	13.3	10.2
Comp4 (low and real)	30	31.8	771.5	36	20	8
	35	78.2		32	20	12
	40	29.6	821.8	13	10	7.5
Comp5 (high and real)	30	24	565.9	37	10.3	9.5
	30 dup.	29.9	586	21	9.6	4.9
	35	48.3	477.6	22	10	4.8
	40	34.5	598.1	11	9.1	3.4
Comp6 (medium and real)	30	2.3	36.1	27	4.1	2.4
	35	41.1		23	11.4	8.1
	40	25.2	280.1	16	10	9.5

Cumulative methane generation is measured in ml/L. Batch time is the time that the reactor generated methane gas. For most reactors, samples were analyzed until the end of the batch time. However, in one case, Composition 3 at 30 ^{0}C, samples were

measured fewer days than batch time. The COD and BOD removal is expressed in percentage. The initial value is taken as the amount after adding the sludge. The final value is the last day water analysis was conducted.

For Composition 1, the highest removal of COD was at 40^0C, and the highest removal for BOD is at 35 ^{0}C. Thus for this composition no relation between COD and BOD removal is observed, meaning if there is high COD removal, there will not necessarily be high BOD removal. . Even though all of the glucose should be removable as COD and BOD, the sludge added will have some non-biodegradable components. Since the sludge added was not uniform for all reactors, the BOD and COD percent removal may not correlate. The methane accumulation was similar for 30 and 35 ^{0}C. Methane volume for 40 ^{0}C was not available thus cannot say if the high COD removal was related to the high methane generation.

Composition 2 had the highest methane generation for 40 ^{0}C. However, the maximum COD and BOD removal was for 30 ^{0}C. The batch time was longer for 30 ^{0}C than the other two reactors. The COD and BOD removal for 35 ^{0}C and 40 ^{0}C was close. However, the relation with methane cannot be determined even in this combination. The 40 ^{0}C reactor generated the highest methane volume but the least COD and BOD removal.

Composition 3 had the highest methane generation for 30 ^{0}C, but the COD removal was not the highest. At this temperature, water analysis was conducted only for 41 days instead of the entire 87 days of the batch time. Since the reactor was active for more than 41 days, it is possible that more degradation of compounds occurred. However, it cannot be said if it would have reached the maximum removal of COD. At 30 ^{0}C, we did reach the highest BOD removal. There seems to be no relation between the

rate of COD and BOD removal within a reactor. At 35 ^{0}C, methane generation was higher than that of 40 ^{0}C. COD and BOD degradation was higher for 35 ^{0}C.

Composition 4 was hybrid. Volume of methane generation was not available for 35 ^{0}C. 30 ^{0}C and 40 ^{0}C had similar methane generation. COD removal was almost double for 30 ^{0}C (20%) than that of 40 ^{0}C (10%). BOD removal was similar for both reactors.

Composition 5 was real vinasse with the maximum initial COD. The cumulative methane generation was similar at all temperatures, including the duplicate at 30 ^{0}C. COD removal was similar for all the reactors. However, at 30 ^{0}C, BOD removal was maximum, almost double (in some cases more than double). The only explanation is the longer batch time for 30 ^{0}C. The longer the batch time, the greater is the BOD removal.

Composition 6 was also real vinasse. The 30 ^{0}C did not perform well because of thin sludge. The methane generation at 35 ^{0}C was not available. Only the reactor at 40 ^{0}C had worked well and also has the methane volume data. So no comparison can be done.

From these comparisons no definitive conclusions can be made regarding the relationship between methane generation and COD and BOD removal. One reason for such behavior is that when the organic compounds are broken, methane is not the only compound that is formed. Carbon dioxide or similar simple compounds are formed that has not been measured. Another reason is obviously the leakage of methane that can occur during measurement of volume, or from the reactor during the treatment.

Some literatures have emphasized on the importance of BOD : COD ratio. The ratio can explain if the waste has reached a stable state or not. Barlaz (2006) stated that at the end of the final stage of a landfill, the BOD;COD ratio of the leachate becomes less than or around 0.1. No prior work on the BOD:COD ratio of vinasse has been

conducted to our knowledge. Figure 4.59 depicts the BOD/COD ratio for Composition 2 at three different temperatures. Nothing can be understood from the graph. We would expect the ratio to decrease during the final stage of the reactor. The graph is undulating and does not decrease or becomes stable at the end. Anaerobic treatments involving vinasse can be very unpredictable. The BOD might not decrease at the same rate as the COD will. Thus such analysis was not meaningful for our study.

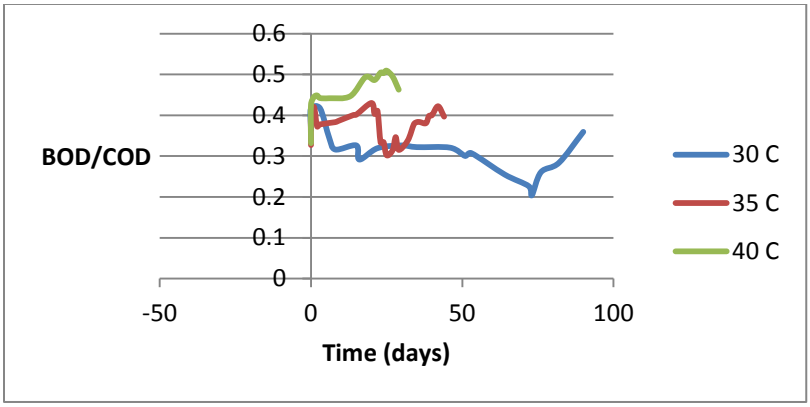

Fig. 4.59 - Comparison between BOD/COD ratio and time for Composition 2 (synthetic and medium COD).

The overall decrease of COD and BOD is less than satisfactory for final vinasse treatment, and must be supplemented by additional processes. This was expected. Anaerobic treatment is mostly chosen for generating energy. As mentioned in detail in Chapter 2, Belhadj (2013) worked with the anaerobic treatment of vinasse obtained from the production of ethyl alcohol in Morocco. The study generated biogas but failed to decrease the organic load of the waste. The author believes it is due to the accumulation of non-biodegradable waste.

4.2.4. Relationship between species richness, Faith PD and COD and BOD removal.

This part is dedicated to finding any relationship between the species richness and the removal of pollutant. It is hypothesized that the greater the microbial diversity, the greater will be the degradation of the organic compounds in the vinasse.

Biodiversity has been defined by Gaston (1996) as the *biology of numbers and difference*. Thus the more species types, the greater are the common metrics of biodiversity like species richness and evenness. Faith (1992) defined phylogenic diversity, "PD", *as the minimum total length of all the phylogenetic branches required to span a given set of taxa on the phylogenetic tree.*

Sabnis (2014) measured the species richness and Faith's PD for the anaerobic treatment of vinasse conducted in this research. Table 4.7 and Fig. 4.60 below examine whether there is any relationship between COD/BOD removal and the species richness. The table and figure show the highest level reached in terms of Faith's PD and species richness for each reactor. From the graph, it seems that there is some kind of upward trend between both COD or BOD removals and species richness. However, trying to fit the curves with trend lines was not that successful. The R^2 were very low for the exponential curves (shown below in Fig. 4.60) and also for other curves, too.

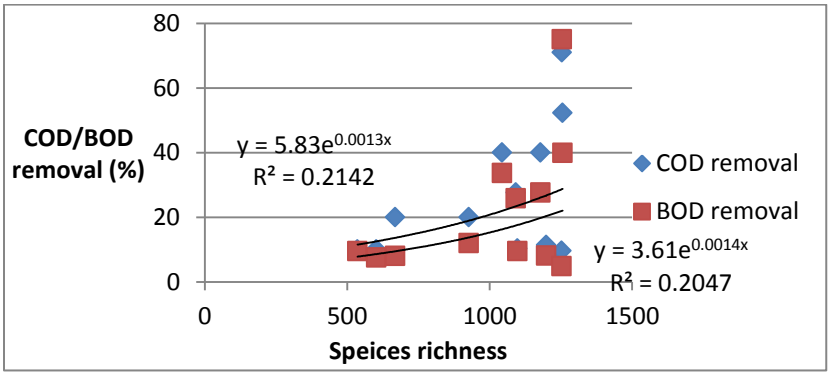

Fig. 4.60 - Comparison between species richness and COD/BOD removal

Table 4.7- Species richness and BOD and COD removal (%)

	Temp.(C)	Species richness	Faith's PD	Batch Time (days)	COD removal (%)	BOD removal (%)
Comp1 (low and synthetic)	30			32	36.2	28.7
	35			16	36.5	46.5
	40	1256	71.	18	52.3	39.9
Comp2 (medium and synthetic)	30	1253	69.	56	71	75.1
	35			39	46	47
	40	1043		31	40	33.7
	40 duplicate	1177		32	40	27.6
Comp3 (high and synthetic)	30	1092	59	87	27.6	25.9
	35			89	40	17.7
	40			11	13.3	10.2
Comp4 (low and real)	30	668	39	36	20	8
	35	927	59	32	20	12
	40	602	32	13	10	7.5
Comp5 (high and real)	30	1097		37	10.3	9.5
	30 duplicate	1251		21	9.6	4.9
	35			22	10	4.8
	40			11	9.1	3.4
Comp6 (medium and real)	30			27	4.1	2.4
	35	1198	68	23	11.4	8.1
	40	536	30	16	10	9.5

The table and figure suggest that there is no strong relationship between the maximum species reached and the BOD or COD removal. It is the methanogens that are highly responsible for methane generation and hence degradation of pollutants. A

comparison between the methanogens and methane generation and water quality removal is recommended in the future.

4.2.5 Ammonia- N

There was no significant reduction of ammonia- N in the reactors. In fact, in some combination, the ammonia – N level increased. According to previous studies in the literature, anaerobic treatment does not decrease the ammonia level. The six combinations at 35 ^{0}C are shown in Figure 4.54. The ammonia levels at 30 ^{0}C and 40 ^{0}C are in Appendix A.

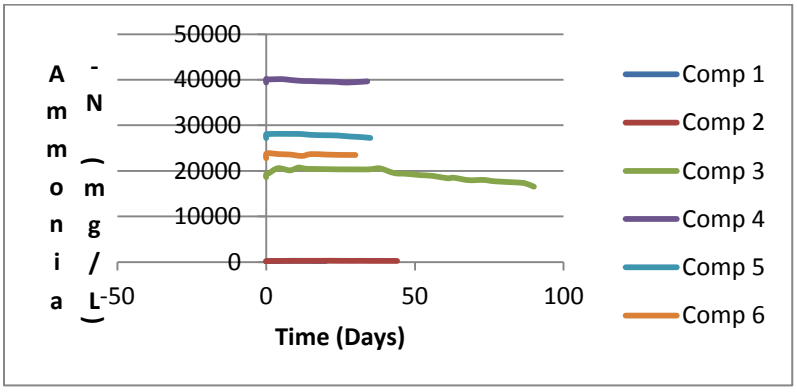

Fig. 4.61 – Ammonia – N at 35 ^{0}C for the six compositions.

4.2.6 Potassium – K

The potassium measured during the anaerobic digestion also shows no decrease from the initial value. The potassium level at 35 ^{0}C for the six combinations is depicted in the following figure. The levels for 30 ^{0}C and 40 ^{0}C are in the Appendix.

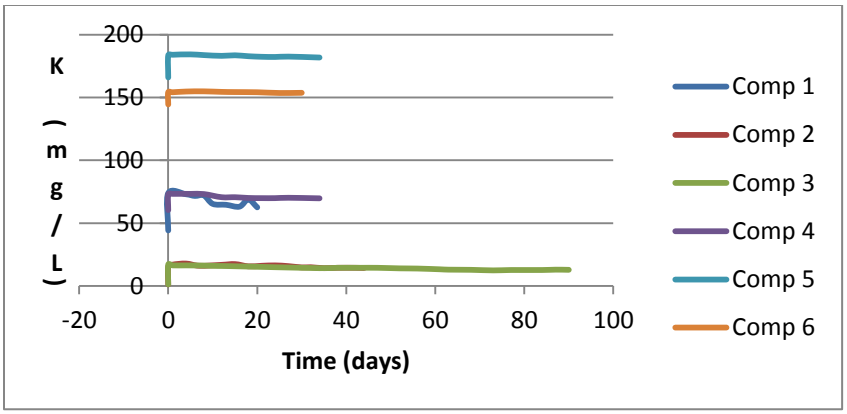

Fig. 4.62 – K at 35 ^{0}C for the six combinations

4.2.7 Phosphorus – Ortho phosphate.

No significant changes in the 0rtho phosphate level was found as shown in the following figure.

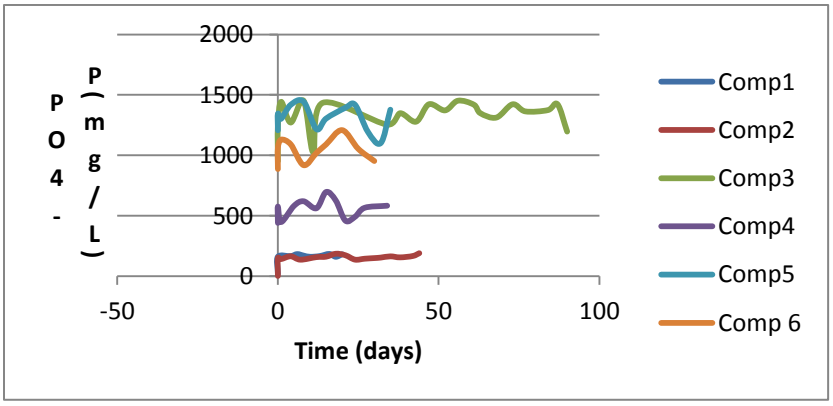

Fig. 4.63 – P at 35 ^{0}C for the six combinations

4.2.8 Sulfur – Sulfate

Sulfate has very little changes. It was expected to have higher changes in sulfur due to the formation of hydrogen sulfide. However, no significant decline in sulfur was found in our experiment, for reasons that are unclear. The figure shows the sulfur level at 35 ^{0}C.

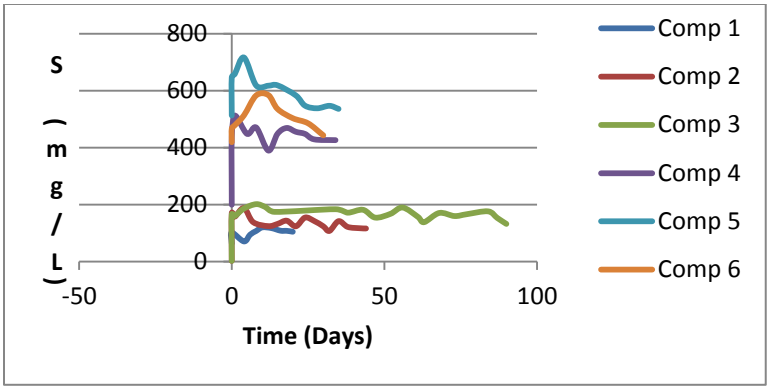

Fig. 4.64 – S at 35 ^{0}C for the six combinations.

4.2.9 Other parameters

Water quality parameters like Total Dissolved Solids (TDS), Conductivity, Total Suspended Solids (TSS) and Volatile Suspended Solids (VSS) were measured before the start of the reactors and after the reactors are dismantled. No significant changes were seen in the parameters. In fact, in many cases, there was an increase of the pollutant level. The two tables below show initial and final values for the various parameters.

Table 4.8 – TDS and Conductivity of the 6 compositions at 3 different temperatures

	Temperature (^{0}C)	30		35		40	
	Parameters	Initial	Final	Initial	Final	Initial	Final
Comp 1	TDS(mg/L)	468	489	420	443	510	519
	Conductivity(us/cm)	821	855	807	864	917	922
Comp 2	TDS(mg/L)	581	603	630	669	597	626
	Conductivity(us/cm)	1062	1105	1178	1219	1097	1124
Comp 3	TDS(mg/L)	1030	1095	1024	1066	1044	1123
	Conductivity(us/cm)	1847	1946	1739	1742	1924	2013
Comp 4	TDS(mg/L)	866	905	820	834	826	821
	Conductivity(us/cm)	1561	1614	1413	1423	1421	1413

Table 4.8 continued

Comp 5	TDS(mg/L)	1012	1026	1029	1121	1035	1108
	Conductivity(us/cm)	1842	1867	1982	2063	1926	1965
Comp 6	TDS(mg/L)	1158	1193	1128	1145	1137	1174
	Conductivity(us/cm)	2185	2194	2068	2098	2044	2086

As expected, the real vinasses had higher TDS and conductivity because of the visible solids in the compositions. For the synthetic vinasses, sludge is the only source of solids.

Table 4.9 - TSS and VSS of the 6 compositions at 3 different temperatures

	Temperature (^{0} C)	30		35		40	
	Parameters	Initial	Final	Initial	Final	Initial	Final
Comp 1	TSS (mg/L)	386	394	297	294	371	369
	VSS (mg/L)	245	265	252	237	326	328
Comp 2	TSS (mg/L)	473	468	458	451	409	439
	VSS (mg/L)	297	285	397	399	357	361
Comp 3	TSS (mg/L)	63	60	267	279	297	343
	VSS (mg/L)	56	55	240	245	254	268
Comp 4	TSS (mg/L)	467	471	521	488	496	452
	VSS (mg/L)	406	401	392	428	385	372
Comp 5	TSS (mg/L)	396	400	414	429	393	384
	VSS (mg/L)	361	358	387	396	347	349
Comp 6	TSS (mg/L)	351	345	367	389	355	328
	VSS (mg/L)	313	311	327	351	316	300

The increase in the parameters (like TDS and TSS) may have been due to an increase in the microbe population, and the dead cells contributed towards the increase of TSS and VSS. Composition 3 at 30 ^{0}C had relatively low TSS and VSS compared to Composition 3 at 35 ^{0}C and 40 ^{0}C and the other compositions. Composition 3 is synthetic and the only source of solids is the sludge. Thus, there must be some

discrepancy in the sludge composition when this particular run was conducted. As discussed before, sludge composition can vary.

Chapter 5

Multiple Linear Regression Analysis

In this chapter the multiple linear regression (MLR) analyses of the first-order reaction rate constants of COD (K_{COD}) and BOD (K_{BOD}) are discussed. It is believed that COD is related to five variables (T, K, N, P and S). Thus, the first-order reaction rate constant of COD (K_{COD}) and the other five parameters were studied. In the same way the relationship between K_{BOD}, first-order reaction rate constant of BOD and the six parameters were also analyzed.

5.1 Preliminary Multiple linear regression model

A multiple linear regression model in the form of the following equation is preliminarily developed:

$$Y = \beta_0 + \beta_1 X_1 + \beta_2 X_2 + \beta_3 X_3 + \beta_4 X_4 + \beta_5 X_5 + \epsilon$$

where the response variable (Y) is the K_{COD} or the K_{BOD} , $X_1, X_2 \ldots\ldots X_5$ are the predictor variables T, K, N, P and S and ϵ is the random error. Y would become ϵ if all the parameters are made zero. The Y intercept in the linear regression is the parameter β_0, and the slope parameters $\beta_1, \ldots, \beta_5$, represent how T, K, N, P and S are related to the response K_{COD} or K_{BOD}.

The MLR model building process consists of four phases:

1- Data collection

2- Model search

3- Model selection

4- Model validation

5.2 Obtaining k values

For our study, due to limitations in data points and resources, k is considered as the decreasing rate of COD or BOD. k values for each reactor were obtained using

EXCEL, assuming that the COD or the BOD followed a first-order trend with time. The Levenberg-Marquardt algorithm (LMA) was used to compute k_{COD} and $k_{BOD.}$ It is also known as the damped least-squares (DLS**)** method and is commonly used to compute non- linear least squares problems. The reactor with Composition 2 at 30 °C for COD was excluded from the model because it visibly did not follow the first-order trend. The fitted curve generated by EXCEL with an equation on the COD or BOD vs. time was used to obtain the k_{COD} and k_{BOD}. Some are shown below and the rest are in the Appendix A. The R^2 of all the graphs for COD are above 0.75. Table 5.1 shows k_{COD} , k_{BOD} , composition numbers, temperature and waste compositions.

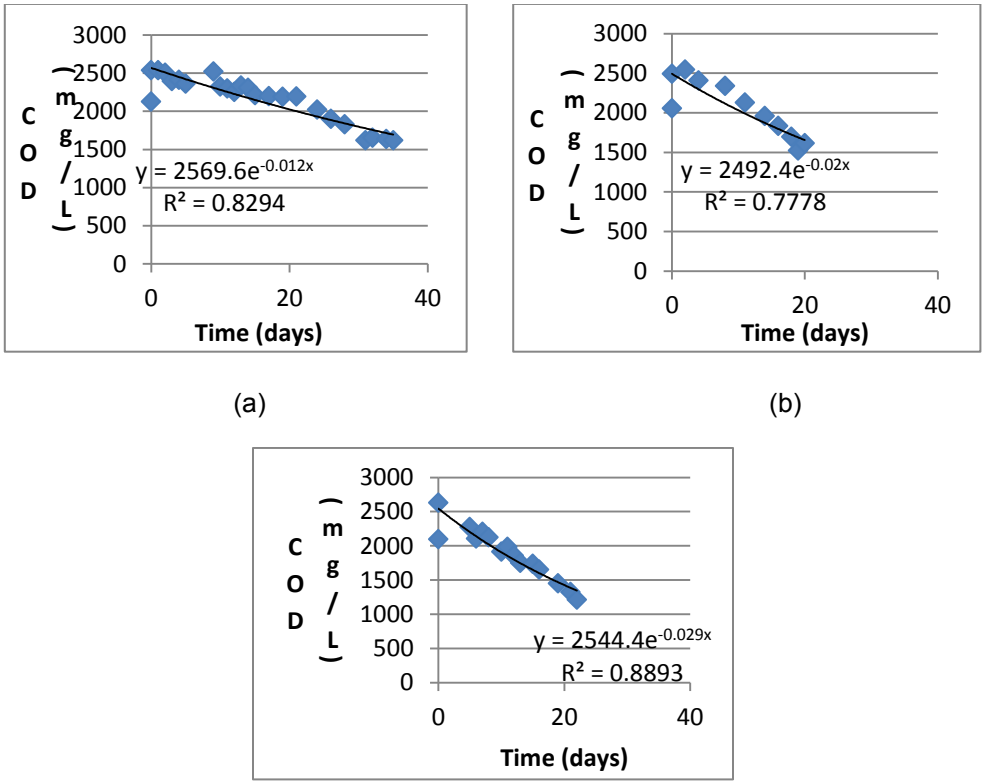

(a) (b)

(c)

Fig. 5.1 – k_{COD} for the vinasse composition 1 (synthetic and low COD) at a.) 30 ^{0}C, b.) 35 ^{0}C and c.) 40 ^{0}C

Calculating k_{BOD} was a little different than calculating k_{COD}. BOD in most reactors tends to increase for some days and then starts to decrease. Since the k is dependent on the assumption of first-order decay, the increasing trend has been omitted while calculating k_{BOD}. An example is shown in Fig. 5.2.

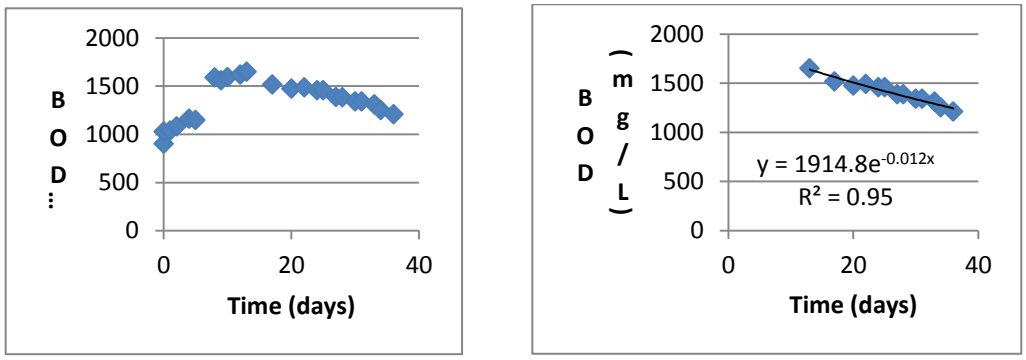

Fig. 5.2- k_{BOD} for the composition 1 (synthetic and low COD) at 30 ^{0}C

For Composition 1 at 30 ^{0}C, the BOD increased for the first 13 days. Then it started to decrease. While calculating k, we omitted the first 12 days and started from the 13th day to the last day of operation. The rest of the k_{BOD} graphs are in Appendix A. The R^2 for all the graphs for BOD are above 0.77. With our limited data points, it was impossible to incorporate the ascending k and the descending k in a single model that would achieve statistical significance. However, it is recommended to conduct research with more real vinasses and include multiple ks in the model development.

Table 5.1– Data Used in Model Building

Composition	k_{COD} (/day)	k_{BOD} (/day)	Temp (^{0}C)	Waste Composition			
				N	P	K	S
1	0.012	0.012	30	185	164	71	83
2		0.025	30	219.12	131.76	22.94	123.53
2	0.008	0.009	30	19055.88	1167.50	12.35	152.35
4	0.006	0.002	30	40095.44	665.74	84.41	438.97
5	0.002	0.003	30	28644.26	1386.32	165.29	624.85
5	0.002	0.002	30	27422.21	1468.23	167.35	642.06
6	0.001	0.0007	30	23689.26	1137.05	146.76	615.44
1	0.02	0.036	35	183.82	161.61	73.82	101.32
2	0.013	0.015	35	203.82	151.32	15	170.29
3	0.006	0.003	35	19252.65	1239.55	16.91	165.44
4	0.008	0.004	35	40173.24	577.06	72.94	436.32
5	0.003	0.002	35	28034.85	1344.56	183.38	646.03
6	0.004	0.003	35	23718.24	1061.47	154.12	465.88
1	0.029	0.05	40	192.64	176.91	85.88	68.09
2	0.018	0.013	40	209.71	187.35	21.76	145.44
2	0.018	0.01	40	203.53	175.59	20.44	161.18
3	0.007	0.006	40	19159.56	1314.56	11.03	127.06
4	0.006	0.004	40	39948.24	762.65	88.09	409.41
5	0.009	0.002	40	28357.06	1505.29	169.41	657.5
6	0.004	0.006	40	23948.09	1065.44	165.29	630.44

5.3 Modelling k_{COD}

5.3.1 Scatter Plots Matrix and Correlation Matrix

The first job is the analysis of the relationship between response predictor and predictor variables using the matrix scatter plot and the coefficient of correlation table. A scatter-plot matrix simply organizes all of the pairwise correlation information as shown in Figure 5.3. The most desirable trend is random for predictor variables (x vs. x). Any kind of upward or downward trend indicates multicollinearity. It seems S and K, S and P and P and K show an upward trend.

The matrix of Pearson correlation coefficients (Table 5.2) is another way of evaluating linear dependence among variables. The r values ranges from -1 to +1. The lower the negative numbers are (i.e, closer to -1) and the higher the positive numbers are (i.e. closer to +1), the stronger is the linear correlation between the variables. The table shows that S and K (0.87719) and S and N (0.72733) have r values greater than 0.7. This indicates there can be some issues with multicollinearity.

For the response vs. predictor graphs (y vs x), we expect a trend. Figure 5.3 states that there is clearly a linear downward relationship between COD vs. P and COD vs. S. COD vs. T also has a trend. COD vs. N and COD vs. k might have a relationship. It is not clear from the scatter plot.

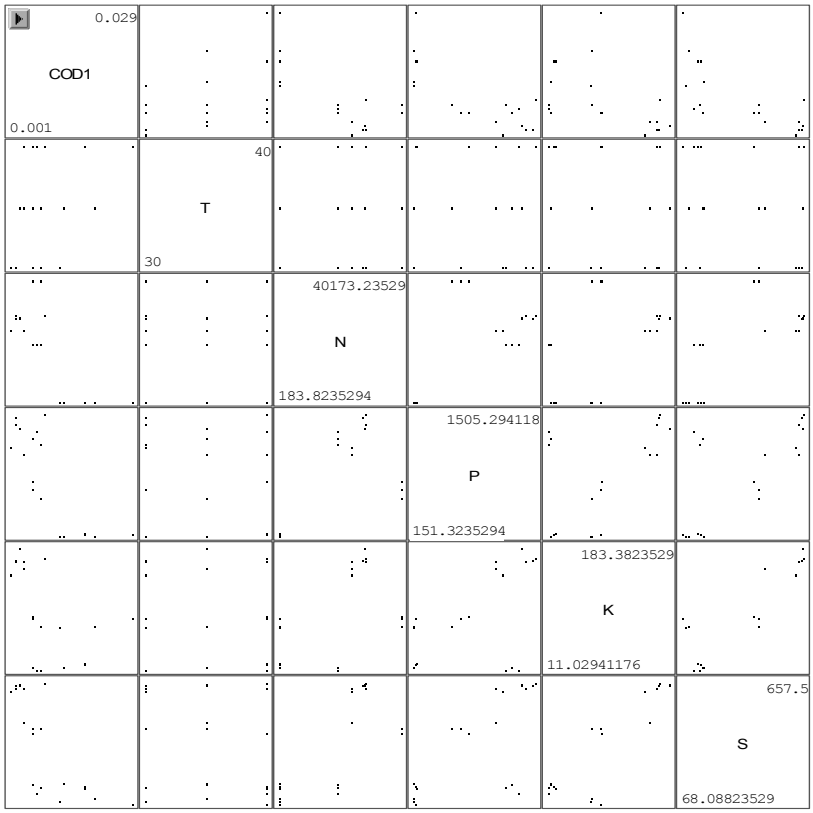

Fig. 5.3 - Matrix Scatter plot

Table 5.2 - Correlation Matrix of k_{COD} and the Predictor Variables

Pearson Correlation Coefficients, N = 19

	T	N	P	K	S
T	1.00000	-0.20661	-0.20513	-0.18169	-0.20128
N	-0.20661	1.00000	0.65596	0.48003	0.72733
P	-0.20513	0.65596	1.00000	0.53505	0.68484
K	-0.18169	0.48003	0.53505	1.00000	0.87719
S	-0.20128	0.72733	0.68484	0.87719	1.00000

5.3.2 Fitting a Preliminary Model

Table 5.3 below shows the preliminary results of regressing K_{COD} with the five predictor variables – temperature, ammonia, potassium, phosphorus and sulfur. It also contains the coefficient estimates, and the ANOVA (Analysis of Variance) table.

Table 5.3 - ANOVA Table, Preliminary Model and the Parameter Estimates.

Analysis of Variance

Source	DF	Sum of Squares	Mean Square	F Value	Pr > F
Model	5	0.00089527	0.00017905	17.98	<.0001
Error	13	0.00012947	0.00000996		
Corrected Total	18	0.00102			

Root MSE	0.00316	R-Square	0.8737
Dependent Mean	0.00947	Adj R-Sq	0.8251
Coeff Var	33.31085		

Parameter Estimates

Variable	DF	Parameter Estimate	Standard Error	t Value	Pr > |t|	Variance Inflation
Intercept	1	0.00488	0.00684	0.71	0.4879	0
T	1	0.00040603	0.00018061	2.25	0.0426	1.06027
N	1	-6.87885E-8	8.775722E-8	-0.78	0.4472	2.98144
P	1	-0.00000608	0.00000208	-2.93	0.0117	2.10680
K	1	0.00006470	0.00002774	2.33	0.0364	5.66642
S	1	-0.00002611	0.00001003	-2.60	0.0218	9.78348

K = 0.00488 + 0.000406T – 6.879E-8N – 0.00000608 P + 0.0000647 K

5.3.3 Model Assumptions Check

Before the preliminary model analysis can be considered valid, it is essential to verify whether the assumptions are satisfied. The model assumptions are as follows:

1. First Assumption - The residuals have constant variance
2. Second Assumption - The current MLR form is reasonable.
3. Third Assumption - The residuals ae normally distributed.

4. Fourth Assumption - The residuals are uncorrelated.
5. Fifth Assumption - There are no outliers
6. Sixth Assumption - The predictors are not highly correlated with each other.

First assumption - The residuals have constant variance

The first assumption can be verified with the residual vs. fitted Y plot. A funnel shape graph is least desired because it indicates that the residuals does not have a constant variance. Our plot in Figure 5.5 does not show any sign of funneling but there was some curvature. Thus we preceded to the next assumption.

Second Assumption - The current MLR form is reasonable

This can be verified with the residuals vs. predictor variables plot. If the graphs do not show curvature, the linear model form assumption is acceptable. Figure 5.4 shows residual vs. P and residual vs. S graphs. The rest are shown in Appendix B. They both potentially show some curvature. Thus the MLR form is NOT reasonable. It was recommended to execute a transformation on the response variable.

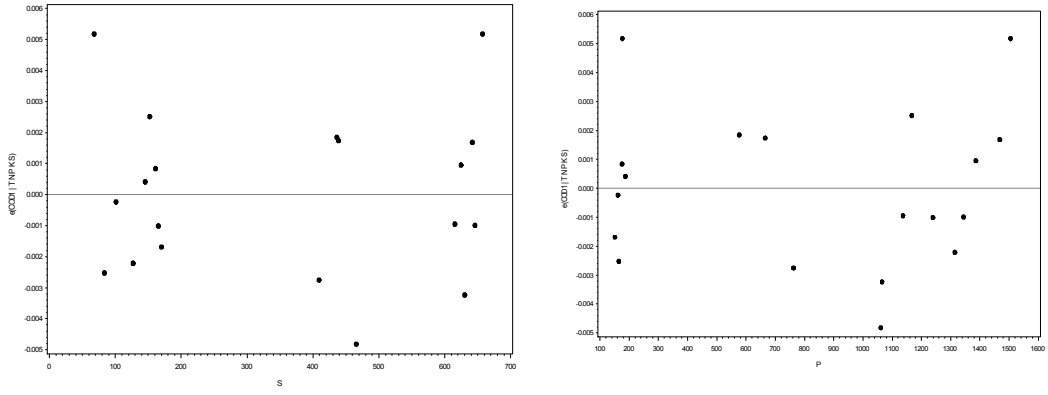

Fig. 5.4 – Residual vs. Predictor graph.

Third Assumption - The residuals ae normally distributed

The normal probability check is conducted usingy a graph where each residual is plotted against its expected value under normality. A linear trend satisfies the normality.

In our case Figure 5.6 exhibits the normal probability plot for our preliminary model. It is not straight or linear. It has a shorter tail at the top and also at the bottom. Thus assumption of normality distribution for the residuals is not correct.

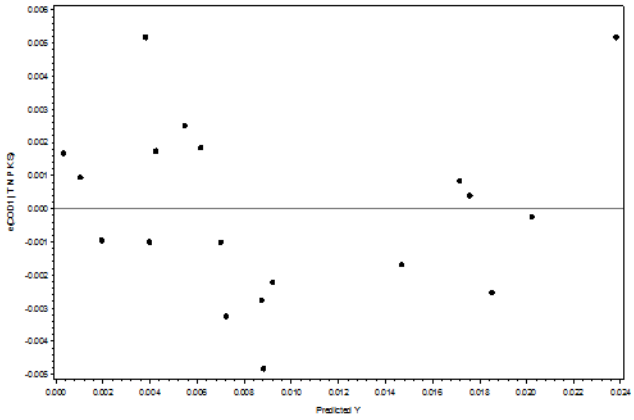

Fig. 5.5- Plot of Residuals vs. k_{COD} Fitted Values

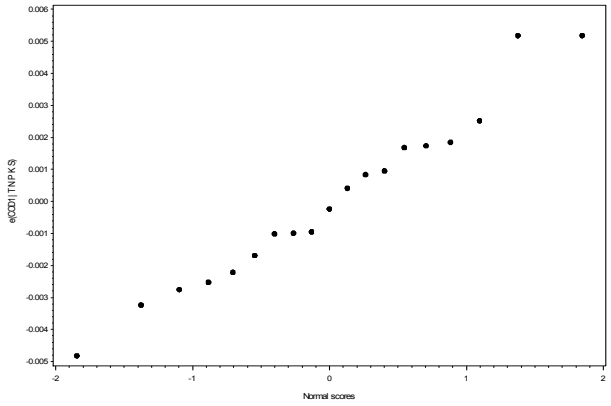

Fig. 5.6 - Normal Probability Plot

Fourth Assumption - The residuals are uncorrelated

This requires a time plot. Since the experiments were conducted at the same time, the observations cannot be correlated over time.

Thus we move to Transformation.

5.3.4 Transformation

Before proceeding any further with outlier analysis, it was decided that the preliminary model was not good enough. The residuals vs. fitted graph do not have any funneling but showed some curvature. Hence we moved forward with the residual vs. predictor graphs. Some of the residual vs. predictor graphs had curvature; thus, it was concluded that the present MLR form is not acceptable. Compression of the response variable could yield a more linear relationship. Before transforming the response variable, it is recommended to examine the normality of the residuals. Any transformation on Y will affect the distribution of Y and the distribution of the residuals. If normality is strongly satisfied, then it would be desirable to lose it via a transformation on Y. In our case, the NPP is actually quite straight, but it is not perfect. A couple of points on the right side exhibit a tail shorter than the normal distribution. Since the NPP is not perfect, we decided to move forward with a transformation on Y.

Simple transformations will be tried first. The first attempt in transformation is conducted on the response variable. The response variable k_{COD} is changed into square root of k_{COD} and the first three assumptions are checked. Appendix B contains the response vs. predictor variables and also the residual vs. fitted value of square root of k_{COD}. The normality plot is also shown in Appendix B. Constant variance was satisfied here, too. However, the residual vs. predictor graphs did not show the expected randomness.

The second transformation was conducted with logarithm (base 10) of the response variable, $\log_{10}(K_{COD})$ and the constant variance and normality assumptions were checked, after fitting the regression model. This had the best result in the normality

check and also in the residual vs. predictor checks. Appendix B contains the detailed plots. Thus the $\log_{10}(K_{COD})$ will be further analyzed.

The transformed model had the following equation:

$$\text{Log}_{10}(K_{COD}) = -2.78 + 0.031T + 0.0000023N - 0.00027P + 0.0012K - 0.0012S$$

Table 5.4 – Parameter estimate of the transformed model

Parameter Estimates

Variable	DF	Parameter Estimate	Standard Error	t Value	Pr > |t|	Variance Inflation
Intercept	1	-2.78037	0.40014	-6.95	<.0001	0
T	1	0.03099	0.01056	2.93	0.0116	1.06027
N	1	0.00000231	0.00000513	0.45	0.6605	2.98144
P	1	-0.00027067	0.00012140	-2.23	0.0440	2.10680
K	1	0.00122	0.00162	0.75	0.4662	5.66642
S	1	-0.00118	0.00058652	-2.01	0.0661	9.78348

First Assumption - The residuals have constant variance

This assumption is satisfied. We can see in Figure 5.8 that the residual vs. predictor Y graph has no funnel shape, confirming that there is constant variance.

Second Assumption - The current MLR form is reasonable

The residual vs. predictor graphs for P and S show that the graphs are better but still some curvature might be there.

Third Assumption

Normality is still slightly off. Plot in Figure 5.9 shows slightly longer tails than the normal distribution. However, this NPP is not worse than the prior one. Thus we can move to the next assumption which is to determine the outliers.

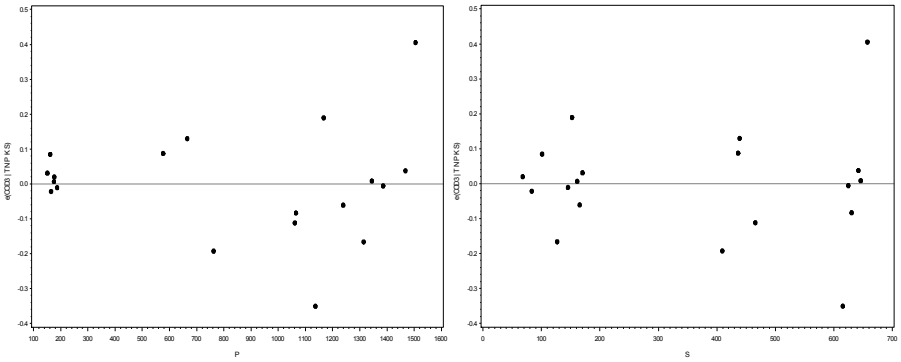

Fig. 5.7– Predictor vs. residual graphs for the transformed model

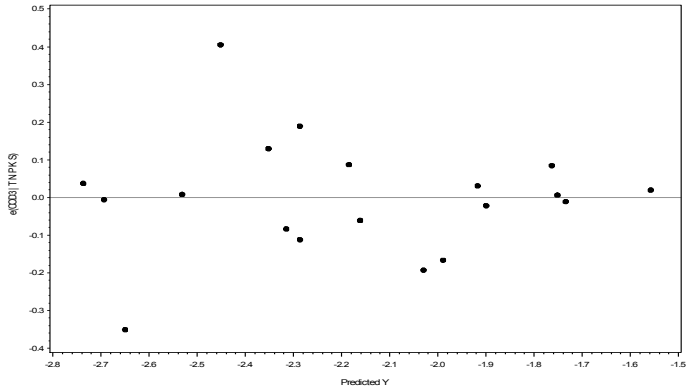

Fig. 5.8 – Residual vs. fitted value for the transformed model

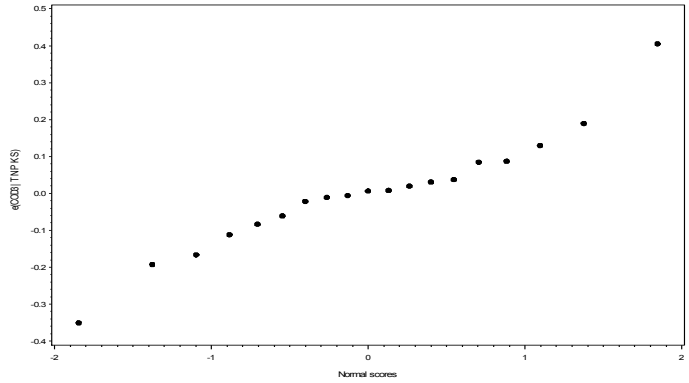

Fig. 5.9 – Normal probability plot of the transformed model

Fifth Assumption - There are no outliers

This is basically a check for the outliers. Since the first three assumptions were satisfied, we proceeded to the fifth assumption which is to check the outliers. The fourth assumption is not required in our case since it demands a time plot and our experiments were conducted around the same time.

X - Outliers

This confirms any outsider or any distant observation from rest of the data. There can be x- outliers and y - outliers. If an outlier is detected, the influence on the regression is determined.

X – Outliers are detected by Leverage values (*hii*) , where an observation with h*ii* $>\frac{2p}{n}$ is an x-outlier . Here, p is the no. of parameters and n is the no. of observations. In our case *hii* = $\frac{2*5}{19}$ = 0.526.

Table 5.5 - Residuals, Leverage Values, and Studentized Deleted Residuals

Observation	tres	hii
1	-0.10688	0.3953
2	1.30525	0.37825
3	0.9121	0.40165
4	-0.03154	0.20558
5	0.23275	0.23628
6	-2.19548	0.25084
7	0.43404	0.25218
8	0.21887	0.36495
9	-0.39526	0.30027
10	0.6006	0.38584
11	0.05341	0.18027
12	-0.64854	0.16832
13	0.18993	0.45009
14	-0.05865	0.27864
15	0.05098	0.31862
16	-1.23224	0.46387

Table 5.5 continued

17	-1.34849	0.40252
18	2.62514	0.30361
19	-0.52712	0.26292
Maximum	2.62514	0.46387

Table 5.6 – ANOVA table for the transformed model

Analysis of Variance

Source	DF	Sum of Squares	Mean Square	F Value	Pr > F
Model	5	2.19434	0.43887	12.88	0.0001
Error	13	0.44292	0.03407		
Corrected Total	18	2.63726			

Root MSE	0.18458	R-Square	0.8321
Dependent Mean	-2.17419	Adj R-Sq	0.7675
Coeff Var	-8.48976		

Sixth Assumption

Variance Inflation factor (VIF) is used to test for multicollinearity. Table 5.4 is the VIF table and it shows that the maximum VIF = 9.78, which is greater than 5. VIF greater than 5 is considered a problem.

Table 5.7 - Correlation matrix for the transformed model

Pearson Correlation Coefficients, N = 19

	T	N	P	K	S
T	1.00000	-0.20661	-0.20513	-0.18169	-0.20128
N	-0.20661	1.00000	0.65596	0.48003	0.72733
P	-0.20513	0.65596	1.00000	0.53505	0.68484
K	-0.18169	0.48003	0.53505	1.00000	0.87719
S	-0.20128	0.72733	0.68484	0.87719	1.00000

5.3.5 Interaction terms

Two or more predictors can have an interaction effect on the response variable. Thus it is important to see which interaction terms are highly correlated with the original response variable and added to the model.

Partial regression plots are constructed to determine which interaction terms can be used to improve the model. Linear trend indicates the possibility of improving the model if added to it. Figure 5.10 shows the four residual plots that were added to the model development. They all have some kind of linear trend. The rest of the residual plots are in Appendix B.

Before adding the terms, it was necessary to check the correlation status of the interaction terms. High r values in Table5.8 indicate severe multicollinearity. Standardization is a common procedure used to decrease the multicollinearity with original predictors. An example is demonstrated below.

Std (TP) =($\frac{T-Tmean}{\sigma T}$) ($\frac{P-Pmean}{\sigma P}$)

Standardization of Std (TP) is simply subtracting the T from the mean and dividing it by the standard deviation of T, and multiplying by the standardized P. Table 5.8 states that the procedure has been successful in reducing the multicollinearity.

Table 5.8 – Correlation matrix of the Interaction terms.

COD3	T	N	P	K	S	
x1x3	-0.65494	-0.00327	0.63504	0.97298	0.50453	0.64829
x1x4	-0.52868	-0.00360	0.45879	0.50486	0.97769	0.84676
x1x5	-0.68289	-0.00873	0.70500	0.65623	0.85597	0.97394
x2x5	-0.72049	-0.21749	0.89390	0.64301	0.78042	0.93912
stdx1x3	0.08270	0.09253	0.15099	0.09035	0.02854	0.00650
stdx1x4	0.22692	0.06112	0.11157	0.02908	0.04962	0.01131
stdx1x5	0.20370	0.07250	0.05533	0.00621	0.01060	-0.01215
stdx2x5	0.56573	0.10924	-0.64625	-0.68886	-0.00342	-0.31176

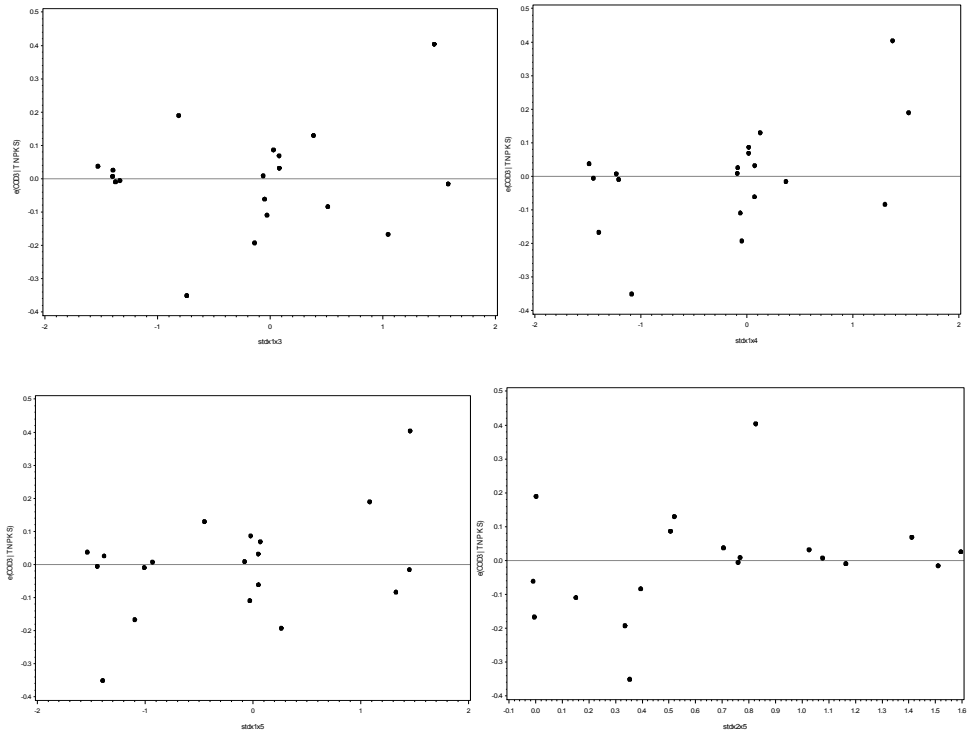

Fig. 5.10 - Partial Regression Plots

5.3.6 Model Search

With the addition of 4 interaction terms, the total number of predictor variables is now 9 :

T,N,P,K,S Std (TP),Std (TK),Std (TS) and Std (NS).

That would make a possibility of 256 models ($2^{9-1} = 256$). This is too tedious to analyze. Three widely used model search methods – Best Subsets, Backward Elimination and Stepwise Regression - will be used for our model search.

Best Subsets

Best Subset procedure, commonly known as **all possible subsets regression** procedure, is a quite comprehensive method where the response variable is regressed against every possible subset of predictor variables to achieve the best models under

each number of predictor variables. The criteria for selecting the best models are as follows:

1. High R^2, the coefficient multiple determination.
2. High adjusted R^2.
3. Low C_p values or close to p (number of parameters) criterion ($C_p \approx p$).
4. Low AIC (Akaike's information criterion) value.
5. Low SBC (Schwarz' Bayesian criterion) value.

Three potentially good models (highlighted in Table 5.9) have been chosen from the nine best subsets models. Only a few are shown below; the rest are in Appendix B. The models were chosen based on high R^2 and adjusted R^2. $C_{p,}$, AIC and SBC were also taken into consideration while choosing the models.

Table 5.9 - Partial SAS Output for Best Subset

Adjusted R-Square Selection Method

Number of Observations Read 19
Number of Observations Used 19

Number in Model	Adjusted R-Square	R-Square	C(p)	AIC	SBC	Variables in Model
4	0.9027	0.9243	5.4669	-76.5616	-71.83943	T K stdx1x4 stdx2x5
4	0.8923	0.9162	7.0091	-74.6371	-69.91487	T S stdx1x4 stdx2x5
5	0.9143	0.9381	4.8369	-78.3739	-72.70726	T N S stdx1x4 stdx2x5
5	0.9089	0.9342	5.5765	-77.2223	-71.55567	T K S stdx1x4 stdx2x5
6	0.9246	0.9497	4.6125	-80.3288	-73.71773	T N K S stdx1x4 stdx2x5
6	0.9123	0.9416	6.1709	-77.4741	-70.86306	T N S stdx1x3 stdx1x4 stdx2x5

The three highlighted models will be analyzed, that is regressed, against k_{COD}. The purpose is to select a single best model.

Backward Elimination

This method considers all the variables in the first step. Then the predictor variable with the highest *p-value in F test* (denoted Pr > F in Table) that exceeds a predetermined level (α = 0.1 in this case) is eliminated because it is statistically insignificant. Then the procedure is repeated with the eliminated variable and the steps continued until the remaining predictor variables in the model are statistically significant. This method also tries to keep the C_p value close to p.

The method picked one model, as shown in Table 5.10, which suggests that three individual predictors and two interactions makes the best model :

T, N, S, Std TK and Std NS.

Stepwise Regression Method

This method starts with no variables and allows addition and removal of variables based on the p values in F test. The SAS Output at α = 0.1 confirms the same model, shown in Table 5.11, as picked in the Backward Elimination, with the following predictor variables:

T,N,S, Std (TK) and Std(NS).

Table 5.10 – SAS Output of Backward Elimination

Backward Elimination: Step 4

Variable K Removed: R-Square = 0.9381 and C(p) = 4.8369

Variable	Parameter Estimate	Standard Error	Type II SS	F Value	Pr > F
Intercept	-3.18486	0.25188	2.00856	159.88	<.0001
T	0.03079	0.00641	0.29028	23.11	0.0003
N	0.00000743	0.00000347	0.05756	4.58	0.0518
S	-0.00129	0.00017519	0.67622	53.83	<.0001
stdx1x4	0.09441	0.02847	0.13814	11.00	0.0056
stdx2x5	0.37052	0.07142	0.33810	26.91	0.0002

Bounds on condition number: 3.6943, 50.194

--------All variables left in the model are significant at the 0.1000 level

Table 5.11 – SAS Output of Stepwise Regression

Variable	Parameter Estimate	Standard Error	Type II SS	F Value	Pr > F
Intercept	-3.18486	0.25188	2.00856	159.88	<.0001
T	0.03079	0.00641	0.29028	23.11	0.0003
N	0.00000743	0.00000347	0.05756	4.58	0.0518
S	-0.00129	0.00017519	0.67622	53.83	<.0001
stdx1x4	0.09441	0.02847	0.13814	11.00	0.0056
stdx2x5	0.37052	0.07142	0.33810	26.91	0.0002

All variables left in the model are significant at the 0.1000 level.

No other variable met the 0.1000 significance level for entry into the model.

5.3.7 Choosing the best model

Backward elimination and stepwise regression had the same model at 0.1 confidence level. Best subset, which is a comprehensive model search, has provided three possible best models. It is worth considering the three highlighted models as our potential best model. The three highlighted models have been fitted and two models (model no. 5 and 6) had an insignificant predictor. The p value of one or more of the

parameters was more than 0.1. Furthermore, the VIFs of these models were high. VIF is used to determine if multicollinearity is an issue. Any value higher than 5 is flagged. It means multicollinearity is a problem in this case. Thus the only model left is the model no. 5 with 0.9143 adjusted R^2 and 0.9381 R^2. Both adjusted R^2 and R^2 are high and close to each other. Furthermore, the model has low VIFs (all under 5) and matches with the selected model of the other two model search methods. The parameter estimate table of the chosen model is shown below in Table 5.12. The parameter estimates of the other two models are in the Appendix B.

Table 5.12 – Parameter estimates of the selected model (model no. 5)

Parameter Estimates

Variable	DF	Parameter Estimate	Standard Error	t Value	Pr > |t|	Variance Inflation
Intercept	1	-3.18486	0.25188	-12.64	<.0001	0
T	1	0.03079	0.00641	4.81	0.0003	1.05742
N	1	0.00000743	0.00000347	2.14	0.0518	3.69432
S	1	-0.00129	0.00017519	-7.34	<.0001	2.36729
stdTK	1	0.09441	0.02847	3.32	0.0056	1.02986
stdNS	1	0.37051	0.07142	5.19	0.0002	1.88994

Thus the selected model is as follows:

$Log_{10}(K_{COD}) = -3.18486 + 0.03079\ T + 0.00000743\ N - 0.00129\ S + 0.09441$ Std (TK) + 0.37052 Std (NS)

5.3.8 Checking the selected model assumptions

Figure 5.11 shows the residual vs. predictor plots without any presence of curvature. The residual vs. fitted plot in Figure 5.12 has no funneling. The normality plot in Fig. 5.13 is not the best one but fairly acceptable. Thus the linearity, constant variance and normality assumptions were reasonable. Furthermore, two hypothesis tests will be conducted to verify the constant variance and normality assumptions.

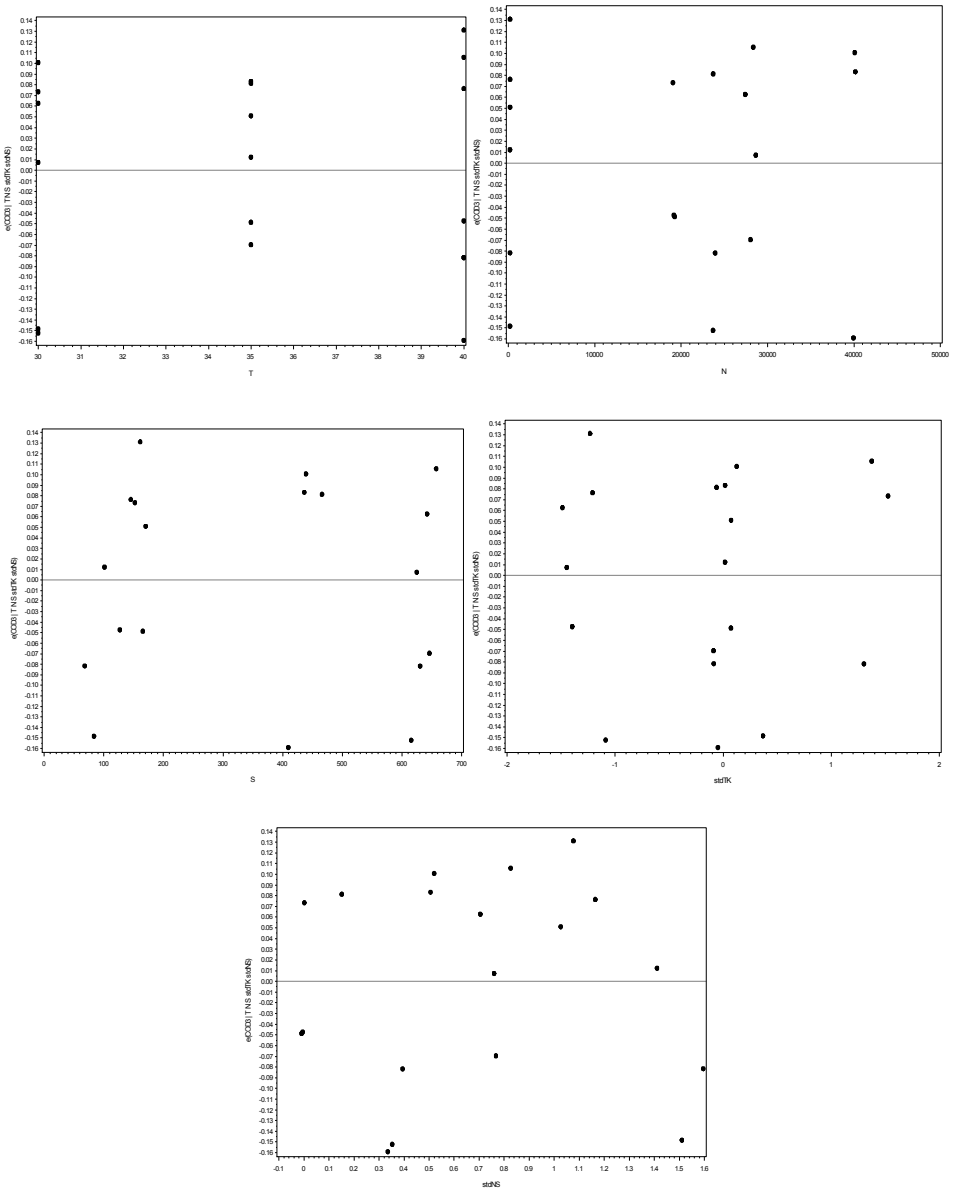

Fig. 5.11- Residual vs. predictor plots for the chosen model

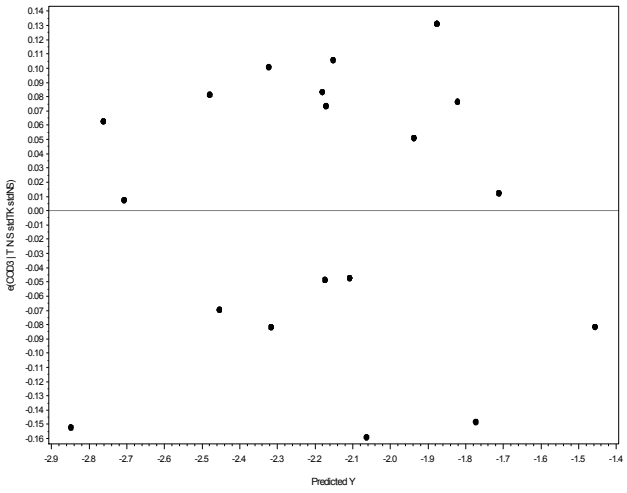

Fig. 5.12 - Residual vs. fitted Y plot for the chosen model.

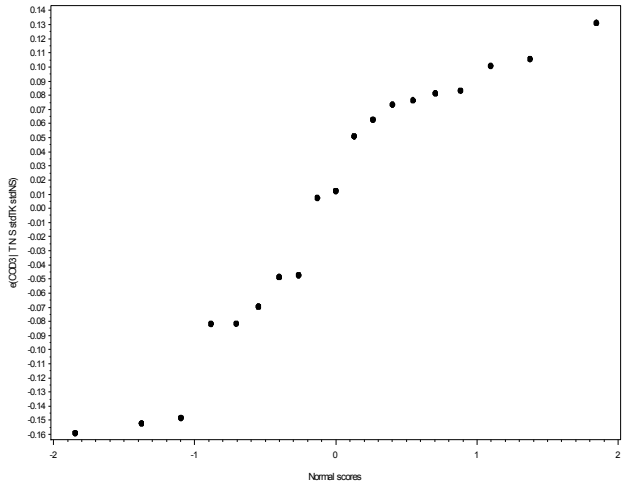

Fig. 5.13 - Normality plot for the chosen model

A- Modified Levene test has been widely used as a recognized method to verify whether residuals have a constant variance.

1. F-test

- Hypothesis

$H_0 : \sigma_{d1} = \sigma_{d2}$

$H_1 : \sigma_{d1} \neq \sigma_{d2}$

- Decision rule

Assuming significance level, $\alpha = 0.10$

From F – test, reject H_0 if p value < 0.10,

P value = 0.7636 (which is greater than 0.10).

Hence, we failed to reject H_0 with 90% confidence. Thus the variance of the two groups are equal ($\sigma_{d1} = \sigma_{d2}$).

- Conclusion

Variances of d1 and d2 are equal.

2. T-test

T-test is performed to check whether the error variance is constant.

- Hypothesis:

H_0 : Constant Error Variance.

H_1 : Constant Error Variance violated.

- Decision rule

If p – value (t test) < 0.10, then reject H_0

P = 0.5634 >0.1. Hence we failed to reject H_0.

- Conclusion

Constant variance assumption is satisfied.

Table 5.13 - The T test table for the selected model

The TTEST Procedure

Variable: d

group	N	Mean	Std Dev	Std Err	Minimum	Maximum
1	10	0.0746	0.0503	0.0159	0.0277	0.1873
2	9	0.0890	0.0557	0.0186	0	0.1714
Diff (1-2)		-0.0143	0.0529	0.0243		

Method	Variances	DF	t Value	Pr > |t|
Pooled	Equal	17	-0.59	0.5634
Satterthwaite	Unequal	16.268	-0.59	0.5659

Equality of Variances

Method	Num DF	Den DF	F Value	Pr > F
Folded F	8	9	1.23	0.7636

B – Normality Test

This verifies whether residuals are normally distributed or not.

- Hypothesis

H_0 : Normality is reasonable.

H_1 : Normality is violated.

- Decision rule

If ρ, the correlation coefficient is < C(α,n), the cutoff value, we reject H_0.

ρ = 0.96287 (from the above table C-2)

Assuming α = 0.1, C (0.1,19) = 0.9585

Since, ρ = 0.96287 >0.9585, we failed to reject H_0.

- Conclusion

Normality is OK.

Table 5.14 – Normality test for the selected model

	e	enrm
e e(COD3 | T N S stdTK stdNS)	1.00000	0.96287
enrm Normal scores	0.96287	1.00000

X – Outliers

One observation has a Leverage value (h_{ii}) that exceeds the cutoff value ($\frac{2p}{n} = \frac{2(5)}{19}$ = 0.526).Thus observation 2 was a x – outlier.

Y – Outliers

Y – Outliers are determined by Bonferroni test. No $|t_i|$ exceeds $t(1 - \frac{\alpha}{2n}; n-p-1)$ = $t(1 - \frac{0.1}{2(19)}; 19 – 5 -1) = t(0.997;13) = 3.28$. Thus there is no y – outlier.

Table 5.15 shows the x outlier. The rest of the h_{ii} and $|t_i|$ are in Appendix B.

Table 5.15 – X– outlier measure for the selected model

Obs	yhat	e	tres	cookdi	hii	dffitsi	enrm
2	-2.17049	0.07358	0.97519	0.19124	0.54681	1.06901	0.40115
18	-2.15166	0.10590	1.24700	0.19228	0.42592	1.09984	1.37597

Since there was an x – outlier, it was necessary to see if the concerned observation is influential. It is accomplished with three measures of influence:

1. DFFITS:

   Guideline : An outlying observation is considered influential if | DFFITS | > ($2\sqrt{p/n}$)

($2\sqrt{\frac{p}{n}}$) = 2 x $\sqrt{5/19}$ = 1.025. Observation 2 and Observation 18 have exceeded the value (table 5.15. But it was not considerably higher than the cutoff.

2. DFBETAS:

Guideline: For large datasets, An outlying observation is considered influential if | DFBETAS |> ($2/\sqrt{n}$) = $2/\sqrt{19}$ = 0.459. For small to medium datasets, flag | DFBETAS |> 1. Ours is a medium range dataset and will be looking for anything larger than 1. None was above 1. The table is in the Appendix B.

3. Cook's distance:

Guideline: If D_i > F (0.5, p, n-p) then observation in considered influential.

F (0.5, 5, 14) = 0.914.

None is above the cutoff. The table is in Appendix B. Thus the x outlier is not influential enough to be removed.

Thus the selected model is as follows:

Log_{10} (K_{COD}) = -3.18486 + 0.03079 T + 0.00000743 N - 0.00129 S + 0.09441 std (TK) + 0.37051 std (NS)

Simplifying the interaction terms,

Std (TK) = $(\frac{Ti-Tmean}{\sigma T})$ $(\frac{Ki-Kmean}{\sigma K})$ = $(\frac{Ti-35.26}{4.24})$ $(\frac{Ki-90.85}{63.83})$

= 0.0037 T_iK_i – 0.336 T_i – 0.130 K_i +11.84

Std (NS) = $(\frac{Ni-Nmean}{\sigma N})$ $(\frac{Si-Smean}{\sigma S})$ = $(\frac{Ni-19088}{14635})$ $(\frac{Si-354.82}{232.01})$

= 2.95 x 10^{-7} N_i S_i – 1.04 x 10^{-4} N_i – 5.62 x 10^{-3} S_i = 1.995

Putting the parameter values in the selected model, we have the final model as follows:

$Log_{10}(K_{COD})$ = - 1.32886 – 0.00091 T – 3.127 * 10^-5 N – 3.37 * 10 ^ -3 S – 0.0123 K + 0.00349 TK + 1.09 * 10^-7 NS

$$K_{COD} = 10^{-1.32886 - 0.00091\ T - 3.127 * 10\text{^-}5\ N - 3.37 * 10\ \text{^}\ -3\ S - 0.0123\ K + 0.00349\ TK + 1.09 * 10\text{^-}7\ NS}$$

5.4 Modeling k_{BOD}

The exact same procedure was followed to model K_{BOD}. The predictors were same as was for COD – temperature, ammonia, potassium, phosphorus and sulfur.

5.4.1 Scatter Plots and Correlation Matrices

The scatter plot of k_{BOD} is depicted in the following Figure 5.11. There is some linear downward trend between BOD vs. N, BOD vs. P and BOD vs. S. There is a trend between BOD and T, too.

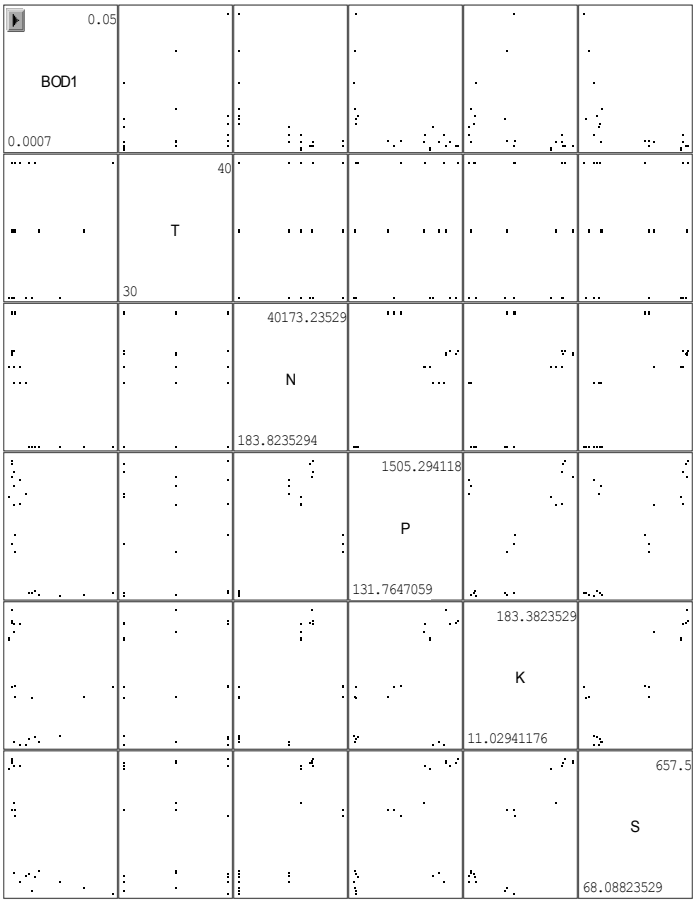

Fig. 5.14 – Scatter plots of the preliminary model

The predictors also show some relationship between each other. If there is a strong relationship, it might lead to multicollinearity. K and S, P and K and P and S show some upward linear trend. Table 5.12 shows the r – values of the k_{BOD} and the predictor variables. It is evident that N and S, P and S, K and S are strongly correlated. Any value above 0.7 is a concern and all the mentioned relations had values above 0.7. Thus multicollinearity can be a problem.

Table 5.16 - Correlation matrix of K_{BOD} vs. predictor variables

Pearson Correlation Coefficients, N = 20					
	T	N	P	K	S
T	1.00000	-0.11264	-0.10809	-0.10462	-0.12746
N	-0.11264	1.00000	0.68461	0.51454	0.74318
P	-0.10809	0.68461	1.00000	0.56655	0.70368
K	-0.10462	0.51454	0.56655	1.00000	0.88360
S	-0.12746	0.74318	0.70368	0.88360	1.00000

5.4.2 Fitting a Preliminary Model and Checking Model Assumptions.

SAS output has provided the parameter estimate of the preliminary model, which is presented in Table 5.13. The result states that the R^2 value is pretty high (73.4%). All the model assumptions are required to be checked before continuing with the significance of regression parameters.

Table 5.17 – Parameter Estimates and ANOVA Table of the k_{BOD} Preliminary Model.

K_{BOD} = 0.01458 + 0.00025119T - 5.54744E-8N - 0.00000741P + 0.00019914K - 0.00006855S

Parameter Estimates

Variable	DF	Parameter Estimate	Standard Error	t Value	Pr > |t|	Variance Inflation
Intercept	1	0.01458	0.01528	0.95	0.3562	0
T	1	0.00025119	0.00041566	0.60	0.5553	1.01762
N	1	-5.54744E-8	2.093872E-7	-0.26	0.7949	3.09406
P	1	-0.00000741	0.00000500	-1.48	0.1605	2.24094
K	1	0.00019914	0.00006628	3.00	0.0095	5.74447
S	1	-0.00006855	0.00002404	-2.85	0.0128	9.91734

Analysis of Variance

Source	DF	Sum of Squares	Mean Square	F Value	Pr > F
Model	5	0.00230	0.00045972	7.74	0.0011
Error	14	0.00083194	0.00005942		
Corrected Total	19	0.00313			

Root MSE	0.00771	R-Square	0.7342
Dependent Mean	0.01039	Adj R-Sq	0.6393

5.4.3 Preliminary model assumption check

1. The residuals do not have a constant variance. The first assumption can be verified with the help of residuals vs. fitted Y plot. There is a funnel shape Figure 5.13. Thus the assumption is violated.

2. The current MLR model form is not reasonable. Since the residual vs. predictor variables depict curvature. Figure 5.12 shows only the plots with curvature. The rest of the graphs are in Appendix B.

3. The third assumption is to check the normality. This is fairly acceptable in this case but not perfect.

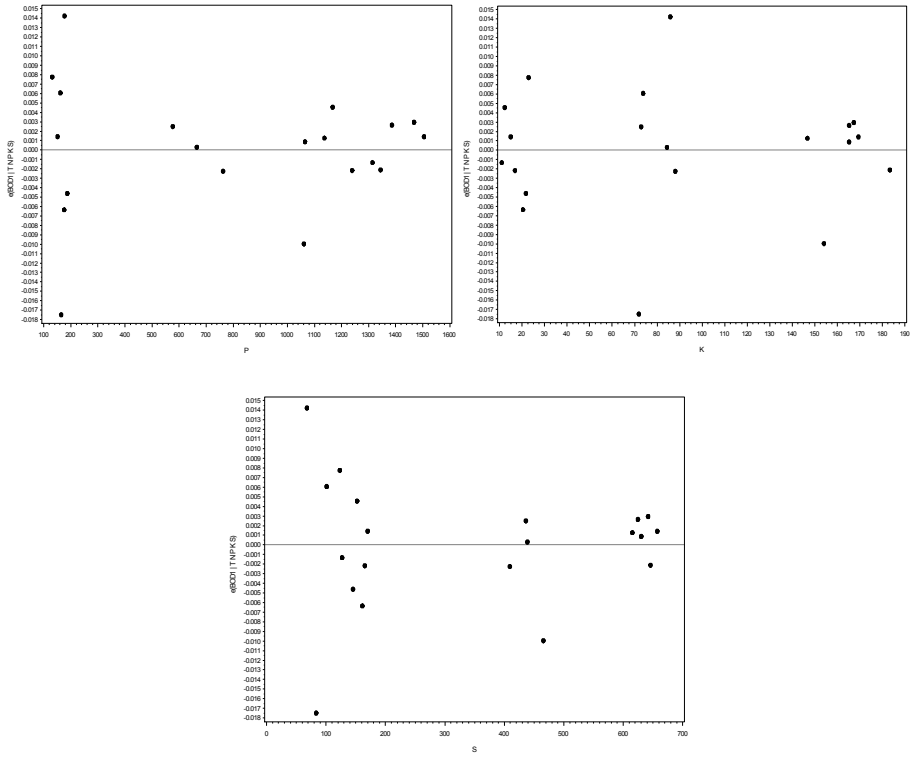

Fig. 5.15 - Residuals vs. Predictor Plots of the Preliminary Model.

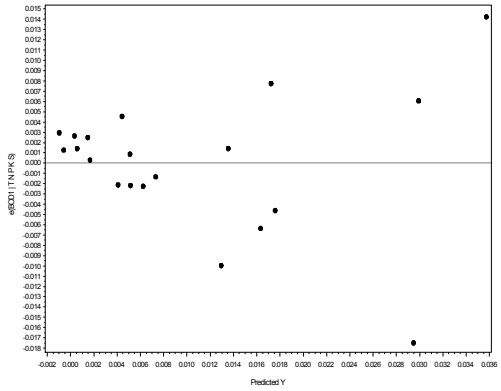

Fig. 5.16 –- Residuals vs. Fits Plot of the Preliminary Model

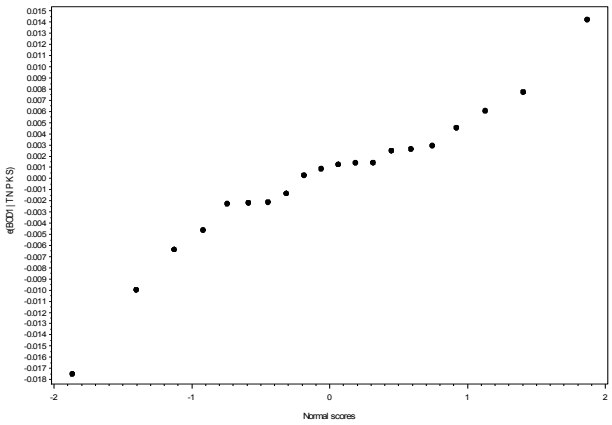

Fig. 5.17 – Normality graph of the preliminary model.

No further analysis has been done for this preliminary model. Since all the first three assumptions were violated, it was decided to conduct transformations.

5.4.4 Transformation

To reduce the violations of the model assumptions, it was necessary to conduct certain transformations. The first attempt of transformation is always to change the response variable and keep the predictor variables as they are. The response variable went through the square root and log transformations. The log transformation looked better in terms of residual vs. predictor variables graphs and also on the residuals vs. fitted Y plot. The results of the square root of k_{BOD} are in the Appendix B.

The transformed response variable, $\log_{10}k_{BOD}$ was regressed on T, N, P, K and S and the new transformed fitted model is shown below:

Table 5.18 – Parameter Estimates of the Transformed Model

K_{BOD} = -2.13592 + 0.01481T - 0.00000535N - 0.00027144P + 0.00339K - 0.00177S

Parameter Estimates

Variable	DF	Parameter Estimate	Standard Error	t Value	Pr > |t|	Variance Inflation
Intercept	1	-2.13592	0.47244	-4.52	0.0005	0
T	1	0.01481	0.01285	1.15	0.2682	1.01762
N	1	-0.00000535	0.00000647	-0.83	0.4219	3.09406
P	1	-0.00027144	0.00015450	-1.76	0.1008	2.24094
K	1	0.00339	0.00205	1.66	0.1201	5.74447
S	1	-0.00177	0.00074303	-2.38	0.0323	9.91734

Now the model assumptions are checked again.

1. The constant variance assumption is satisfied since the figure which depicts the predictor vs. fitted Y in Figure 5.16 has no funnel shape.

2. The residual vs. the predictor variables are shown in Figure 5.15. No curvature is seen.

3. The normality plot in Figure 5.17 also looks better in the transformed model.

4. There are no outliers.

X – Outliers

The cutoff value is $\frac{2p}{n}$ = $\frac{2(5)}{20}$ = 0.50. None of the leverage values shown in Table 5.19 exceeds the cutoff value.

Y – Outliers

The Bonferroni is a common test procedure to detect Y – Outliers.

t(1 - $\frac{\alpha}{2n}$; n-p-1) = t (1 - $\frac{0.1}{2(20)}$; $20 - 5 - 1$) = t (0.9975; 14) = 3.32.

None of the $|t_i|$ exceeds 3.32. Thus there are no Y – outliers.

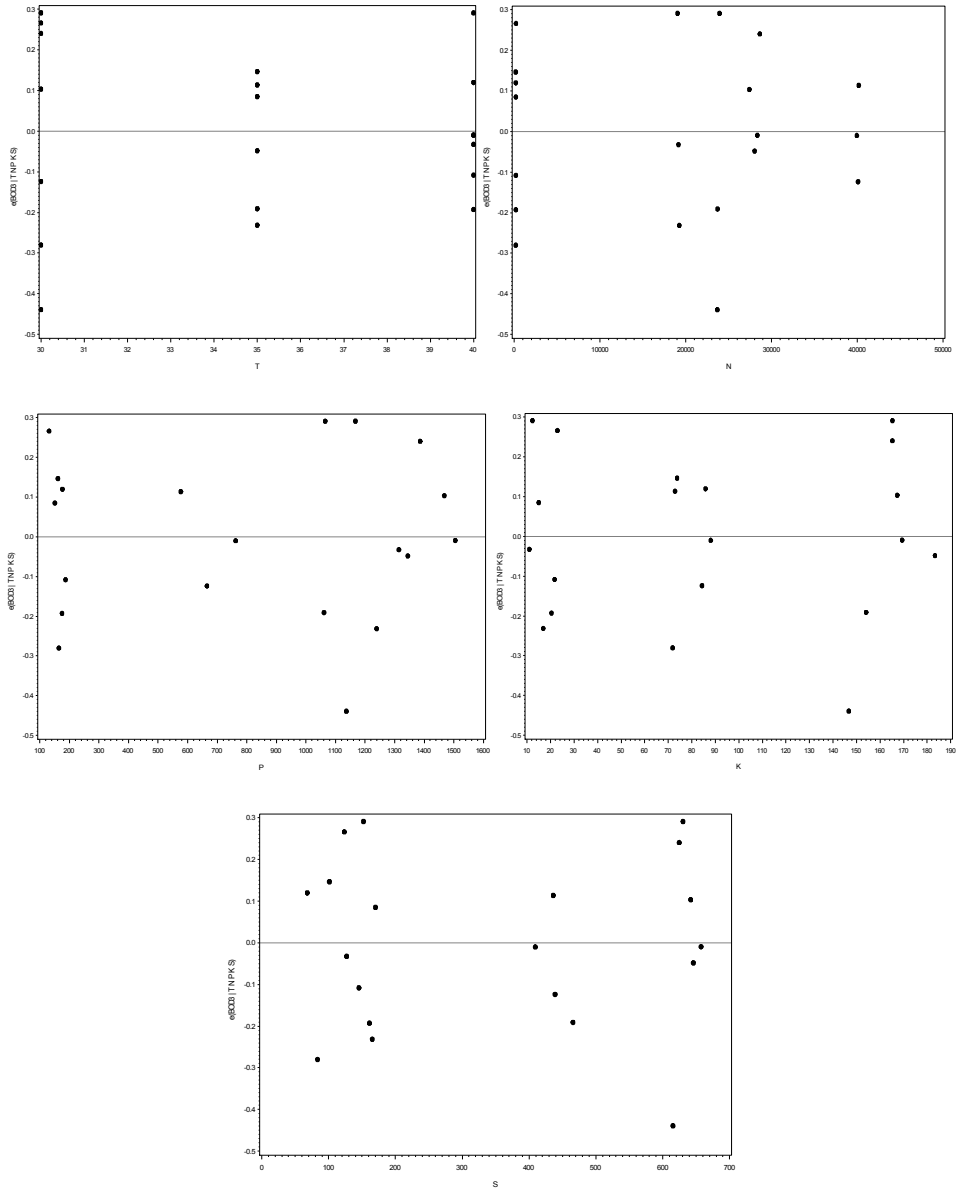

Fig. 5.18 – Residuals vs. Predictor Plots of the Transformed Model

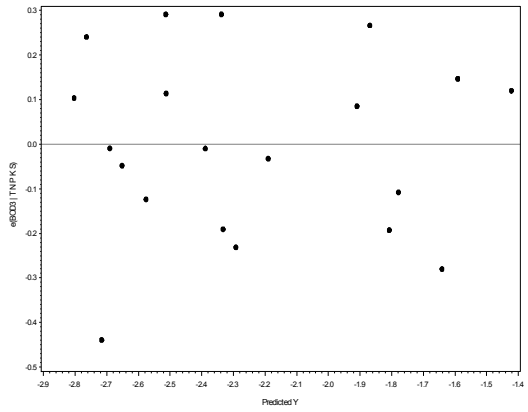

Fig. 5.19 - Residuals vs. Fits Plot of the Transformed Model

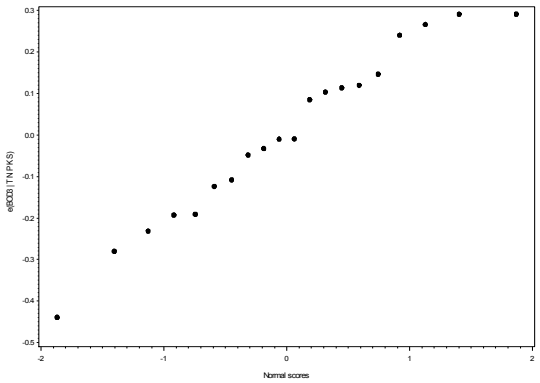

Fig. 5.20 - Normal Probability Plot of the Transformed Model

Table 5.19 – Measures for Outlier Analysis.

Obs	tres	hii
1	-1.46285	0.35505
2	1.31154	0.27153
3	1.53281	0.36164
4	-0.66333	0.39133
5	1.1324	0.20247
6	0.49802	0.23259
7	-2.1012	0.23098
8	0.70839	0.23954
9	0.42769	0.29568
10	-1.15914	0.29972
11	0.61118	0.38466
12	-0.22097	0.17756
13	-0.87488	0.16567
14	0.68112	0.44933
15	-0.52548	0.26022
16	-0.96363	0.2964
17	-0.18257	0.45526
18	-0.0511	0.38693
19	-0.04384	0.28536
20	1.42031	0.25811
Maximum	1.53281	0.45526

5.4.5 Interaction terms.

Regression plots were drawn to see the possibilities of adding interaction terms. Only one plot, std TK showed some linear relationship, and was decided to include in the model. The graph is shown below. The rest of the graphs are in the Appendix B.

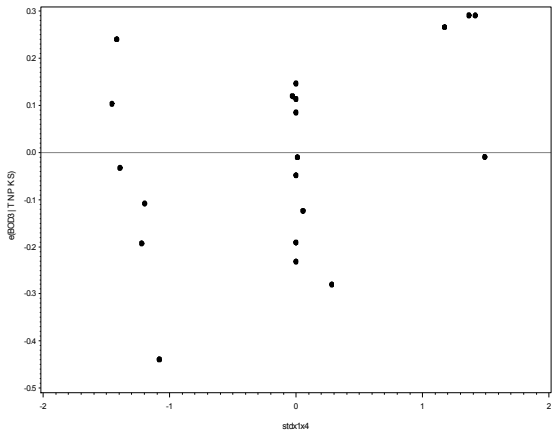

Fig. 5.21 – Partial Regression Plot

Interaction terms are added to improve the model quality. However, it is necessary to see if there is any correlation with the predictor variables. Standardization is a common procedure to mitigate the correlation issue. Table 5.16 shows that the multicollineatity has been drastically reduced after standardization of the interaction term.

Table 5.20 – Correlation matrix between TK and stdTK with the Model Variables.

	BOD3	T	N	P	K	S
x1x4	-0.50211	0.06385	0.49609	0.53985	0.97895	0.85493
stdx1x4	0.19489	0.00995	0.02996	-0.04423	0.02204	-0.01676

5.4.6 Model Search

Best Subsets, Backward Elimination and Stepwise regression were utilized in model search. SAS outputs of the different results are shown in the following graphs. Along with T, N. P, K and S, STDTK were used to achieve the best model.

Table 5.21- SAS Output of the Best Subsets Model Search Method

Number in Model	Adjusted R-Square	R-Square	C(p)	AIC	SBC	Variables in Model
1	0.6245	0.6443	13.9276	-47.0061	-45.01463	S
1	0.5957	0.6170	16.2238	-45.5276	-43.53613	N
2	0.7024	0.7337	8.4033	-50.7976	-47.81039	K S
2	0.6956	0.7276	8.9166	-50.3445	-47.35727	P S
3	0.7536	0.7925	5.4598	-53.7837	-49.80077	P K S
3	0.7221	0.7660	7.6874	-51.3822	-47.39927	N P S
4	0.7658	0.8151	5.5552	-54.0938	-49.11515	P K S stdx1x4
4	0.7594	0.8100	5.9813	-53.5533	-48.57466	T P K S
5	0.7726	0.8325	6.0960	-54.0640	-48.08956	T P K S stdx1x4
5	0.7674	0.8286	6.4188	-53.6111	-47.63674	N P K S stdx1x4
6	0.7742	0.8455	7.0000	-53.6827	-46.71262	T N P K S stdx1x4

Table 5.22 - SAS Output of the Backward Elimination Model Search Method

Variable	Parameter Estimate	Standard Error	Type II SS	F Value	Pr > F
Intercept	-1.60765	0.10395	13.61472	239.17	<.0001
P	-0.00031394	0.00014750	0.25787	4.53	0.0492
K	0.00415	0.00185	0.28465	5.00	0.0399
S	-0.00217	0.00059341	0.76198	13.39	0.0021

Bounds on condition number: 6.3085, 39.107

All variables left in the model are significant at the 0.1000 level.

Table 5.23 - SAS Output of the Stepwise Selection Model Search Method

Stepwise Selection: Step 3

Variable P Entered: R-Square = 0.7925 and C(p) = 5.4598

Variable	Parameter Estimate	Standard Error	Type II SS	F Value	Pr > F
Intercept	-1.60765	0.10395	13.61472	239.17	<.0001
P	-0.00031394	0.00014750	0.25787	4.53	0.0492
K	0.00415	0.00185	0.28465	5.00	0.0399
S	-0.00217	0.00059341	0.76198	13.39	0.0021

Bounds on condition number: 6.3085, 39.107

All variables left in the model are significant at the 0.1000 level.

No other variable met the 0.1000 significance level for entry into the model.

The Best Subset model is the most trust worthy model search method since it includes every single possibility. The four highlighted models in the Best Subsets are the possibilities. Anyone can be used. Both Backward Elimination and Stepwise Regression are pointing towards the Model 3 in Best Subsets. All the models were fitted.

Model nos. 4 ,4 and 5 with the interaction terms std (TK) had one or more insignificant predictors. The p value of one or more of the parameters was more than 0.1. The parameter estimate tables are shown in Appendix B. Model 3 is the only one that satisfies all conditions. The R^2 and the adjusted R^2 are pretty high and the values are close. Furthermore, the model has been chosen by the other two model search methods. Most importantly, there is no insignificant predictor. The table for parameter estimates of model 3 is shown below in Table 5.20.

Table 5.24 – Parameter estimates for the selected model (model 3)

Parameter Estimates

Variable	DF	Parameter Estimate	Standard Error	t Value	Pr > |t|	Variance Inflation
Intercept	1	-1.60765	0.10395	-15.47	<.0001	0
P	1	-0.00031394	0.00014750	-2.13	0.0492	2.03693
K	1	0.00415	0.00185	2.24	0.0399	4.69028
S	1	-0.00217	0.00059341	-3.66	0.0021	6.30850

The selected model is as follows:

$Log_{10}(K_{BOD}) = -1.60765 - 0.00031394\ P + 0.00415\ K - -0.00217\ S$

5.4.7 Checking Assumption of the Selected Model

The following figures of residual plots of the selected model are used to check the assumptions of the model selection. Residual – *Predictor* plots have no curvature, the residual fitted plot shows no funneling and the normality plot also looks pretty straight. Thus the linearity, constant variance and normality assumptions are satisfied. Two hypothesis tests were conducted to verify the normality and the constant variance of the selected model.

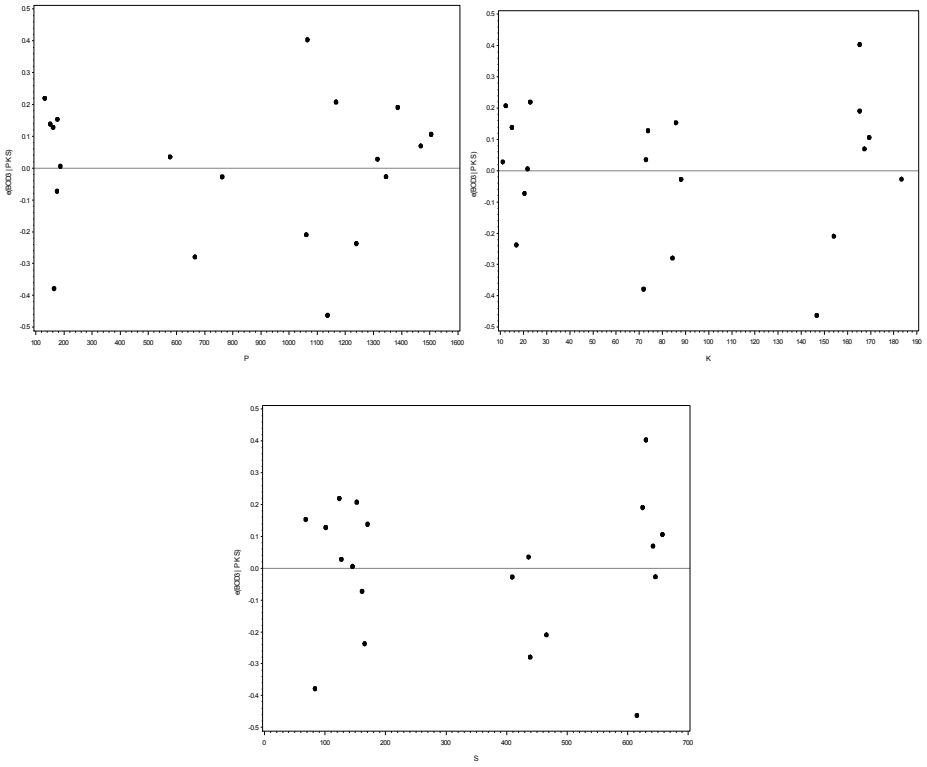

Fig. 5.22 – Residual vs. predictor graphs of the selected model.

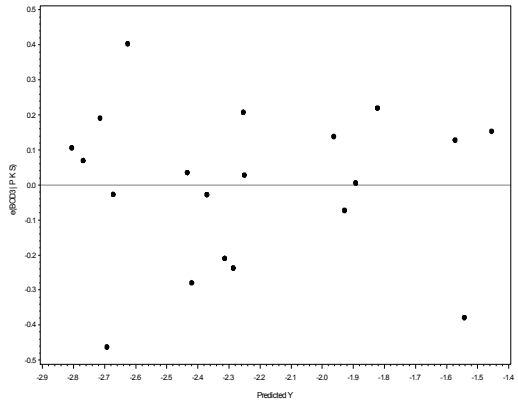

Fig. 5.23 – Residual vs. fits plot of the selected model.

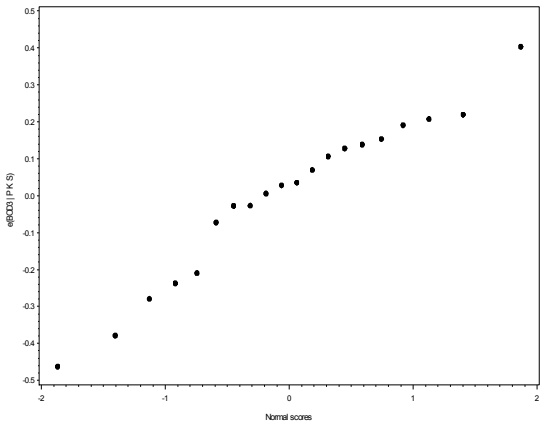

Fig. 5.24 – Normality probability plot of the selected model.

Hypothesis Tests for the k_{BOD} Selected Model:

A - Modified Levene test is used to ascertain whether the error terms have constant variance. The test is robust against serious departures from normality.

1. F-test

- Hypothesis

$H_0 : \sigma_{d1} = \sigma_{d2}$

$H_1 : \sigma_{d1} \neq \sigma_{d2}$

- Decision rule

Assuming significance level, $\alpha = 0.10$

From F – test , reject H_0 if p value < 0.10,

P value = 0.6174 (which is greater than 0.10).

Hence, we failed to reject H_0 with 90% confidence. Thus, the variance of the two groups are equal ($\sigma_{d1} = \sigma_{d2}$).

- Conclusion

Variances of d1 and d2 are equal.

T-test is performed to whether the error variance is constant.

- Hypothesis:

H_0 : Constant Error Variance.

H_1 : Constant Error Variance violated.

- Decision rule

If p – value (t test) < 0.10, then reject H_0

P = 0.6428 >0.1. Hence we failed to reject H_0.

- Conclusion

Constant Variance assumption is satisfied

Table 5.25 – SAS Output of the Modified Levene Test for the Selected Model.

The TTEST Procedure

Variable: d

group	N	Mean	Std Dev	Std Err	Minimum	Maximum
1	10	0.1812	0.1591	0.0503	0.0313	0.4670
2	10	0.1502	0.1340	0.0424	0.0500	0.4568
Diff (1-2)		0.0310	0.1471	0.0658		

Method	Variances	DF	t Value	Pr > |t|
Pooled	Equal	18	0.47	0.6428
Satterthwaite	Unequal	17.495	0.47	0.6429

Equality of Variances

Method	Num DF	Den DF	F Value	Pr > F
Folded F	9	9	1.41	0.6174

B – Normality Test

This verifies whether residuals are normally distributed or not.

- Hypothesis

H_0 : Normality is reasonable.

H_1 : Normality is violated.

- Decision rule

If ρ, the correlation coefficient is < C(α,n), the cutoff value, we reject H_0.

ρ = 0.978 (from the above table C-2)

Assuming α = 0.1, C (0.1,20) = 0.960

Since, ρ = 0.978 >0.960, we failed to reject H_0.

- Conclusion

Normality is OK.

Table 5.26 – SAS Output for the Normality Test

	e	enrm
e e(BOD3 | P K S)	1.00000	0.97819
enrm Normal scores	0.97819	1.00000

X _ Outliers

The Leverage values (h_{ii}) for all the observation is shown in the Appendix B. The cutoff value is ($\frac{2p}{n} = \frac{2(3)}{20} = 0.3$).

Observation 14 and 17 has higher values than the cutoff as shown in Table 5.23. Thus there are two X – Outliers.

Table 5.27– SAS Output for the X – Outliers

Obs	e	tres	cookdi	hii	dffitsi	enrm
14	0.15401	0.81775	0.10112	0.37690	0.62908	0.74414
17	0.02864	0.15324	0.00369	0.38621	0.11778	-0.06193
20	0.40390	1.83170	0.14318	0.14581	0.82426	1.86824

Y _ Outliers

The Bonferroni test was conducted to see if there are any Y – Outliers. No I t_i I is greater than t (1 - $\frac{\alpha}{2n}$; n-p-1) = t (1 - $\frac{0.1}{2(20)}$; $20-3-1$) = t(0.9975;16) = 3.252.

No value exceeds the cutoff thus there are no Y – outliers.

Since there were two x – outliers, it was necessary to determine how influential they are. There are three measures to determine it.

4. DFFITS:

Guideline : An outlying observation is considered influential if | DFFITS | > ($2\sqrt{p/n}$)

($2\sqrt{\frac{p}{n}}$) = 2 x $\sqrt{3/20}$ = 0.775. Observation 20 exceeded the value. But it was not considerably higher than the cutoff (table 5.23). And the x – outliers had DFFITS values less than the cutoff.

5. DFBETAS:

Guideline: For large datasets, An outlying observation is considered influential if | DFBETAS |> ($2/\sqrt{n}$) = $2/\sqrt{20}$ = 0.447. For small to medium datasets, flag | DFBETAS |> 1. Ours is a medium range dataset and will be looking for anything larger than 1. None was above 1. The table is in the Appendix B.

6. Cook's distance:

   Guideline: If $D_i > F(0.5, p, n-p)$ then observation in considered influential.

   F (0.5, 3, 17) = 0.829 (Kutner, Table B.4).

   No value exceeded the cutoff.

   Thus the outliers were not influential enough to remove them.

   Thus the final form of model is:

   $Log_{10}(K_{BOD}) = -1.60765 - 0.00031394\ P + 0.00415\ K - -0.00217\ S$

   Or,

   $K_{BOD} = 10^{-1.60765 - 0.00031394\ P + 0.00415\ K - 0.00217\ S}$

5.5 Model Interpretation

It was a little surprising that T was not part of the BOD model. Temperature plays an important role in the rate of the anaerobic treatments. One reason can be that the range of temperature was from 30 – 40 ^{0}C. Within this range, rate of BOD removal might not vary significantly. Thus it is recommended to try wider ranges of temperature in the future.

Moreover, the predictors that are significant in the COD model did not necessarily play a role in BOD. For example T, N, S, K and interactions of TK and NS were present in COD model. In BOD, T and N were not present. Only P, K and S were seen in BOD the model. P was insignificant in COD model but was important for BOD model.

It is important to visualize the importance of each predictor in the model. For example, in COD we have an entire model with all predictors that are significant. To have an idea how potassium affects the decay constant at three temperatures, we varied the K (mg/L), made the other predictors constant and studied the changes in k (/day) with increasing K (mg/L). K was varied based on the lowest to highest initial value of K in the

six combinations of vinasses used. The mean values of T, S and N were used as constants. The same procedures were repeated to find the effects of individual N and S on the k(/days).

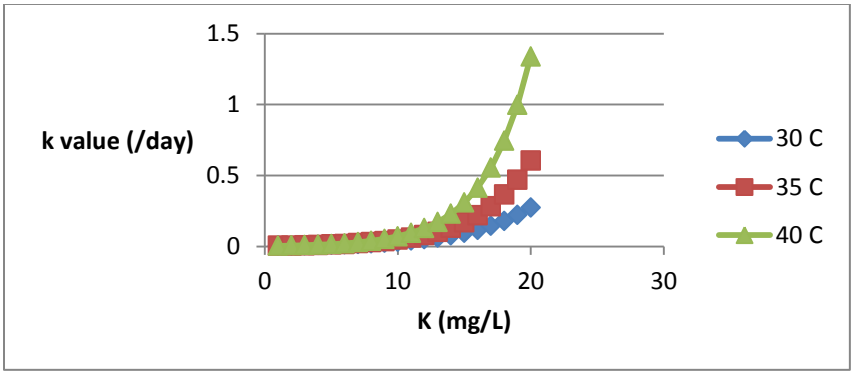

Fig. 5.25 - Effect of changes on K (mg/L) and T (^{0} C) on k_{COD} (/day)

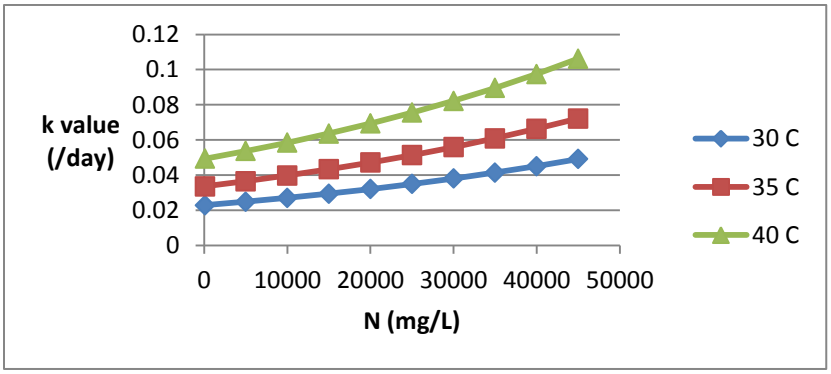

Fig. 5.26 – Effect of changes on N (mg/L) and T (^{0}C) on k_{COD} (/day)

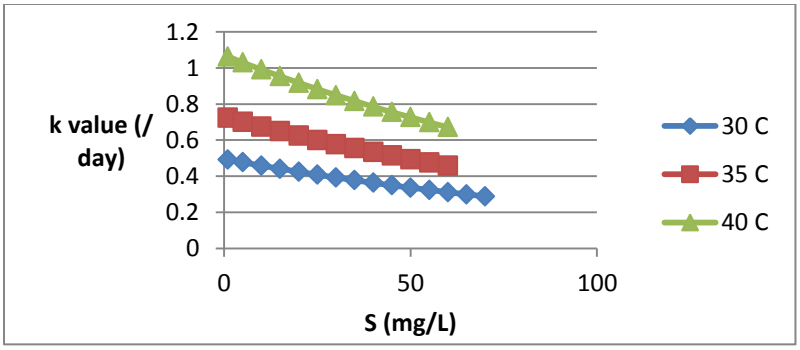

Fig. 5.27 – Effect of changes on S (mg/l) and T (^{0} C) on k_{COD} (/day)

The above graphs are useful in interpreting how a single nutrient will affect the decay rate rather than the combined effect of all the predictors. From Fig. 5.25, it is evident that increasing the K (mg/L), there is an increase in k, provided the other predictors are constant. Moreover, with increasing temperature there is an increase in decay rate, too. The same trend is observed in Fig. 5.26 for N (mg/L). However, S shows the opposite trend: increasing S (mg/L) decreases the k (/day).

For BOD models, the same procedures were applied and Fig. 5.28 to Fig. 5.30 depict the results of increasing a single nutrient. K (mg/L) and S (mg/L) behaved in accordance with the COD model. Phosphorus was not part of COD model. Increasing the P (mg/L), it tends to decrease the k value (/day), provided the other predictors are constant.

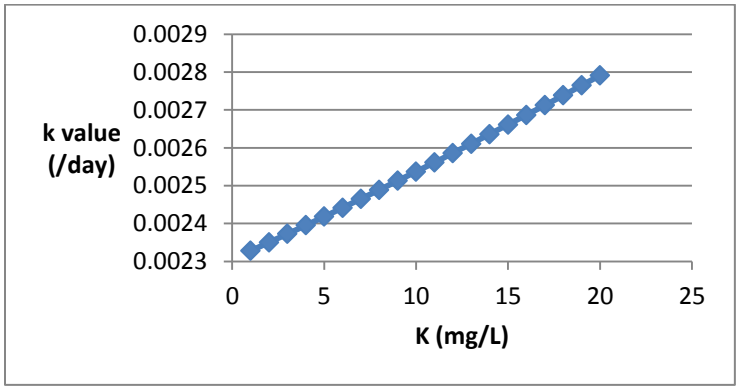

Fig. 5.28 – Effect of change on K (mg/L) on k_{BOD} (/day)

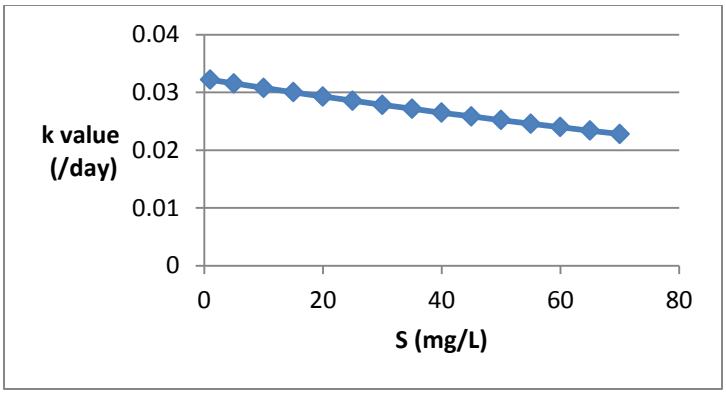

Fig. 5.29 - Effect of change on S (mg/L) on k_{BOD}(day)

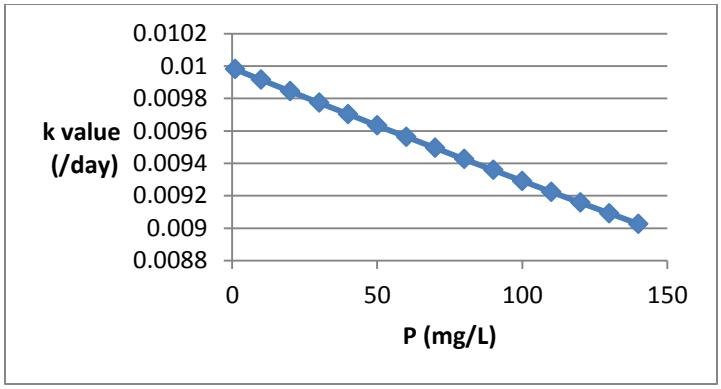

Fig. 5.30 – Effect of change on P (mg/L) on k_{BOD}(/day)

Chapter 6

Conclusions and Recommendations

6.1 Conclusions

The primary goal of the research was to develop a relationship between the water quality parameters COD and BOD of vinasse and the temperature and composition of vinasse. Ammonia, potassium, phosphorus and sulfur were considered in the composition of vinasse. 20 lab scale reactors with different compositions of vinasse at three mesophilic temperatures were run to develop the relationship. Multiple linear regression analysis was utilized to build the two models.

- The reactors at 40^0 C have a higher reaction rate and came to a stable state much earlier than the other two temperatures. This was expected. However, in terms of methane generation and the removal of COD and BOD, 35 ^{0}C was more effective in most cases. Thus for the kind of microbes used, we can say 35 ^{0}C is the optimum temperature.
- To develop the model, we obtained the k values from the COD or BOD vs. time graphs. Since we assumed that it is a first-order decay, we omitted the reactors that did not follow the graph (only one COD vs. time graph displayed a non-first-order trend).
- As expected, the synthetic vinasses were easier to degrade and had a higher methane generation than the real vinasse. Synthetic vinasse was composed of simple glucose and other chemicals which are far simpler than the complex lignin and cellulose of the real vinasse. Thus, the microbes had a tough time in breaking the real vinasse compared to the synthetic vinasse.

- Initially the scope was to model all the parameters like COD, BOD, K, N, P, and S. Only COD and BOD followed first-order decay, however. The rest had little decay and the trend did not follow any pattern.
- The two models developed in the study were:

  $k_{COD} = 10^{5.041 - 0.0009318\ T - 0.0000311\ N - 0.003372\ S - 0.0123\ K + 0.000349\ TK + 0.000000\ NS}$

  $k_{BOD} = 10^{-1.60765 - 0.00031394\ P + 0.00415\ K - -0.00217\ S}$

It is a little surprising that T was not a part of the BOD model. Temperature was a main determinant in terms of the breakdown of COD. It was expected to have the similar determinants in both the models. However, this was not seen in our case. Microbe behavior can be unpredictable; a simple change can cause discrepancies.

The primarily advantage of the research is that the models that were developed can be used in any vinasse treatment facilities to estimate the pollutant level after certain time and at a particular temperature. The model can also be used in design of vinasse treatment systems (estimate residence time for a given percent removal and reactor size, or determine reactor size for a given residence time and percent removal).

6.2 Recommendation

Ideas for future research include:

- Inclusion of more real vinasses. Synthetic and real vinasse vary considerably in composition and behavior. In our research we used vinasse obtained from corn and milo. Vinasse is produced from sugarcane, beet crops and many other crops. More variety will enrich the understanding of anaerobic treatment of vinasse.

- Only 6.8 L of vinasse was used in our experiment. In real world scenario, thousands of gallons of vinasse are expected to discharge every day. Thus it is essential to conduct pilot-scale testing.
- We assumed the COD/BOD vs. time graph followed first order trend. In future model development might consider incorporating multiple ks.
- Though substantial removal of COD and BOD was achieved in some instances, it is not enough. Treatments like UV, sonication and advanced oxidation treatment can be used in moderation on the anaerobically treated waste.
- Studies have shown that thermophilic temperatures are better suited for anaerobic treatment. More studies using thermophilic temperatures can be conducted.
- Relationships between the degradation of pollutants and the microbe species can be studied more extensively.
- Model validation is required.

Appendix A

Figures for obtaining k values for COD and BOD and some figures for water quality parameters.

Obtaining k values for COD

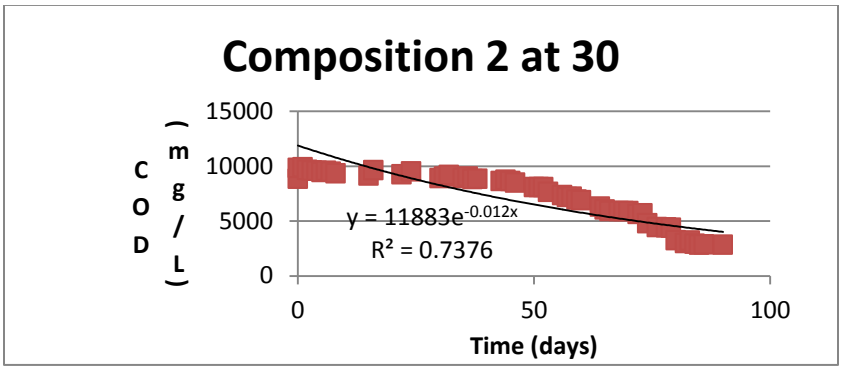

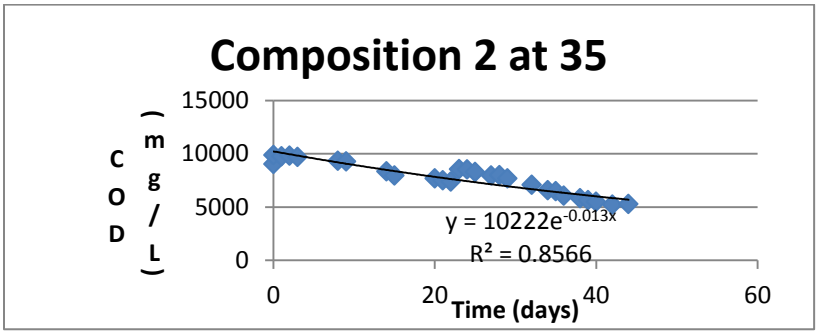

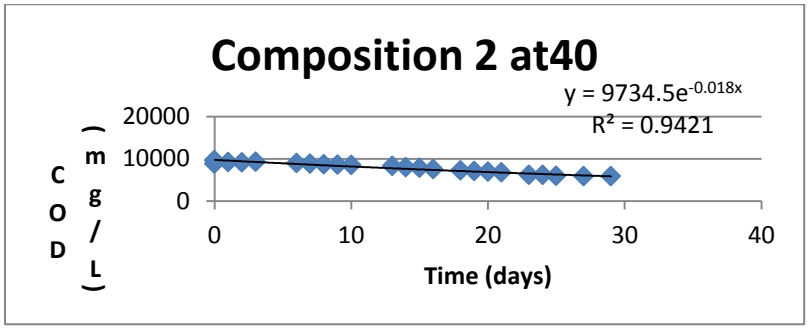

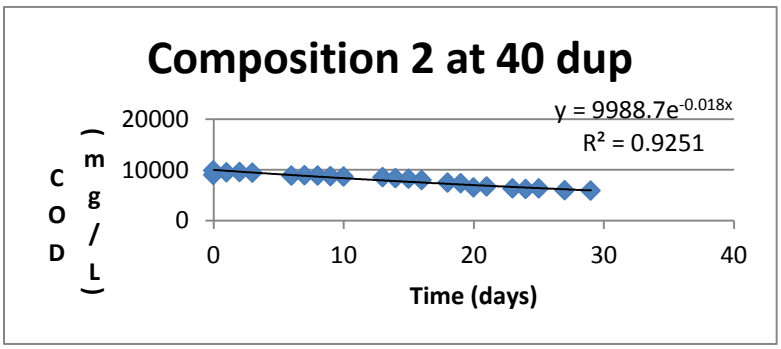

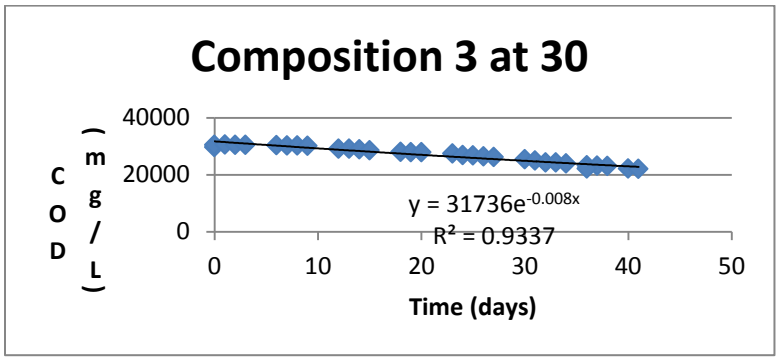
Composition 3 at 30
COD (mg/L)
40000
20000
0
y = 31736e-0.008x
R² = 0.9337
0
10
20
30
40
50
Time (days)

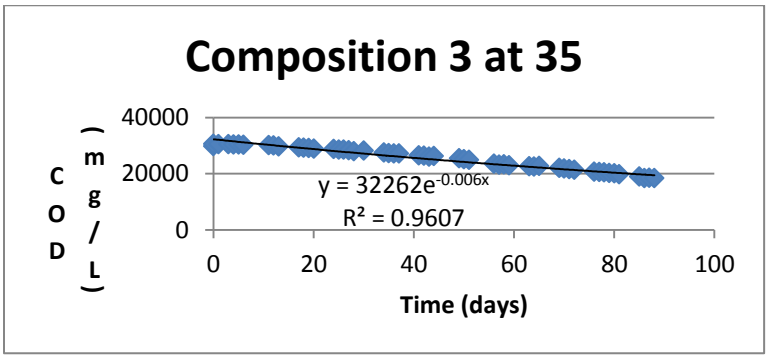
Composition 3 at 35
COD (mg/L)
40000
20000
0
y = 32262e-0.006x
R² = 0.9607
0
20
40
60
80
100
Time (days)

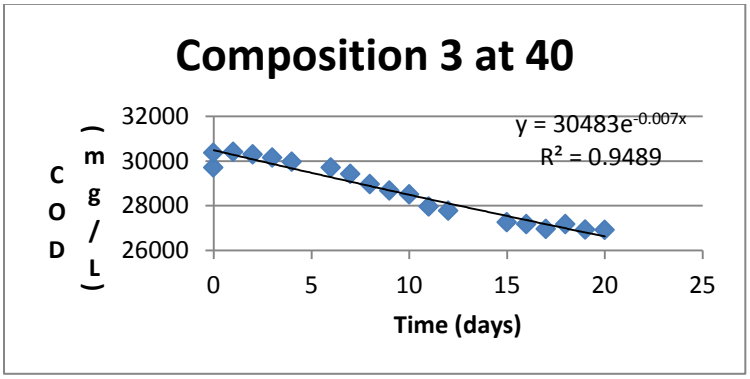
Composition 3 at 40
COD (mg/L)
32000
30000
28000
26000
y = 30483e-0.007x
R² = 0.9489
0
5
10
15
20
25
Time (days)

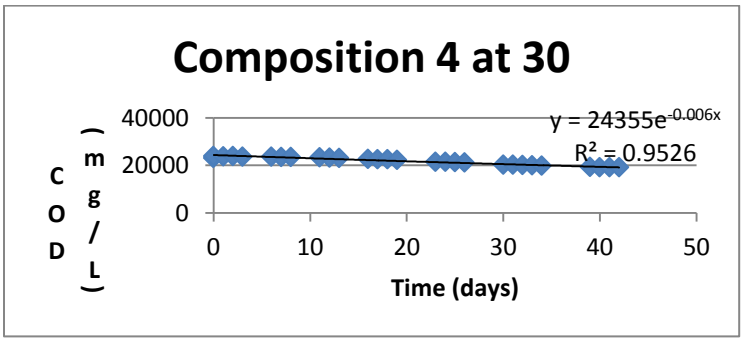
Composition 4 at 30
COD (mg/L)
40000
20000
0
y = 24355e-0.006x
R² = 0.9526
0
10
20
30
40
50
Time (days)

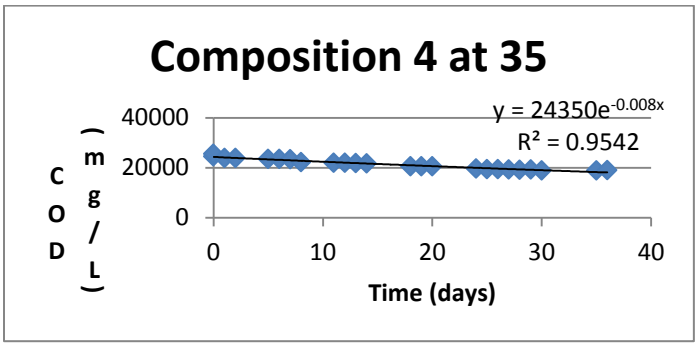
Composition 4 at 35
y = 24350e-0.008x
R² = 0.9542
COD (mg/L)
40000
20000
0
0
10
20
30
40
Time (days)

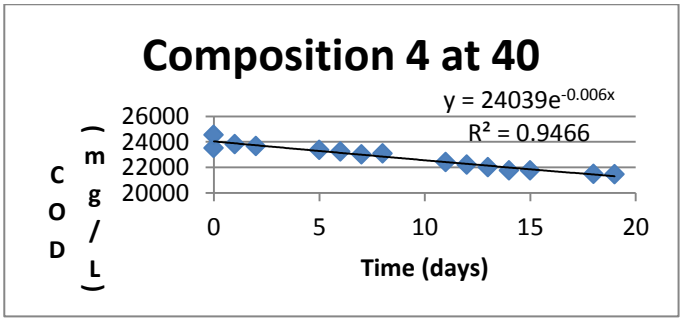
Composition 4 at 40
y = 24039e-0.006x
R² = 0.9466
COD (mg/L)
26000
24000
22000
20000
0
5
10
15
20
Time (days)

\

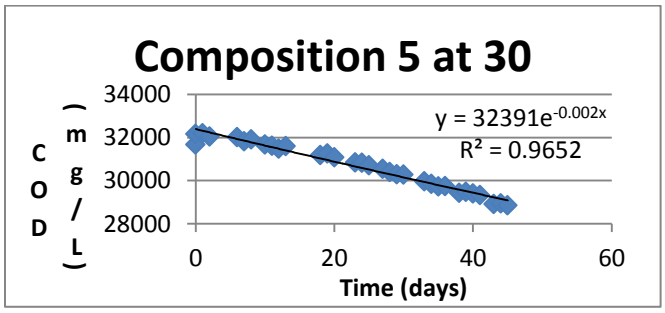
Composition 5 at 30
y = 32391e-0.002x
R² = 0.9652
COD (mg/L)
34000
32000
30000
28000
0
20
40
60
Time (days)

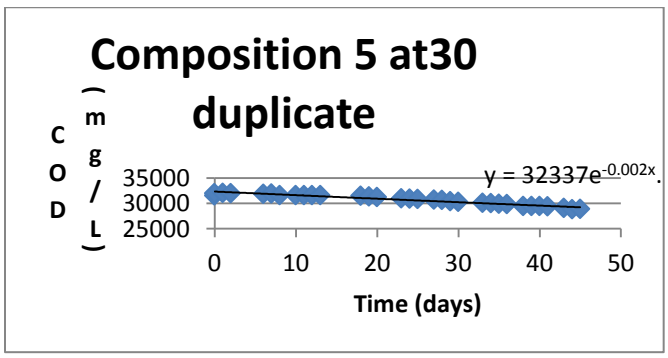
Composition 5 at30 duplicate
y = 32337e-0.002x
COD (mg/L)
35000
30000
25000
0
10
20
30
40
50
Time (days)

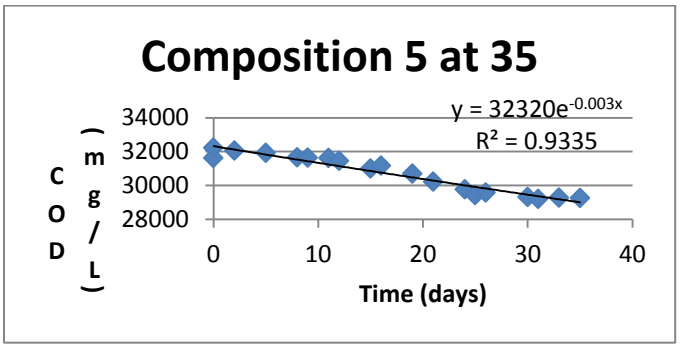
Composition 5 at 35
y = 32320e-0.003x
R² = 0.9335
COD (mg/L)
34000
32000
30000
28000
0
10
20
30
40
Time (days)

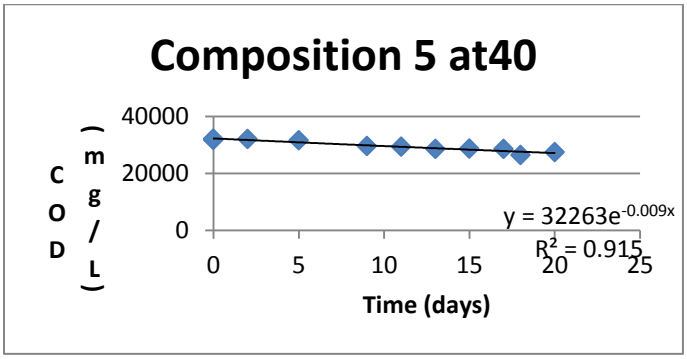
Composition 5 at40
COD (mg/L)
40000
20000
0
y = 32263e-0.009x
R² = 0.915
0
5
10
15
20
25
Time (days)

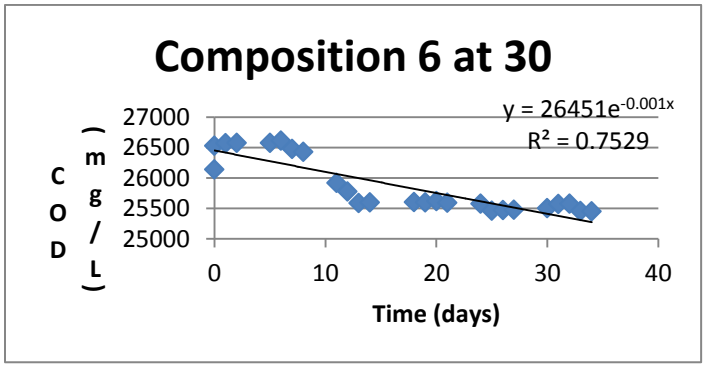
Composition 6 at 30
y = 26451e-0.001x
R² = 0.7529
COD (mg/L)
27000
26500
26000
25500
25000
0
10
20
30
40
Time (days)

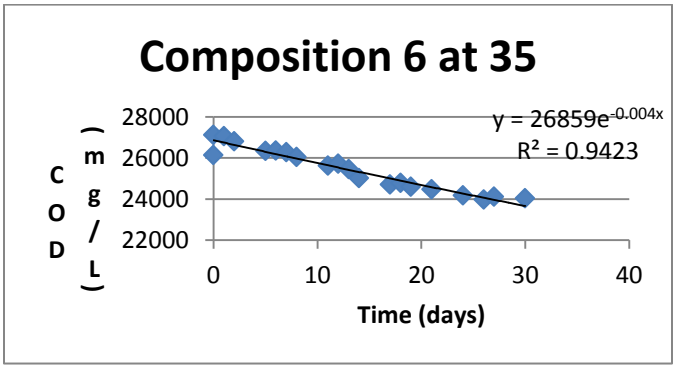
Composition 6 at 35
y = 26859e-0.004x
R² = 0.9423
COD (mg/L)
28000
26000
24000
22000
0
10
20
30
40
Time (days)

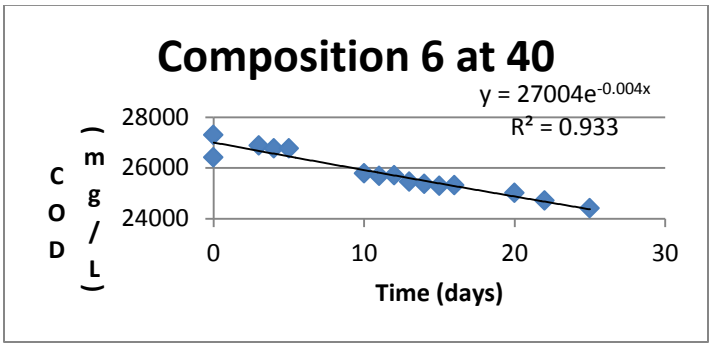

Obtaining k values for BOD

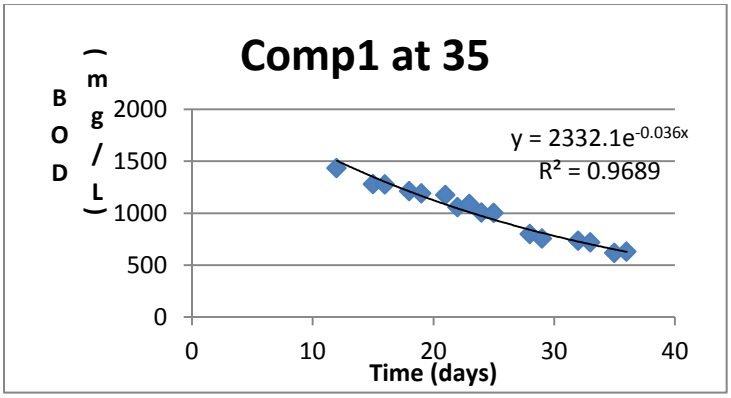

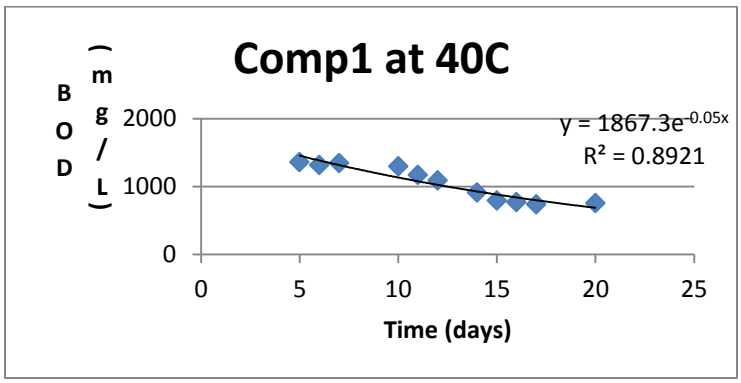

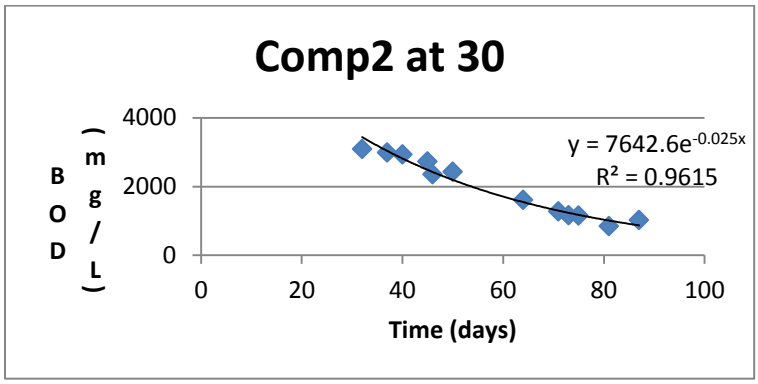
Comp2 at 30
BOD (mg/L)
4000
2000
0
0
20
40
60
80
100
Time (days)
y = 7642.6e-0.025x
R² = 0.9615

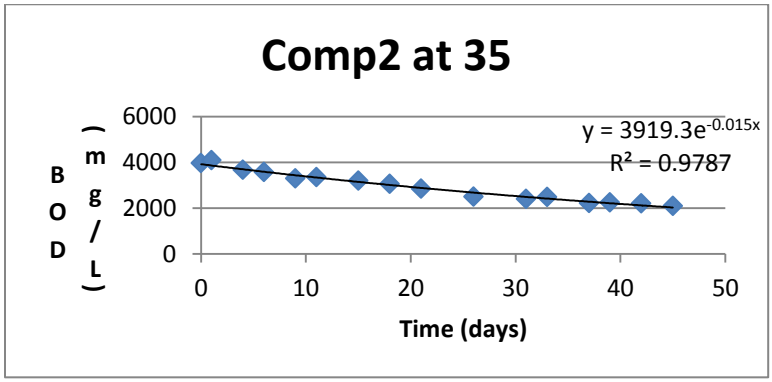
Comp2 at 35
BOD (mg/L)
6000
4000
2000
0
0
10
20
30
40
50
Time (days)
y = 3919.3e-0.015x
R² = 0.9787

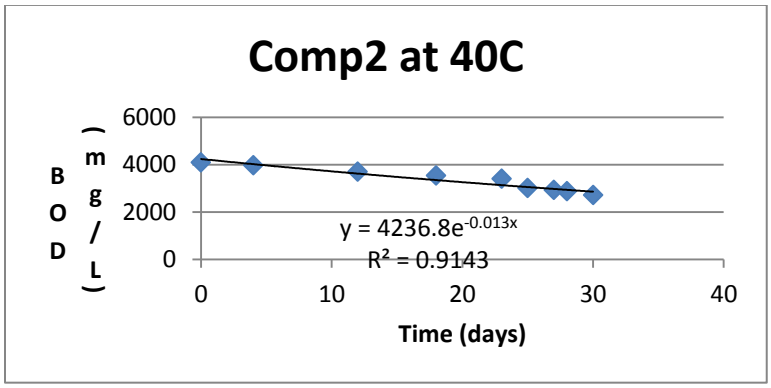
Comp2 at 40C
BOD (mg/L)
6000
4000
2000
0
0
10
20
30
40
Time (days)
y = 4236.8e-0.013x
R² = 0.9143

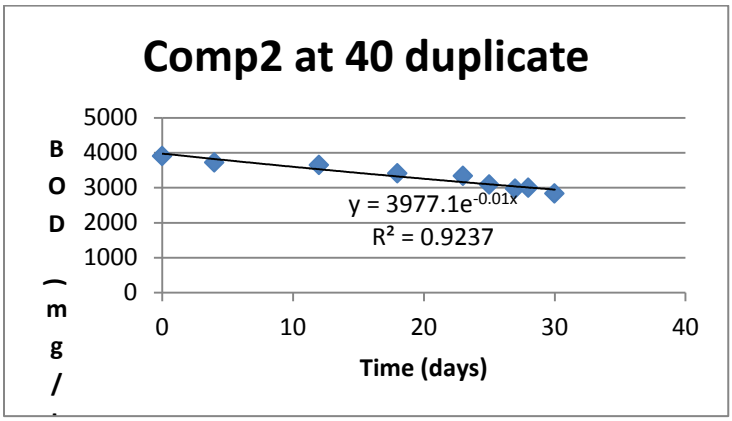
Comp2 at 40 duplicate
BOD (mg/
5000
4000
3000
2000
1000
0
0
10
20
30
40
Time (days)
y = 3977.1e-0.01x
R² = 0.9237

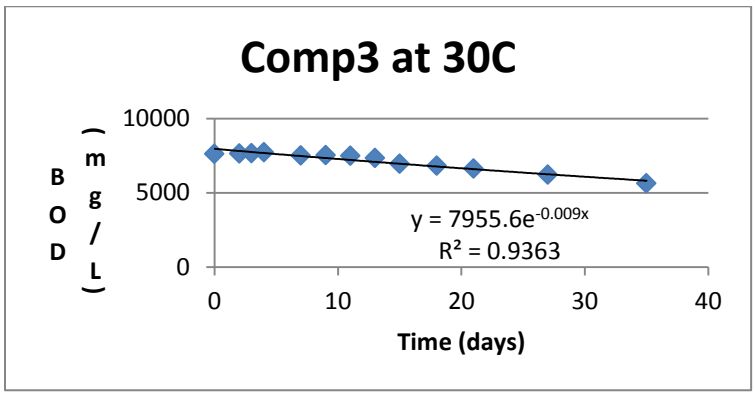
Comp3 at 30C
BOD (mg/L)
10000
5000
0
0
10
20
30
40
Time (days)
y = 7955.6e-0.009x
R² = 0.9363

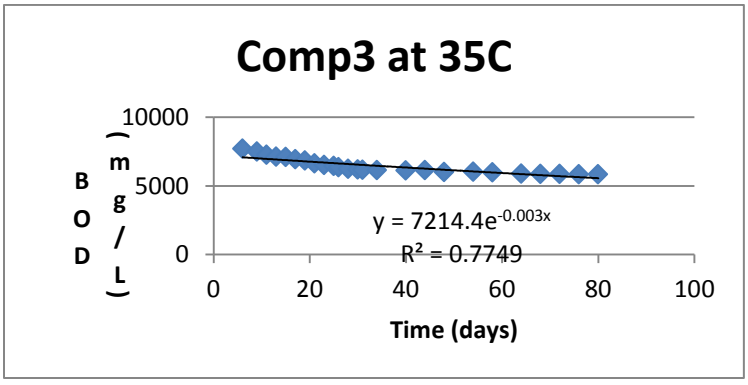
Comp3 at 35C
BOD (mg/L)
10000
5000
0
0
20
40
60
80
100
Time (days)
y = 7214.4e-0.003x
R² = 0.7749

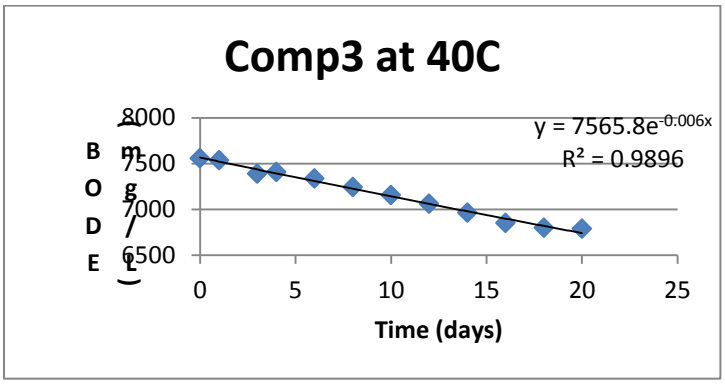
Comp3 at 40C
y = 7565.8e-0.006x
R² = 0.9896
BOD (mg/L)
8000
7500
7000
6500
0
5
10
15
20
25
Time (days)

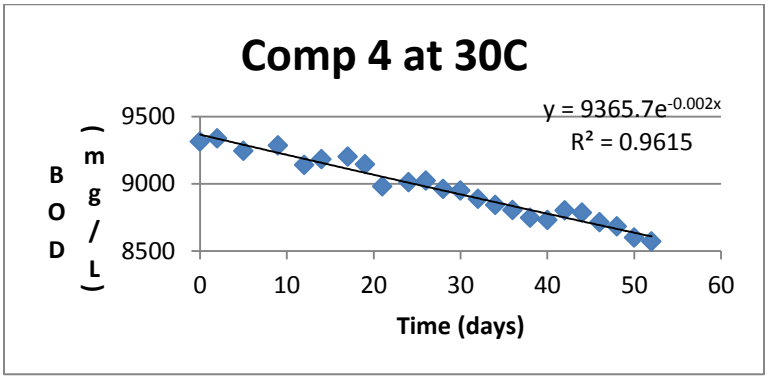
Comp 4 at 30C
y = 9365.7e-0.002x
R² = 0.9615
BOD (mg/L)
9500
9000
8500
0
10
20
30
40
50
60
Time (days)

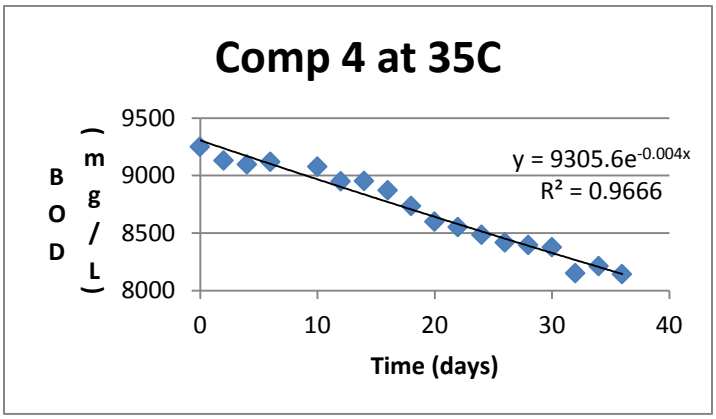
Comp 4 at 35C
y = 9305.6e-0.004x
R² = 0.9666
BOD (mg/L)
9500
9000
8500
8000
0
10
20
30
40
Time (days)

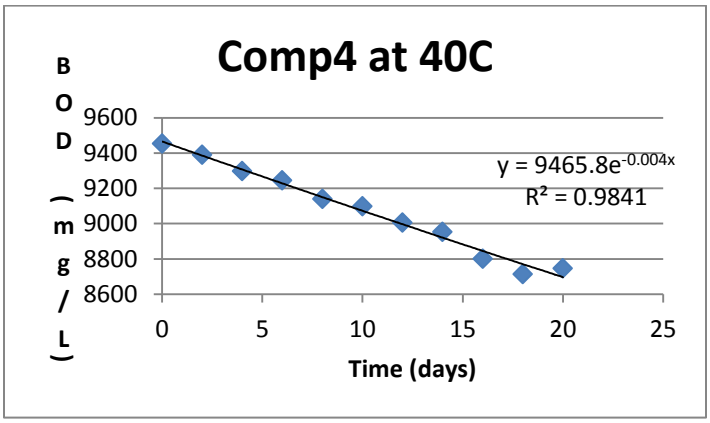
Comp4 at 40C
BOD (mg/L)
9600
9400
9200
9000
8800
8600
0
5
10
15
20
25
Time (days)
y = 9465.8e-0.004x
R² = 0.9841

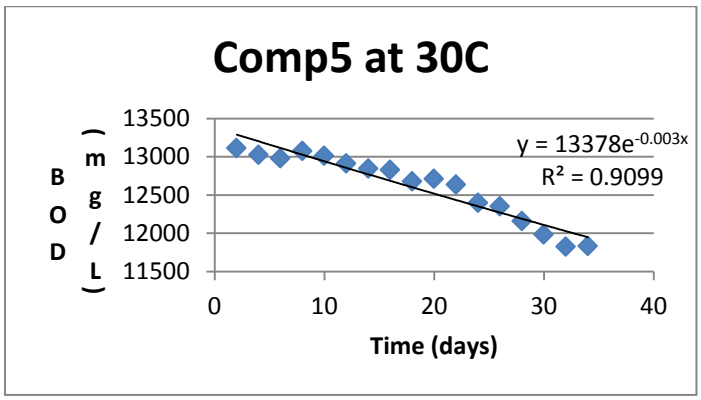
Comp5 at 30C
BOD (mg/L)
13500
13000
12500
12000
11500
0
10
20
30
40
Time (days)
y = 13378e-0.003x
R² = 0.9099

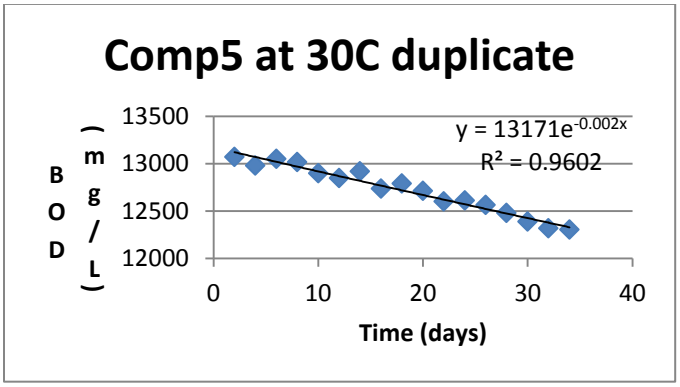
Comp5 at 30C duplicate
BOD (mg/L)
13500
13000
12500
12000
0
10
20
30
40
Time (days)
y = 13171e-0.002x
R² = 0.9602

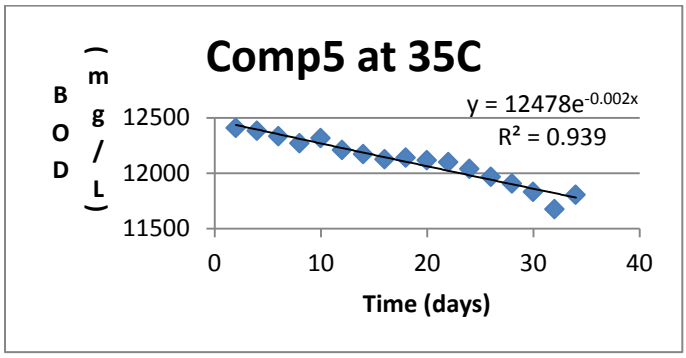
Comp5 at 35C
BOD (mg/L)
y = 12478e-0.002x
R² = 0.939
12500
12000
11500
0
10
20
30
40
Time (days)

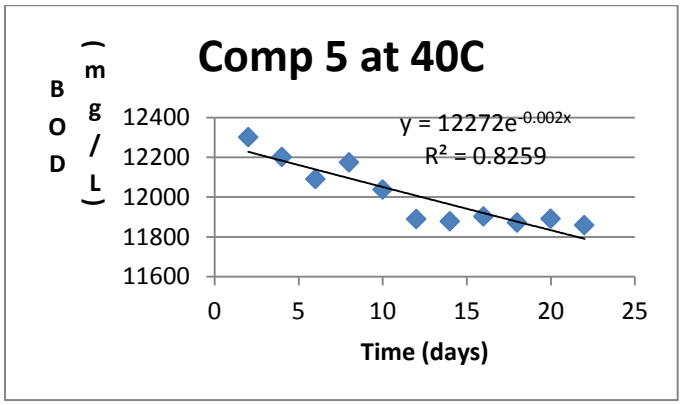
Comp 5 at 40C
BOD (mg/L)
y = 12272e-0.002x
R² = 0.8259
12400
12200
12000
11800
11600
0
5
10
15
20
25
Time (days)

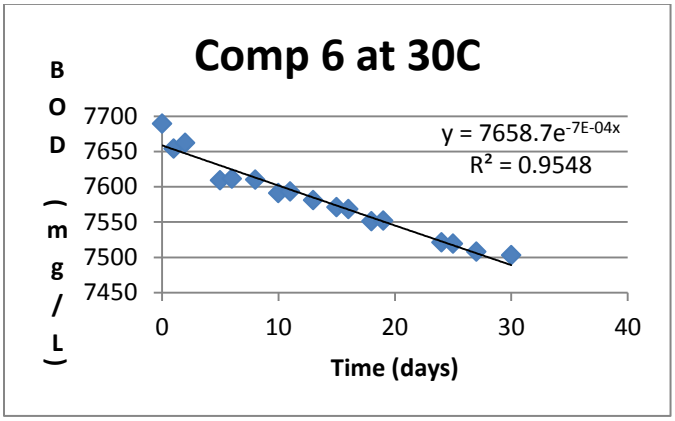
Comp 6 at 30C
BOD (mg/L)
y = 7658.7e-7E-04x
R² = 0.9548
7700
7650
7600
7550
7500
7450
0
10
20
30
40
Time (days)

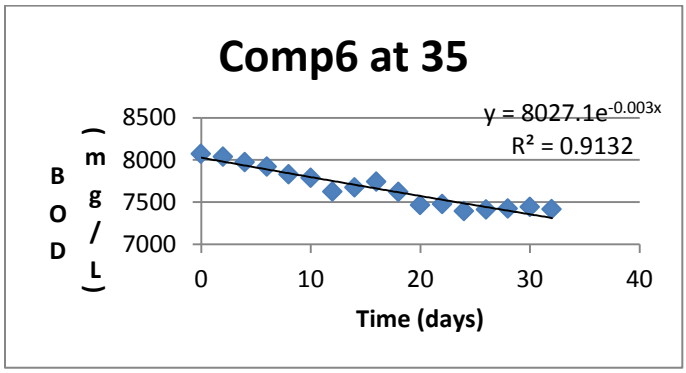

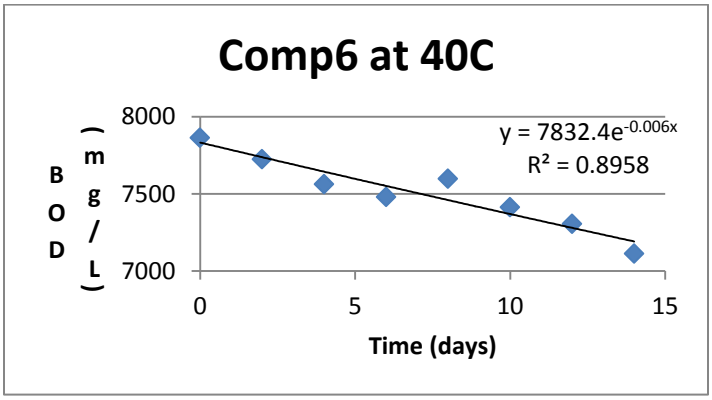

Water quality parameters

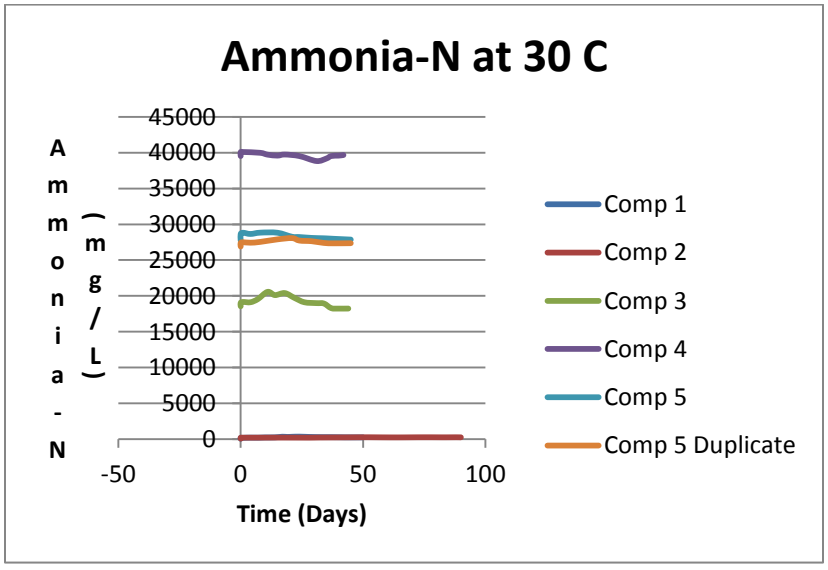

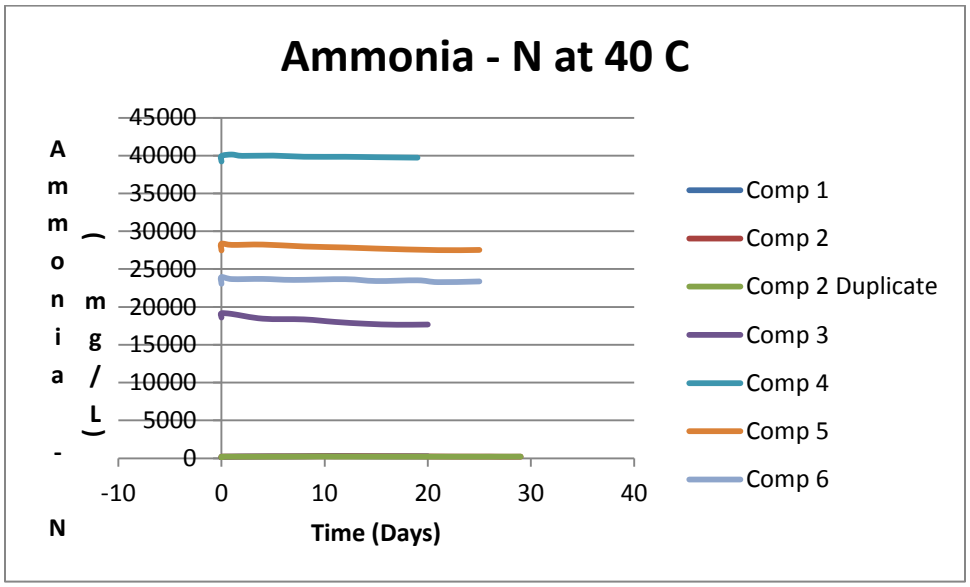
Ammonia - N at 40 C
Ammonia - N (mg/L)
45000
40000
35000
30000
25000
20000
15000
10000
5000
0
-10
0
10
20
30
40
Time (Days)
Comp 1
Comp 2
Comp 2 Duplicate
Comp 3
Comp 4
Comp 5
Comp 6

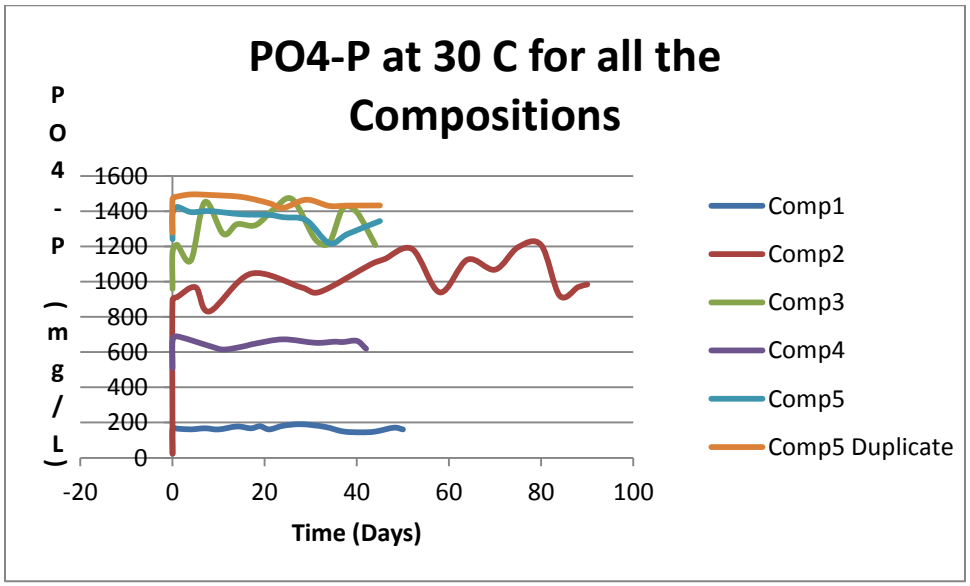
PO4-P at 30 C for all the Compositions
PO4-P (mg/L)
1600
1400
1200
1000
800
600
400
200
0
-20
0
20
40
60
80
100
Time (Days)
Comp1
Comp2
Comp3
Comp4
Comp5
Comp5 Duplicate

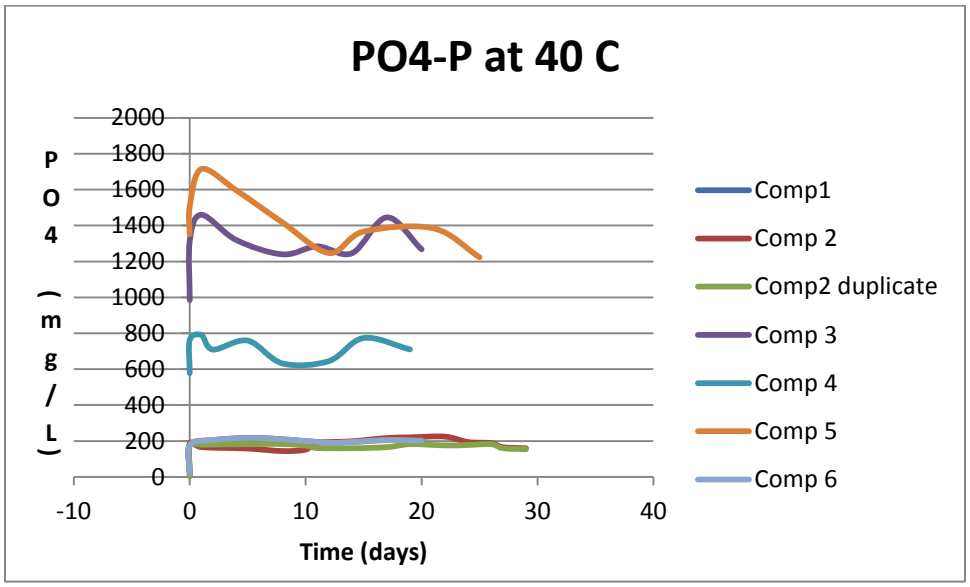
PO4-P at 40 C
PO4 (mg/L)
2000
1800
1600
1400
1200
1000
800
600
400
200
0
-10
0
10
20
30
40
Time (days)
Comp1
Comp 2
Comp2 duplicate
Comp 3
Comp 4
Comp 5
Comp 6

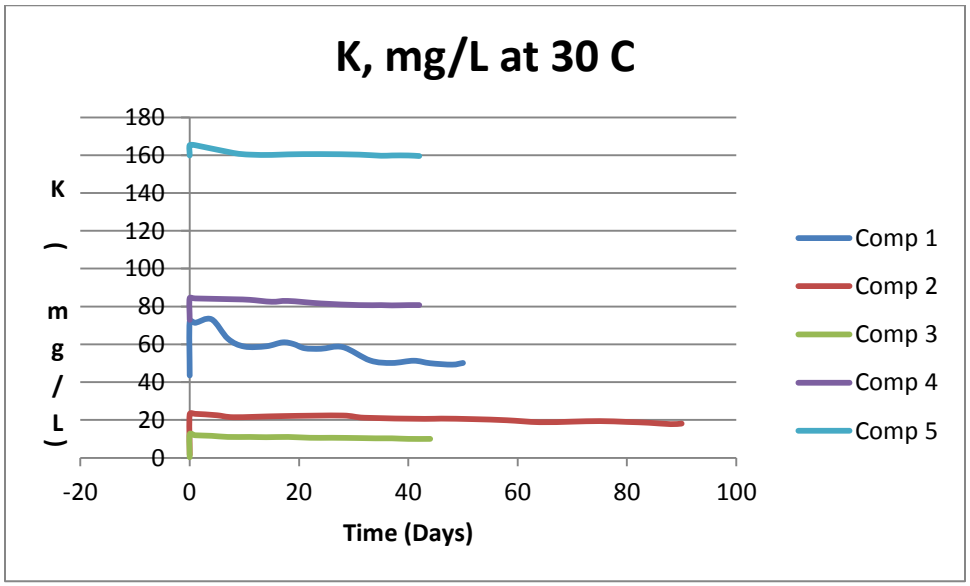
K, mg/L at 30 C
K (mg/L)
180
160
140
120
100
80
60
40
20
0
-20
0
20
40
60
80
100
Time (Days)
Comp 1
Comp 2
Comp 3
Comp 4
Comp 5

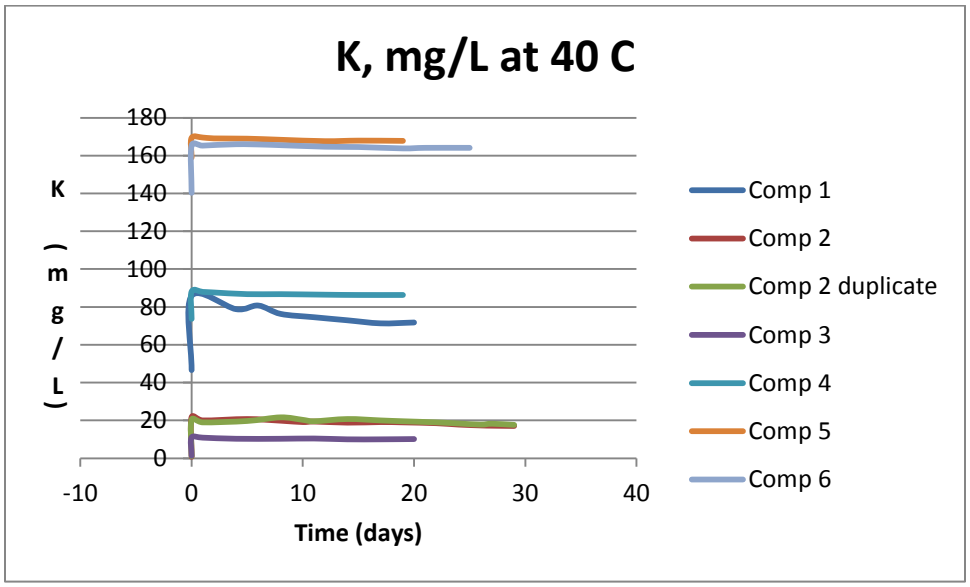
K, mg/L at 40 C
K (mg/L)
180
160
140
120
100
80
60
40
20
0
-10
0
10
20
30
40
Time (days)
Comp 1
Comp 2
Comp 2 duplicate
Comp 3
Comp 4
Comp 5
Comp 6

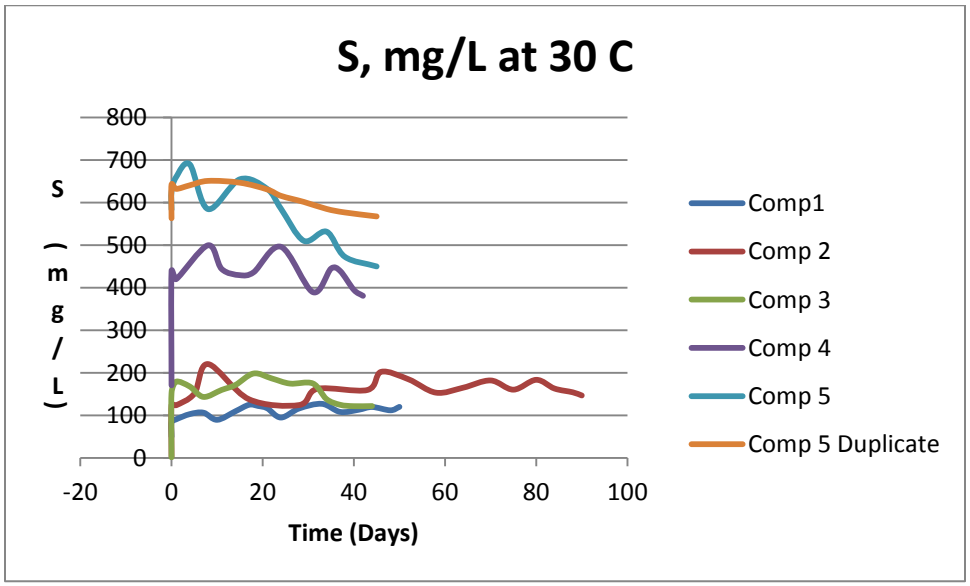
S, mg/L at 30 C
S (mg/L)
800
700
600
500
400
300
200
100
0
-20
0
20
40
60
80
100
Time (Days)
Comp1
Comp 2
Comp 3
Comp 4
Comp 5
Comp 5 Duplicate

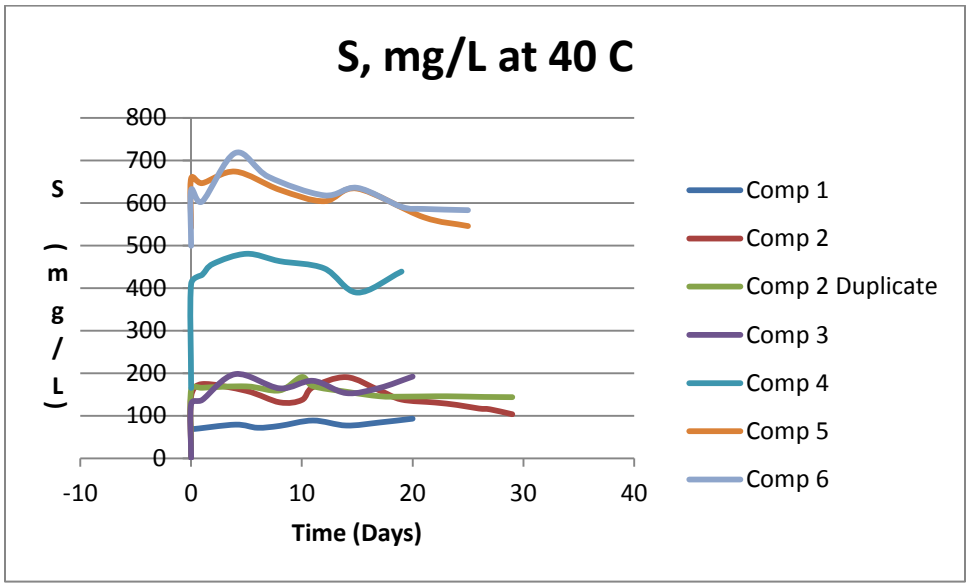
S, mg/L at 40 C
800
700
600
500
400
300
200
100
0
S (mg/L)
-10
0
10
20
30
40
Time (Days)
Comp 1
Comp 2
Comp 2 Duplicate
Comp 3
Comp 4
Comp 5
Comp 6

Appendix B

Residual Plots for Several Transformations and Hypothesis Tests

K_{COD} on T,N,P,K and S.

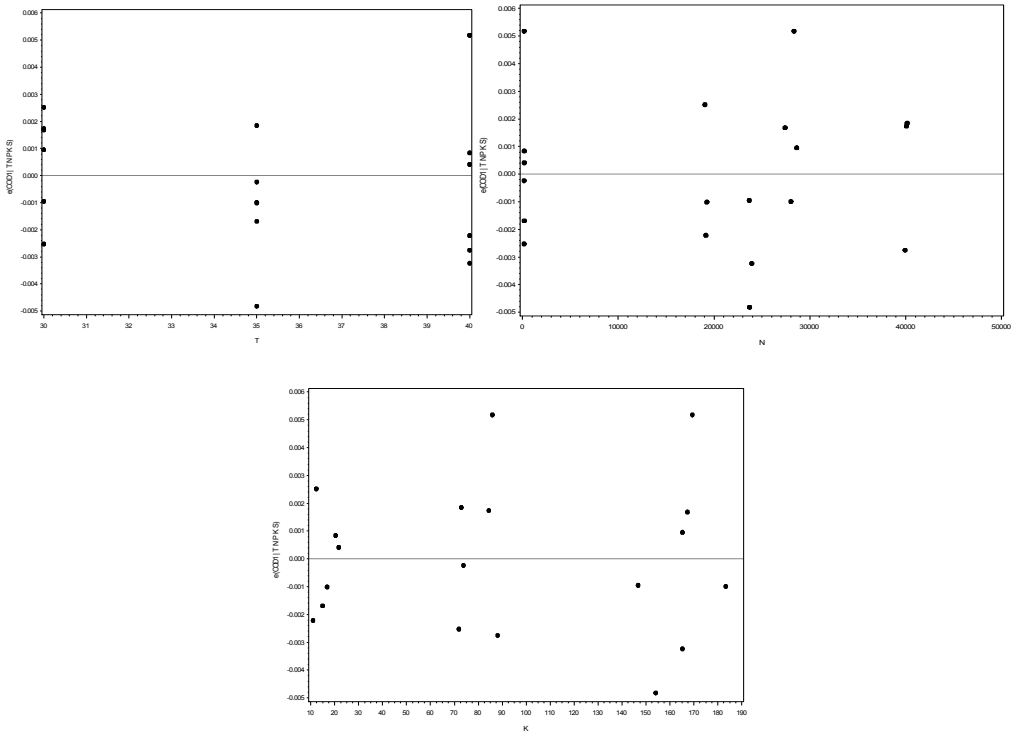

Fig. B.1-Residual vs. Predictor graph for the preliminary model.

Square root to K_{COD} on T,N,P,K and S.

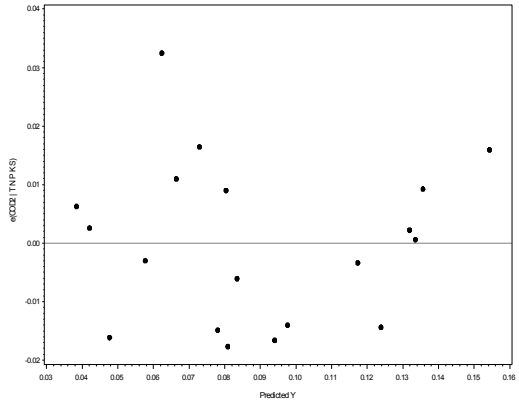

Fig. B.2 -- Residuals vs. Fitted Values

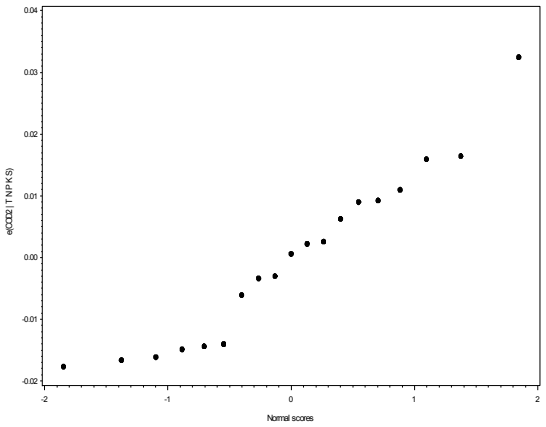

Fig. B.3 - Normal Probability Plot

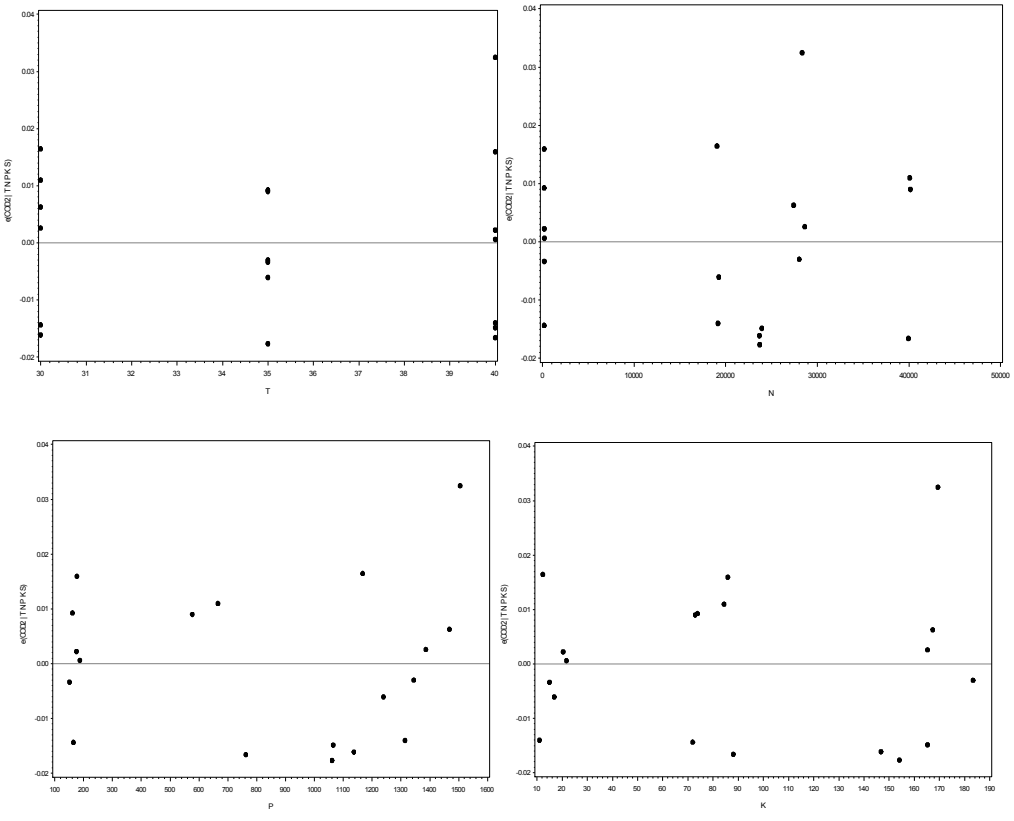

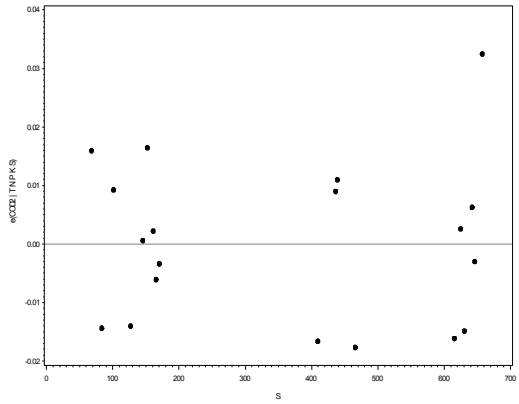

Fig. B.4 - Plots of Residuals vs. Predictor Variables

Log(K_{COD}) on T,N,P,K and S.

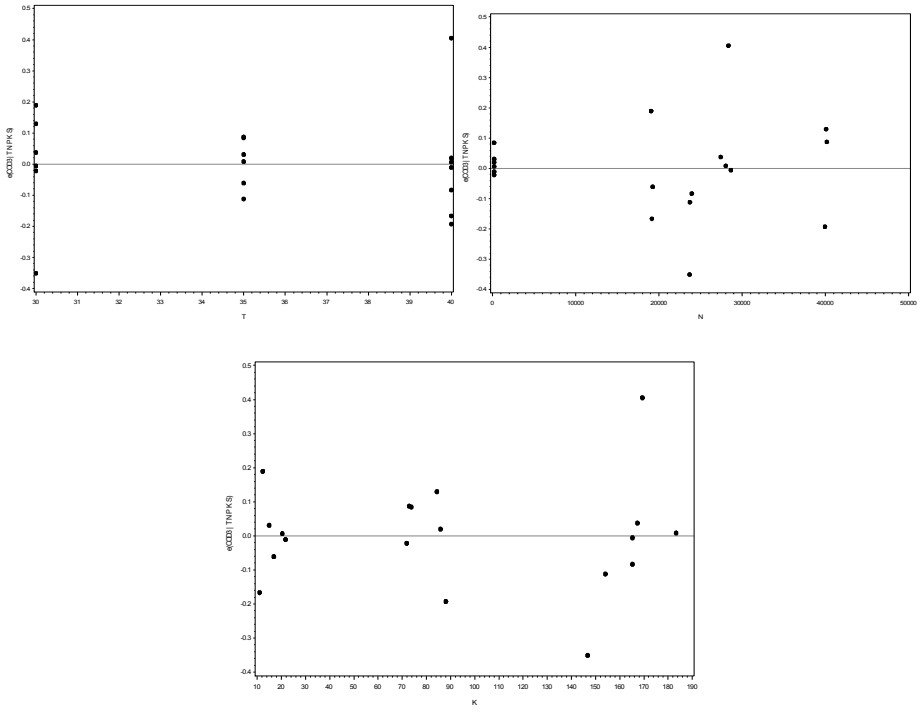

Fig. B.5 - Plots of Residuals vs. Predictor Variables

Hypothesis Tests for the kCOD Transformed Model:

A - Modified Levene test is used to ascertain whether the error terms have constant variance. The test is robust against serious departures from normality.

1. F-test

- Hypothesis

$H_0 : \sigma_{d1} = \sigma_{d2}$

$H_1 : \sigma_{d1} \neq \sigma_{d2}$

- Decision rule

Assuming significance level, $\alpha = 0.10$

From F – test , reject H_0 if p value < 0.10,

P value = 0.0289(which is less than 0.10).

Hence, we reject H_0 with 90% confidence. Thus the variance of the two groups are not equal ($\sigma_{d1} \neq \sigma_{d2}$).

- Conclusion

Variances of d1 and d2 are equal.

2. T-test

T-test is performed to check whether the error variance is constant.

- Hypothesis:

H_0 : Constant Error Variance.

H_1 : Constant Error Variance violated.

- Decision rule

If p – value (t test) < 0.10, then reject H_0

P = 0.1589 >0.1. Hence we failed to reject H_0.

- Conclusion

Constant Variance assumption is satisfied.

Table B.1 SAS Output of the Modified Levene Test

The TTEST Procedure

Variable: d

group	N	Mean	Std Dev	Std Err	Minimum	Maximum
1	9	0.1456	0.1440	0.0480	0	0.3954
2	10	0.0667	0.0651	0.0206	0.00848	0.1917
Diff (1-2)		0.0790	0.1095	0.0503		

group	Method	Mean	95% CL Mean		Std Dev	95% CL Std Dev	
1		0.1456	0.0350	0.2563	0.1440	0.0973	0.2758
2		0.0667	0.0201	0.1132	0.0651	0.0448	0.1189
Diff (1-2)	Pooled	0.0790	-0.0272	0.1852	0.1095	0.0822	0.1642
Diff (1-2)	Satterthwaite	0.0790	-0.0361	0.1941			

Method	Variances	DF	t Value	Pr > |t|
Pooled	Equal	17	1.57	0.1351
Satterthwaite	Unequal	10.889	1.51	0.1589

Equality of Variances

Method	Num DF	Den DF	F Value	Pr > F
Folded F	8	9	4.89	0.0289

Table B.2- SAS Output of the Normality Test

Pearson Correlation Coefficients, N = 19

	e	enrm
e	1.00000	0.96111
e(COD3 | T N P K S)		
enrm	0.96111	1.00000
Normal scores		

B – Normality Test

This verifies whether residuals are normally distributed or not.

- Hypothesis

H_0 : Normality is reasonable.

H_1 : Normality is violated.

- Decision rule

If ρ, the correlation coefficient is < C(α,n), the cutoff value, we reject H_0.

ρ = 0.961 (from the above Table C-2)

Assuming α = 0.1, C (0.1,19) = 0.9585

Since, ρ = 0.961 > 0.9585, we failed to reject H_0.

- Conclusion

Normality is OK.

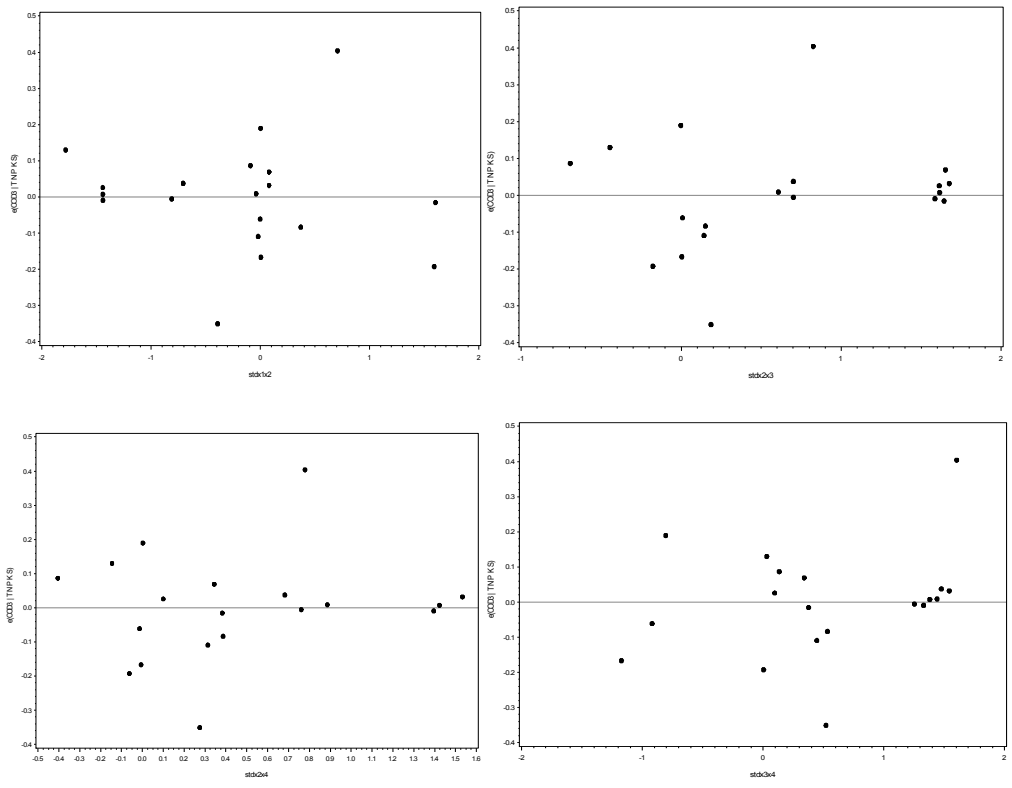

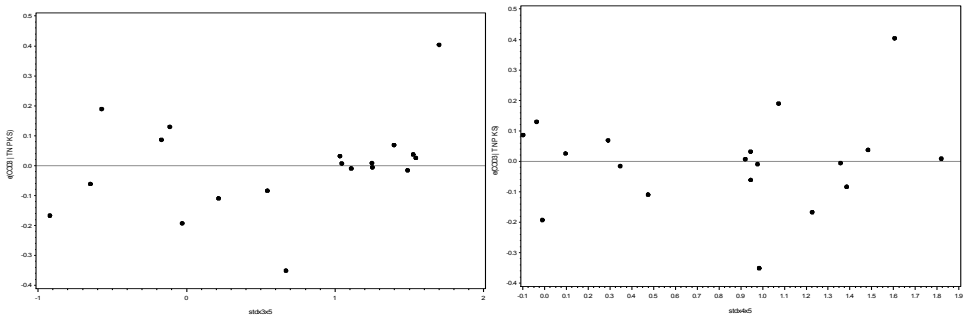

Fig. B.6– Partial Regression plots

Table B.3 - SAS Output of Best Subsets Model Search Method for K_{COD}

The REG Procedure
Model: MODEL1
Dependent Variable: COD3

Adjusted R-Square Selection Method

Number of Observations Read 19
Number of Observations Used 19

Number in Model	R-Square	Adjusted R-Square	C(p)	AIC	SBC	Variables in Model
1	0.6054	0.6274	56.2274	-52.2754	-50.38651	S
1	0.5532	0.5780	65.6614	-49.9121	-48.02323	P
2	0.7227	0.7535	34.1223	-58.1249	-55.29155	T S
2	0.7074	0.7399	36.7095	-57.1093	-54.27602	S stdx2x5
3	0.8257	0.8547	16.7712	-66.1710	-62.39328	T S stdx2x5
3	0.8086	0.8405	19.4953	-64.3932	-60.61541	T K stdx2x5
4	0.9027	0.9243	5.4669	-76.5616	-71.83943	T K stdx1x4 stdx2x5
4	0.8923	0.9162	7.0091	-74.6371	-69.91487	T S stdx1x4 stdx2x5
5	0.9143	0.9381	4.8369	-78.3739	-72.70726	T N S stdx1x4 stdx2x5
5	0.9089	0.9342	5.5765	-77.2223	-71.55567	T K S stdx1x4 stdx2x5
6	0.9246	0.9497	4.6125	-80.3288	-73.71773	T N K S stdx1x4 stdx2x5
6	0.9123	0.9416	6.1709	-77.4741	-70.86306	T N S stdx1x3 stdx1x4 stdx2x5
7	0.9215	0.9520	6.1746	-79.2147	-71.65916	T N K S stdx1x3 stdx1x4 stdx2x5
7	0.9212	0.9518	6.2071	-79.1476	-71.59210	T N K S stdx1x4 stdx1x5 stdx2x5
8	0.9147	0.9526	8.0623	-77.4487	-68.94877	T N P K S stdx1x3 stdx1x4 stdx2x5
8	0.9143	0.9524	8.0998	-77.3704	-68.87041	T N K S stdx1x3 stdx1x4 stdx1x5 stdx2x5
9	0.9058	0.9529	10.0000	-75.5798	-66.13540	T N P K S stdx1x3 stdx1x4 stdx1x5 stdx2x5

Table B.4 - Parameter estimates of Model 5

Parameter Estimates

Variable	DF	Parameter Estimate	Standard Error	t Value	Pr > |t|	Variance Inflation
Intercept	1	-3.06402	0.24933	-12.29	<.0001	0
T	1	0.02885	0.00659	4.38	0.0008	1.05432
K	1	-0.00211	0.00112	-1.88	0.0822	6.92346
S	1	-0.00045297	0.00032404	-1.40	0.1855	7.62261
stdTK	1	0.11177	0.02964	3.77	0.0023	1.05029
stdNS	1	0.35485	0.07143	4.97	0.0003	1.77938

Table B.5 Parameter estimate of Model 6

Parameter Estimates

Variable	DF	Parameter Estimate	Standard Error	t Value	Pr > |t|	Variance Inflation
Intercept	1	-3.19091	0.23628	-13.50	<.0001	0
T	1	0.02998	0.00603	4.97	0.0003	1.06441
N	1	0.00000638	0.00000331	1.92	0.0785	3.83301
K	1	-0.00173	0.00104	-1.67	0.1215	7.18336
S	1	-0.00078577	0.00034187	-2.30	0.0403	10.24688
stdTK	1	0.10376	0.02729	3.80	0.0025	1.07534
stdNS	1	0.42376	0.07422	5.71	<.0001	2.31987

Table B.6 – Measures of outliers for the selected model

Obs	yhat	e	tres	cookdi	hii	dffitsi	enrm
1	-1.77266	-0.14816	-1.70886	0.32671	0.40165	-1.52764	-1.09680
2	-2.17049	0.07358	0.97519	0.19124	0.54681	1.06901	0.40115
3	-2.32275	0.10090	1.11984	0.11439	0.35373	0.83739	1.09680
4	-2.70653	0.00756	0.08023	0.00045	0.29328	0.04967	-0.13058
5	-2.76186	0.06289	0.67287	0.03304	0.30454	0.43545	0.26344
6	-2.84794	-0.15206	-1.64289	0.20983	0.31808	-1.21106	-1.37597
7	-1.71144	0.01247	0.12477	0.00067	0.20448	0.06081	-0.00000
8	-1.93722	0.05116	0.50105	0.00857	0.17000	0.22000	0.13058
9	-2.17332	-0.04853	-0.50331	0.01483	0.25994	-0.28943	-0.40115
10	-2.18035	0.08344	0.88682	0.05491	0.29526	0.56897	0.88413
11	-2.45341	-0.06946	-0.67673	0.01468	0.16127	-0.29026	-0.54695
12	-2.47941	0.08147	0.79225	0.01966	0.15823	0.33828	0.70547
13	-1.45618	-0.08142	-0.87607	0.05811	0.31238	-0.58485	-0.70547
14	-1.82129	0.07657	0.78792	0.03418	0.24832	0.44587	0.54695
15	-1.87603	0.13131	1.35477	0.10319	0.25225	0.81577	1.84570
16	-2.10775	-0.04715	-0.57868	0.04980	0.47153	-0.53207	-0.26344
17	-2.06292	-0.15892	-1.79211	0.31981	0.37401	-1.53376	-1.84570
18	-2.15166	0.10590	1.24700	0.19228	0.42592	1.09984	1.37597
19	-2.31639	-0.08155	-0.97959	0.12996	0.44831	-0.88156	-0.88413

Table B.7 - DFBEATS for the selected model

	DFBETAS					
Obs	Intercept	T	N	S	stdTK	stdNS
1	-0.8528	0.9204	-0.0283	0.4001	-0.4687	-0.6630
2	0.7160	-0.5189	-0.1859	-0.2375	0.6139	-0.4982
3	0.2126	-0.3453	0.6381	-0.4444	0.0478	0.3733
4	0.0140	-0.0205	0.0031	0.0136	-0.0272	0.0094
5	0.1355	-0.1775	-0.0348	0.1670	-0.2367	0.0282
6	-0.6094	0.5312	0.6110	-0.7072	0.4070	0.5351
7	0.0127	-0.0118	-0.0019	-0.0148	0.0114	0.0277
8	0.0870	-0.0452	-0.1328	0.0386	0.0574	-0.0380
9	-0.1080	0.0239	0.0421	0.0919	-0.0191	0.2004
10	-0.1229	0.0445	0.5025	-0.3179	-0.0176	0.2736
11	0.0570	-0.0253	0.0161	-0.1750	-0.0223	-0.0651
12	0.0781	0.0018	-0.1738	0.1485	0.0224	-0.2578
13	0.2181	-0.2071	-0.1313	0.1902	-0.0330	-0.3576
14	-0.1442	0.2017	-0.0917	-0.0043	-0.2183	0.0265
15	-0.2379	0.3685	-0.2517	0.0585	-0.4027	-0.0543
16	0.0862	-0.2087	-0.0278	0.1835	0.2846	0.2581
17	0.8786	-0.8161	-1.1530	0.7323	0.1498	-0.4095
18	-0.5481	0.4948	-0.0359	0.4937	0.6418	0.2246
19	0.2682	-0.3665	0.3956	-0.5654	-0.4917	0.2847

K_{BOD} on T,N,P,K and S.

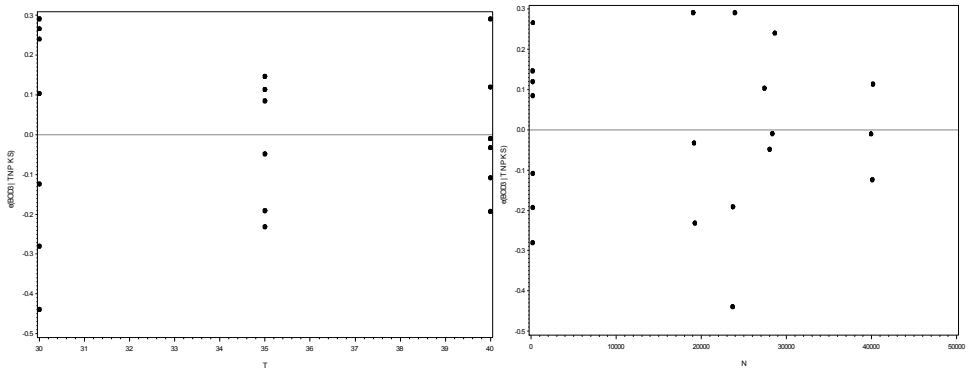

Fig. B.7- Residuals vs. Predictor Plots

Square root of k_{BOD} on T,N,P,K and S.

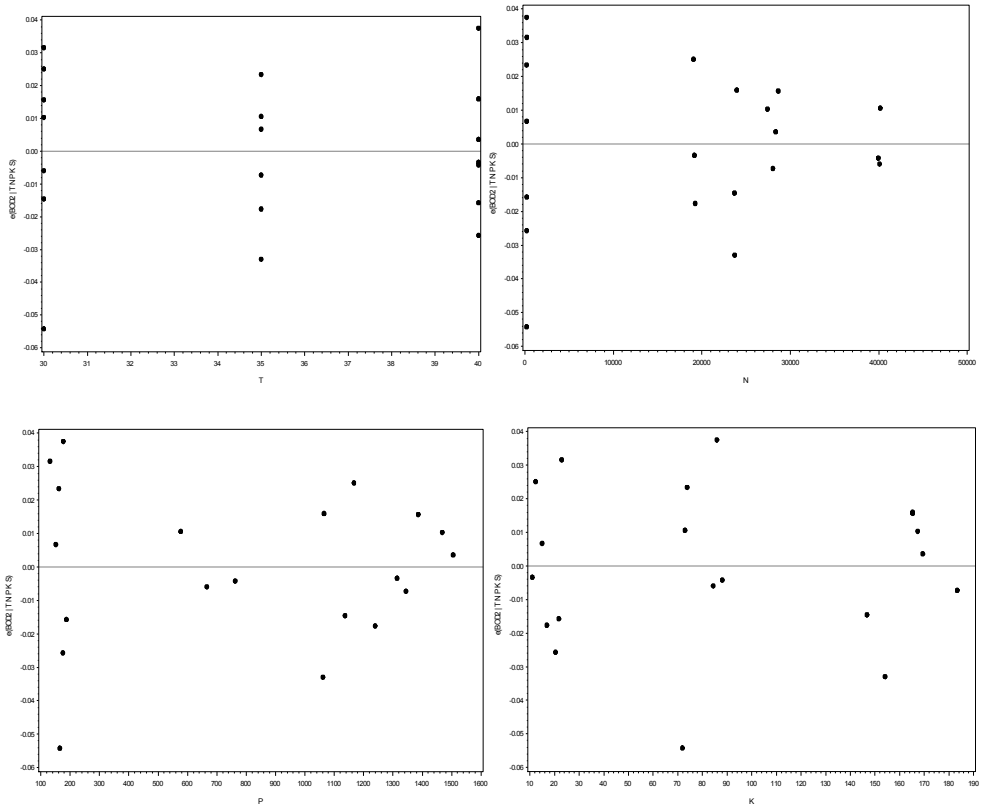

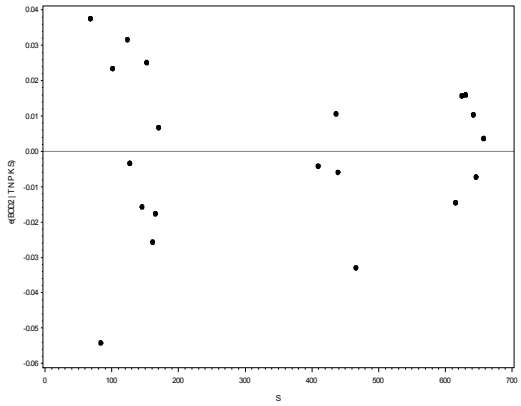

Fig. B.8 - Residuals vs. Predictor Plots

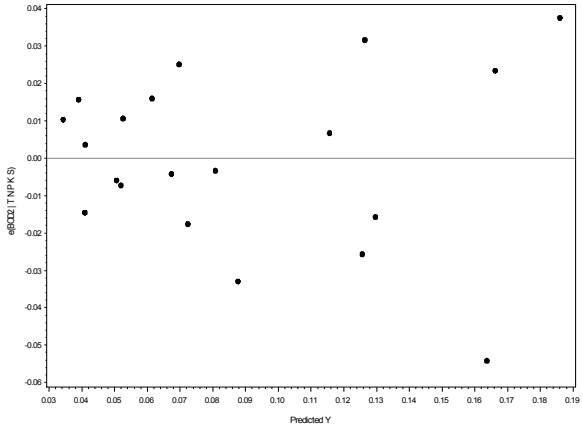

Fig. B.9 - Residuals vs. Fits Plot of the Preliminary Model

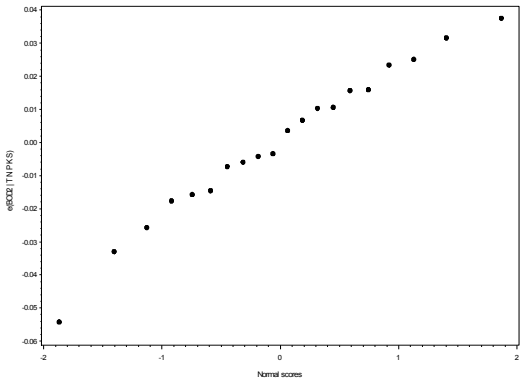

Fig. B.10 – Normality Graph of the Preliminary Model.

$Log_{10}(k_{BOD})$on T,N,P,K and S.

Hypothesis Tests for the k_{BOD} Transformed Model:

A - Modified Levene test is used to ascertain whether the error terms have constant variance. The test is robust against serious departures from normality.

1. F-test

- Hypothesis

$H_0 : \sigma_{d1} = \sigma_{d2}$

$H_1 : \sigma_{d1} \neq \sigma_{d2}$

- Decision rule

Assuming significance level, $\alpha = 0.10$

From F – test , reject H_0 if p value < 0.10,

P value = 0.2244(which is greater than 0.10).

Hence, we failed to reject H_0 with 90% confidence. Thus the variance of the two groups are equal ($\sigma_{d1} = \sigma_{d2}$).

- Conclusion

Variances of d1 and d2 are equal.

2. T-test

T-test is performed to check whether the error variance is constant.

- Hypothesis:

H_0 : Constant Error Variance.

H_1 : Constant Error Variance violated.

- Decision rule

If p – value (t test) < 0.10, then reject H_0

P = 0.8627 >0.1. Hence we failed to reject H_0.

- Conclusion

Constant Variance assumption is satisfied.

Table B.8 –SAS Output of the Modified Levine Test

The TTEST Procedure

Variable: d

group	N	Mean	Std Dev	Std Err	Minimum	Maximum
1	11	0.1684	0.1384	0.0417	0	0.4302
2	9	0.1590	0.0891	0.0297	0	0.2988
Diff (1-2)		0.00939	0.1190	0.0535		

group	Method	Mean	95% CL Mean		Std Dev	95% CL Std Dev	
1		0.1684	0.0754	0.2614	0.1384	0.0967	0.2429
2		0.1590	0.0906	0.2275	0.0891	0.0602	0.1706
Diff (1-2)	Pooled	0.00939	-0.1030	0.1218	0.1190	0.0899	0.1760
Diff (1-2)	Satterthwaite	0.00939	-0.0986	0.1173			

Method	Variances	DF	t Value	Pr > |t|
Pooled	Equal	18	0.18	0.8627
Satterthwaite	Unequal	17.182	0.18	0.8567

Equality of Variances

Method	Num DF	Den DF	F Value	Pr > F
Folded F	10	8	2.42	0.2244

B – Normality Test

This verifies whether residuals are normally distributed or not.

- Hypothesis

H_0 : Normality is OK.

H_1 : Normality is violated.

- Decision rule

If ρ, the correlation coefficient is < C(α,n), the cutoff value, we reject H_0.

ρ = 0.986 (from the above Table C-2)

Assuming α = 0.1, C (0.1,20) = 0.960

Since, ρ = 0.986 >0.960, we failed to reject H_0.

- Conclusion

Normality is OK.

Table B.9 - SAS Output of the Normality Test.

Pearson Correlation Coefficients, N = 20		
	e	enrm
e	1.00000	0.98604
	e(BOD3 | T N P K S)	
enrm	0.98604	1.00000
	Normal scores	

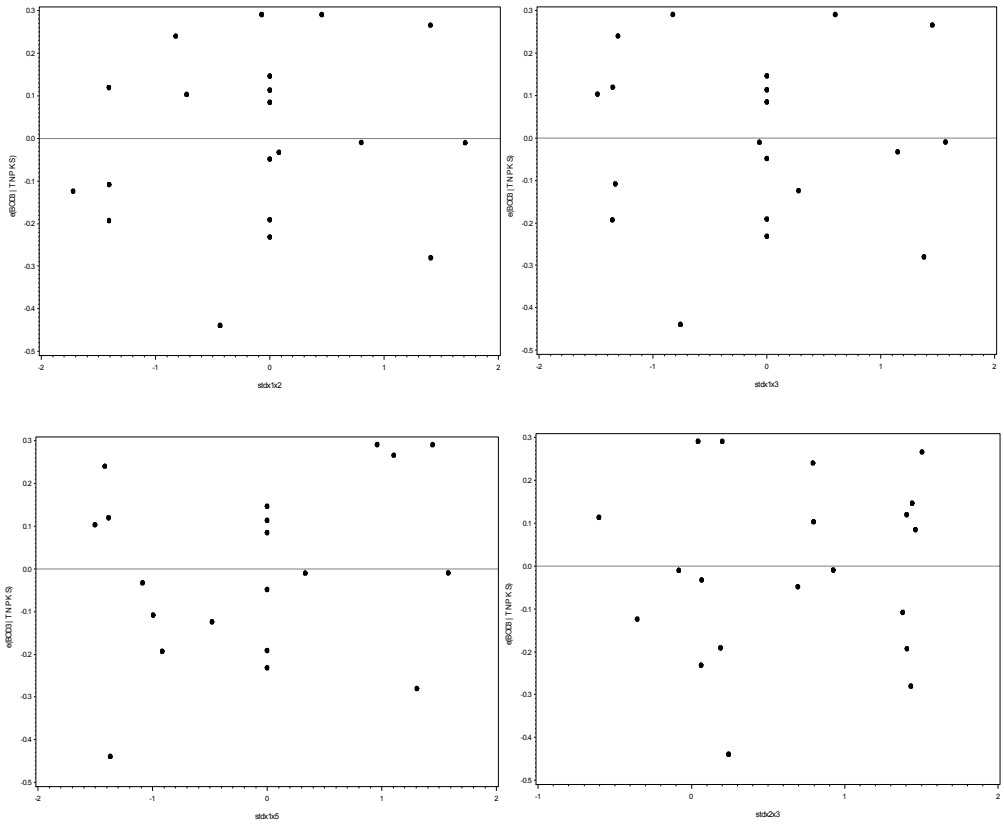

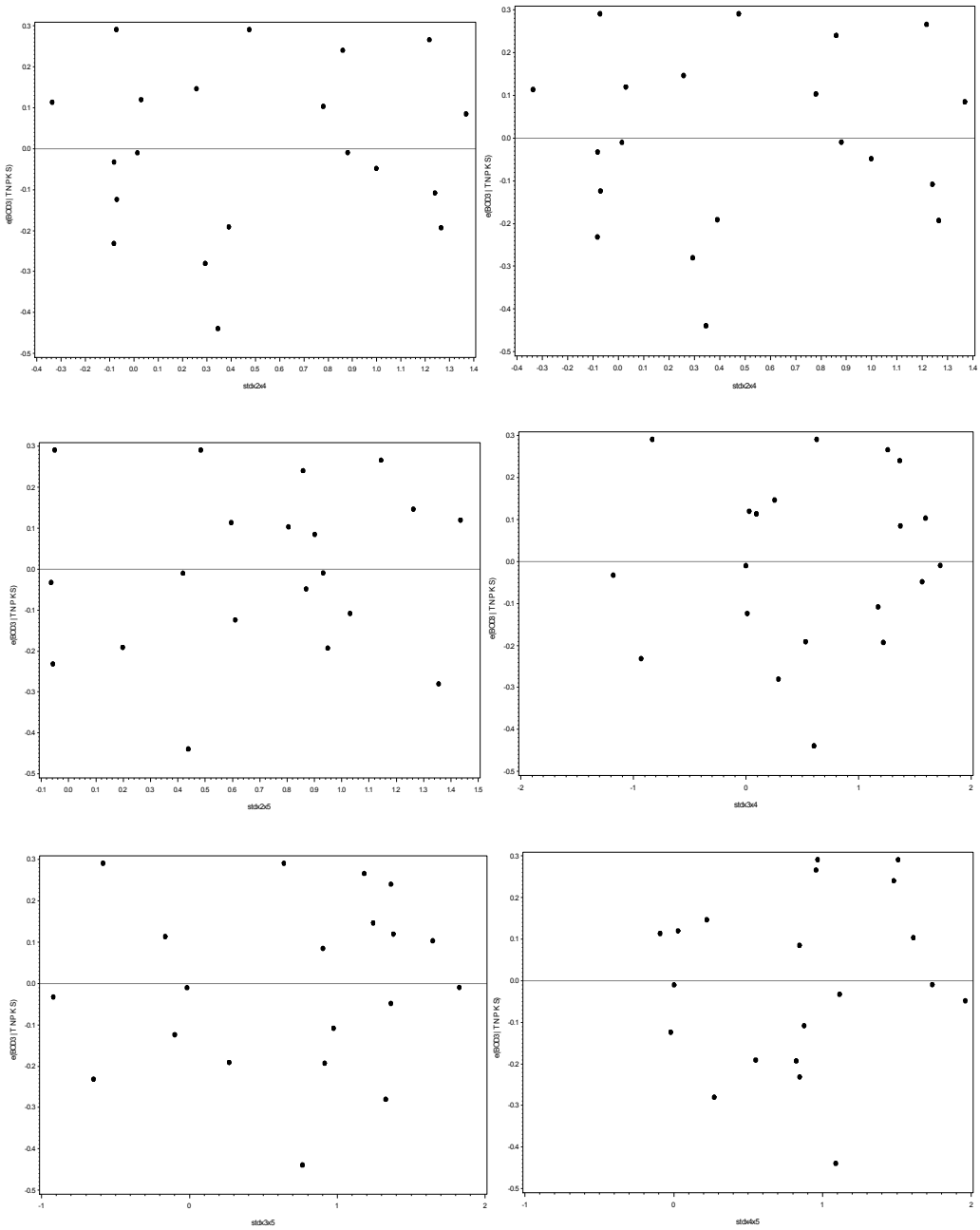

Fig. B.11– Partial Regression Plots

Table B.10 – Parameter estimate of Model 4

Parameter Estimates

Variable	DF	Parameter Estimate	Standard Error	t Value	Pr > |t|	Variance Inflation
Intercept	1	-2.14471	0.46733	-4.59	0.0004	0
T	1	0.01497	0.01271	1.18	0.2571	1.01738
P	1	-0.00030989	0.00014579	-2.13	0.0505	2.03806
K	1	0.00412	0.00183	2.25	0.0401	4.69108
S	1	-0.00214	0.00058713	-3.64	0.0024	6.32539

Table B.11 - Parameter estimate of Model 4

Parameter Estimates

Variable	DF	Parameter Estimate	Standard Error	t Value	Pr > |t|	Variance Inflation
Intercept	1	-1.60004	0.10474	-15.28	<.0001	0
P	1	-0.00036089	0.00015658	-2.30	0.0359	2.27506
K	1	0.00439	0.00188	2.33	0.0339	4.78492
S	1	-0.00213	0.00059753	-3.57	0.0028	6.34001
stdTK	1	0.05652	0.06099	0.93	0.3687	1.16877

Table B.12– Parameter estimate of Model 5

Parameter Estimates

Variable	DF	Parameter Estimate	Standard Error	t Value	Pr > |t|	Variance Inflation
Intercept	1	-2.12993	0.47011	-4.53	0.0005	0
T	1	0.01477	0.01278	1.16	0.2672	1.01769
P	1	-0.00035589	0.00015492	-2.30	0.0375	2.27684
K	1	0.00436	0.00186	2.34	0.0345	4.78606
S	1	-0.00210	0.00059171	-3.55	0.0032	6.35611
stdTK	1	0.05531	0.06033	0.92	0.3748	1.16913

Table B.13 – Measures for Outliers for the Selected Model

Obs	e	tres	cookdi	hii	dffitsi	enrm
1	-0.37813	-1.83609	0.28834	0.25491	-1.17044	-1.40341
2	0.22006	0.99805	0.04254	0.14591	0.41247	1.40341
3	0.20800	1.02870	0.10381	0.28181	0.64564	1.12814
4	-0.27915	-1.26377	0.06656	0.14289	-0.52658	-1.12814
5	0.19148	0.86667	0.03120	0.14248	0.35038	0.91914
6	0.06993	0.31926	0.00476	0.15729	0.13398	0.18676
7	-0.46243	-2.07800	0.16135	0.13003	-0.91034	-1.86824
8	0.12868	0.61725	0.02950	0.23650	0.33666	0.44777
9	0.13880	0.65143	0.02692	0.20241	0.32204	0.58946
10	-0.23698	-1.18664	0.15041	0.29935	-0.78642	-0.91914
11	0.03584	0.16951	0.00196	0.21462	0.08587	0.06193
12	-0.02672	-0.12318	0.00079	0.17323	-0.05462	-0.31457
13	-0.20932	-0.95299	0.04085	0.15247	-0.40297	-0.74414
14	0.15401	0.81775	0.10112	0.37690	0.62908	0.74414
15	0.00597	0.02707	0.00003	0.14612	0.01084	-0.18676
16	-0.07202	-0.33035	0.00539	0.16507	-0.14271	-0.58946
17	0.02864	0.15324	0.00369	0.38621	0.11778	-0.06193
18	-0.02711	-0.11841	0.00030	0.07923	-0.03365	-0.44777
19	0.10655	0.48924	0.01198	0.16675	0.21352	0.31457
20	0.40390	1.83170	0.14318	0.14581	0.82426	1.86824

Table B.14 - DFBETAS for the selected model

	DFBETAS			
Obs	Intercept	P	K	S
1	-0.7309	0.1575	-0.8112	0.7924
2	0.3906	-0.2202	-0.1256	0.0902
3	0.1717	0.4683	-0.1845	-0.1382
4	-0.1770	0.2890	0.3257	-0.4163
5	-0.1320	0.0919	0.0794	0.0058
6	-0.0558	0.0439	0.0252	0.0031
7	0.1730	0.1682	0.1630	-0.4623
8	0.2151	-0.0628	0.2269	-0.2138
9	0.2550	-0.1884	-0.1950	0.1751
10	-0.1706	-0.6013	0.1953	0.1924
11	0.0292	-0.0507	-0.0605	0.0732
12	0.0203	-0.0090	-0.0234	0.0058
13	0.0317	-0.0948	-0.3023	0.2183
14	0.3097	-0.0228	0.5036	-0.4858
15	0.0098	-0.0057	-0.0047	0.0036
16	-0.1220	0.0805	0.0734	-0.0629
17	0.0218	0.0962	-0.0180	-0.0409
18	-0.0129	0.0124	0.0161	-0.0203
19	-0.0932	0.0707	0.0327	0.0116
20	-0.1587	-0.2302	0.0888	0.2688

References

Aguiar MM, Ferreira LFR, Monteiro RTR. 2010. *Use of vinasse and sugarcane bagasse for the production of enzymes by lignocellulolytic fungi*. Brazilian Archives of Biology and Technology 53:1245–1254; 444 doi:10.1590/S1516-89132010000500030.

Akunna, J.C., Clark, M., 2000. *Performance of a granular-bed anaerobic baffled reactor (GRABBR) treating whisky distillery wastewater*. Bioresource Technology 74 (3), 257–261.

Alfafara, C.G., Migo, V.P., Amrante, J.A., Dallo, R.F., Matsumara, M., 2000. *Ozone treatment of distillery slop waste*. Water Science and Technology 42 (3–4), 193–198.

A. Ryznar-Luty*, M. Krzywonos, E. Cibis, T. Miśkiewicz. *Aerobic Biodegradation of Vinasse by a Mixed Culture of Bacteria of the Genus Bacillus: Optimization of Temperature, pH and Oxygenation State* Polish J. of Environ. Stud. Vol. 17, No. 1 (2008), 101-112

Belhadj S, Karouach F., El Bari H., Joute Y. *The biogas production from mesophilic anaerobic digestion of vinasse.* IOSR Journal Of Environmental Science, Toxicology And Food Technology (IOSR-JESTFT) e-ISSN: 2319-2402,p-ISSN: 2319-2399.Volume 5, Issue 6 (Sep. - Oct. 2013), PP 72-77

Bernardo, E.C., Egashira, R., Kawasaki, J., 1997*. Decolorization of molasses wastewater using activated carbon prepared from cane bagasse*. Carbon 35 (9), 1217–1221

Bhandari, H.C., Mitra, A.K., Kumar, S., 2004. Crest's integrated system: reduction and recycling of effluents in distilleries. In: Tewari, P.K. (Ed.), Liquid Asset, Proceedings of Indo-EU Workshop on Promoting Efficient Water Use in Agro-based Industries. TERI Press, New Delhi, India, pp. 167–169.

Bories, A., Raynal, J., Bazile, F., 1988. Anaerobic digestion of high strength distillery wastewater (cane molasses stillage) in a fixed-film reactor. Biological Wastes 23 (4), 251–267.

Campbell, A. Kumar, F.G. La Rosa, K.N. Prasad, S.C. Bondy . *Aluminium increases levels of ß-amyloid and ubiquitin in neuroblastoma but not in glioma cells*. Proc. Soc. Exp. Biol. Med., 223 (2000), pp. 397–402.

Carmen Baez-Smith, 2006. *Anaerobic Digestion of Vinasse for the Production of Methane in the Sugar Cane Distillery*. SPRI Conference on Sugar Processing.

CiBiSe. *Aerobic biodegradation of starch stillages from rural distilleries by means of mixed culture of thermo- and mesophilic bacteria of the genus Bacillus*.; Prace Nau-kowe Akademiie konomicznej im. oskara langego we wrocławiu, vol. 1028, 1, 2004.

Cortez LAB, Pérez B. 1997. *Experiences on vinasse disposal: Part III: Combustion of vinasse-# 6 Fuel oil emissions*. Brazilian Journal of Chemical Engineering 14; doi:10.1590/S0104-66321997000100002. Retrieved 477 January 9, 2013.

Cronin C, Lo KV: Anaerobic treatment of brewery wastewater using UASB reactors seeded with activated sludge. Bioresource Technol 1998, 64:33-38

Dahiya, J., Singh, D., Nigam, P., 2001a. *Decolorization of synthetic and spentwash melanoidins using the white-rot fungus Phanerochaete chrysosporium* JAG-40. Bioresource Technology 78 (1), 95–98.

Elda I España-Gamboa, Javier O Mijangos-Cortés, Galdy Hernández-Zárate, Jorge A Domínguez Maldonado and Liliana M Alzate-Gaviria, 2012. *Methane production by treating vinasses from hydrous ethanol using a modified UASB reactor*. Biotechnology for Biofuels.

Fahrasmane, Ganou-Parfait. 1998. *Microbial flora of rum fermentation media*. Journal of Applied 495 Microbiology 84:921–928; doi:10.1046/j.1365-2672.1998.00380.x.

Faith DP. Conservation evaluation and phylogenetic diversity. . Biol. Conserv. 1992a;61:1–10

G. Iñiguez-Cobarrubias, F. Peraza-Luna *Reduction of solids and organic load concentration in tequila vinasses using polyacrylamide (PAM) polymer flocculant* Rev. Int. Contam. Ambient., 23 (2007), pp. 17–24.

Gaikwad, R.W., Naik, P.K., 2000. *Technology for the removal of sulfate from distillery wastewater*. Indian Journal of Environmental Protection 20 (2), 106–108.

Garcı´a-Bernet, D., Buffie´ re, P., Elmaleh, S., Moletta, R., 1998. *Application of the down-flow fluidized bed to the anaerobic treatment of wine distillery wastewater.* Water Science and Technology 38 (8–9), 393–399.

Gaston, Kevin J., Biodiversity, August 1996.

Ghosh, M., Ganguli, A., Tripathi, A.K., 2002. *Treatment of anaerobically digested distillery spentwash in a two-stage bioreactor using Pseudomonas putida and Aeromonas sp*. Process Biochemistry 37 (8), 857–862.

Goodwin, J.A.S., Stuart, J.B., 1994. *Anaerobic digestion of malt whisky distillery pot ale using upflow anaerobic sludge blanket reactors*. Bioresource Technology 49 (1), 75–81

Gulati, N., 2004. *Conservation of resources using evaporation and spray drying technology for distillery and paper industries. In: Tewari, P.K. (Ed.), Liquid Asset, Proceedings of Indo-EU Workshop on Promoting Efficient Water Use in Agro-Based Industries*. TERI Press, New Delhi, India, pp. 163–166.

Harada H, Uemura S, Chen A, Jayadevan J: *Anaerobic treatment of a recalcitrant distillery wastewater by a thermophilic UASB reactor*. Bioresource Technol 1996, 55:215-221

Hidalgo K, Rodríguez B, López M, Iben C, Albelo A, Cárdenas M. 2011. *Distillery Vinasse as an Alternative Additive in Poultry Feed*. Retrieved February 8, 2013.

Invitti JH, Sampaio LAS de A. 2012. *Water, Decontaminant and Drying of Vinasse by Micronization and 505 Formulation of an Organic Mineral Fertilizer Made From Vinasse*. Patent US20120210759 A1. Retrieved 506 January 9, 2013

Jiminez A , or a R, art n A. 2003. *Aerobic–anaerobic biodegradation of beet molasses alcoholic 508 fermentation wastewater.* Process Biochemistry 38:1275–1284; doi:10.1016/S0032-9592(02)00325-4.

Joshi, H.C., 1999. *Bio-energy potential of distillery effluents*. Bio Energy News 3 (3), 10–15.

Rodrı´guez, J.G.O., 2000. Effects of vinasse on sugarcane (saccharum officinarum) productivity. Revista de la Facultad de Agronomia, Universidad del Zulia 17, pp. 318–326

Kalavathi, D.F., Uma, L., Subramanian, G., 2001. *Degradation and metabolization of the pigment- melanoidin in a distillery effluent by the marine cyanobacterium Oscillatoria boryana BDU 92181.* Enzyme and Microbial Technology 29 (4–5), 246–251

Kaparaju P, Serrano M, Angelidaki I: Optimization of biogas production from wheat straw stillage in UASB reactor. Appl Energ 2010, 87:3779-3783.

Kapdi SS, Vijay VK, Rajesh SK, Prasad R (2005) *Biogas scrubbing, compression and storage.* Renew Energy 30:1195–1202.

Kumar, V., Wati, L., Nigam, P., Banat, I.M., Yadav, B.S., Singh, D., Marchant, R., 1998. *Decolorization and biodegradation of anaerobically digested sugarcane molasses spentwash effluent from biomethanation plants by white-rot fungi*. Process Biochemistry 33 (1), 83–88

L. Shih, Y.-T. Van, The production of poly-(-γ-glutamic acid) from microorganisms and its various applications Bioresour. Technol., 79 (2001), pp. 207–225

Mall, I.D., Kumar, V., 1997. *Removal of organic matter from distillery effluent using low cost adsorbent*. Chemical Engineering World XXXII (7), 89–96.

Mandal, A., Ojha, K., Ghosh, D.N., 2003. *Removal of color from distillery wastewater by different processes*. Indian Chemical Engineer Section B 45 (4), 264–267.

Mane, J.D., Modi, S., Nagawade, S., Phadnis, S.P., Bhandari, V.M., 2006. *Treatment of spentwash using chemically modified bagasse and color removal studies*. Bioresource Technology 97 (14), 1752–1755.

Miltner M, Makaruk A, Bala H, Harasek M (2009) *Biogas upgrading for transportation purposes — operational experiences with Austria's first bio-CNG fuelling station*. Chem Eng Trans 18:617–622

Miyata, N., Iwahori, K., Fujita, M., 1998. *Manganese-independent and manganese-dependent decolorization of melanoidin by extracellular hydrogen peroxide and peroxidases from Coriolus hirsutus pellets*. Journal of Fermentation and Bioengineering 85 (5), 550–553

Migo, V.P., Matsumara, M., Rosario, E.J.D., Kataoka, H., 1993. *Decolorization of molasses wastewater using an inorganic flocculant*. Journal of Fermentation and Bioengineering 75 (6), 438–442.

Molina F, Ruiz G, García C, Roca E, Lema JM: *Winery effluent treatment at an anaerobic hybrid USBF pilot plant under normal and abnormal operation*. Water Sci Technol 2007, 56:25-31.

Octavio Carvajal-Zarrabal, Cirilo Nolasco-Hipólito, Dulce Ma. Barradas-Dermitz, Patricia M. Hayward-Jones,Ma. Guadalupe Aguilar-Uscanga, Kopli Bujang. *Treatment of vinasse from tequila production using polyglutamic acid*. Journal of Environmental Management Volume 95, Supplement, March 2012, Pages S66–S70

Ostrem, K. 2004: Greening Waste: *Anaerobic Digestion For Treating The Organic Fraction Of Municipal Solid Wastes*. Earth Engineering Center Columbia University.

Paananen H, Lindroos M, Nurmi J, Viljava T. 2000. *Process for fractioning vinasse*. U.S. Patent # 6022394. 518 Retrieved January 9, 2013.

Pen˜ a, M., Coca, M., Gonza´ lez, R., Rioja, R., Garcı´a, M.T., 2003. *Chemical oxidation of wastewater from molasses fermentation with ozone*. Chemosphere 51 (9), 893–900.

Petersson A (2008) *New biogas upgrading processes*. Brochure of IEA Task 37 “Energy from Biogas and Landfill Gas”.

Pikaev, A.K., Ponomarev, A.V., Bludenko, A.V., Minin, V.N., Elizar’eva, L.M., 2001. *Combined electronic-beam and coagulation purification of molasses distillery slops. Features of the method, technical and economic evaluation of large scale facility*. Radiation Physics and Chemistry 61 (1), 81–87.

Sabnis Madhu, Investigation of how microbes involved in anaerobic digestion of vinasse change as function of temperature, vinasse compositions and time, August 2014.

Salman Zafar, Alternative Energy news, August 25th 2008.

Stuart Peter. The Advantages and Disadvantages of Anaerobic Digestion As A Renewable Energy Source.

Sánchez F, Córdoba P, Siñeriz F*: Use of the UASB reactor for the anaerobic treatment of stillage from sugar cane molasses.* Biotechnol Bioeng 1985, 27:1710-1716

Sa´ nchez Riera, F., Co´ rdoba, P., Sin˜ eriz, F., 1985. *Use of the UASB reactor for the anaerobic treatment of stillage from sugarcane molasses.* Biotechnology and Bioengineering 27 (12), 1710–1716.

Sangave, P.C., Pandit, A.B., 2004*. Ultrasound pre-treatment for enhanced biodegradability of the distillery wastewater.* Ultrasonics Sonochemistry 11 (3–4), 197–203.

Schneider R, Quicker P, Anzer T, Prechtl S, Faulstich M (2002) Grundlegende Untersuchungen zur effektiven, kostengünstigen Entfernung von Schwefelwasserstoff aus Biogas. In: Biogasanla- gen Anforderungen zur Luftreinhaltung, Bayerisches Landesamtfür Umweltschutz, Augsburg.

Schulte-Schulze Berndt A (2005) *Biogas upgrading with pressure swing adsorption versus biogas reforming*. In: Lens P, Westermann P, Haberbauer M, Moreno A (eds) Biofuels for fuel cells. IWA Publishing, pp 414–429.

Sennitt, T., 2005. *Emissions and economics of biogas and power*. In: 68th Annual Water Industry Engineers and Operators' Conference, Schweppes Centre, Bendigo, 7 and 8 September 2005.

Seth, R., Goyal, S.K., Handa, B.K., 1995. *Fixed film biomethanation of distillery spentwash using low cost porous media*. Resources, Conservation and Recycling 14 (2), 79–89.

Sheehan, G.J., Greenfield, P.F., 1980. *Utilization, treatment and disposal of distillery wastewater*. Water Research 14 (3), 257–277.

Siles JA, García-García I, Martín A, Martín MA (2011):*Integrated ozonation and biomethanization treatments of vinasse derived from ethanol manufacturing*. J hazard mater 2011 Apr 15; 188(1-3):247-53

Sirianuntapiboon, S., Zohsalam, P., Ohmomo, S., 2004a. *Decolorization of molasses wastewater by Citeromyces sp. WR-43-6*. Process Biochemistry 39 (8), 917–924.

Subba Rao, B., 1972*. A low cost waste treatment method for the disposal of distillery waste (spentwash).* Water Research 6 (11), 1275–1282.

Syutsubo, K., Harada, H., Ohashi, A., Suzuki, H., 1997. *An effective start-up of thermophilic UASB reactor by seeding mesophilically grown granular sludge*. Water Science and Technology 36 (6–7), 391–398.

T. Takahashia, M. Yoshii, T. Kawano, T. Kosaka, H. Hosoya. A new approach for the assessment of acrylamide toxicity using a green paramecium Toxicol. In Vitro, 19 (1) (2005), pp. 99–105.

Trivedy, R.K., Nakate, S.S., 2000. Treatment of diluted distillery waste by constructed wetlands. Indian Journal of Environmental Protection 20 (10), 749–753.

The Biogas. *Biogas composition.* http://www.biogas-renewable-energy.info/biogas_composition.html.11/22/2014.

Valderrama, L.T., Del Campo, C.M., Rodriguez, C.M., de- Bashan, L.E., Bashan, Y., 2002. Treatment of recalcitrant wastewater from ethanol and citric acid production using the microalga Chlorella vulgaris and the macrophyte Lemna minuscula. Water Research 36 (17), 4185–4192.

Verma, S., 2002: Anaerobic Digestion of Biodegradable Organics In Municipal Solid Wastes. Department of Earth & Environmental Engineering (Henry Krumb School of Mines) Fu Foundation School of Engineering & Applied Science Columbia University

Vlyssides, A., Barampouti, E. M. & Mai, S. 2007. Effect of ferrous ion on the biological activity in a UASB reactor. Mathematical modeling and verification. Biotechnol. Bioeng. 96(5), 853 –861.

Vlyssides, A., Barampouti, E. M. & Mai, S. 2008 Granulation mechanism of a UASB reactor supplemented with iron. Anaerobe 14(5), 275– 279.

Vorion Chemicals & Distilleries Ltd., 1999. Distillery Effluent Treatment and Gold Fish Culture Project.

Waste to energy research and technology council. 'Anaerobic digestion process'.http://www.wtert.eu/default.asp?Menue=13&ShowDok=12, 11/20/2014.

Wempe J, Dumont M (2008) Lets give full Gas! New Gas Platform, Green Gas Working Group, Netherland.

Willington IP, Marten GG. 1982. *Options for handling stillage waste from sugar-based fuel ethanol production*. Resources and Conservation 8:111–129; doi:10.1016/0166-3097(82)90036-0.

Wünsche K (2008) Praxiserfahrungen drucklose Aminwäsche. Proc. Biogas upgrading to biomethane, 6th Hanauer Dialog, pp 136–145.

Yeoh BG: Two-phase anaerobic treatment of cane-molasses alcohol stillage. *Water Sci Technol* 1997, 36:441-448.

Biographical Information

Shammi Rahman received her Bachelors from University of Dhaka, Bangladesh in Geography and Environment in 2005. She obtained her Masters on Civil Engineering form University of Alabama at Birmingham. She was chosen as a Life member of Chi Epsilon from UAB due to excellence in academics. She joined University of Texas at Arlington in January 2011 to pursue her Ph.D. on civil engineering. She was awarded UT Arlington Honorable Mention on her Annual Celebration of Excellence by Students (ACES) oral presentation on the research described in this dissertation. Her research interests include wastewater, energy and climate change.